THESE de l'Université de Lyon

Délivrée par l'Ecole Centrale de Lyon

Spécialité: **Matériaux de L'Ecole Doctorale EDML**

21 Janvier 2016, Lyon

par

Paula USSA

"Tungsten disulfide nanoparticles as lubricant additives for the automotive industry"

préparée au Laboratoire de Tribologie et Dynamique des Systèmes

Pr	Mitjan **KALIN**	Université de Ljubljana	Rapporteur
Pr.	Stefan **CSILLAG**	Université de Stockholm	Rapporteur
Dr.	Pierre **MONTMITONNET**	CNRS. Mines, Paritech	Examinateur
Dr.	Monica **RATOI**	Université de Southampton	Examinateur
Pr.	Fabrice **DASSENOY**	Ecole Centrale de Lyon	Directeur de thèse
	Benoît **THIEBAUT**	Total	Encadrant Industriel

Abstract

The growing environmental concerns, along with the continuous increase of energy demand, have encouraged research to improve energy efficiency in every technological field. In the transport industry, responsible of more than half of the world's oil consumption, manufacturers have bet on hybrid fuel technologies, more aerodynamic car profiles, innovative tires and even downsizing of engines and gearboxes to reduce the weight of the vehicles to face the problem. However, according to VTT Technical Research Centre of Finland, in passenger cars one third of fuel consumption is due to friction loss. This means that several millions of liters of fuel are used every year to overcome friction around the world. As a consequence, reduction on the friction losses would have a direct impact in oil consumption. For this reason, research in the tribology field has specially focused in the development of low friction materials and more efficient lubricants.

This work investigates the potential of metal dichalcogenide nanoparticles as lubricant additives for automobile applications with the aim of formulating more efficient lubricants. These nanoparticles which were synthetized for the first time in the 90's have shown interesting tribological properties when added to base oil under specific laboratory test conditions. However, their future use in real-life mechanical systems needs a better comprehension of their behavior on rough surfaces and in the presence of additives commonly used in industrial lubricants.

Industrially produced tungsten disulfide nanoparticles were used in this work. First of all, the industrial context of this work and the basis of tribology science in general and of tribology in the automotive industry in particular are exposed in the state of the art part. In this section, a literature review of the lubricating properties of laboratory scale produced metal dichalcogenides nanoparticles of tungsten and molybdenum disulfide is exposed. The effect of different conditions (temperature, concentration in oil, contact pressure, among others) is also presented in this first section.

The research work done for this thesis is divided in two main parts. In the first one, the nanoparticles were first morphologically and chemically characterized and their tribological potential in base oil was investigated on smooth and rough surfaces under different test conditions. Then, their tribological behavior in the presence of additives that are commonly used in industrial applications, in the boundary lubrication regime and at 100°C was studied.

In the second part, the use of nanoparticles for a gearbox application was explored. The potential of the nanoparticles in base oil and in the presence of a commercial package of additives for this application was studied, first at the laboratory scale, and then in scaled-up tests with gearboxes used in cars. The results suggest that nanoparticles can be used to increase life span of the mechanical parts of gears.

Key words: Nanoparticles, lubrication, gears, additives, rough surfaces

Résumé

Les normes environnementales toujours plus sévères associées à une constante augmentation de la demande énergétique rendent nécessaires les actions à entreprendre en vue d'améliorer l'efficacité énergétique. Dans le domaine du transport, responsable à lui seul de plus de la moitié de la consommation des ressources pétrolières, les actions visant à optimiser la consommation énergétique se traduisent par la mise en place de nouvelles technologies hybrides, par un travail sur l'aérodynamisme des véhicules, la conception de pneumatiques plus performants ou bien encore la réduction de la taille des moteurs et des boites de vitesse afin de réduire le poids des véhicules. Cependant, selon le VTT (Centre de recherche technique finlandais), dans les voitures particulières, les pertes par frottement représentent un tiers de la consommation totale de carburant. Plusieurs millions de litres de carburant sont ainsi utilisés dans le monde chaque année pour vaincre les forces de frottement. Pour cette raison la recherche en tribologie dans le domaine de l'automobile s'est plus particulièrement focalisée ces dernières années sur le développement de matériaux à faible coefficient de frottement ainsi que lubrifiants plus performants.

Ce travail de thèse a pour objectif d'étudier le potentiel des nanoparticules de dichalcogénures métalliques en tant qu'additifs de lubrification pour applications automobiles dans le but de développer de nouveaux lubrifiants hautement performants. Ces nanoparticules, synthétisées pour la première fois dans les années 90, ont déjà montré des propriétés tribologiques intéressantes lors de tests effectués en laboratoire, en régime de lubrification limite. Toutefois, leur utilisation dans des systèmes mécaniques réels nécessite une meilleure compréhension de leurs performances dans des conditions plus proches de la réalité, à savoir en présence de surfaces rugueuses ainsi qu'en présence d'additifs couramment utilisés dans les lubrifiants industriels.

Au cours de ce travail, nous nous sommes focalisés sur des nanoparticules de bisulfures de tungstène produites industriellement. Le contexte industriel de ce travail de thèse ainsi que les bases de la tribologie seront exposés dans un premier chapitre consacré à l'état de l'art. Dans ce même chapitre, une revue bibliographique des propriétés lubrifiantes des nanoparticules de bisulfures métalliques (MoS_2, WS_2) observées lors d'essais tribologiques effectués en laboratoire sera également présentée. L'influence de certains paramètres tels que les conditions d'essais, l'effet de la température, de la concentration, de la cristallinité sera également présentée dans ce premier chapitre.

Les résultats de mon travail de thèse seront présentés à travers deux grandes parties. Dans une première, les caractéristiques morphologiques et chimiques des nanoparticules étudiées seront présentées. Leurs propriétés tribologiques dans l'huile de base en présence de surfaces en acier de différentes rugosités seront discutées. Enfin, leurs performances en présence d'additifs couramment utilisés dans les applications industrielles ont également été étudiées. Tous ces essais ont été réalisés en régime de lubrification limite et à 100°C.

Dans une seconde partie, le potentiel des nanoparticules pour une application boîte de vitesses a été exploré. Des essais tribologiques ont été réalisés à la fois dans une huile de base ainsi qu'en présence d'un cocktail d'additifs, tout d'abord à l'échelle du laboratoire puis lors de tests réels effectués avec des boites de vitesses utilisées dans l'automobile. Les résultats montrent que les nanoparticules peuvent être utilisées pour augmenter la durée de vie des engrenages.

Mots cléfs : Nanoparticules, lubrification, engrainages, additifs, surfaces rugueuses

Acknowledgments

First and foremost, I would like to thank my academic supervisor, Professor Fabrice DASSENOY for his constant availability and all the time he dedicated to this project. Thanks for your patience, your advices, and all the good times and the laughs we shared during these three years. I would also like to thank you for the very careful reading the manuscripts we submitted and the thesis. It was a pleasure to work with you. This work would not have been possible without your support and encouragement.

I also would like to thank my industrial supervisor, Benoît THIEBAUT for his commitment to this work and the nice scientific talks that we had thought it. It was also a pleasure to work with you and I hope it will continue to be that way for the next years.

My sincere gratitude to the members of the jury not only for accepting to review my thesis, but also for their advices and the interesting discussion held during the defense.

I gratefully acknowledge the members of LTDS that contributed to this work. Thierry for his XPS expertise, his time and his precious help when the machine was not working; Didier for the metal working and the visit to Loche's Castle with my parents; Beatrice for the TEM images; Michel for his help with the tribometer, Helene for the administrative assistance, the fashion talks and the coffee breaks and Istvan for reading my thesis, the chocolates and the English help.

I extend these acknowledgments to the people from Total that contributed to this work. Eric for giving me the opportunity to do this thesis; Stephane for the transmission experiments, the time he dedicated to this project and his attendance to the meetings; Bernadette for the MTM training, the nice talks and the rides downtown.

This thesis has been carried out with the support and help of many people from a personal point of view, for this reason, I would also like to thank all the people from LTDS and Total that supported me during these three years. Special thanks go to Sophie. Thank you for the nice talks, the good meals, the great parties, the victory dances, the Alsacian and Japanese trips and all the good times we had spent together. I would also like to thank Chacha, Gael, Clara and Ju for their friendship. You guys arrived to my life when I needed it the most and I'm so glad I found friends like you. It is nice to know that besides being friends we'll continue to be colleagues because that will give us plenty of good opportunities to have fun! A big thanks to Adalberto, Alexia, Clara, Irene, Thomas M., Miguel, Mickael, Rafael, Modestino, Catia Gilles, Deepthi, Paule, Marieme, Anton and all the other post docs, PhD students and LTDS colleges for the overall atmosphere, the coffee breaks we shared and the volleyball matches (for those that were there every Friday). All those moments really allowed me to keep things in perspective.

Finally, I thank my family (mom, dad, Nana and now Florian) for their constant support, their love and for believing in me even when I didn't believe in myself. You all are the reason why I did this PhD, so I dedicate this work to you.

Preface

This dissertation is submitted for the degree of Doctor of Philosophy at the *Ecole Doctorale Matériaux* of Lyon. This work was financed by Total Marketing Services through a CIFRE convention with *Ecole Centrale de Lyon*. The research described herein was conducted under the academic supervision of Professor Fabrice DASSENOY in LTDS (*Laboratoire de Tribologie et Dynamique des Systèmes*) laboratory at *Ecole Centrale de Lyon* and the industrial supervision of Benoît THIEBAUT in TOTAL Marketing Services.

This dissertation is the fruit of the research done by the author between September 2012 and September 2015

Scientific Contribution

Part of this work has been patented in France in February 2014 (N° de depot: FR 1451648).

A version of the first part of this work has been published in Tribology Letters Journal: P.Ussa. B. Vacher, T. Le Mogne, M. Belin, B. Thiebaut, F. Dassenoy, "Action mechanism of WS_2 nanoparticles with ZDDP additive in boundary lubrication regime", Volume 56, Issue 2, pp 249-258, 2014. An oral communication of this chapter was done during ITC 2015 in Tokyo, Japan. Additionally, another part of this first section has been recently submitted to Tribology International Journal: P.Ussa. F. Dassenoy, B. Vacher, T. Le Mogne, B. Thiebaut, "WS_2 nanoparticles anti-wear and friction reducing properties on rough surfaces in the presence of ZDDP additive" (paper under review).

The second part of this work has been published in Tribology Transactions Journal: P. Ussa, F. Dassenoy, B. Vacher, T. Le Mogne, B. Thiebaut, A. Bouffet, "Anti spalling effect of WS_2 nanoparticles on the lubrication of automotive gearboxes", in press. The results of this part were presented in an oral communication in STLE 2015 conference in Dallas, Texas and in ITC 2015 conference in Tokyo, Japan. A poster was also presented during STLE 2015 (silver best poster award).

Table of Contents

Table de matières

List of Tables

List of Figures

18

Notations

h_{min} Elastohydrodynamic film thickness
Ra   Average roughness
μ   Friction coefficient
λ   Lambda ratio

Abbreviation and acronyms

AFM	Atomic Force Microscopy
AW	Anti-wear
BL	Boundary Lubrication
CVT	Continuously Variable Transmission
CO	Carbon monoxide
COF	Coefficient Of Friction
DLC	Diamond-Like Carbon
DOC	Diesel Oxidation Catalyst
DPF	Diesel Particulate Filter
EDX	Energy Dispersive X-ray spectrometer
EP	Extreme Pressure
ECR	Electrical Contact Resistance
FIB	Focused Ion Beam
FM	Friction Modifier
HD	Hydrodynamic lubrication
HFRR	High Frequency Reciprocating Rig
IEA	International Energy Agency
IF	Inorganic Fullerene-like
MoDTC	Molybdenum Dithiocarbamate
MTM	Mini Traction Machine
NMHC	Non-Methane Hydrocarbons
NOx	Nitrogen Oxides
NP	Nanoparticle
NT	Nanotube
NS	Neutral Solvent
OFM	Organic Friction Modifiers
PAO	Polyalphaolefin
PM	Particulate Matter
S	Solvent
SCR	Selective Catalytic Reduction
SEM	Scanning Electron Microscope

SSU	Second Saybolt Universal
TDS	Total Dissolved Solids
TEM	Transmission Electronic Microscope
TGA	Thermogravimetric Analysis
THC	Total hydrocarbon
XANES	X-ray Absorption Near Edge Structure
XPS	X-Ray Photoelectron Spectroscopy
ZDDP	Zinc Dialkyl DithoPhosphate

State of the art

The aim of the State of the art part is to present a general overview about lubrication science in the automotive industry, followed by a synopsis about the research that has been done on metal dichalcogenide nanoparticles. The first part includes the description of tribology and its fundamental principles as well as the generalities of lubricants and their composition. The role of the different additives is also presented. The second part consists on a bibliographic review of nanoparticles as lubricant additives which exposes the results obtained by different research groups around the world.

1. Industrial context

It is known that energy is the main fuel for economic and social development and that its demand has always been linked to population growth. Generation of energy can be done from different sources such as coal, oil and natural gas (among others). However, for decades, oil has been the main source of the energy we used. According to the International Energy Agency (IEA), 64% of the oil consumed in 2012, was consumed by the transport industry (*1*) as illustrated by Figure 1. Research done by the VTT Technical Research Centre of Finland revealed that, in passenger cars, one third of the fuel energy is used to overcome friction on engine, transmission, tires and brakes (*2*). This means that 208,000 million liters of fuel (gasoline and diesel) were used to overcome friction in 2009. The global energy demand for transportation is projected to increase by 40 percent from 2010 to 2040 (*3*), at the same time the vehicle fleet is expected to duplicate to 1.7 billion in 2035 and is expected to be 2.2 billion in 2050 (*4*). As a consequence, research in tribology has been specially focused in the development of low friction materials and more efficient lubricants, which may be able to reduce fuel consumption, increase energy efficiency and thus reduce emissions.
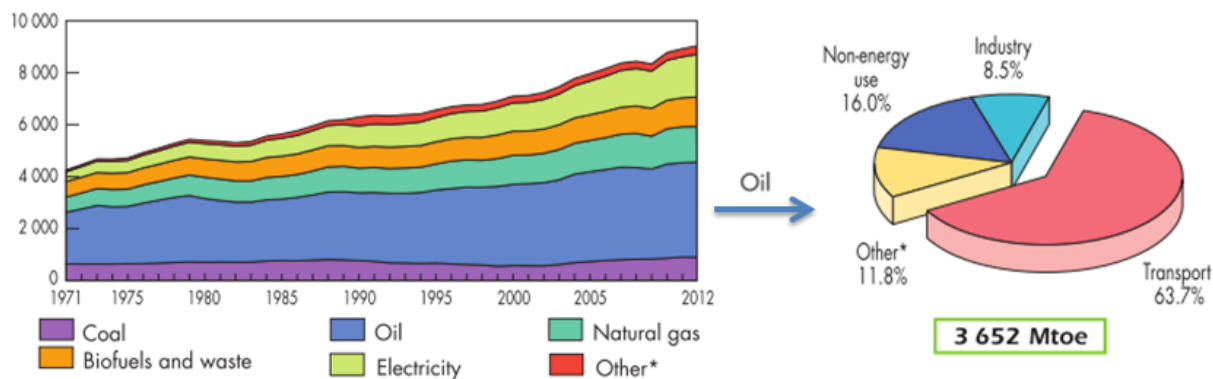
Figure 1. World energy consumption from 1971 to 2012 by fuel in million tonnes of oil equivalent (Mtoe) and oil world consumption by sector (*1*).

Since 1992, when the *Earth Summit* was signed in Brazil during the *United Nations Conference on Environment and Development*, the governments recognized the need to redirect international plans and policies to reduce vehicle emissions. In the European Union, the acceptable limits for exhaust emissions of new cars are defined by the European Emission Standards. These regulations concern emissions of nitrogen oxides (NOx), total hydrocarbon (THC), non-methane hydrocarbons (NMHC), carbon monoxide (CO) and particulate matter (PM). The emission standards have been progressively tightened. Figure 2 illustrates the evolution of these regulations concerning NOx and PM for diesel passenger cars. Euro 6 standard became mandatory from the beginning of 2015.
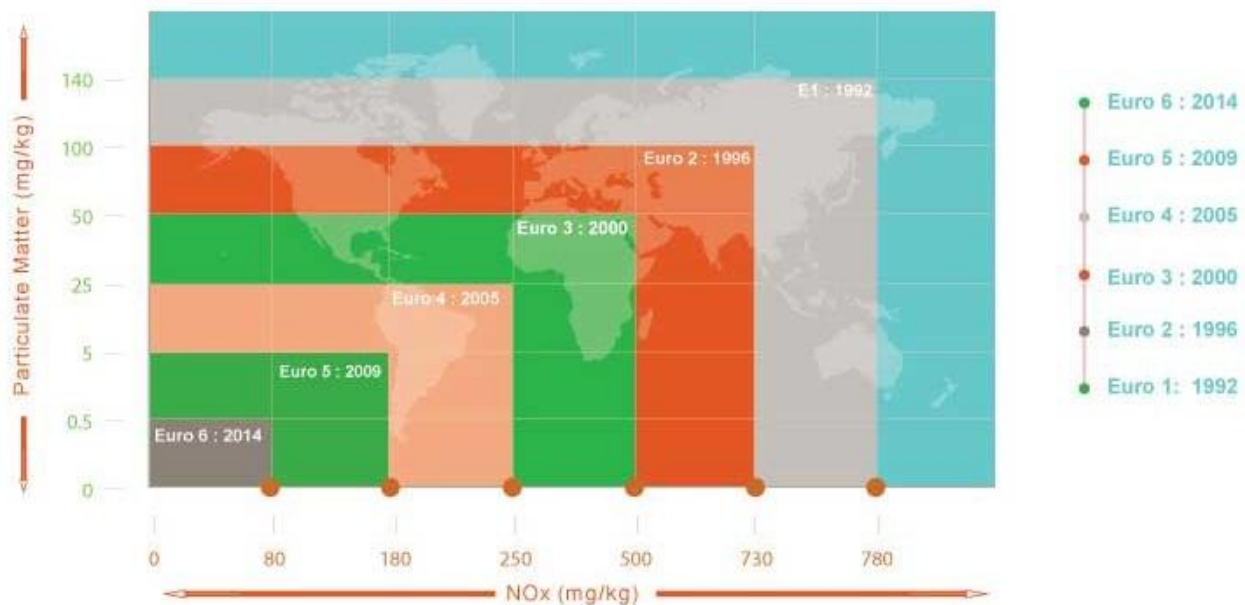
Figure 2. Evolution of Euro Emissions Standards for diesel passenger cars (taken from: http://www.clm.co.uk/diesel-emissions-crackdown/)

In order to improve energy efficiency and to reduce emissions, manufacturer's strategies include developments in lubrication and surfaces to minimize internal friction and weight of the vehicle. The use of lighter materials and the downsizing of components would reduce the automobile weight. However, reducing the size of contacting components will probably cause friction and wear to increase. Lubricants must be able to work under more severe conditions to guarantee lifespan of the mechanical parts of cars. For this reason, research in tribology, the science of friction and wear needs to be done.

2. Friction and wear principles

Despite the fact that humanity has been facing tribology problems since a long time ago, it was not until the 60's that this term was employed for the first time. The term tribology comes from the Greek word "tribos" which means "rubbing" and from the suffix "ology" which means "the study of". Therefore, tribology is the study of rubbing or the study of things that rub. Nowadays, tribology is known as the study of friction, lubrication and wear.

2.1 Friction principles

Friction is defined as the resistance encountered when one body moves tangentially over another with which it is in contact. Friction force always acts in the opposite direction to that of the relative displacement between the contacting surfaces and is a function of the normal load of the contact. It is also the principal cause of wear and energy dissipation. As a matter of fact, friction has been a part of humanity's history since its very beginning. In ancient Egypt, wooden sledges where used to haul the heavy stones for the construction of the pyramids. Later, at around 3000 BCE, the invention of the wheel was also a response to friction.

Leonardo Da Vinci (1452-1519) is considered the first scientist that studied the basics of friction. However, Guillome Amontons (1663-1705) was the first to formulate the friction laws. Further understanding of friction phenomena was made by Hertz, Reynolds, Coulomb, Bowden and Tabor.

Friction between moving surfaces can be reduced by the use of lubricants. Lubricants can be solid, gases or liquids. In the automobile industry, lubricants are liquids composed mainly of base oil and a package of additives.

In the case of liquid lubrication, three different regimes can be distinguished: full film or hydrodynamic, mixed and boundary lubrication. These are based on the lambda parameter or specific film thickness, which is the ratio of the fluid film thickness to the surface roughness as defined by the equation 1.

$$\lambda = \frac{h_{min}}{[(Rq_1)^2 + (Rq_2)^2]^{1/2}} \qquad \text{(Eq 1)}$$

Where h_{min} is the elastohydrodynamic film thickness for smooth surfaces and Rq_1 and Rq_2 are the roughness values of the two bearing surfaces. All the lubrication regimes and their relationship to the lambda parameter are illustrated in the Stribeck curve in Figure 3. Full film or hydrodynamic lubrication (HD) regime occurs when the two surfaces in motion are completely separated by a film of fluid, this means that the lubricant film is thicker than the height of the asperities. On the other hand, boundary lubrication (BL) occurs when the two surfaces are mostly in contact with each other even though a fluid is present. Mixed lubrication (ML) is a cross between boundary and full film lubrication where the bulk of the surfaces are separated but the asperities are in contact.
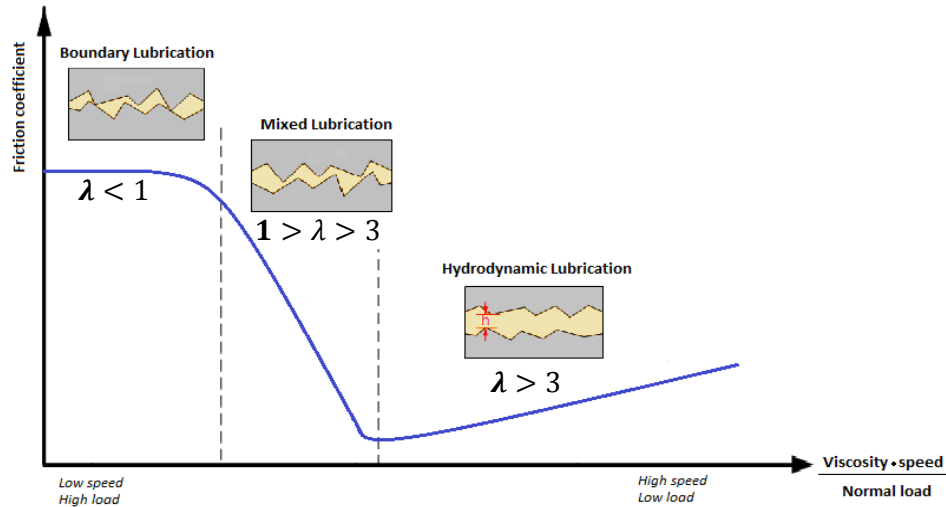
Figure 3. Stribeck curve showing the different lubrication regimes as a function of the film thickness, the viscosity and the normal load.

2.2 Wear principles

Wear is defined as the removal or displacement of material from one body when subjected to contact and relative motion with another, in other words when subjected to friction. There are several types of wear. However, the most representatives and important ones are: abrasive, adhesive, rolling contact fatigue and corrosive. In reality, wear does not normally take place through just one wear mode but through a combination of them. An explanation about the wear modes in presented below and schematic images of each wear mode are illustrated in Figure 4.

(a)Adhesive wear

(b) Abrasive wear

(c) Fatigue wear

(d) Corrosive wear
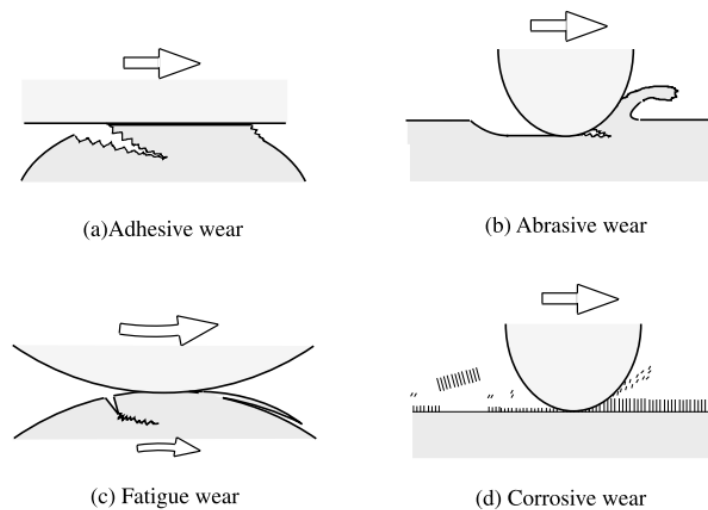
Figure 4. Schematic images of the wear modes (5).

26

- **Abrasive wear** occurs between surfaces of different relative hardness. In this wear mechanism the asperities of the hardest material scratch the softer one. This mode is also known as Scratching. The three different abrasive modes are shown in Figure 5: microcutting, wedge forming and ploughing. The wear particles have different forms depending on these three modes. In the first one, curled and long ribbon-like wear particles are formed; in the second one, wedge-like particles are formed at the tip of the grooving asperity while in the third one a shallow groove is formed on the surface but repeated sliding and accumulation of plastic flow are necessary to generate a wear particle.

Microcutting	Wedge forming	Ploughing
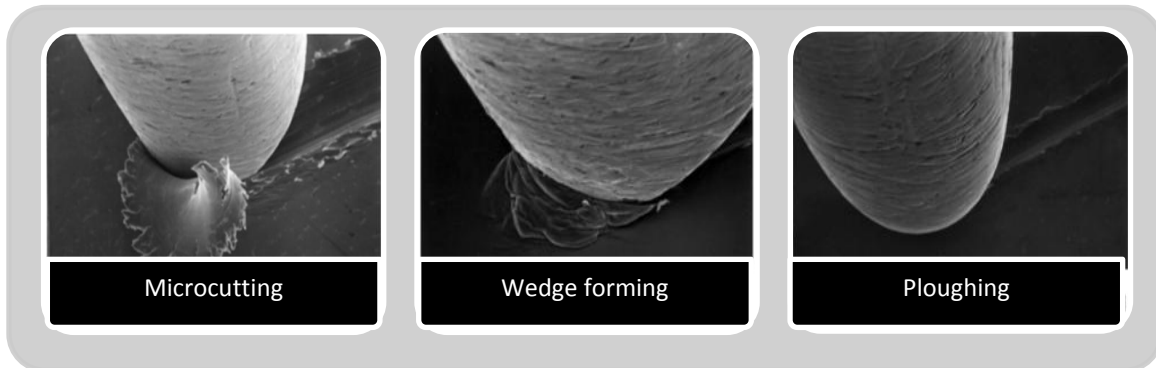
Figure 5. TEM images of the different abrasive wear modes (*6*)

- **Adhesive wear** occurs when adhesive bonding strength of the contact interface between two surfaces can resist their relative sliding. Thus, deformation occurs under the compressed zone initiating a crack which propagates in the combined fracture mode of tensile and shearing until it reaches the contact interface and creates a wear particle. Wear particles can leave the contact interface or stay on either surface. Transfer and retransfer from one surface to the mating surfaces take place in many cases. Compatibility of the materials is important for this wear mechanism.

- **Corrosive Wear** takes place in the case where a tribochemical reaction produces a layer on the surface which is continuously removed by friction. This layer behaves in most of the cases differently from the bulk material.

- **Rolling contact fatigue** is due to the stress developed in the subsurface of the material under repeated or cyclic loading conditions. This can cause subsurface delamination and cracking. In the case of metallic materials, shallows are formed by the ploughing mode and after repeated contact of abrasive sliding at the same grooves, plastic burnishing becomes more predominant and after a critical number of cycles fatigue mode appears.

3. Tribology in the automotive industry

Vehicles are one of the most common machines used nowadays. A car consists in thousands of different parts which are commonly in motion. Thus, we can find many hundreds of tribological parts in cars like bearings, gears, tires among many others. All the lubrication regimes and the wear modes presented above are met in automotive applications. According to Tung et al. (*7*) for the purpose of classifying tribological components, vehicles can be divided into engine, transmission and ancillaries (tires, brakes and windshield wipers). In the framework of this investigation, only the engine and transmission will be discussed and special focus will be put on transmission failure.

3.1 Engine

Engines or motors are machines designed to convert energy into mechanical motion. Car engines are internal combustion engines which produce the power necessary to move vehicles by controlled explosions. Car engines use fuel, such as petrol or diesel, which is ignited to produce the power required to move the vehicle. The power is then transferred to the driveshaft via the transmission drive. Most engines use a four stroke combustion cycle which consists of: intake, compression, combustion and exhaust. The cycle is repeated in quick succession to generate the required power. The different components of an engine can be seen in Figure 6.

© 2006 Merriam-Webster, Inc.
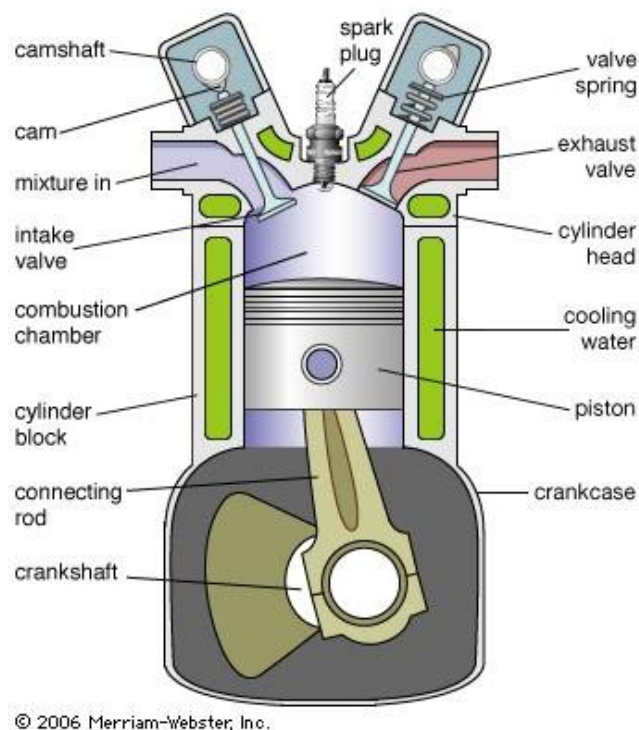
Figure 6. Parts of an internal combustion engine (source: Merriam-Webster, Inc).

Engines work under a wide range of operating conditions of speed, temperature and load. The lubrication system makes sure that every moving part in the engine gets lubricant so it can easily move. According Taylor et al. (*8*) 80% of the mechanical losses of an internal combustion engine are due to friction. Some examples of moving parts where lubrication is needed are pistons which slide in the cylinders and bearings that allow rotation of the crankshaft and camshafts. A representation of the engine lubrication system can be observed in Figure 7. The lubricant is taken from the sump by the pump that drives it to the oil filter to remove sludge as well as potentially abrasive particles such as debris resulting from engine wear. It is then squirted under high pressure onto the main bearings and the cylinder walls. After the entire engine is lubricated, the lubricant is collected in the sump where the heat is transferred to the surrounding air and the cycle is then repeated.
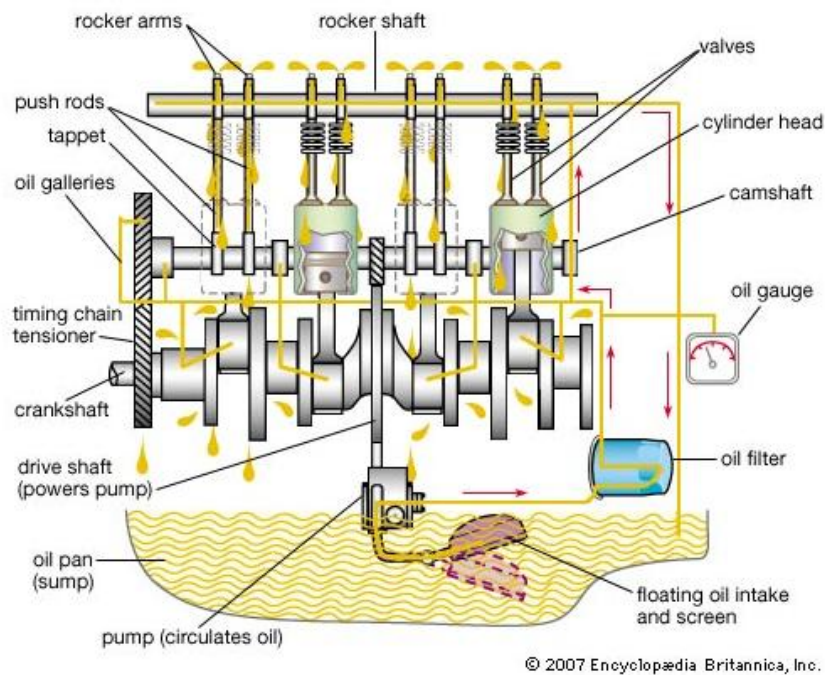
Figure 7. Engine lubrication system (source: Encyclopedia Britannica, Inc.).

Therefore, all the lubrication regimes can be easily found in engines. In fact, some components are known to operate in specific lubrication regimes as illustrated in Figure 8.
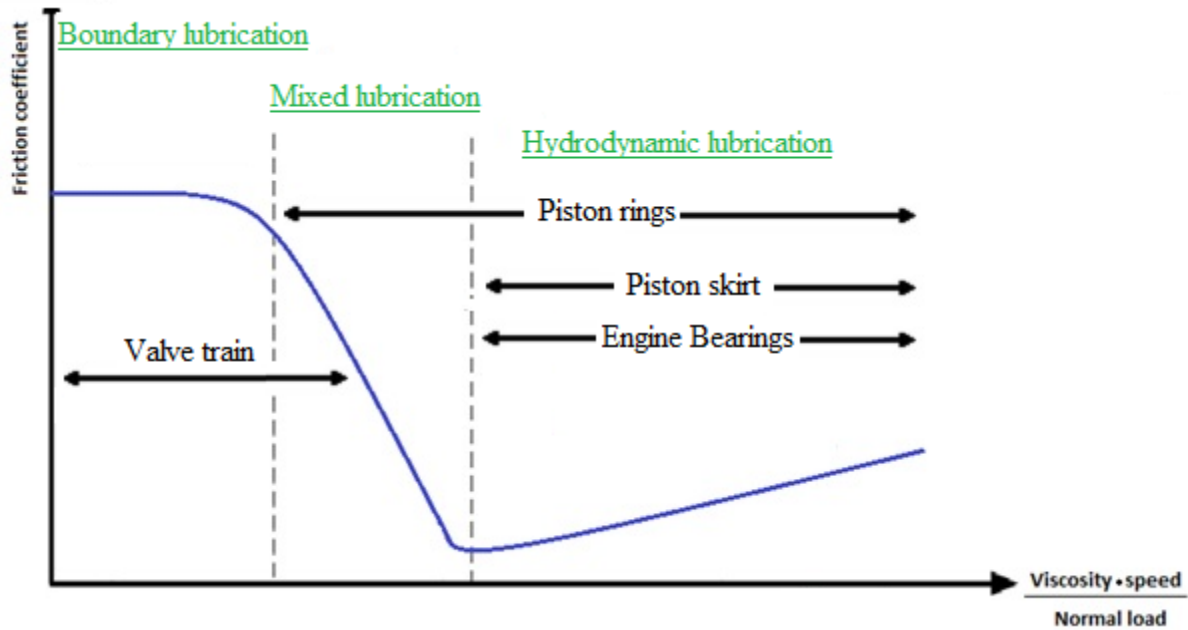
Figure 8. Lubrication regimes for engine components.

As a result, lubricants used in engines must resist the high heat of combustion and must not degrade when exposed to combustion products. They must also be capable of removing metal debris away from the contact zones, produced during the running in of rough surfaces, and to protect matting surfaces working under the mixed and boundary lubrication regimes as it is the case of the valve trains.

Proper lubrication yields to reduction on both fuel and oil consumption and increase in engine lifespan. Thus, improvements in tribology have a direct impact on these items and should focus on the reduction of harmful exhaust emissions. According to Culley et al. (*9, 10*) an increasing concern with modern engine oils is the influence of presence of phosphorus that deteriorates the emission systems components by poisoning the after treatment catalysts.

3.2   Transmission

The transmission system is responsible for the power transfer from the engine to the drive wheels. This is done by variation of torque from the engine through manual gear operation, or torque conversion in the case of automatic transmission cars. A car's transmission system enables the engine to provide a wide range of output speeds which allow vehicles to function in different driving conditions by the use of different gears.

The first stage of the transmission system is the clutch which is then followed by the gearbox. Manual transmission cars have normally four or five forward speeds, one reverse and a neutral position. Figure 9

shows one of the most common configurations of a five-speed gearbox. Power enters the transmission though the input shaft which is connected to the engine via the clutch. When the cutch is fully engaged, the layshaft is always turning. All the helical gears on the layshaft are permanently attached to it so they all turn at the same rate. They mesh with a series of gears on the output shaft that are mounted on sliprings so they permanently spin around the output shaft but don't make it turn. The gear level which is operated by the driver is connected to selector rods and forks that move the synchromesh units back and forth and allows transferring movement from the layshaft to the output shaft, according to which gear is selected. All this is done by the action of friction so lubricants must be used.
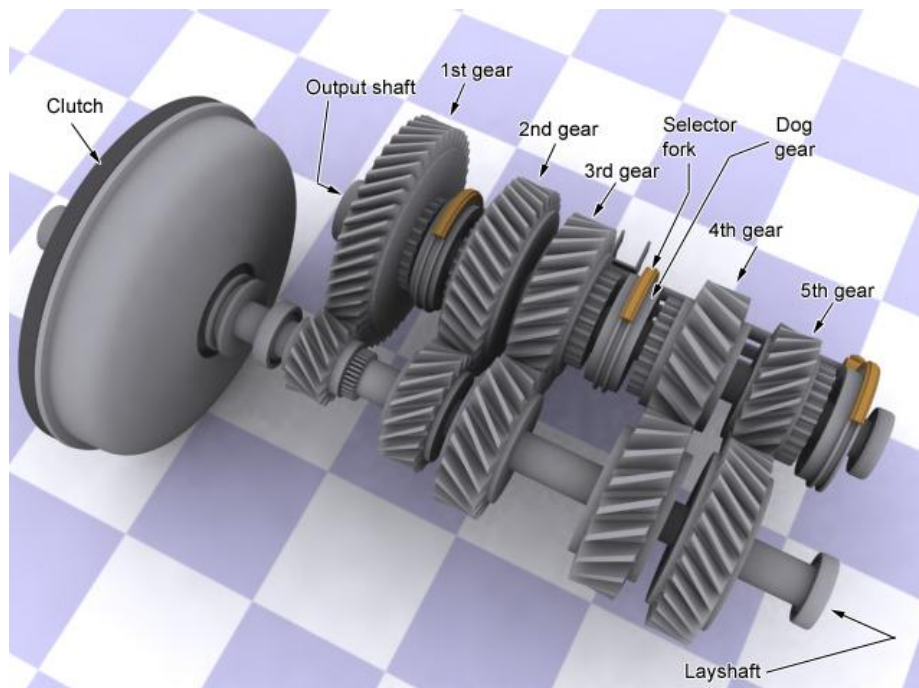
Figure 9. Typical five-speed gearbox (source: www.carbibles .com)

Gear lubricants must have good thermal and oxidative stability, extreme pressure resistance and protection against wear to reduce the failure risk. The most common form of failure in gears is known to be rolling contact fatigue (*11, 12*).

3.2.1   Failure of gears

3.2.1.1   *Surface contact fatigue principles*

Rolling contact fatigue is one of the most common wear modes. As explained in section 2.2, it occurs when two surfaces in contact experience Hertzian stress of a great magnitude and number of cycles. This localized stress results when curved surfaces are in contact under a normal load. So it can be

observed not only in gears but also in bearings where the contact geometry and the motion of the rolling elements produce an alternating subsurface shear stress. As a matter of fact, all surfaces in rolling and/or sliding contact are exposed to fatigue.

Fadjdiga et al. (*13*) defined fatigue as a kind of damage caused by changes in the material microstructure which results in crack initiation followed by crack propagation. Therefore, the initiation of cracks represents one of the most important stages in fatigue process.

The chemical and physical properties of lubricants play a significant role in fatigue wear (*14*). The lambda parameter or specific film thickness, water content and lubricant additives are all considered to have significant effect on fatigue life.

The lambda parameter is considered to be an important parameter affecting fatigue life of bearings as illustrated in Figure 10. Consequently, the selection of lubricants with a proper viscosity is important to ensure longer lifespan of the bearings.
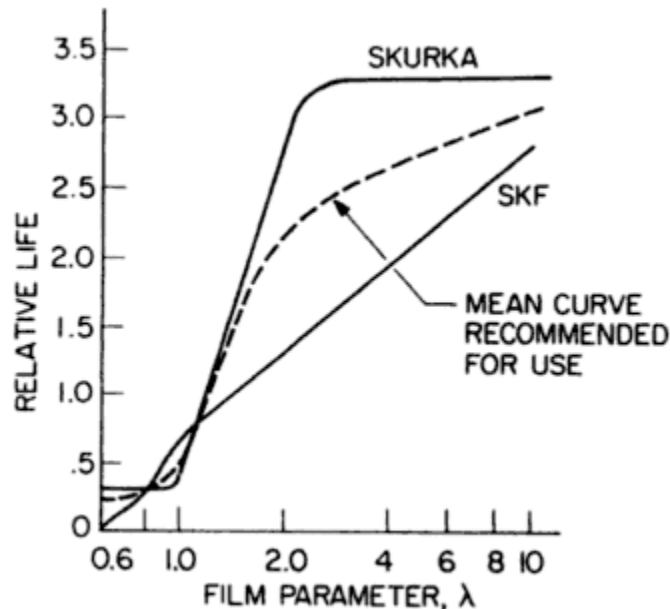
Figure 10. Relative fatigue life as a function of film parameter (*15*)

Water content has also proven to have a detrimental effect on rolling contact fatigue life. Different research groups have demonstrated that water contents of around 1% may reduce contact fatigue life of mineral (*16, 17*) and hydraulic oils (*18*) by 40-50%. Water molecules produce embrittlement of the steel by the production of atomic hydrogen when they reach the highly reactive surface of cracks as illustrated in Figure 11. The use of additives able to neutralize protons, sequester water or form hydrophobic films may help deal with this problem.
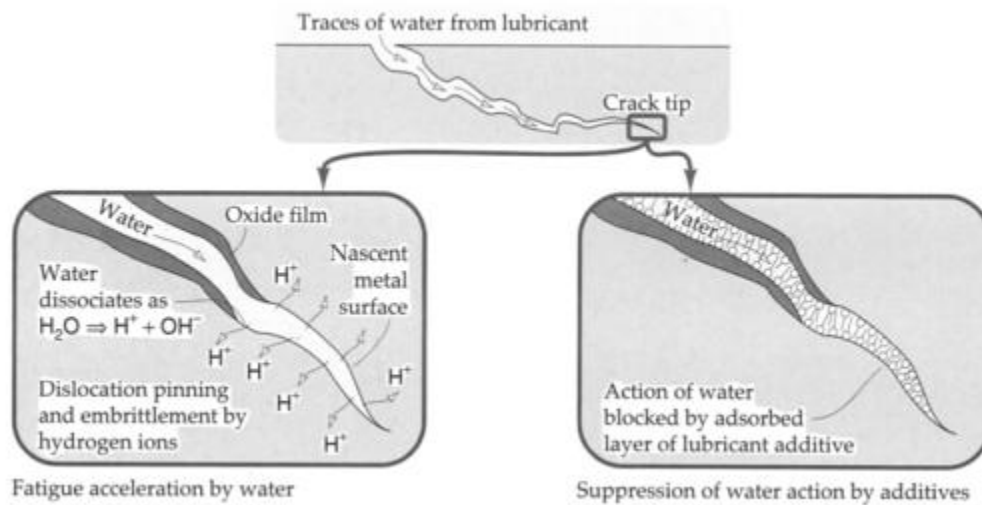
Figure 11. Effect of water on the propagation of cracks (*19*).

Some lubricant additives may also have a significant influence on contact fatigue life. This will be discussed below.

3.2.1.2   Rolling contact Fatigue in Gears

Gear drives have non conformal interacting surfaces and have both rolling and sliding action at the teeth interfaces. Due to the severe conditions and even if correctly lubricated, gear drives will eventually fail as a result of surface fatigue phenomenon. Cracks can occur anywhere on the gear tooth flank but are most likely to appear where the contact conditions are more severe (*20, 21*). The teeth terminology can be seen in Figure 12.
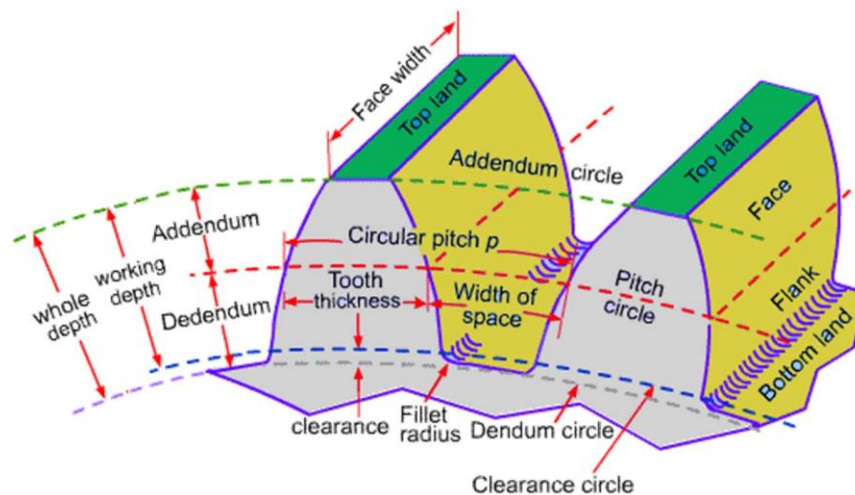
Figure 12. Gear tooth terminology (source: http://en.wikiversity.org/wiki/File:Gearnomenclature.jpg).

Below the pitch diameter, in the dedendum zone, conditions are known to be the most critical due to the fact that sliding and rolling directions are opposite. Thus, fatigue failure normally begins at this point of the teeth.

Surface fatigue modes are: pitting, micro-pitting and spalling. Even if spalling and pitting are the most common forms of surface contact fatigue, spalling results in more rapid deterioration of surface durability when particles of the material break out. Thus, it is considered as the more destructive surface failure mode for gear contacts. The presence of cracks in the material promotes and accelerates spalling. Cracking can start either at the surface or in a subsurface level when defects and inclusions are present in the material (*11, 20, 22, 23*). Both kinds of cracks propagate and subsurface cracks may open to the surface. Cracks can occur anywhere on the gear tooth flank but are most likely to appear where the contact conditions are more severe (*20, 21*)

In 1935, Way, et al. (*24*) suggested that pit nucleation is brought about by the propagation of a tiny surface crack due to oil hydraulic pressure caused by oil penetrated into the crack. Later, Kaneta, et al. (*25*) proved that oil sealed into the cracks do promote crack propagation. It has been suggested that the process occurs in three stages: a crack opening phase caused by traction forces ahead of the rolling contact, followed by the filling of the crack by the liquid lubricant which is finally squeezed when the traction forces and contact stress close the crack (*26*). Pit nucleation is also thought to be due to hydrogen embrittlement. In fact, it has been shown that hydrogen decreases dramatically rolling contact fatigue life (*27-29*).

The role of additives in the formation and propagation of cracks is not completely understood. Special interest has been paid these last past years to the effect of anti-wear and extreme pressure additives on rolling fatigue life. In some instances, these additives have demonstrated to be able to increase the rolling contact fatigue life of gears (*30-32*). In others, results have shown detrimental effect on pitting life (*33-36*) which scientist link to chemical reactivity of the additive that would attack the metal surface promoting crack initiation by the creation of corrosion pits. On the other hand, other researchers state that the effect of these additives depends on their concentration in the oil (*33, 37-39*). An increment of the fatigue life can be obtained at low concentrations while a decrement is observed at high concentrations. The fact that additives can go inside cracks and react with crack faces was demonstrated for the first time by Meheux et al. (*40*).

The use of solid additives has also been studied. Arizmendi et al. (*41*) tested the effect of a solid nonstoichiometry inorganic glassy compound consisting of B, P, Mg, and K (known as nsic-bp1) oxides with a particle size of 16 μm, and a solid MoS_2 of colloidal grain size, on fatigue life. Their results show that both solid particles improve more than twice the fatigue life of the base oils. Only the results obtained with the first solid additive were analyzed. No oxidation of the base oil was observed with this additive. The authors proposed that all the heat was used for softening the solid compound, so there was no heat available for the oxidation of the base oil, thus inhibiting the generation of hydrogen preventing crack nucleation and growth. Other alternative mechanism proposed by the authors is the formation of a protective film of the softened compound which may delay crack initiation produced by chemical attack from active substances in the oil, and would also inhibit oil penetration once the cracks

are formed, delaying crack propagation. Nevertheless, no chemical analyses were done on the surfaces to observe such protective film, nor physical analyses where made to observe the presence of cracks in the material. On the other hand, Rico et al. (*42*) have shown that PTFE nanoparticles used as additive in both mineral and synthetic base oils at concentrations lower than 3% increase the fatigue life of steel. The authors measured the contact angle between the counter parts and found that it decreased in the presence of PTFE. This led them to the conclusion that these nanoparticles improve the adsorption phenomena increasing the lubricant's unctuosity. They also claim that simple mechanical interposition of PTFE particles between the surfaces could protect them from fatigue. However, no surface analyses were done to observe the presence of cracks in the steel.

To resume, rolling contact fatigue is known to be one of the most common forms of failure fatigue in gears. Thus, the reduction of wear in gearboxes requires the use of powerful lubricants able to minimize the disastrous consequences of the contact fatigue.

3.3 Lubricant composition and function

As it has been stated before, a lubricant is a substance that is used to reduce friction between moving surfaces. Lubricants perform a number of critical functions: to provide cooling, transport debris away from the interface, prevent deposits on the surfaces, among others. Additionally, they must be effective in all the lubrication regimes. In order to help the oils accomplish all these tasks, additives are used. Additives are substances that are mixed into the base oil either to suppress or enhance its intrinsic properties or to add properties it does not have by itself. The composition of a lubricant is illustrated in Figure 13. The concentration and the chemical nature of the additives directly depend on the application in which it is used. In the automobile industry, lubricants need good oxidation resistance, suitable low and high temperature viscosities and good cleaning and dispersing ability. On the other hand, metalworking lubricants need antiwear performance, corrosion control and cooling ability.
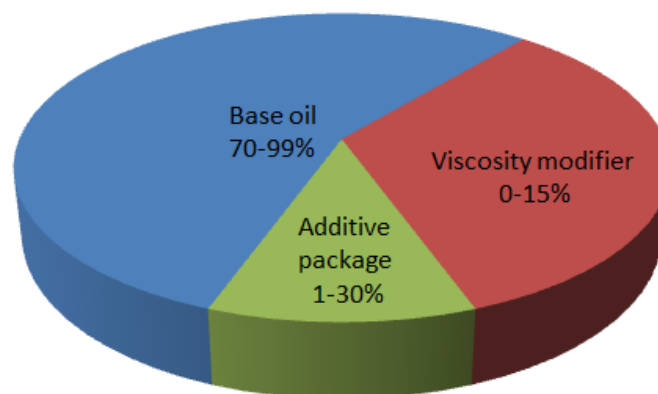
Figure 13. Composition of a lubricant

3.3.1 Base oil

Base oils can be classified depending on their origin into mineral oils or synthetic lubricating oils

- **Mineral oils** are the most commonly used throughout the industry. They are produced from crude oil by distillation. Their properties depend both on the composition of the original crude oil and the processes used for its manufacture which can be solvent extraction or hydrotreatment. They can be classified into: paraffinic and iso-paraffinic base oils. Paraffinic base oils have a good oxidation stability and high viscosity index (of around 100). However their high molecular weight can produce crystallization even at room temperature.
On the other hand, iso-paraffinic base oils, which have a lower viscosity index, don't present this problem. They are named after their viscosity measured at 37.8°C in Second Saybolt Universal (SSU) and the letter S (solvent) or NS (neutral solvent). In this group, the naphthenic base oils can also be found. They have low oxidation stability but good properties at low temperatures.
- **Synthetic oils** are artificial substitutes for mineral oils. They are obtained by chemical synthesis. As a consequence, they have better properties than the natural base oils but are more expensive. The most common synthetic base oils used in the automobile industry are the polyalphaolefines (PAO) which are composed of carbon and hydrogen, and the esters composed of oxygen, carbon and hydrogen.

3.3.2 Lubricant additives

As said before, lubricants must have a good performance in all the lubrication regimes, so additives are added to the base oils to improve its performance. The additives can be present in a lubricant at concentrations ranging from 1 to 30%. Their concentration and chemical nature depend on the lubricant's further use. Additives can act to protect the counter surfaces, to improve the base oil performance and to protect the lubricated surfaces. The most commonly used additives and their classification according to their function is illustrated in Figure 14. The specific function of each additive is described below. A special focus will be made on the mechanism of the tribological active additives.
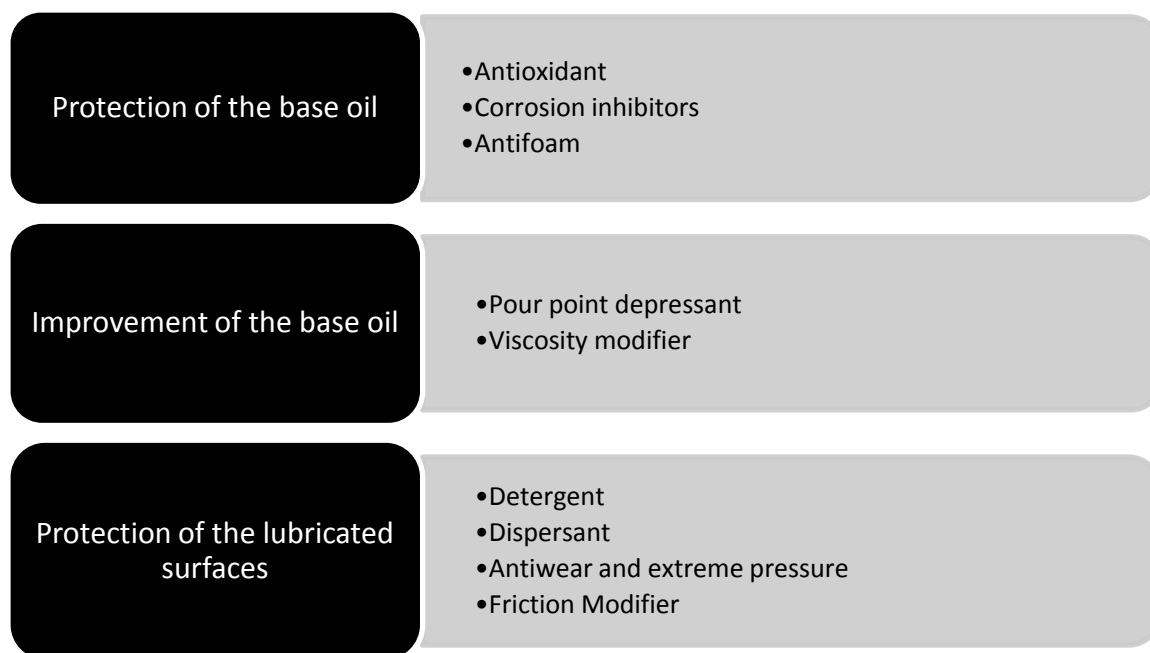
Figure 14. Classification of the additives used in lubrication by the function they accomplish.

- **Antioxidant**

Oxidation leads to oil thickening (increase of the viscosity), sludge and deposit formation and corrosion. Thus the use of antioxidants delays the degradation of the oil that is activated by the presence of air, high temperatures and acids. Antioxidant additives reduce then the oxidation rate of the base oil which determines the useful life of the lubricant. Aromatic amines, sulfur and phosphorous compounds are used as antioxidant additives.

- **Corrosion inhibitors**

These additives protect metal surfaces against chemical attack by the adsorption onto the surface via a high polar group to form a protective film. Some used molecules are amine succinate and alkaline earth surfonates.

- **Pour point depressant**

Polymeric compounds are used to interfere the crystallization process of paraffin present in oil improving the flow properties at low temperatures.

- **Viscosity modifier**

The viscosity modifier additives are used to improve the viscosity temperatures properties of lubricants. High molecular polymers are used to increase the oil viscosity of the oil at high temperatures by steric effect. Poly-alkyl-methacrylate and olefin's copolymer are widely used.

- **Detergents**

Detergents keep the surfaces clean by preventing the formation of carbon-based deposits at high temperature. They have a micellar structure with an alkaline core surrounded by surfactant chains. They can have neutral pH or be overbased in order to neutralize acid compounds which could be generated. Sulfonates, phenates, salicylates and phosphonates are commonly used.

- **Dispersants**

Dispersants are non-metallic or ashless cleaning agents that solubilize and disperse contaminants. They are fully organic compounds with polar head and hydrocarbon tail. Succinimides are the most widely used dispersant.

- **Antifoam**

These additives are used to inhibit foaming caused by dispersants and detergents. Mainly silicon based molecules are used.

- **Anti-wear and extreme pressure**

These additives form a protective film on the surface by chemical reaction. Typical additives contain sulfur and or phosphorus. The most widely used is Zinc dialkyl dithiophsphate (ZDDP).

- **Friction modifiers**

The friction modifiers additives are used to reduce friction between the counter surfaces. Organomolybdenum compounds are the most widely used friction modifier additives. Through chemical reaction they produce a tribofilm on the surface composed of sheets of MoS_2 which allows friction reduction. Molybdenum dithiocarbamate (MoDTC) is the most used organomolybdenum compound used in the automobile industry.

Therefore, the additives with a tribological action are the friction modifiers, the anti-wear and the extreme pressure additives. They are active in the boundary lubrication regime where they can create a tribofilm to protect the surfaces and allow reduction of wear and/or friction. So in this section, the lubrication mechanisms of these additives under severe conditions will be explained.

3.3.2.1 Tribological active additives

3.3.2.1.1 Zinc-dialkyl-dithiophosphate (ZDDP)

Despite the fact that the ZDDP additive has been used as the primary anti-wear additive, it was first used as corrosion and oxidation inhibitor in engine oils (*43*) and it also has extreme-pressure properties (*44*). Its molecular structure is shown in Figure 15.
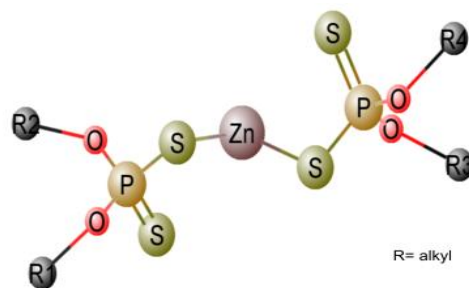
Figure 15. Molecular structure of ZDDP molecule.

When tribo-stressed in a lubricated tribological contact under severe contact conditions, ZDDP molecules form an anti-wear tribofilm on the steel rubbing surfaces which is consumed and regenerated continuously preventing steel/steel contact. Chemical analyses have demonstrated that this tribofilm is mostly composed of amorphous zinc/iron polyphosphates with variable chain lengths with inclusions of ZnS and FeS (*43*). A schematic representation of the tribofilm formed by ZDDP under friction and shear is illustrated in Figure 16.
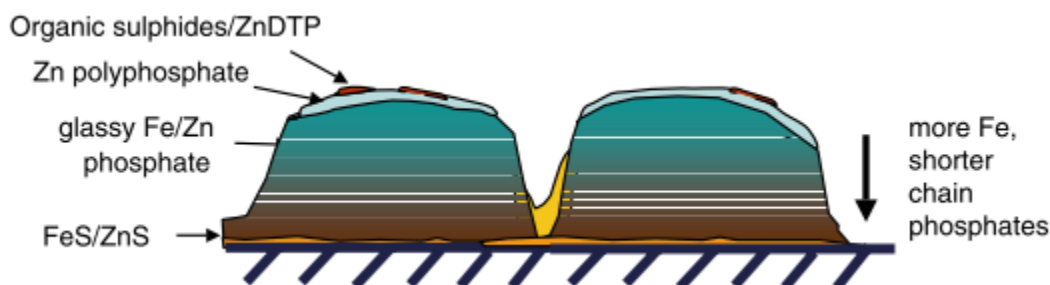
Figure 16. Schematic diagram of the composition of ZDDP tribofilms (*43*).

The anti-wear properties of ZDDP seems to be linked to the ability of phosphate glasses to digest iron oxides that would cause abrasive wear to produce relatively soft iron phosphate (*45, 46*).

With the aim to elucidate the mechanisms of this tribofilm formation research has been done on the reactions of the molecule in the oil and on its adsorption on the surfaces.

3.3.2.1.1.1   Reactions of the molecule in oil

The literature suggests that ZDDP can show different types of chemical behavior in solution: antioxidant activity and thermal degradation.

It has been shown that ZDDP can not only decompose hydroperoxides (*47*) but also peroxy-radicals (*48*) which are at the heart of the hydrocarbon oxidation chain reaction. Additionally, ZDDP can sequester pro

oxidant metal cations like copper, lead and iron in solution that catalyze redox reactions by ligand exchange (*43*). These reasons explain the good anti-oxidant properties that this molecule exhibits.

On the other hand, thermal degradation reactions lead to the formation of zinc phosphates, alkyl sulfides, mercaptans, hydrogen sulfides and olefins (*43, 49*). The temperature of this degradation depends on the alkyl groups and the metal cation but are usually between 130 and 230°C. Coy el al. (*50*) have demonstrated that alkyl groups are transferred to sulfur atoms which explain the large amount of sulfur compounds found after the thermal decomposition of ZDDP molecule suggesting that an O/S exchange took place.

3.3.2.1.1.2   Tribofilm formation

According to Willermet et al. (*51*) different authors agree in the fact that the formation of a tribofilm in steel surfaces happens in a four-step process as follows:

- Step 1: Physisorption of ZDDP molecule on the metallic surfaces.
- Step 2: Reaction of the molecule to form phosphate /phosphothionic moieties chemically bounded to the metal surface.
- Step 3: Formation of phosphate film precursors from the antioxidant reactions of ZDDP
- Step 4: Reaction of the phosphates chains with the zinc-containing compounds.

Armstrong et al. (*52*) have demonstrated that ZDDP molecules adsorb on iron via the sulfur atom of the P=S bond. This adsorption is reversible below 80°C; whereas, above 80°C the absorbed molecules undergo thermo-oxidative decomposition due to the presence of peroxide radicals and oxygen in the oil. As a consequence, the formation of a zinc polyphosphate and polythiophosphate coating occurs on the surface (formation of a chemical tribofilm). Under mild contact conditions, phosphates rather than polyphosphates are formed releasing organosulfur species into the lubricant which under severe conditions react with the steel surfaces to form FeS.

3.3.2.1.1.3   Interaction with other additives

Chemical interaction between ZDDP and detergent additives has been reported in the literature (*53, 54*). Yamaguchi et al. (*54*) studied the boundary film formation by ZDDP and three different detergents (calcium phenate, calcium sulfonate and magnesium sulfonate). The authors found that adding overbased detergents to oils containing ZDDP increases the induction time for tribofilm formation compared to the individual components. Though, the authors don't know if this is due to competitive adsorption, effects of calcium or magnesium carbonate on phosphate glass formation or to phase

relation in the detergent/phosphate glass system. However, no chemical analyses of the tribofilms formed by the different samples were carried out by the authors. On the contrary, chemical analyses done by Wan et al. (*55*) after doing friction tests with an overbased calcium and magnesium salycilate detergents and ZDDP showed that the metallic element from the detergent may have been involved in the surface of the tribofilms. Nevertheless, calcium or magnesium salicylate impedes ZDDP to form a tribofilm and this results in thinner films.

On the other hand, the interaction of ZDDP with MoDTC additive has been investigated by several authors (*56-59*). The addition of MoDTC to ZDDP containing oil decreases friction coefficient due to MoS$_2$ formation in the contact. MoS$_2$ formation mechanism from MoDTC will be discussed in the following section.

To summarize, the anti-wear properties of ZDDP in oil can be explained by the formation of a mechanical protective film that prevents abrasive wear by its capability to remove corrosive peroxides or peroxy-radicals and the ability of phosphate glasses to "digest" iron oxide particles. Chemical interaction with detergent additives and ZDDP is known to happen.

3.3.2.1.2   Molybdenum Dialkyldithiocarbamate (MoDTC)

It has been reported that in the mixed and boundary lubrication regime, MoDTC is able to reduce friction to values around 0.05 when added to a base oil (*57, 60-62*). The effectiveness in friction reduction of MoDTC has been attributed to the formation of MoS$_2$ (*60-62*) single sheets in the contact as the result of complex tribochemical reactions that are not yet fully understood (*63, 64*). Grossiord et al. (*62*) proposed a two-step mechanism (Figure 17): the first phase corresponds to electron transfer on Mo-S chemical bonding leading to the formation of free radicals, while recombination of two radicals and decomposition into MoS$_2$ and MoO$_3$ takes place in the second phase. So, an induction period is needed to produce the chemical reaction.
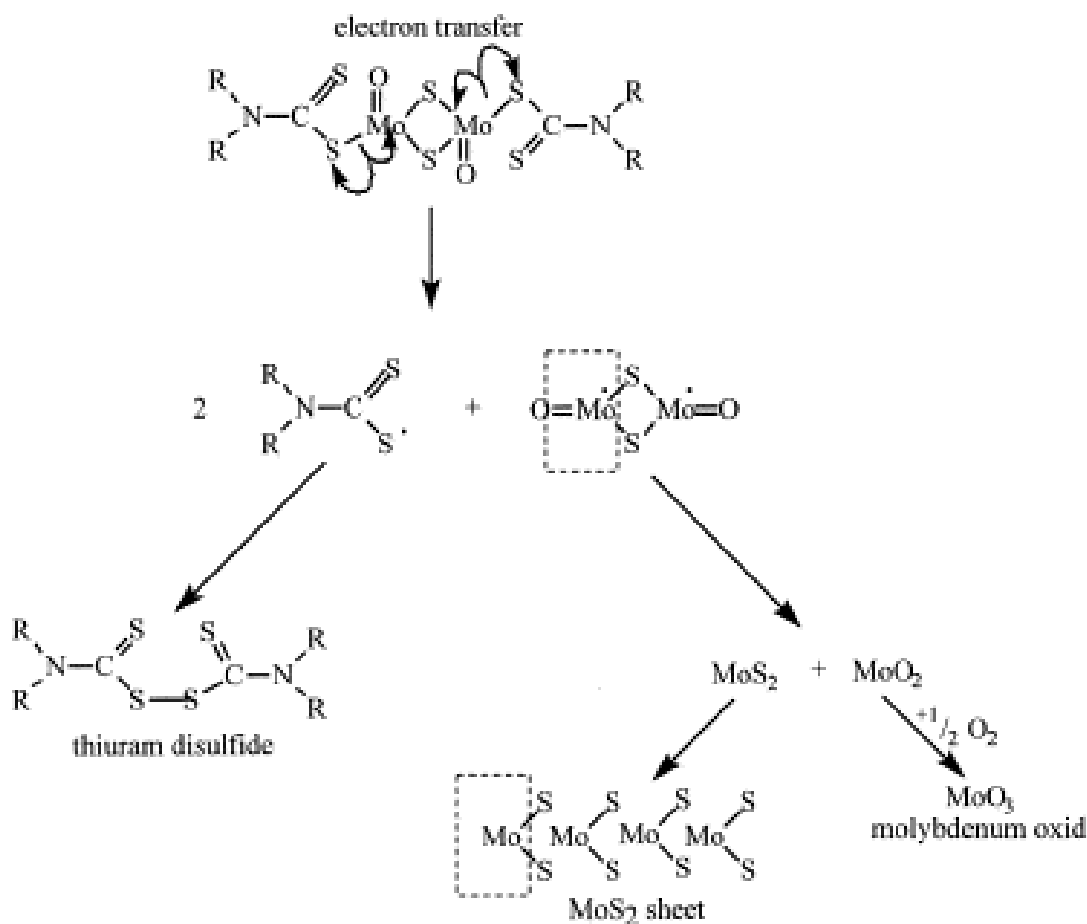
Figure 17. MoS$_2$ chemical process formation from MoDTC (*62*).

The lubricating properties of MoS$_2$ have been attributed to its lamellar structure. Some researchers say that weak van der Waals forces between adjacent lamellar provide easy inter lamellar shear of the structure (*56, 57, 65*). However, Onodera et al. (*66*) found by computational chemistry that the predominant interactions between two sulfur layer in different MoS$_2$ sheets was Coulombic repulsion. Figure 18 shows the lubrication mechanism of MoS$_2$ single sheets proposed by the authors. The electron transfer from nascent Fe substrate to MoS$_2$ increases the sulfur atoms negative charge which increases Coulombic repulsive interaction and makes a much lower friction state. On the other hand, the increment of oxygen content in MoS$_2$ sheets gives a higher friction state due to a decrease of interlayer Coulombic repulsion.
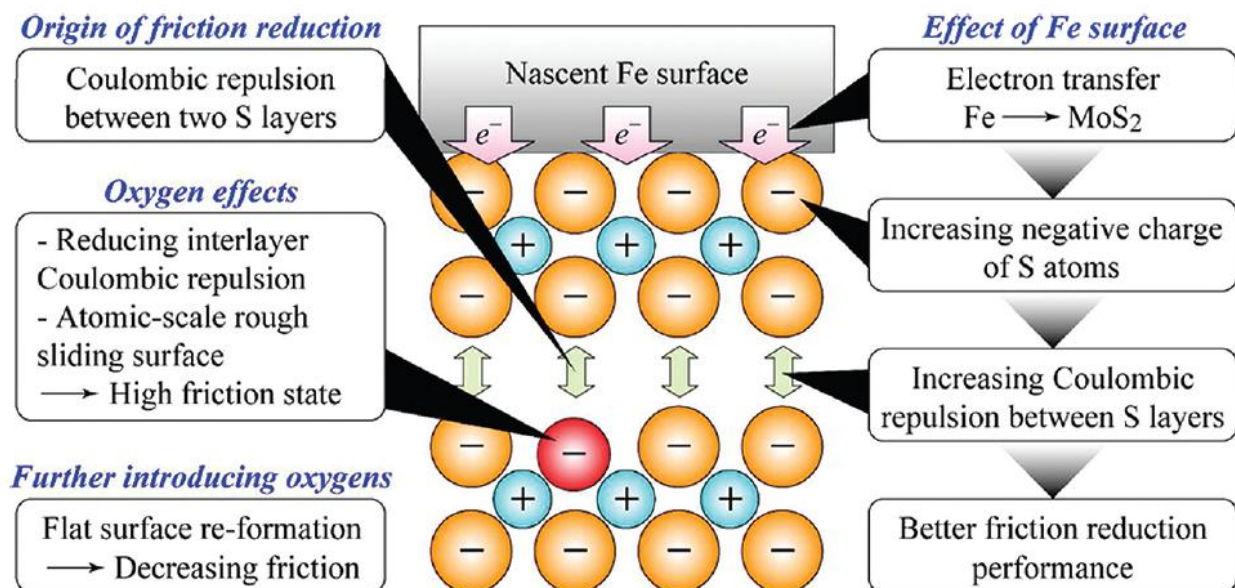
Figure 18. MoS₂ single sheets lubrication schema proposed by Onodera et al. (*66*)

According to the literature (*67*), MoDTC is the most effective in reducing friction at a combination of high additive concentration (up to 0.4 wt%) and high temperature (higher than 60°C).

The tribological additives used nowadays not only need to be activated but are also known to have a detrimental effect on sensitive exhaust emission systems. This is due to the presence of sulfur and phosphorous that poisons the catalytic converters in cars. Hence, research in energy efficiency to decrease friction losses and the reduction of emissions is directly linked to the modification or substitution of these additives which act mainly under the boundary lubrication regime. Ionic liquids, organic friction modifiers and nanoparticles have been widely studied during the last few years as possible candidates to replace the molecules used nowadays. This work will focus on nanoparticles and their lubricating properties for their use in the automotive industry.

3.4   Nanoparticles as lubricant additives

The advent of nanotechnology has allowed the synthesis of nanoparticles of different materials that can be used in different applications. In tribology, researchers have explored the possibility of using nanoparticles as lubricant additives to reduce friction and wear.

It was first believed that nanoparticles could act as small ball-bearings between the sliding surfaces (*68*). As a consequence, carbon based nanoparticles and nanotubes (NT) (*69-71*), as well as other nano chemical compounds like Cu (*72*), ZnO (*73*), TIO₂ (*74*), NiMoO₂S₂ (*75*), Zn (*76*), among others have been studied during the last decades. However, special interest has been paid on metal diacolgenides

nanomaterials like MoS_2 and WS_2 due to their layered structure. Analyses made by Joly-Pottuz et al. (*77*) on steel-worn surfaces lubricated by IF-WS_2 nanoparticles in PAO under the boundary lubrication regime and at room temperature, revealed the presence of WS_2 sheets. Based on this observation, the author proposed an exfoliation mechanism of IF nanoparticles governed by morphological changes caused by pressure and shear stress. The fact that these nanoparticles are able to provide sheets of the material into the contact that provides a lamellar lubrication may explain why both friction and wear reduction are obtained for this kind of nanoparticles whereas other nanoparticles don't give similar results.

This review covers most of the relevant work related to the use of nanoparticles of MoS_2 and WS_2 fullerene like nanoparticles and nanotubes as lubricant additives. The majority of the research done until now concern steel surfaces. However the few results found for diamond-like coatings will be also presented here.

3.4.1 Metal dichalcogenides nanoparticles. State of art

Metal dichalcogenides are materials with the formula MX_2, where M is a transition metal from groups IV-VI, while X is a chalcogen atom (S, Se or Te). These materials have an anisotropic layered structure of the form X-M-X with the chalcogen atoms in two hexagonal planes separated by a plane of metal atoms as illustrated in Figure 19. The overall symmetry can be hexagonal or rhombohedral, and the metal atoms have octahedral or trigonal prismatic coordination (*78*). These material exhibit electronic properties, ranging from metallic to semiconductors (*78, 79*). Metal dichalcogenides, like MoS_2 and WS_2 have been extensively studied and used for a long time as solid lubricants (*80*). Strong covalent forces bond sulfur and metal atoms within a lamella, while adjacent lamellae interact through weak van der Waals forces which facilitates easy inter lamellar shear of the structure. The interlayer spacing is 0.62nm (*81*). However, their use in liquid lubricants had never been considered until they were synthetized in a nanoscale.
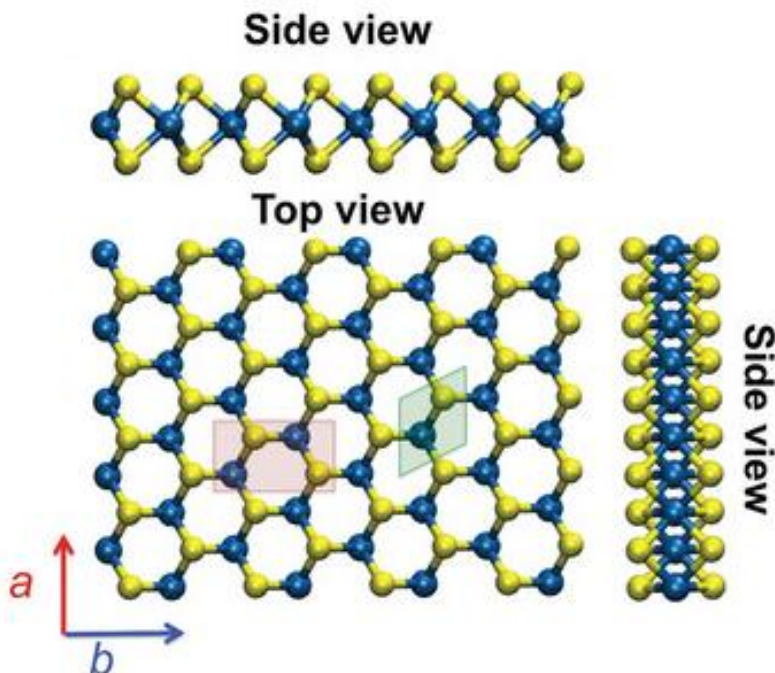
Figure 19. Atomic structure of MX$_2$ materials (*79*).

The synthesis of inorganic fullerene (IF) nanoparticles and nanotubes (NT) of WS$_2$ was done for the first time by Tenne et al. (*82*) in 1992. Concentric polyhedral and cylindrical structures (IF) with a ranging size from 10 to 100 nm were obtained after heating a thin tungsten film in an atmosphere of hydrogen sulfide. A year later, the same research group, was able to synthetize IF-MoS$_2$ nanoparticles for the first time after oxidation of a molybdenum thin layer and further exposure to a stream of H$_2$S and N$_2$/H$_2$ mixture (*83*). Improvement in the synthesis techniques have permitted to control nanoparticles size, shape and crystallinity. This has made their synthesis scale-up possible and now they are commercialized worldwide by companies specialized in nanotechnologies.

Since the synthesis of the first nanoparticles at the lab-scale in 1992, research on their lubrication properties has been done. Special interest has been paid to IF nanoparticles because tribologists believed that their closed-caged structure made them chemically more stable than NT, and allowed them to roll in the contact surface as small bearings (*68*). Consequently, studies have been mainly made for this kind of nanoparticles in the boundary lubrication regime where the rolling effect could allow them to protect the counter surfaces and decrease the friction coefficient. Nonetheless, research has demonstrated that exfoliation of the nanoparticles takes place in the contact under pressure and shear at room temperature (*77, 84-87*). The IF nanoparticles lubrication mechanism is represented in Figure 20.
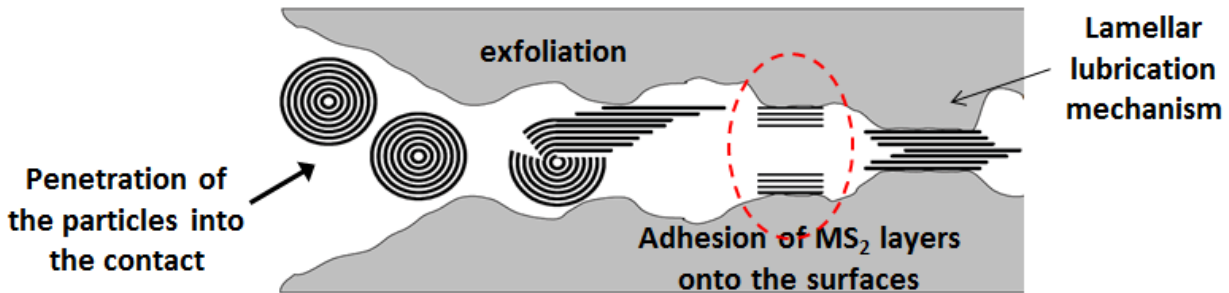
Figure 20. Lubrication mechanism of the MS$_2$ fullerene like nanoparticles in a steel/steel contact.

The tribologist have demonstrated that nanoparticles are able not only to decrease the friction coefficient until 70% compared to the base oil, but that they also have interesting anti-wear properties in the boundary lubrication regime (*77, 88*). In the hydrodynamic lubrication regime, they have actually proven to have non detrimental effect in the on steel surfaces (*65, 71, 77, 84, 85, 89-92*). Additionally, their friction modifier and anti-wear properties has not only been proven in liquid lubricants when added to synthetic (*77, 93*), mineral (*94-96*) and natural base oils (*97-99*), but also in greases (*100*)

With the aim to elucidate the action mechanism of IF nanoparticles, the researchers have studied their behavior under different contact conditions. The main results for fullerene like nanoparticles are presented below.

3.4.1.1 *Nanoparticles concentration in oil*

Joly-Pottuz et al.(*77*) have studied the effect of IF-WS$_2$ nanoparticles concentration in PAO base oil at room temperature under the boundary lubrication regime. They found that the increase in the nanoparticles concentration produced a decrease in the coefficient of friction and that even at very low concentration (0.1wt %) the nanoparticles exhibited a significantly positive effect compared to PAO base oil alone. However, above 1wt% the authors claim that the value of the friction coefficient settles and no further reduction is observed as illustrated in Figure 21. The same behavior was observed by the same research group for IF-MoS$_2$ nanoparticles in base oil (*101*).

These results agree with those found by Hu et al. (*95*) for hollow nanoparticles of MoS$_2$ in liquid paraffin; they stated that the optimal concentration was 1.5 wt% not only for the best results in the friction coefficient but also on wear reduction. The authors claim that at higher concentrations the probability for collisions between the nanoparticles would be increased producing their agglomeration and resulting in a negative impact on their tribological performance.
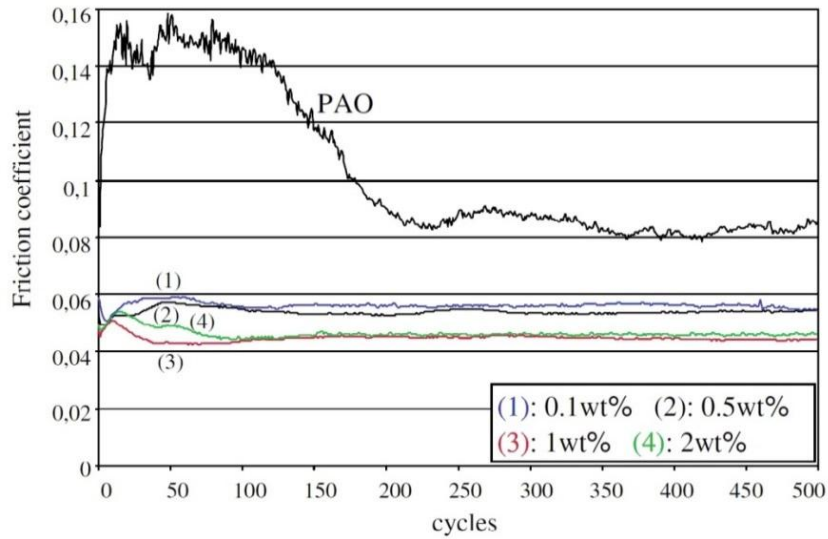
Figure 21.Influence of IF-WS$_2$ concentration in PAO on the friction coefficient (*77*).

3.4.1.2 *Contact pressure effect*

Joly-Pottuz et al. (*77*) have studied the effect of the contact pressure on the tribological properties of IF-WS$_2$ nanoparticles in a PAO base oil at room temperature in the boundary lubrication regime. The increase of the contact pressure from 330MPa to 830MPa gave a diminution of the friction coefficient as illustrated in Figure 22. Further increase of the contact pressure above 830MPa did not have significant effect on the friction coefficient. They led to the conclusion that a critical limit pressure needed to be reached to cause structural modification of the nanoparticles into sheets to obtain low friction coefficients. The authors found that a low and stable friction coefficient is obtained since the very first cycles for all the particle concentrations tested.
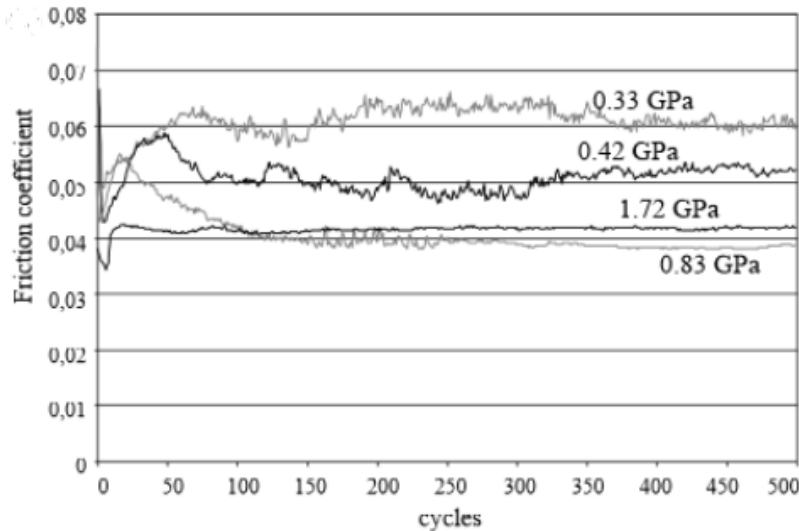
Figure 22. Influence of contact pressure in the friction coefficient for IF-WS$_2$ in PAO (*77*).

Later, in 2009, Rosentsveig et al. (*102*) observed the same behavior for IF-MoS$_2$ nanoparticles in PAO under the same lubrication regime. Additionally, the nanoparticles exhibited to have anti-wear properties and to be effective since the beginning of the test. The authors claim that an exfoliation mechanism is in the origin of the decrease in the friction coefficient and in the wear performance. Such exfoliation process was observed *in situ* by TEM imaging in 2012 by Lahouij et al.(*86, 87*) proving that the authors hypothesis was right.

3.4.1.3   *Temperature Effect*

The influence of temperature on the tribological performances of IF-MoS$_2$ nanoparticles has been studied by Joly-Pottuz et al. (*90*). They compared the friction coefficient of these nanoparticles blended at a concentration of 1wt% in PAO base oil at 20°C and at 70°C. Their results showed a high and unstable friction coefficient at 70°C while good results were seen at 20°C as illustrated in Figure 23. They explain these results by the fact that at high temperature the particles tend to agglomerate more. They claim that a dispersant able to avoid this undesired agglomeration is needed for the use of nanoparticles at high temperature.
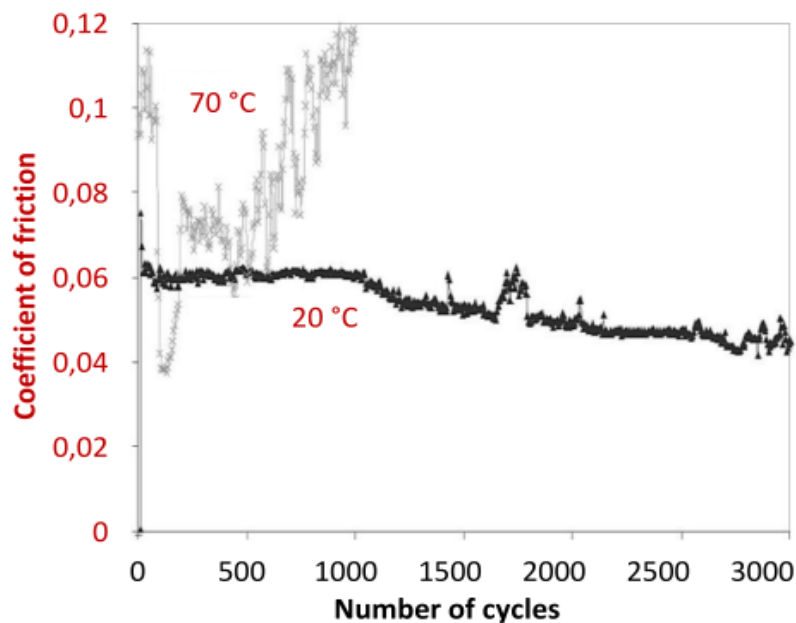
Figure 23. Temperature effect on the friction coefficient for IF-MoS$_2$ nanoparticles (*90*).

In contrast, Ratoi et al. (*103*) observed good tribological response when using sheets of 2H-WS$_2$ nanoparticles in PAO at 100°C. The tests were carried out on a mini traction machine (MTM) which combines sliding and rolling. After characterization of the tribofilm formed on the steel surface made by XPS etching and SIMS, the authors concluded that the tribofilm is formed of several layers as illustrated in Figure 24. They claim that the presence of tungsten in the tribofilm explains the excellent mechanical and anti-wear properties and that the squashed WS$_2$ nanoparticles are responsible of the friction reduction.
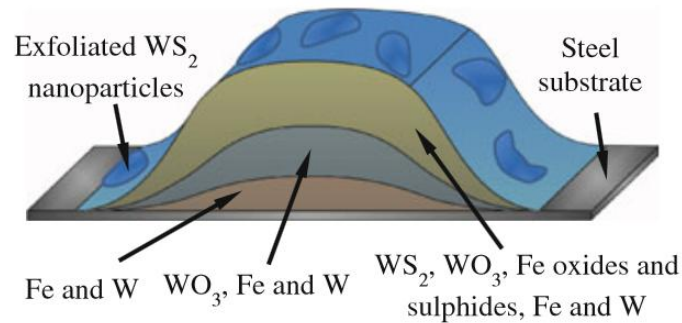
Figure 24. Composition of the tribofilm generated by WS$_2$ NP in PAO oil at 100°C proposed by Ratoi et al. (*103*).

More recently, in 2014, Rabaso et al. (*104*) studied the friction performance of PAO base oil with and without IF-MoS$_2$ nanoparticles at 80°C using a HFRR (High Frequency Reciprocating Rig) under the boundary lubrication regime. Their results showed that MoS$_2$ fullerene like nanoparticles were able to reduce friction coefficient by almost 70% compared to the base oil as shown in Figure 25.
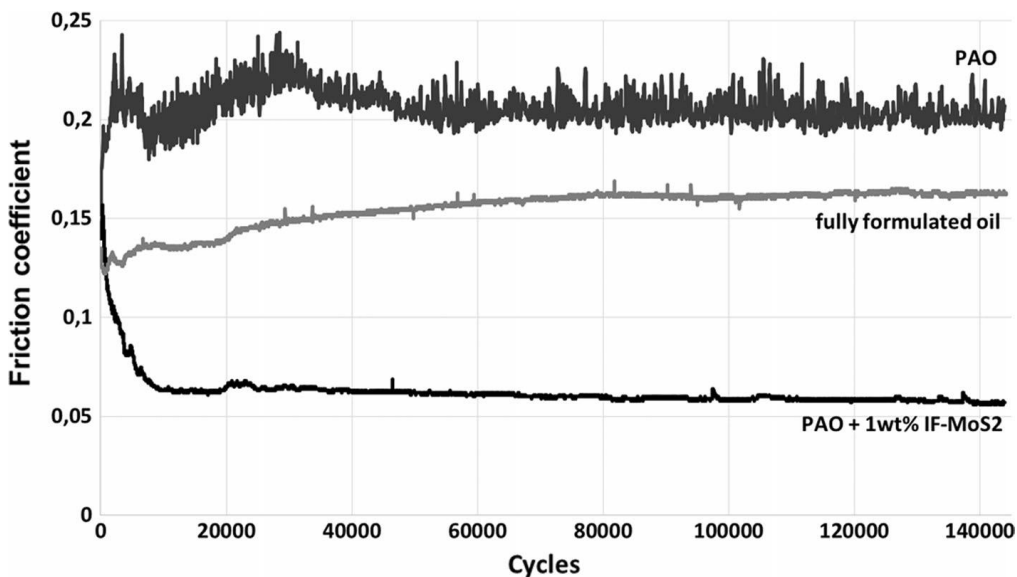
Figure 25. Friction coefficient of IF-MoS$_2$ nanoparticles in PAO and in a fully formulated oil at 80°C (*104*).

The results obtained under high temperatures seem somehow contradictory. However, the nanoparticles can be more easily fed to the contact zone in a MTM machine by the fact that there is not only sliding between the surfaces but also rolling of the upper surface against the other one which can explain the difference on the results presented here for the WS_2 nanoparticles. On the other hand, the differences obtained for the IF-MoS_2 nanoparticles is much more difficult to understand. Nevertheless either differences on the test conditions or differences on the nanoparticles due to their structure may be responsible for this. As a matter of fact, higher speeds were used for the test carried out by the first research group (where no friction reduction was observed with the nanoparticles) than the other study. It is possible to think that nanoparticles can be pushed out of the contact because of the speed. Additionally, if the nanoparticles are not well dispersed they would have difficulties to reach the contact zone.

3.4.1.4   Effect of the dispersion of the nanoparticles

It is a known fact that nanoparticles tend to agglomerate. Researchers have observed that WS_2 seems to agglomerate more than MoS_2 (*92*). As a consequence, Moshkovith et al. (*105*) studied the sedimentation of IF-WS_2 aggregates and their influence in the reproducibility of the tribological data. The authors carried out experiments with IF-WS_2 nanoparticles in paraffin oil and studied the influence of the mixing time on the size and distribution of the nanoparticles and their tribological performance. It was found that the reproducibility of the results was determinate by the size of the IF aggregates and that the fraction of small aggregates increased with longer mixing time giving lower friction coefficients.

3.4.1.4.1   Dispersion alternatives

In order to face the dispersion problem different solutions have been proposed. The results of the research done on this are shown below.

3.4.1.4.1.1   Doped nanoparticles

By the partial replacement of Molybdenum or Tungsten atoms by Rhenium atoms which act as electron donors, the nanoparticles would be negatively charged repelling each other. This would reduce their tendency to agglomerate. As a consequence, Rappoport et al. (*106, 107*) and Yadgarov et al. (*107*) have tribologically tested Rhenium doped IF-MoS_2 nanoparticles and compared the results to undoped IF and 2H nanoparticles under the same test conditions. The doped nanoparticles did exhibited reduced

agglomeration producing stable suspensions in PAO base oil. The tribological results showed a better wear rate and friction coefficient reduction for these doped nanoparticles than for the un-doped ones. As a matter of fact, the authors claim that the un-doped nanoparticles reduced friction coefficient by 40% compared to the PAO base oil, whereas a reduction of 80% was seen for the doped particles as illustrated in Figure 26. The authors attributed this to the improved dispersion of the Re doped particles and to the increased conductivity of the formed tribofilm by those particles which should decrease the effects of tribocharging at the surface.
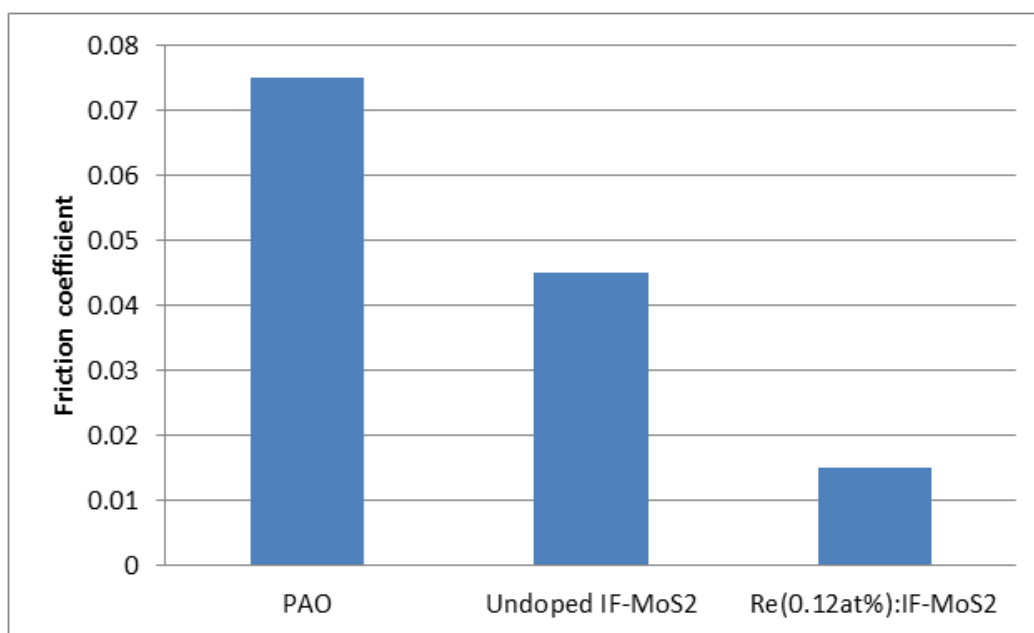
Figure 26. Friction coefficient for PAO alone, MoS$_2$ in PAO and Rhenium doped nanoparticles in PAO oil (*106, 107*).

3.4.1.4.1.2   Addition of a dispersant

Other solution to face this problem is to improve the stability of the particles by surface modification with organic molecules.

Sahoo et al. (*108*) demonstrated that polyisobuttylene succinimide (PIBS) which is commonly used as dispersant in lubricants is able to decrease the size of the agglomerates of MoS$_2$ in hexadecane. However, the friction coefficient obtained for the sample containing PIBS was the same than for the agglomerated MoS$_2$. More recently, Rabaso et al. (*104*) have also demonstrated that succinimide-based dispersants have a detrimental effect on the tribological performance of IF-MoS$_2$ nanoparticles as it can be seen in Figure 27. Their investigation has shown that nanoparticles do exfoliate in the presence of the dispersant additive but that the liberated nanoparticle sheets cannot form a tribofilm on the steel surfaces when the dispersant concentration is between 0.5 wt% and 0.5 w %. The authors have shown that the use of this dispersant in a concentration of 0.05% would allow dispersing the nanoparticles and finding the good tribological performance of the nanoparticles after a running-in period. However,

dispersants are used in higher concentrations in commercial lubricants so it seems that the use of succinimide-based dispersants is not suitable for nanoparticles-containing lubricants.
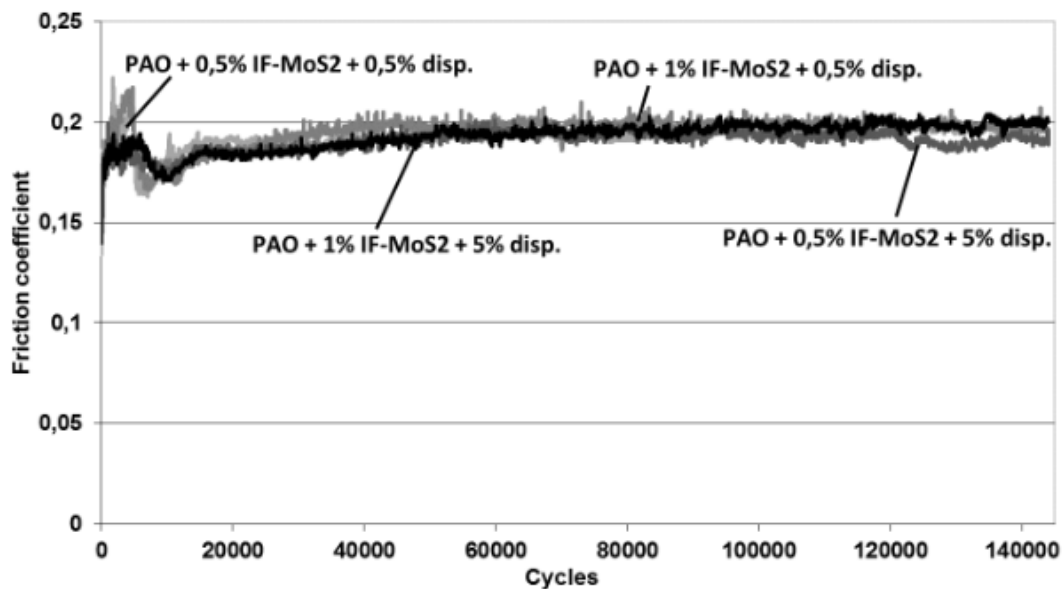
Figure 27. Tribological response of a PAO base oil containing various concentrations of IF-MoS$_2$ and succinimide-based dispersants (104).

As a consequence, Aralihalli et al. (109) have studied the tribological performance of MoS$_2$ nanoparticles in base oil in the presence of different surfactants. The dispersants used were:

- Aminopropyl trimethoxy silane (ATS) which is a methoxy silane with one amine functional group
- Sorbital monoleate (SPAN 80) which is an oxygen-based polymeric dispersant with three –OH groups and one furan ring
- Octadecyltrimethoxysilane (OTS) that is a long chain HC with a methoxy silane head group
- Perfluorodecyltriethoxysilane (PTS) is a long chain hydrofluorocarbon with an ethoxy silane head group
- Perfluorooctyltrichlorosilane (PTCS) which is a long chain hydrofluorocarbon with a chloro silane head group.

The lowest friction coefficients were exhibited by the mixtures containing ATS and SPAN as illustrated in Figure 28 . Actually, the measured particle size of MoS$_2$ was smaller when these additives were used compared to the others. The authors claim that the molecules of the ATS and SPAN remain strongly grafted to the particles preventing agglomeration even under shear stress which seems not to be the case for the others additives. They say that the amine group can bind covalently the molecules of ATS to MoS$_2$ while the hydrogen of the -OH group combines with sulfur atom of MoS$_2$.

The difference between ATS and PIBS is actually that the amine of the first one is a free amine which can be expected to be able to bind with metals.
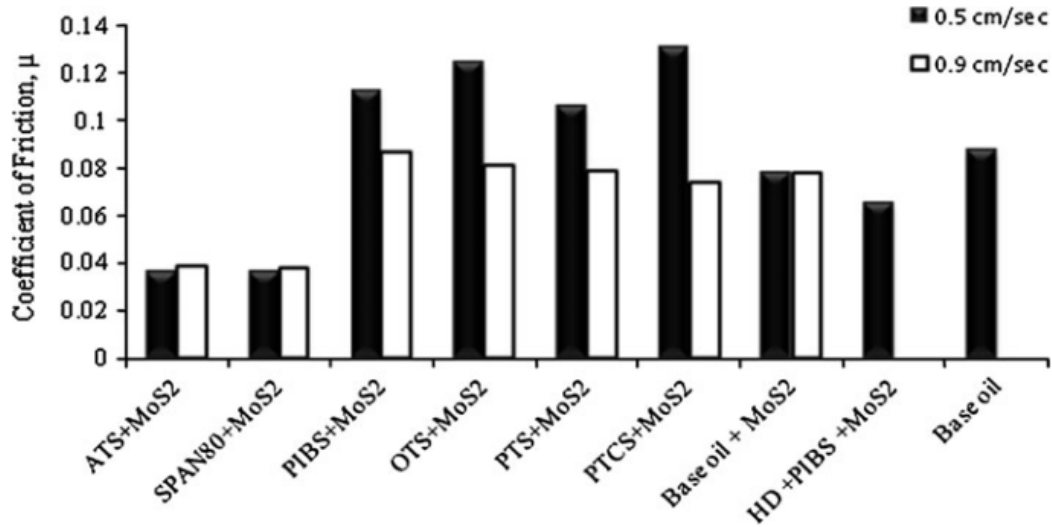
Figure 28. Friction coefficient of MoS₂ nanoparticles suspended in oil using different dispersants (*109*).

3.4.1.4.1.3 Coatings

Other possible solution for the dispersion problem is to use the nanoparticles not in the lubricant but as a coating on the counter surfaces.

The research work done by Cho et al. (*110*) evaluated the tribological properties of gray cast iron surfaces with and without a MoS₂ nanoparticles coating lubricated with either mineral oil or IF-MoS₂ nanoparticles in mineral oil. Their results showed (Figure 29) a diminution of around 35% for the MoS₂ coated surface compared to the non-coated lubricated with mineral oil. Nevertheless, the friction coefficient obtained for the uncoated surface lubricated with mineral oil blended with the nanoparticles exhibited a reduction of the friction coefficient of around 75% compared to the mineral oil alone. The best performance was seen for the coated surface using the nanoparticles additivated oil. Their results show that nanoparticles used as lubricant additives outperform coatings even is some beneficial effect is seen for the coating.
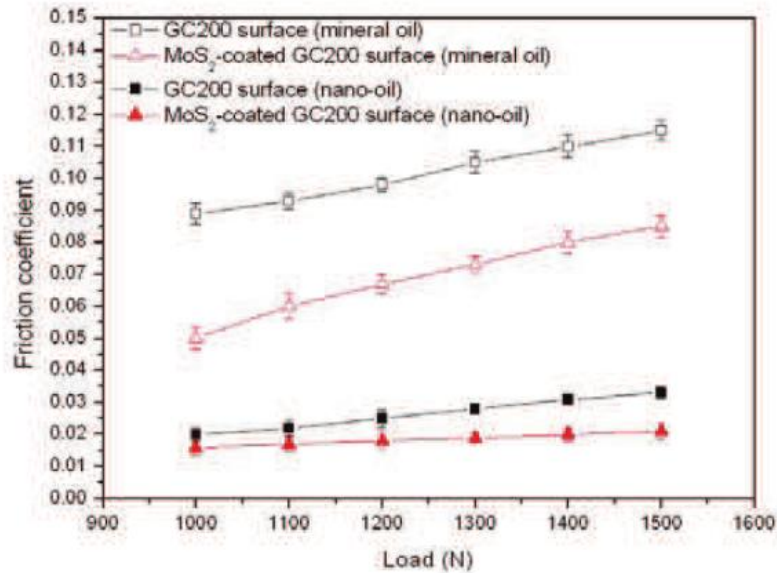
Figure 29. Friction coefficient of MoS₂ doped and un-doped gray cast iron surfaces lubricated with mineral oil and nanoparticles containing oil (*110*).

3.4.1.5 *Particle shape, size and crystallinity*

The influence of the particle size, shape and crystallinity on the tribological performance of nanoparticles has been studied by some authors. The main results of their research is shown in this part of this work.

3.4.1.5.1 Shape

Despite the fact that research has been mainly made for IF nanoparticles, some data can be found for NT of metal diacholgenides. Results of the research work done by Kogovsek et al. (*92*) with nanotubes and fullerene like WS₂ and MoS₂ nanoparticles indicate that the same reduction in the friction coefficient is obtained when using any of these two shapes as illustrated in Figure 30. A reduction of 55-60% in the friction coefficient was observed for both shapes of MoS₂ nanoparticles whereas 35-40% reduction was seen for both WS₂ shapes. The authors concluded that exfoliation of NT and IF is the main mechanism in their tribological behavior.

As a matter of fact, Jelenc et al. (*111*) have observed by Atomic Force Microscopy (AFM) the sliding of a MoS₂ nanotube while they were measuring its friction coefficient under ultra-high vacuum which was reported to be 0.023. NT exfoliation or fracture into individual layers has been seen under high loads by molecular dynamics simulations performed by Stefanov et al. (*112*). The authors claim that the exfoliation process forms what they called "a local nanocoating" based on MoS₂ platelets responsible for friction reduction.
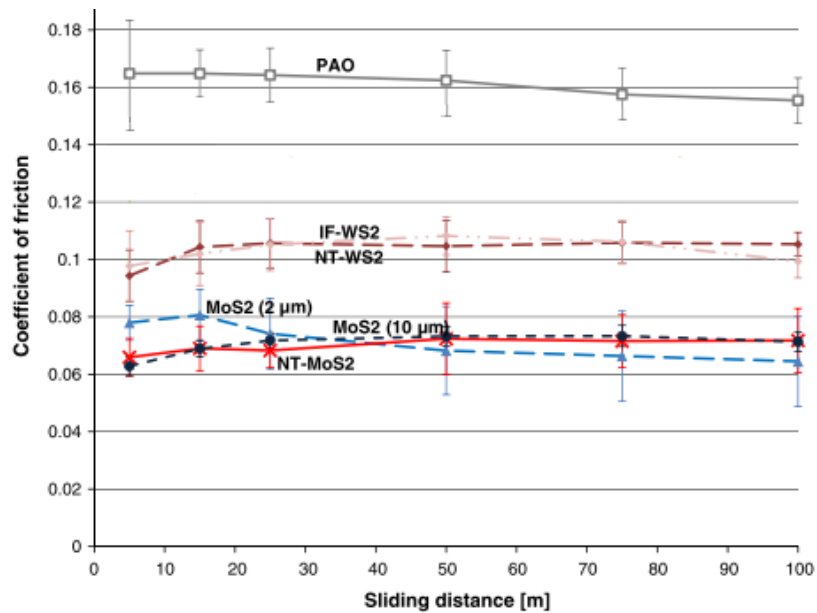
Figure 30. Friction coefficient of WS$_2$ and MoS$_2$ nanotubes and fullerene like nanoparticles in PAO base oil (*92*).

The research work done by Hu et al. (*95*) with hollow nanoparticles of MoS$_2$ (nanoballs) and nano-slices of the same material, showed that the first ones have a better performance than the last ones. This was attributed to the chemical stability of the hollow nanoparticles against oxidation as it was shown by chemical analyses.

All these results seems to suggest that the same friction reduction can be obtained for nanoparticles of different shapes on condition that the chemical structure does not change.

3.4.1.5.2   Size

3.4.1.5.2.1   Micro vs nano scale

Huang et al. (*96*) compared the tribological performance of IF-MoS$_2$ nanoparticles and 2H-MoS$_2$ platelets (average size: 0.5 µm) in oil in the boundary lubrication regime using a contact pressure of 1,6 GPa. The lowest values of the friction coefficient were obtained for the nanoparticles as illustrated in Figure 31. Wear reduction was also better for the IF-MoS$_2$ nanoparticles. Other authors agree on the fact that the fullerene nanoparticles provide a greater reduction in friction and wear than the 2H platelets (*90, 95, 101, 113-115*) which is attributed to their smaller size which would allow them entry easily the contact zone.
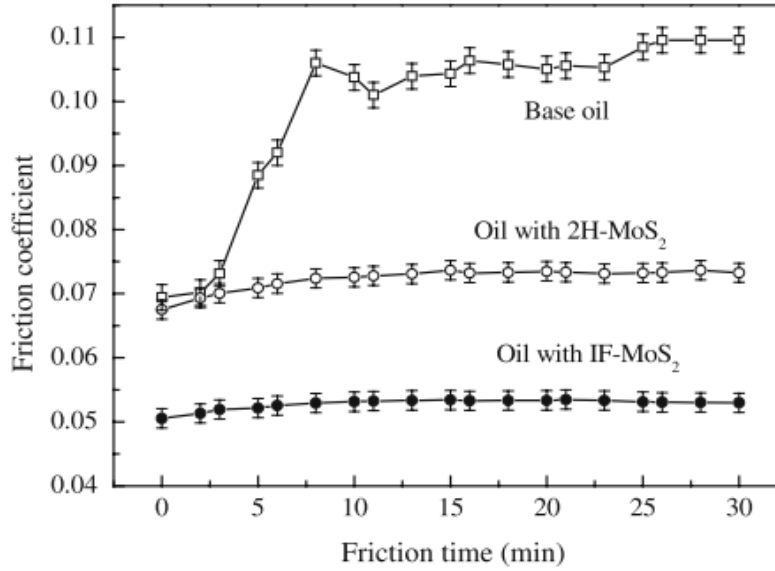
Figure 31. Evolution of the friction coefficient of IF-MoS$_2$, IF-WS$_2$ and platelets of 2H-MoS$_2$ in PAO (*96*).

3.4.1.5.2.2   Nano scale

The research work done by Njiwa et al. (*116*) with IF-MoS$_2$ nanoparticles of different sizes have shown that lower friction coefficients are obtained for nanoparticles of 50-60 nm size (Mo/Zn=2 and 5) compared to nanoparticles of more than 100 nm (Mo/Zn=10) as illustrated on Figure 32. The same conclusion was reached by Rosentsveig et al. (*102*) after comparing the results obtained for IF-WS$_2$ to those of IF-MoS$_2$, where lower friction coefficient (0.04) was obtained for the molybdenum particles (50-80nm) which were smaller than the tungsten ones (80-140nm).
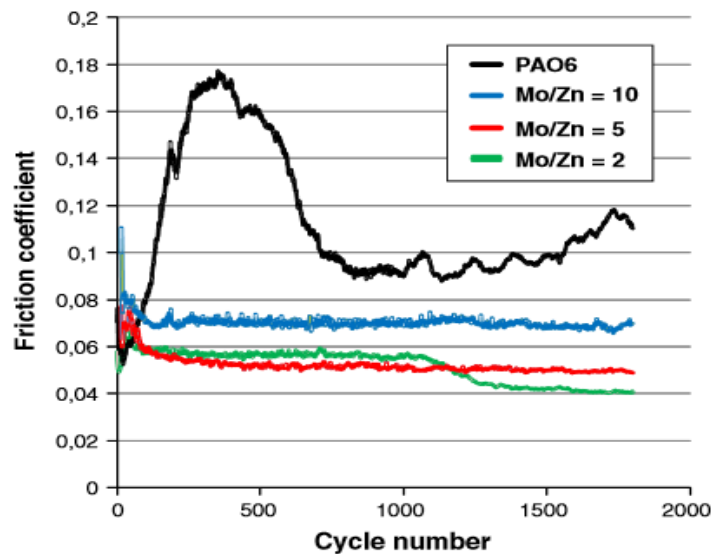
Figure 32. Friction coefficient of IF-MoS$_2$ nanoparticles of different size in PAO6 (*116*).

3.4.1.5.3 Crystallinity

Tannous et al. (*117*) studied the performance of IF WS_2, MoS_2 and of $Mo_xW_{1-x}S_2$ nanoparticles in PAO under the boundary lubrication regime. Their results are somehow difficult to compare because change in the molecule stoichiometry led to a variation of the particle size and its crystallinity which also affects the tribological performance. However, the authors claim that the large number of defects present in the MoS_2 nanoparticles tested led to an easy exfoliation of the nanoparticle's sheets which served as a third body and provided easy shear between the metallic surfaces.

More recently, Lahouij et al. (*84*) carried out experiments with very well crystallized and poorly crystalized IF-MoS_2 nanoparticles and obtained better results for the poorly crystallized ones as illustrated in Figure 33. Chemical characterization of the particles after the friction tests showed that the poorly crystallized ones were strongly damaged in comparison with the well crystallized. These results are in agreement with those obtained by Njiwa et al. (*116*) for the same kind of IF nanoparticles. Chemical characterization of the formed tribofilm made by the first research group, showed a more homogenous tribofilm on the metal surface for the poorly crystallized nanoparticles, mainly composed of MoS_2 layers, while a more discontinuous tribofilm was seen for the other nanoparticles. The authors attributed these results to an easier delamination of the poorly crystallized nanoparticles by the defects present in their structure.
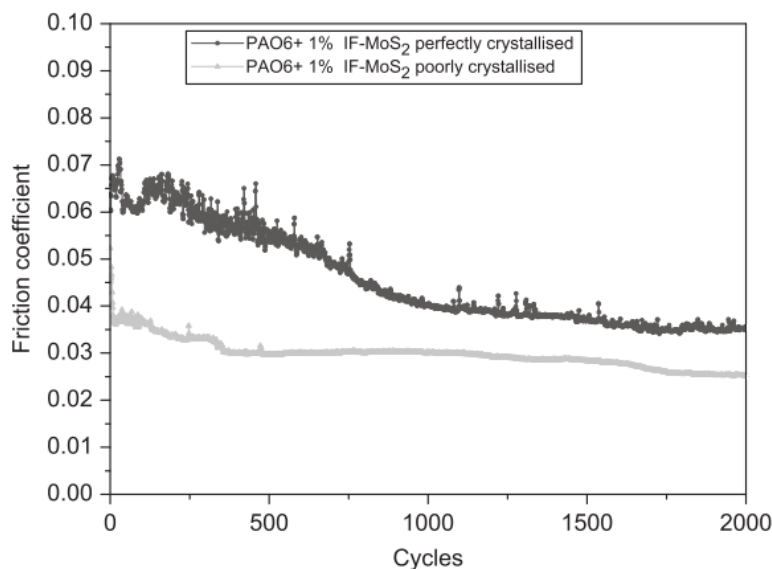
Figure 33. Tribological reponse of perfectly crystallised and poorly crystallised IF-MoS_2 nanoparticles (*84*).

Latter, Lahouij et al. (*86, 87*) demonstrated, by in-situ observation using transmission electron microscopy, that well crystallized nanoparticles are able to roll and slide under the effect of shear stress and pressure, whereas the poorly crystallized nanoparticles exfoliate immediately under the same conditions Experimental work and molecular dynamics simulations done by the same research group

have also demonstrated that hollow fullerene like nanoparticles exfoliate more easily than well crystallized nanoparticles (*85*).

These results allowed elucidating the lubrication mechanisms at room temperature of the nanoparticles and their tribological properties at the macro-scale, proving that their lubrication mechanisms are directly linked to their intrinsic characteristics.

As a conclusion, tribologists agree that better results are obtained when using nanoparticles instead of 2H platelets. Additionally, as published by Tannous et al. (*117*) in 2009, the lowest friction coefficients can be obtained with small and poorly crystallized IF nanoparticles.

3.4.1.6 *Influence of the surface roughness*

The majority of the research work done until now has been carried out with smooth surfaces. However, surfaces used in industry are rougher that those used in the laboratory. Thus, the industrial use of the nanoparticles involves research on their behavior on rough surfaces.

Consequently, Kogovsek et al. (*91*) studied in 2013, the influence of surface roughness on the lubrication behavior of NT-MoS$_2$ in PAO base oil on steel surfaces. They carried out their experiments on smooth (Ra=6nm) and on rough (Ra=40nm) surfaces using a MTM. Their results showed that regardless the roughness of the samples the same value of the friction coefficient is obtained when using the nanoparticles in all the lubrication regimes as illustrated in Figure 34. On the other hand, the results for the base oil alone exhibited a higher friction coefficient for the rough samples than for the smooth ones. The authors state that the MoS$_2$ tribofilm that is formed on the steel surfaces completely governs the friction coefficient.
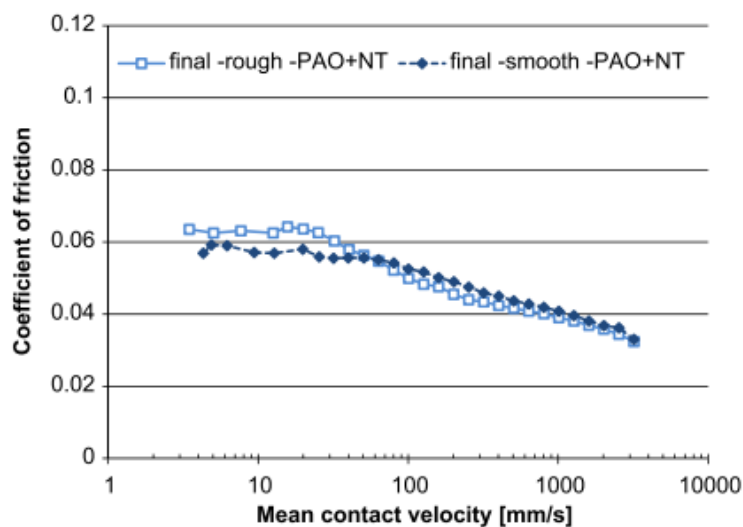
Figure 34. Influence of the surface roughness in the tribological behavior of NT-MoS$_2$ (*91*).

The same research group has also evaluated the influence of the surface roughness for diamond like carbon (DLC) coatings when using NT-MoS$_2$ in PAO (*93*). Their results are shown in section 3.4.1.7.

3.4.1.7 Influence of the surface material

The use of Diamond-like coatings (DLC) in the automobile industry is becoming more frequent. They are used on some parts of the engine as shown in Figure 35, and in some cases (Nascar and Formula 1) we can find them on the entire engine.
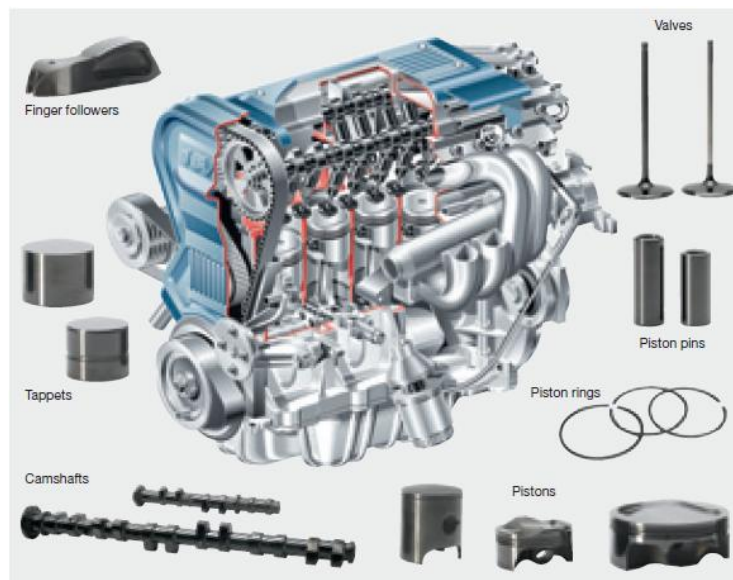
Figure 35. DLC coating on various engine components (source: Sulzer Group)

As a consequence, Kalin et al. (*118*) decided to study the effect of nanoparticles on this kind of surfaces. For this, samples containing NT-MoS$_2$ in PAO were tested on non-doped amorphous hydrogenated DLC coating (a-C:H). The results were compared to those obtained for steel surfaces. A reduction on the friction coefficient was observed for both surfaces but the lowest value was obtained for DLC as illustrated in Figure 36. However, chemical analyses revealed that the main difference between the two surfaces was the extent to which the MoS$_2$ based tribofilm covered the surface. The surface was twice more covered for the steel surface than for the DLC one (*119*). The authors claim this is clear evidence that the action mechanism is predominately physical and not chemical.
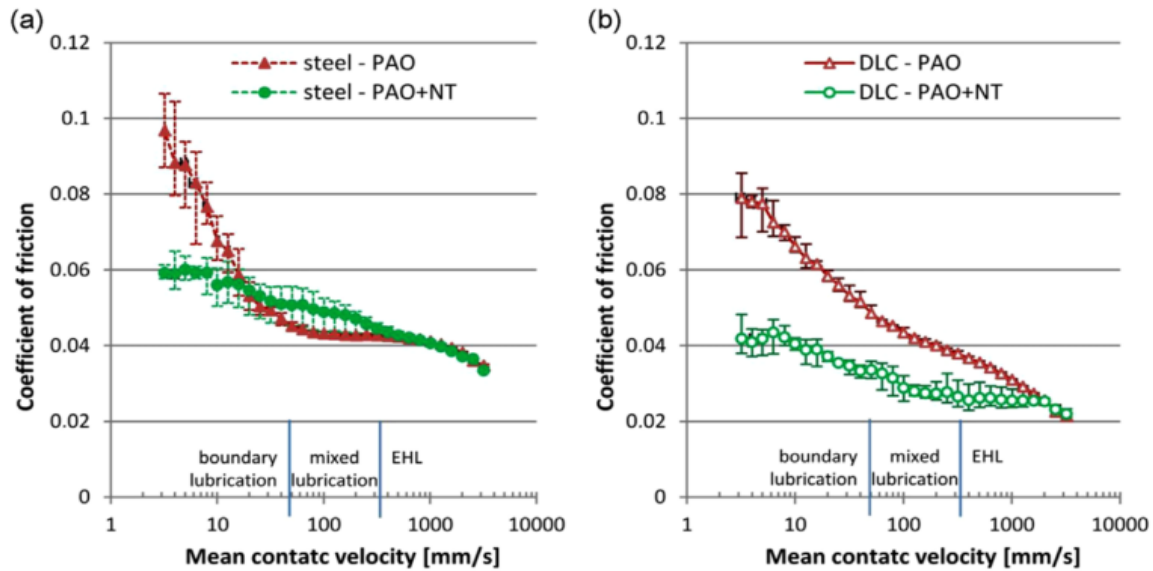
Figure 36. Friction coefficient on a) steel and b) DLC surfaces lubricated with PAO base oil and base oil with MoS₂ nanotubes
(*118*).

The same research group has also studied the influence of the DLC coating surface roughness when using NT-MoS$_2$ in PAO (*93*) and found surprisingly that lower friction coefficients are obtained for smooth surfaces than for the rough ones. However, long-duration tests showed a detrimental effect on the tribological performance of the NT on both surfaces but more important for the smooth ones. The authors claim that in the rough surfaces the nanotubes withdraw to the valleys and contact between the asperities may happen, giving higher friction coefficient values. With time, the NT are pushed away from the contact more easily for the smooth surfaces while the groves of the rough surfaces entrapped the nanoparticles in the contact. This phenomenon was not observed in the steel surfaces where the same value of the friction coefficient was obtained no matter the roughness of the surface (same average roughness for the DLC coated surfaces than for the steel surfaces tested)

On the other hand, Rapoport et al. (*94*) have proven that nanoparticles can also reduce the friction coefficient and wear of porous materials in the boundary lubrication regime. The tests were carried out with IF-WS$_2$ nanoparticles in mineral oil in a ball on disk set-up. The ball was made out of Si$_3$N$_4$ and the flat of alumina.

3.4.1.8 Nanoparticles compatibility with the after-treatment catalysis

The commercial use of nanoparticles in the automotive industry, involves investigation on their effect in the catalytic activity of the after-treatment catalysts used in vehicles. In fact, exhaust catalysts are usually poisoned by sulfur and phosphorous elements commonly found in the anti-wear additives (ZDDP) used in engine lubricants. These elements can be released into the flue gases after in-cylinder combustion.

Castillo Marcano et al. (*120*) have studied the effect of the nanoparticles containing lubricant in a real diesel engine composed of three Euro V compliant catalysts. The results where compared to those obtained with a reference oil without nanoparticles.

A diesel oxidation, a soot oxidation and a Selective Catalytic Reduction (SCR) catalyst were used. Their action mode is explained below:

•   A Diesel Oxidation Catalyst (DOC) whose function is to oxidize CO and hydrocarbons (HC) present in the flue gases to produce CO_2 and water.

•   A catalytic Diesel particulate Filter (DPF) or soot combustion catalyst which reduce the soot burn-out temperature during the filter regeneration leading to fuel saving.

•   A Selective Catalytic Reduction (SCR) or de-NOx catalysts that reduces the nitrogen oxides present in the exhaust gases to diatomic nitrogen and water. Ammonia is typically used as reductant agent.

MoS_2 nanoparticles were blended into commercial oil (ARL-1 from Fuchs Lubricants) at a concentration of 0.5 wt%. The authors found that the DOC and DPF catalysts reduced the gas and solid pollutants obtained with the lubricant containing nanoparticles to the same levels of those observed for the reference lubricant. An endurance test of 100h (equivalent to 10,000 km) proved that no substantial differences in HC, CO and NO concentration at the engine exit occurred during time. Thus, it has been demonstrated that the commercial after-treatment catalysts besides of not been poisoned by the emissions of the lubricant containing nanoparticles can also control them.

3.4.1.9   *Influence of other additives on the tribological performance of IF nanoparticles*

Lubricants are complex mixtures of base oil with different additives as explained in section 3.3. Nanoparticles have proven to be able to reduce both wear and friction for different kind of materials. However, their performance in the presence of other additives commonly used in a lubricant is not well known. Rabaso et al (*104*) have demonstrated that no decrease on the friction coefficient is observed by the addition of IF-MoS_2 nanoparticles to a fully formulated engine oil compared to the engine oil alone (Figure 37). The authors have attributed this to the presence of dispersants which may have affected the tribochemistry of the contact by an excessive adsorption on the steel and/or by encapsulation of the released sheets impeding tribofilm adhesion. On the other hand, Jenei et al. (*121*) have also observed the same loss on nanoparticles performance but this time for WS_2 when added to a fully formulated engine oil (Table 1). Their results showed that even if the friction coefficient of the base oil decreased by 50% with the use of nanoparticles, no significant effect was seen for the engine oil which suggests possible interactions between the nanoparticles and the other additives. Unfortunately, no chemical analyses were made on the worn surfaces for the samples lubricated with the engine oil which would be a key element to understand what happened.
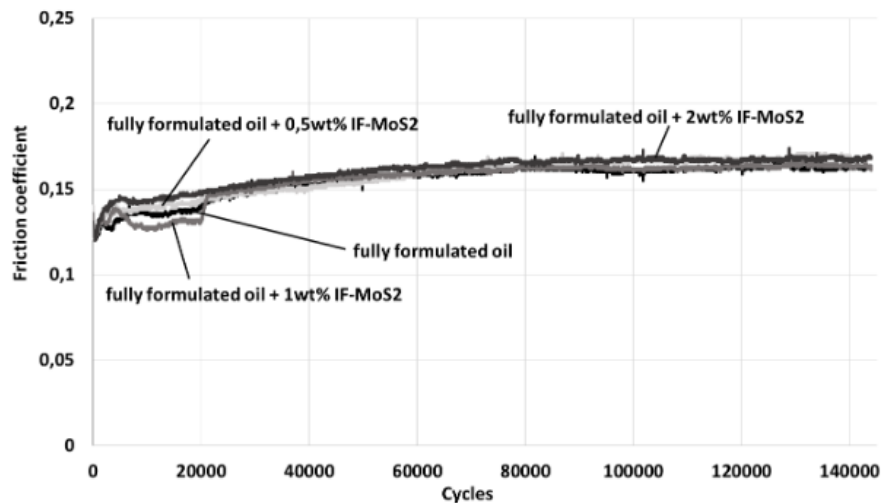
Figure 37. Tribological response of a fully formulated engine oil and of the same oil doped with IF-MoS$_2$ nanoparticles at different concentrations (*104*)

It seems that investigation for a better understanding on the possible effect of additives on the tribological performance of nanoparticles needs to be done. As a matter of fact, besides the investigation done for the dispersion of the nanoparticles, little information can be found concerning the influence of other additives in the performance of the nanoparticles.

The first work on this topic was done by Jenei et al. (*121*) in 2013. This research group studied the tribological response of WS$_2$ nanoparticles in the presence of different additives (anti-wear, anti-oxidant, pour-point depressant, viscosity modifier) in the boundary lubrication regime at room temperature. Their results are summarized in Table 1.

Table 1. Results obtained for the different samples tested by Jenei et al. (*121*)

Lubricants	Friction coefficient	Wear rate (μm^3/Nm)
PAO	0.103	33
PAO+WS$_2$	0.046-0.050	23-28
PAO+Anti-wear	0.079	27
PAO+Anti-wear+WS$_2$	0.073-0.075	23-29
PAO+Antiox1	0.087	18
PAO+Antiox1+WS$_2$	0.048-0.050	18-23
PAO+Antiox2	0.090	13
PAO+Antiox2+WS$_2$	0.058-0.066	18-22
PAO+pp depressant	0.088	21
PAO+pp depressant+WS$_2$	0.059-0.068	17-22
PAO+visc mod	0.109	41
PAO+visc mod+WS$_2$	0.050-0.053	24-28
Engine oil	0.103	14
Engine oil+WS$_2$	0.094-0.096	15-24

The authors compared the results obtained for the PAO + additive to those obtained for the PAO + additive + WS$_2$. This led to the conclusion that the anti-wear additive inhibits the nanoparticles from reducing friction. A correlation between tungsten content in the tribofilm and the friction coefficient was proposed: low friction coefficient values are associated with relatively high tungsten contents in the center part of the wear track. Thus, a low tungsten concentration leads to higher friction coefficients. The other correlations found by the authors are summarized in Figure 38.
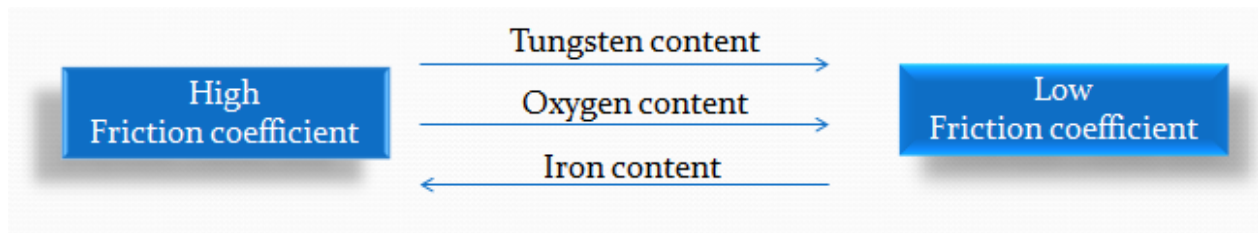
Figure 38. Correlations found by Jenei et al. (*121*)

4. Conclusions and overall methodology

To summarize, nanoparticles of metal diacholgenides have proven to have better tribological properties than 2H platelets. However, both kinds of nanoparticles have exhibited friction modifier and anti-wear properties when blended in base oil at room temperature in the boundary lubrication regime. The optimal concentration when used as additives in pure base oil has been estimated to be 1wt% and the contact pressure 1GPa. Their effect has been observed in both synthetic and mineral base oils not only on steel, but also on DLC coated surfaces.

Low friction coefficients are then due to the layered structure of the metal diacholgenides materials which allows easy inter-lamellar shear. This is the reason why nanoparticles of different shapes give the same coefficient of friction (COF) values. However, it is important to note that chemical changes can affect the beneficial effect of the nanoparticles.

The research done on the lubrication mechanism of IF nanoparticles has demonstrated that under the effect of shear and pressure they can either roll-slide or exfoliate. It has been demonstrated that poorly crystallized IF particles and hollow IF nanoparticles exfoliate more easily than well crystallized nanoparticles. Thus, better results would be obtained with small and poorly crystallized IF nanoparticles.

At high temperatures, when the nanoparticles reach the contact zone, they chemically react to form a tribofilm on the surface which is composed on the upper part by smashed nanoparticles that continues to lubricate the counter-surfaces.

Additionally, the commercial after treatment catalysts have proven to be capable of controlling the emissions produced by the nanoparticles without poisoning them. This is an important step for the use of nanoparticles in the automobile industry.

It is important to highlight that proper dispersion of the nanoparticles in the oil is crucial. Succinimide-based dispersants which are commonly used in the automotive industry have shown to have a detrimental effect on nanoparticles tribological performance. The use of other dispersants like ATS and SPAN80 should be considered.

Concerning the effect of other additives in the tribological performance of the nanoparticles, some information can be found but only for experiments made at room temperature. Thus, research under real life conditions needs to be carried out to be able to formulate nanoparticles-containing lubricants.

The aim of this work is to get a better understanding of the lubricating properties of fullerene like nanoparticles of metal diacholgenides for their use in lubricants for the automotive industry. The first part of this work will focus on the tribological properties of industrially produced tungsten disulfide fullerene like nanoparticles when tested at the laboratory scale under specific tests conditions. In this part, the effect of nanoparticles on smooth and rough surfaces will be investigated at room temperature

and at 100°C. Then, their lubricating properties, in the presence of additives commonly used in the automotive industry, will be investigated.

In the second part of this work the behavior of nanoparticles in a transmission application for the automotive industry will be explored not only at the lab scale but also at the industrial scale.

In order to achieve a better understanding of the phenomena occurring during the lubrication of two contacting surfaces when using nanoparticles, a characterization of the raw materials is needed. Then, a tribological testing must be carried out and the rubbed surfaces should be chemically and morphologically characterized. The general methodology used throughout this research work is summarized in Figure 39. The different materials, like tribometers and characterization techniques that were used for will be presented in the following sections.
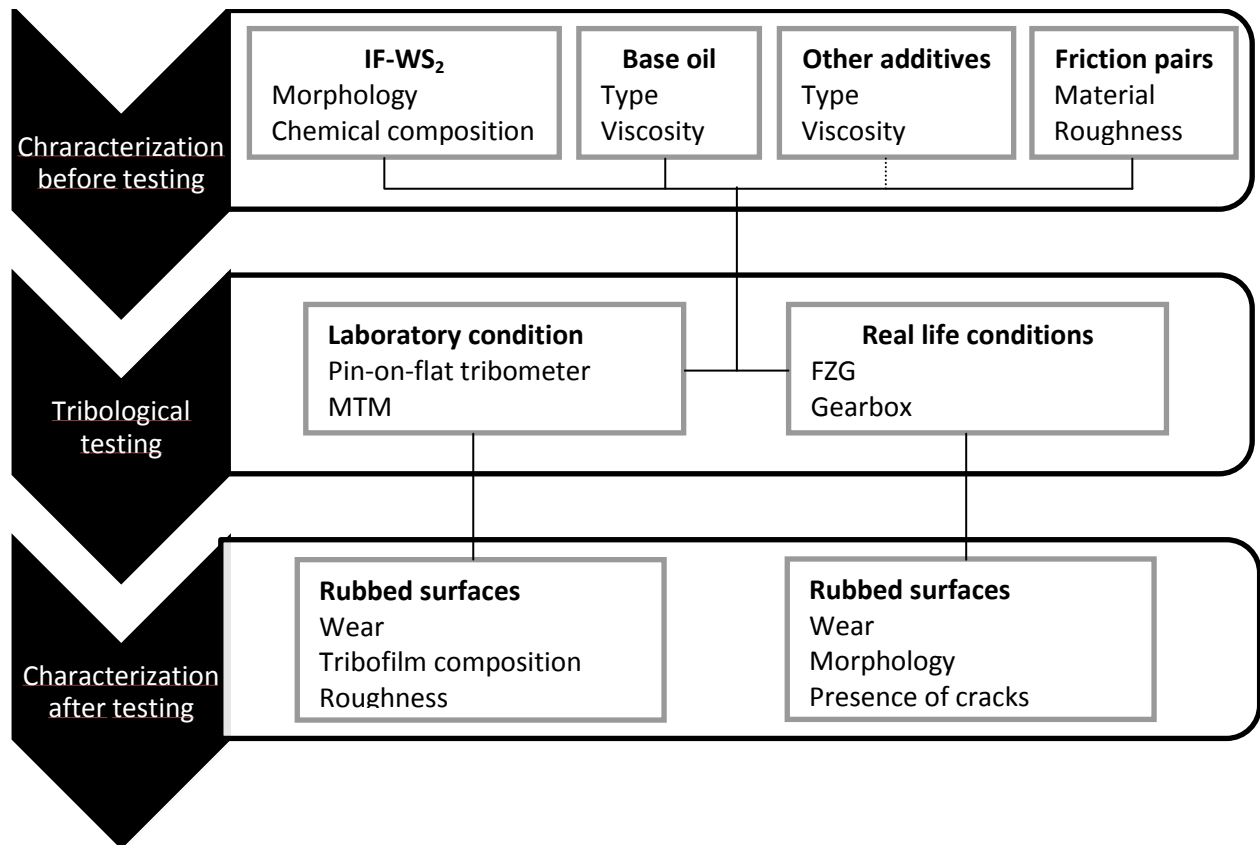
Figure 39. Overview of the methodology used for this work.

Résumé. Etat de l'art

De nos jours, l'une des principales préoccupations de notre société est la réduction de la consommation énergétique. L'industrie des transports est celle qui consomme le plus de pétrole dans le monde. Ainsi, des efforts sont menés au niveau des constructeurs automobiles pour améliorer les systèmes mécaniques et leurs rendements. Les pétroliers se doivent eux aussi d'être en mesure de proposer des lubrifiants répondant aux évolutions techniques mais également plus performants en terme de réduction du frottement et de l'usure.

Les nanoparticules de dichalcogénures métalliques se sont avérées être intéressantes ces dernières années pour les applications tribologiques. Ces nanoparticules ont été synthétisées pour la première fois dans les années 90. Les essais menés en laboratoire ont montré que lorsqu'elles sont dispersées dans une base lubrifiante, les nanoparticules présentent des propriétés tribologiques (réductrice de frottement et anti-usure) extrêmement intéressantes à température ambiante et en régime de lubrification limite. Il a notamment été démontré que les fullerènes inorganiques (IF) de bisulfures métalliques peuvent rouler ou s'exfolier sous l'effet de la pression et du cisaillement dans un contact tribologique. Ainsi, les nanoparticules avec un haut degré de cristallinité ont plutôt tendance à rouler tandis que la présence de défauts dans la structure des particules faciliterait leur exfoliation permettant d'alimenter en permanence le contact en nano feuillets de disulfure métalliques bien connus pour leurs propriétés lubrifiantes.

Cependant, un lubrifiant complètement formulé comprend une base lubrifiante et un ensemble d'additifs permettant soit d'améliorer les propriétés naturelles de l'huile de base, soit d'en conférer de nouvelles. D'un point de vue tribologique, les études faites par le passé ont montré que les dispersants de type succinimide empêchent les nanoparticules de former un tribofilm sur les surfaces en acier et donc de réduire le frottement. L'interaction (synergie ou antagoniste) de ces nanoparticules avec les autres additifs utilisés dans les lubrifiants dans des conditions de sollicitation proches de celles rencontrées dans les applications réelles reste donc inconnue.

Dans le cadre de cette thèse nous nous sommes intéressés à ce sujet. Nous avons utilisé des fullerènes inorganiques de disulfure de tungstène produits industriellement. Après les avoir caractérisé, nous les avons ensuite sollicité tribologiquement dans des conditions dites «idéales et contrôlées» (échelle laboratoire) avant de les tester dans des boîtes de vitesse automobiles (échelle industrielle). Cette démarche est présentée dans ce manuscrit à travers deux parties: la première présente les résultats obtenus avec ces nanoparticules sur des surfaces de rugosités différentes (surfaces lisses et rugueuses) à température ambiante et 100°C ainsi que leur comportement tribologique en présence des additifs utilisés dans la formulation des huiles automobiles. La deuxième partie présente les résultats obtenus lors de tests réalisés pour l'application transmission.

Afin de comprendre les résultats obtenus lors de cette thèse, différentes techniques d'analyses de surface et chimiques ont été utilisées.

Part 1. Lubricating properties of industrially produced tungsten disulfide nanoparticles

Researchers have demonstrated that factors like the nanoparticle's size and structure have an influence on the nanoparticle's tribological properties. For this reason, industrially produced nanoparticles must now be first characterized and then tribologically studied to validate their further use in lubricants.

This part of this work is divided in three main sections. In the first one, the chemical and morphological characterization of tungsten disulfide nanoparticles produced at the industrial scale is presented. Then, the friction and wear reduction potential properties of these nanoparticles, in PAO base oil and under different tests conditions, are studied in the second part. Finally, the tribological behavior of these nanoparticles in the presence of other additives that are commonly used in the automotive industry is investigated in the third part.

5. Characterization of industrial IF-WS$_2$ nanoparticles

The production and commercialization of nanoparticle-doped lubricants requires large-scale synthesis of these materials. The evolution of the synthesis techniques allows nowadays the production of fullerene like WS$_2$ nanoparticles at an industrial scale so they can be currently found in the market. Thus, an important step for the production of lubricants containing nanoparticles has been achieved. However, these industrially produced WS$_2$ nanoparticles are not expected to be perfectly crystalized fullerene like closed caged structures as those synthetized at the lab-scale where the growth mechanism can be more easily controlled. For this reason, these industrially produced nanoparticles must now be first characterized and then tribologically studied to validate their further use in lubricants.

The tungsten disulfide nanoparticles used for this research work were purchased from NanoMaterials Ltd. by TOTAL in 2012. They were sold by the company dispersed at a concentration of 20 wt% in base oil.

The morphological and chemical characterization of the nanoparticles was carried out at the laboratory before the friction tests were done. High Resolution Transmission Electron Microscopy (HR-TEM) and laser granulometry were used to morphologically characterize the sample while X-ray photoelectron spectroscopy (XPS) was used for the chemical characterization. The results obtained with the different techniques are presented below.

5.1 High Resolution Transmission Electron Microscopy (HR-TEM)

The morphological characterization of the nanoparticles was done by High Resolution Transmission Electron Microscopy (HR-TEM). All the TEM observations presented in this work were performed on a JEOL 2010 operating with 200 KV acceleration voltage equipped with energy dispersive spectroscopy (EDX).

For the analysis, the solid nanoparticles were dropped off in a copper grid after they were cleaned with heptane in an ultrasonic bath and centrifuged twice. The grid was immersed in pure heptane for complete oil removal before the analysis. TEM imaging revealed the presence of clusters of nanoparticles formed mainly by IF-NP and the presence of some WS$_2$ sheets (Figure 40a). The nanoparticles were present in spherical and polyhedral shapes as observed in Figure 40(b) and (c), respectively. Their size varies between 50 nm and 130 nm showing that these industrially produced nanoparticles are much more heterogeneous in size than those produced at the lab scale that have been widely studied during the last decade.
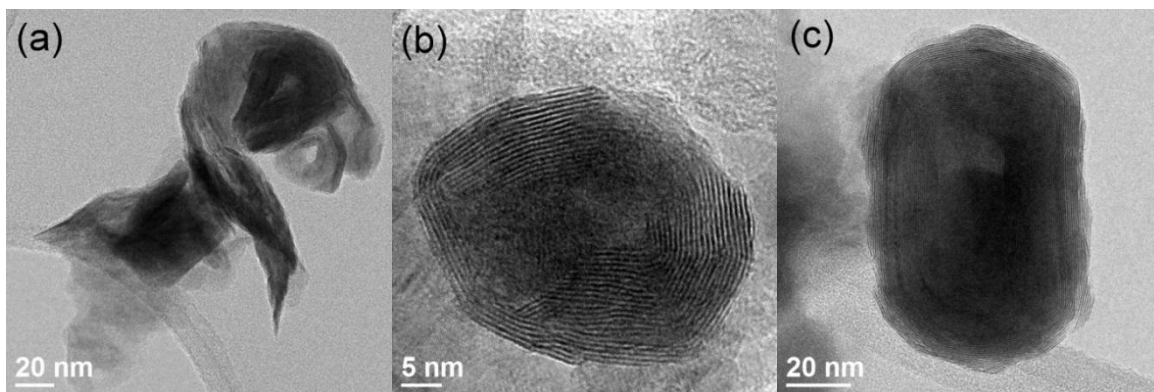
Figure 40. TEM images of WS$_2$ nanoparticles used for the tribological tests: (a) cluster with IF nanoparticles and 2H-WS$_2$ sheets, (b) spherical shape WS$_2$-IFLNP and (c) polyhedral shape nanoparticle

5.2 Laser granulometry

The particle size distribution of the sample was measured by laser granulometry (CILAS 1064L) using 150 NS as solvent and ultrasound to disagglomerate the particles before the measurements. Figure 41 shows the particle size distribution obtained for the nanoparticles.
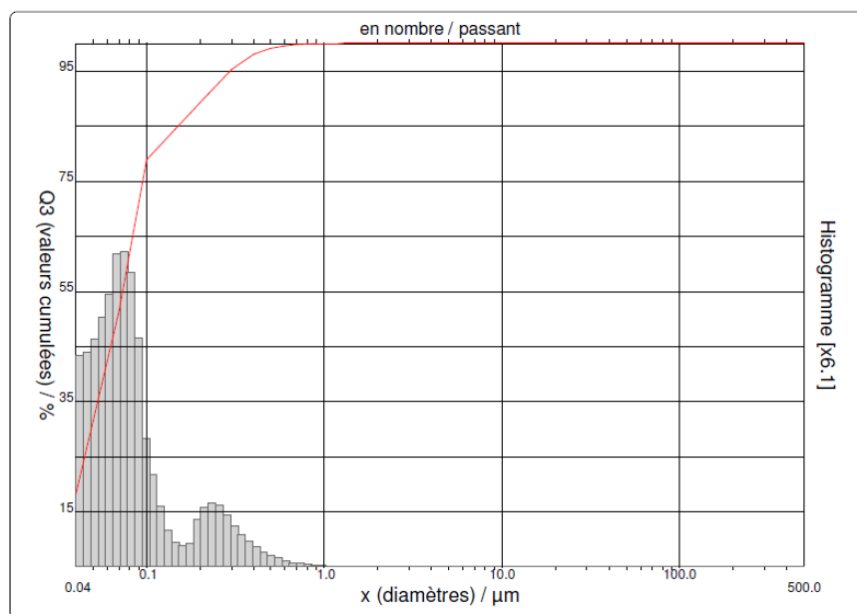
Figure 41. Particle size distribution of the nanoparticles

From this figure it can be concluded that the sample presents 2 main particle size populations: one around 0.07 μm and a second one at 0.40 μm. The second size population clearly shows the tendency of the nanoparticles to agglomerate, whereas the first population corresponds to isolated nanoparticles, which agrees with the nanoparticle size observed by TEM (50 to 130 nm).

5.3 X-ray Photoelectron Spectroscopy (XPS)

Chemical characterization of the nanoparticles was done by X-ray Photoelectron Spectroscopy (XPS). To get the nanoparticles in a powder form for the XPS analysis, oil removal was done by heptane washing and sonication followed by a centrifugation step. The process was repeated several times to accomplish complete oil removal. The nanoparticles were then dried in an oven for 10 hours at 35°C.

All the X-Ray Photoelectron Spectrometry (XPS) analyses presented in this work were carried out with a ULVAC-PHI VersaProbe II electron spectrometer using a monochromatized AlKα X-ray source. Calibration of the machine was done using Ag, Cu and Au elements following the calibration procedure of the fabricant. Constant pass energy of 23.5 eV was used for the analyses. Data treatment was made using PHI multipack software. The charging effect was corrected by fixing the C1s peak (adventitious carbon) at 284.8 eV.

Characterization of the nanoparticles was made using a spot size of 100 μm with a power of 24.8 W. Figure 42 shows the W4f (a) and the S2p (b) spectra recorded from the WS_2 powder. The binding energies and the corresponding chemical species present in the sample are summarized in Table 2.
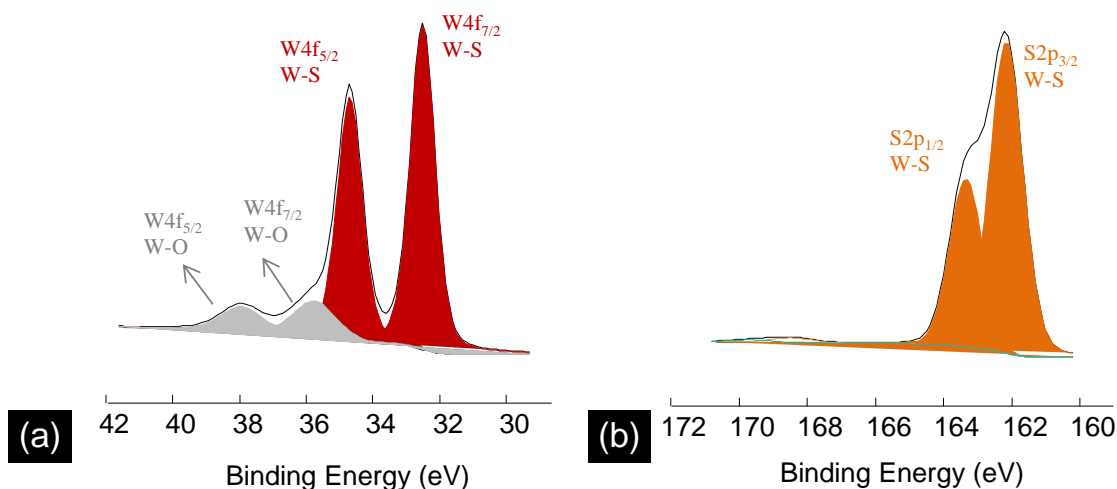
Figure 42. XPS spectra of WS_2 nanoparticles: (a) W4f region, (b) S2p region

Table 2. XPS binding energies and corresponding chemical species present in the nanoparticles

W4f peaks		S2p peaks	
Peak	% at	Peak	% at
32.5 eV (WS_2)	33.5%	162.3 eV (WS_2)	60.1%
35.9 eV (WO_x)	5.5%	168.5 eV (SO_x)	0.9%

Treatment of tungsten spectra (Figure 42a) shows the presence of two W4f$_{7/2}$ peaks, one at 32.5 eV which corresponds to W-S bond and another one at 35.9 eV that corresponds to W-O bond. Since, the nanoparticles were synthetized by reaction of WO$_3$ with a sulfur source; the W-O bond could be explained by unreacted WO$_3$. However, a small/light surface oxidation of the nanoparticles cannot be excluded. The tungsten oxide concentration in the sample is nevertheless low (5.5 at%). Deconvolution of the sulfur spectra (Figure 42b), shows one peak S2p$_{3/2}$ at 162.3 eV corresponding to S-W bond, the W/S ratio is 1.80. A small peak is present at 168.5 eV which can be attributed to a contribution of sulfur bonded to oxygen.

6. Tribological behavior of industrial WS$_2$ nanoparticles in PAO base oil on smooth and rough surfaces

Research done during the last decades on the tribological properties of metal dichalcogenides fullerene like nanoparticles has demonstrated that they have very interesting friction and wear reducing properties in boundary lubrication regime. Their lubrication mechanism has been attributed to their ability to exfoliate under high pressures to produce sheets that adhere to the steel surfaces to form a tribofilm and provide a lamellar lubrication mechanism. The research done until now used nanoparticles produced at the laboratory scale as raw product (a brief summary can be found in the State of the art part). The results have demonstrated that factors like nanoparticle's size and structure have an influence on their tribological properties.

The morphological characterization of the IF-WS$_2$ used for this study, revealed that the sample is heterogeneous in terms of shape, size and morphology. For this reason, the aim of the first experiments carried out in this work was to validate whether the commercially available nanoparticles exhibit the same lubrication properties than those produced in the laboratories, or not. First of all, MTM technique was used to study the Stribeck curve obtained for these nanoparticles in PAO. Then, a reciprocating pin-on-flat tribometer was used to study the nanoparticles behavior under more specific test conditions (boundary lubrication regime).

All the tests were carried out using synthetic polyalphaolephin (PAO) with kinematic viscosity of 5.9 mm^2/s at 100°C as base oil. WS$_2$ nanoparticles were blended in a concentration of 1 wt% in this base oil.

6.1 MTM experiments

In order to study the performance of the WS$_2$ nanoparticles in a wide range of operating conditions a PCS MTM was used (Figure 43). In this machine, a ball is loaded against a disc. Both friction pairs are driven independently to obtain the desired Slide-to Roll Ratio (SRR). Traction curves (varying SRR for a given velocity) and Stribeck curves (varying rolling velocity, load or temperature for a given SRR) can be

obtained with this machine. The standard specimens (ball and disc) are made of AISI 52100 (100Cr6). The balls used had a diameter of ½'' (12.70 mm) and the discs have a roughness inferior to 0.01 µm. For an easier cleaning of the machine, PCS provided a mini-pot assembly which reduces the sample volume from 35 mL to 4 mL. All the blends tested on the MTM were mixed using a magnetic agitator and were sonicated for 15 minutes. The complete test procedure is summarized in Table 3.
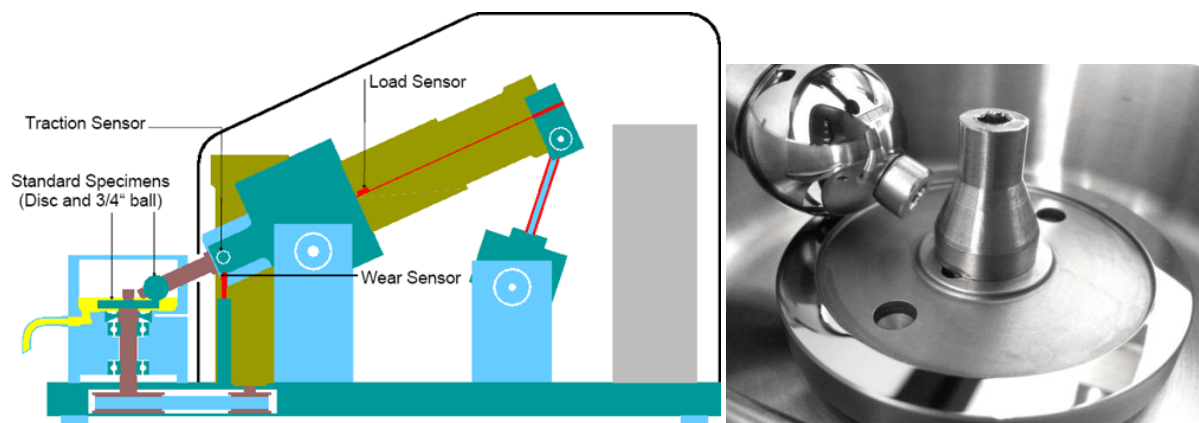
Figure 43. MTM schema (left) and picture (right) (source: PCS instruments)

A series of Stribeck curves were plotted for different Slide-to-Roll Ratios (SRR) after a running period of 10 minutes. Two traction curves were plotted at 0.3 m/s rolling velocity, one at 30°C at the beginning and another one at 100°C at the end of the test procedure. The experiments were run at 30°C and 100°C with an initial maximum contact pressure of 1.3 GPa. The lubricant tested consisted of PAO with 1 wt% WS_2 nanoparticles and the results were compared to those obtained when using the base oil (PAO) alone.

Table 3. MTM test procedure for the evaluation of the potential of the industrial WS_2 nanoparticles in PAO

Step	Description	SRR (%)	T (°C)
1	Traction	-	
2	Timed step 10 min	20	
3	Stribeck		
4	Timed step 10 min	50	30
5	Stribeck		
6	Timed step 10 min	100	
7	Stribeck		
8	Timed step 10 min	20	
9	Stribeck		
10	Timed step 10 min	50	100
11	Stribeck		
12	Timed step 10 min	100	
13	Stribeck		
14	Traction	-	

The traction curves obtained at 30°C and 100°C for a mean rolling sliding velocity of 0.3 m/s can be observed in Figure 44. The reference curves (dotted lines) exhibited very typical behavior: the traction coefficient increases with the SRR. Nanoparticles seem to have no effect at 30°C while lower traction coefficients are obtained for all SRR at 100°C. This can be explained by the fact that oil viscosity decreases dramatically as a function of temperature. Lower viscosities give thinner oil film so contact between the asperities of the friction pairs can happen. This result suggests that mixed lubrication was reached for a mean velocity of 0.3 m/s at 100°C as confirms the Stribeck curves plotted for PAO in Figure 45. At both temperatures and both SRR, the rise in friction attests the transition from the full film to the mixed lubrication regime. The results obtained for the nanoparticles show that they are able to reduce friction under low speeds in mixed lubrication regime. This is in agreement with the results reported in the literature for laboratory produced nanoparticles as described in Chapter 1.
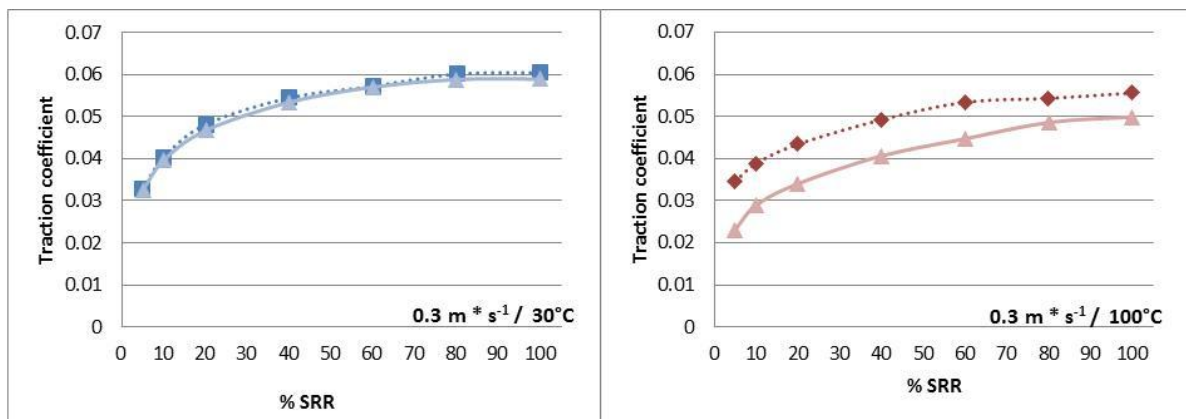
Figure 44. Traction curves for PAO base oil (doted lines) and PAO + WS$_2$ (full lines) at 30°C (blue, left) and 100°C (red, right) measured at 0.3 m/s

74
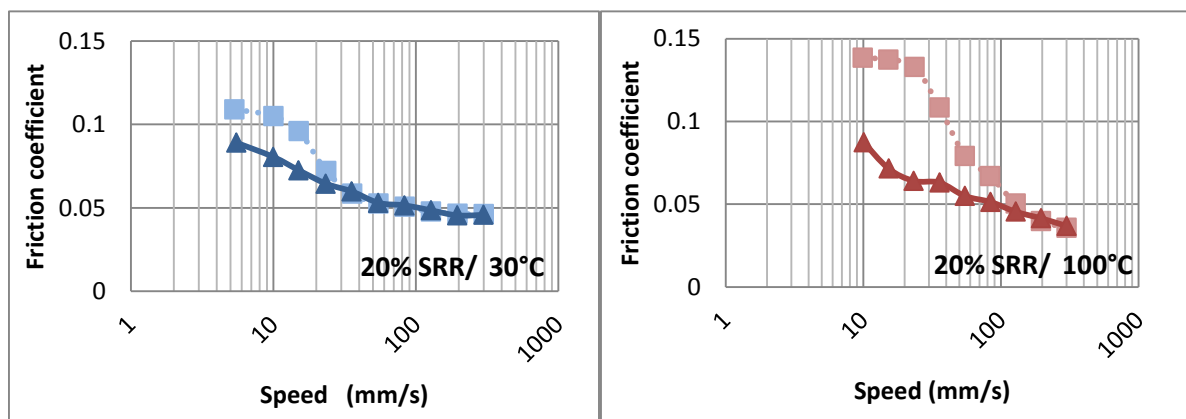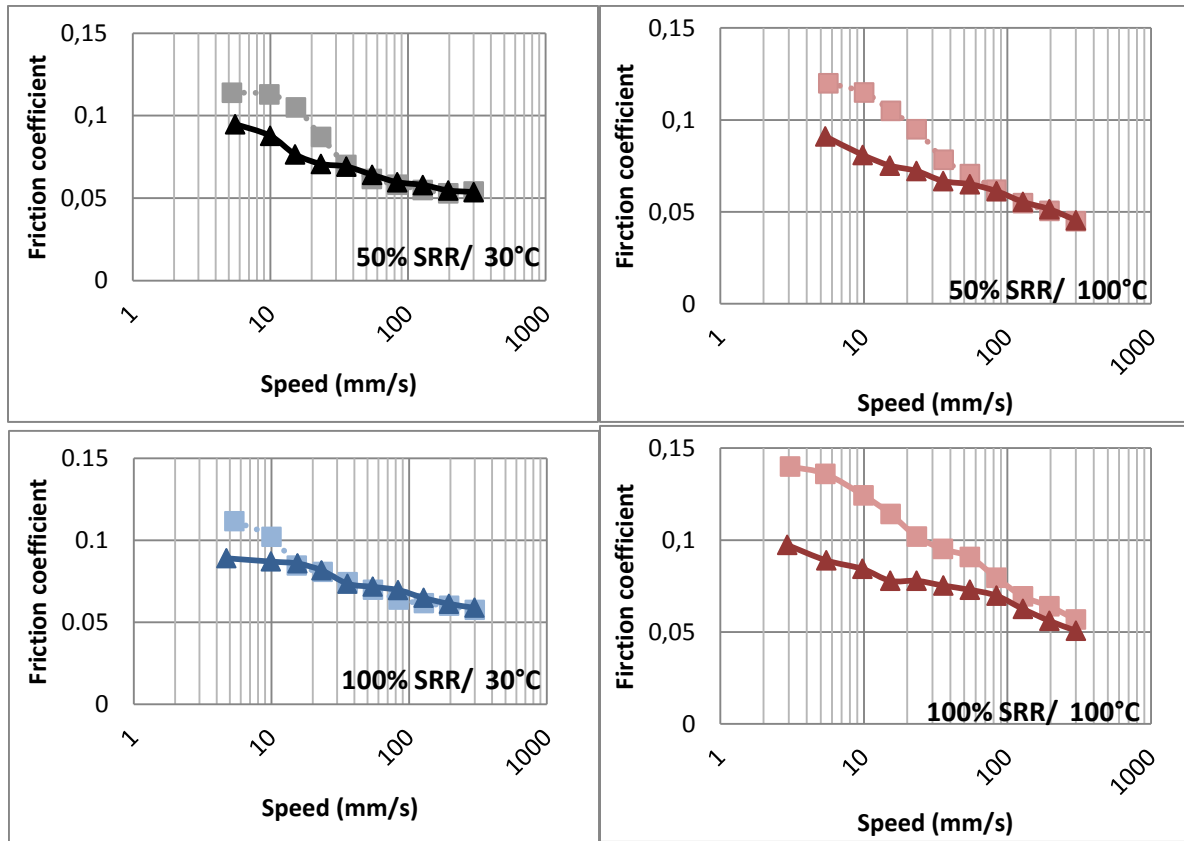
Figure 45. Stribeck curves obtained for PAO (dotted lines) and PAO + WS₂ nanoparticles (full lines) at 30°C (blue, right) and 100°C (red, left).

From these tests, industrially produced WS$_2$ nanoparticles appear to be efficient in reducing friction coefficient in the most severe conditions. Thus, it looks like industrially produced nanoparticles have a similar behavior than those produced at the lab-scale. As a consequence, the experiments that will be carried out in this work will be done under the boundary lubrication regime, because is in this regime that nanoparticles produced at the lab-scale have proven their ability to reduce friction and wear.

6.2   Pin-on-flat tribometer experiments

A home-made tribometer was used to evaluate the friction and wear reducing properties of the nanoparticles in severe boundary lubrication conditions. The test consists in a pure-sliding reciprocating motion between a pin on a flat disc using one drop of lubricant. A picture of the tribometer and a schematic representation of the contact can be observed in Figure 46. The friction coefficient is deduced from the friction force generated between the ball and the disc during the test, which is measured by a piezoelectric force transducer placed against the heater block supporting the lower specimen holder.

The experiments were carried out on smooth and rough surfaces. For this, 6.00 mm diameter balls (Ra < 20nm) were used for all the tests whereas two types of flat discs were used: smooth with a Ra < 20nm

and rough with a Ra = 300 nm (the furnisher reported Ra=150 nm for the rough samples). All the specimens were made of AISI 52100 (100Cr6) steel hardened to 800HV produced by PCS instruments
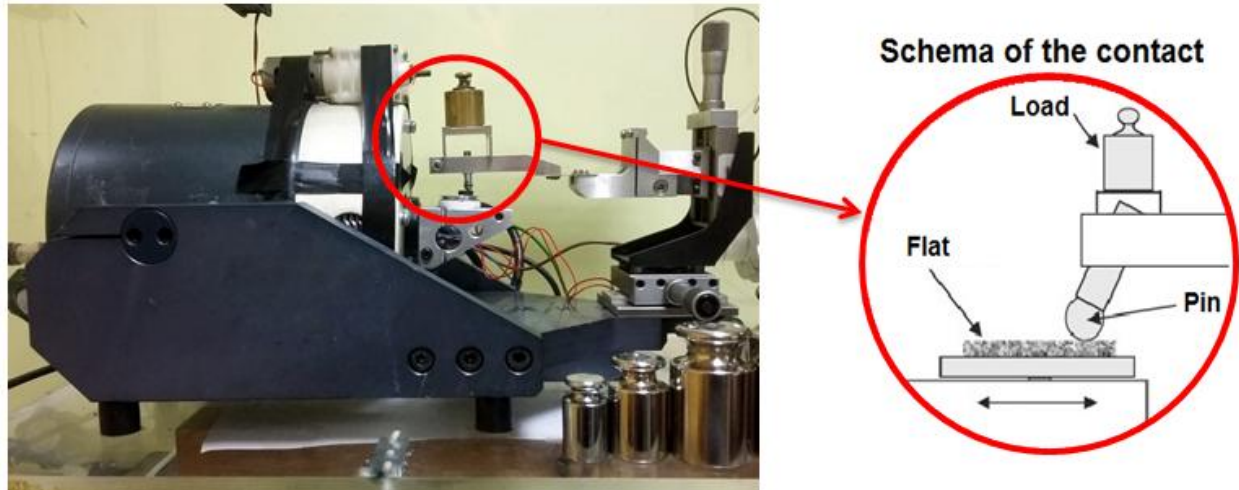
Figure 46. Picture of the pin-on-flat tribometer used for the experiments and schema of the contact

The friction pairs were cleaned before the tests in an ultrasonic bath using three different solvents: first acetone, then isopropanol and finally heptane. The samples were sonicated for fifteen minutes in each solvent before the test. The experiments were performed in ambient atmosphere (RH 35-45%). The mean sliding velocity was 3mm/s with a strike frequency of 0.5 Hz and initial maximum Hertzian contact pressure of 1.12 GPa (obtained by the use of a load of 5N). The experiments were run at room temperature and 100°C for 8 hours. All the tests were done four times to study their reproducibility. The test conditions are summarized in Table 4

Table 4. Test conditions for the pin-on-flat tribometer experiments

Load (N)	5
Maximum Hertzian pressure (GPa)	1.12
Temperature (°C)	Room temperature and 100°C
Sliding velocity (mm/s)	3
Strike frequency (Hz)	0.5
Length of the experiments (h)	8
Number of cycles	14400
Samples tested	Base oil
	Base oil + 1 wt% WS_2
Friction pairs	Ball Ra < 20 nm
AINSI 52100 (100Cr6)	Smooth flat Ra < 20 nm
	Rough flat Ra = 300 nm
Hertz diameter for the tests conditions (µm)	92

6.2.1 Nanoparticles behavior on smooth surfaces

The friction coefficient of the nanoparticles in the base oil and of the base oil alone (without nanoparticles) obtained at room temperature and 100°C on the smooth surfaces is shown in Figure 47.
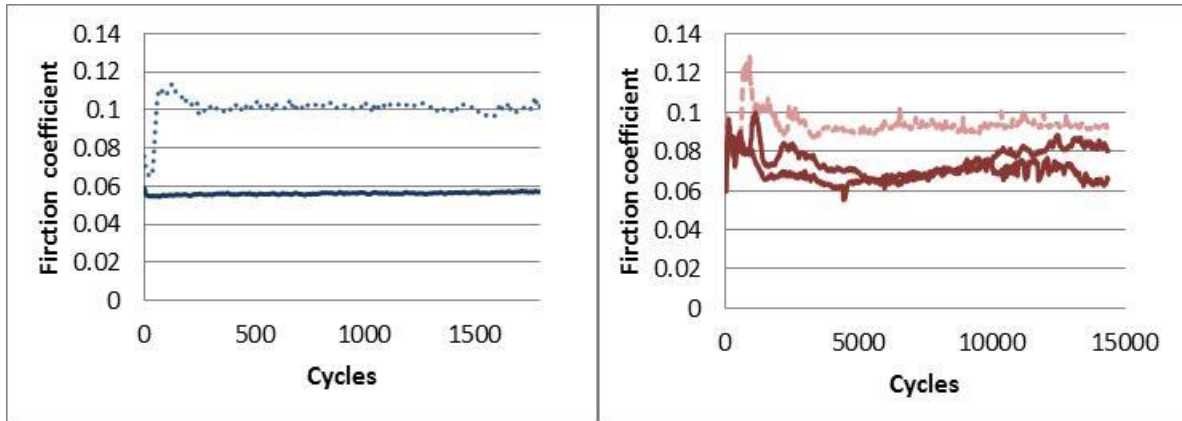
Figure 47. Friction coefficient for the nanoparticles (full line) and the reference (dotted line) as a function of cycles at room temperature (blue, left) and 100°C (red, right)

The reference test for the PAO oil gave a fairly constant friction coefficient of 0.1 under both working temperatures. At room temperature, clear friction reduction can be observed when nanoparticles are added to the base oil. A low and stable friction coefficient of 0.6 is obtained since the very first cycles and tests are highly reproducible. This result agrees with those obtained by other research group (*92*) where 35-40% reduction in friction coefficient was obtained with the WS_2 nanoparticles compared to the base oil, using an unidirectional sliding tester with a fixed ball and rotating disc with similar test conditions.

On the other hand, at 100°C, not only important fluctuations of the friction coefficient from 0.06 to 0.08 along the friction test were seen, but also reproducibility problems were observed. As described in Chapter 1, there is no much information about the nanoparticles behavior under high temperatures in the literature, and information found seems to be contradictory. Additionally, none of the previous studies done either with MoS_2 (*90, 104*) or WS_2 (*103*) nanoparticles reported reproducibility problems. However, those results were obtained when using more homogeneous samples than the one used in the present work. It is possible to think that the presence of some sheets and of not perfectly close caged nanoparticles may have some consequences on nanoparticles tribological behavior. It is known that shear can catalyze some reactions in the contact, like oxidation that may affect the performance of the particles. A chemical characterization of the tribofilm formed on the worn surfaces needs to be done to help understanding these results.

In order to check the effectiveness of the lubricants tested for wear reduction, the wear coefficient K_i was calculated using Archard wear equation:

$$K_i = \frac{V_i}{F * S}$$

where F is the nomal load (N), S the sliding distance (m), V_i the wear volume (m^3) which is the volume of the lost segment calculated from the wear scar diameter on the pin. The obtained values are summarized in Figure 48. Figure 49 shows the worn surfaces for all the samples. It can be seen that the presence of WS_2 nanoparticles in PAO improves drastically the anti-wear properties of the dispersion at both temperatures. However, the best anti-wear properties were obtained for the nanoparticles tested at room temperature where actually the wear scar corresponds to the calculated Hertz diameter. The friction reproducibility problems encountered at 100°C with the use of the nanoparticles causes more uncertainty in the wear coefficient value for this sample than for the others (Figure 48).
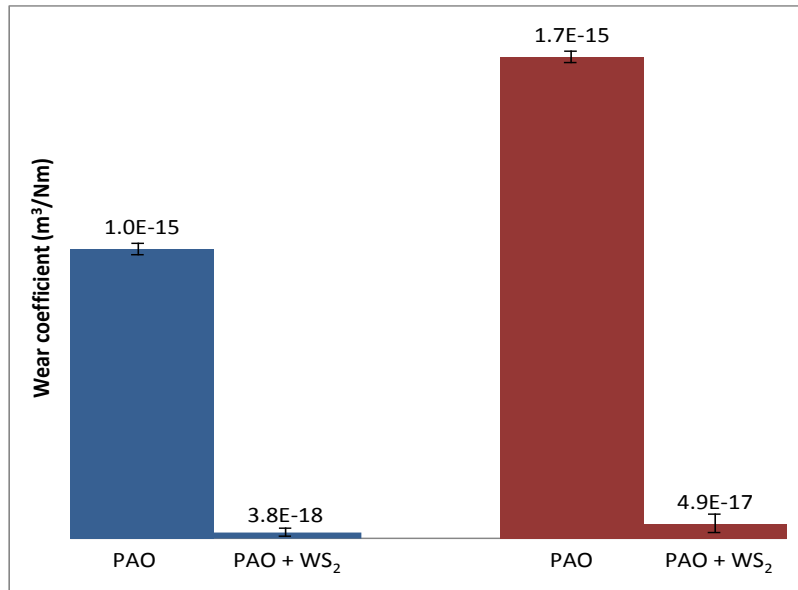
Figure 48. Wear coefficient calculated for PAO and PAO + WS$_2$ nanoparticles at room temperature (blue) and 100°C (red)
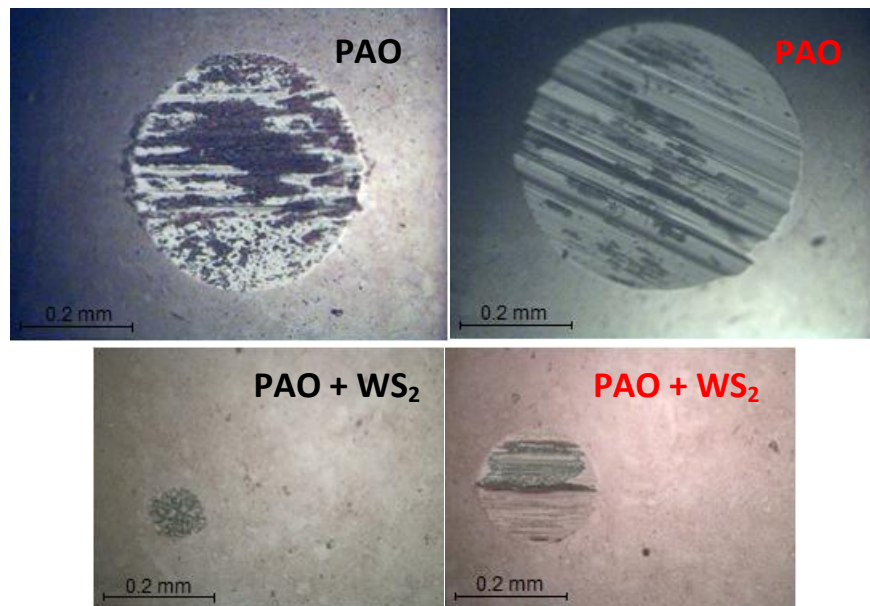
Figure 49. Wear scars of the pin when lubricating smooth surfaces with PAO and PAO + WS$_2$ nanoparticles at room temperature (blue, left) and 100°C (red, right)

To understand the friction coefficient fluctuations observed at high temperature, a chemical characterization of the tribofilms obtained at both temperatures was carried out by XPS. The spot size was 50 µm with a power of 12.5W. The analyses were made twice for each sample and showed good reproducibility. Concerning the experiments carried out at 100°C, only the worn surface of the sample that gave the highest friction coefficient in Figure 47 was analyzed. The tungsten and sulfur spectra recorded for the tribofilm formed at room temperature and at 100°C are shown in Figure 50.
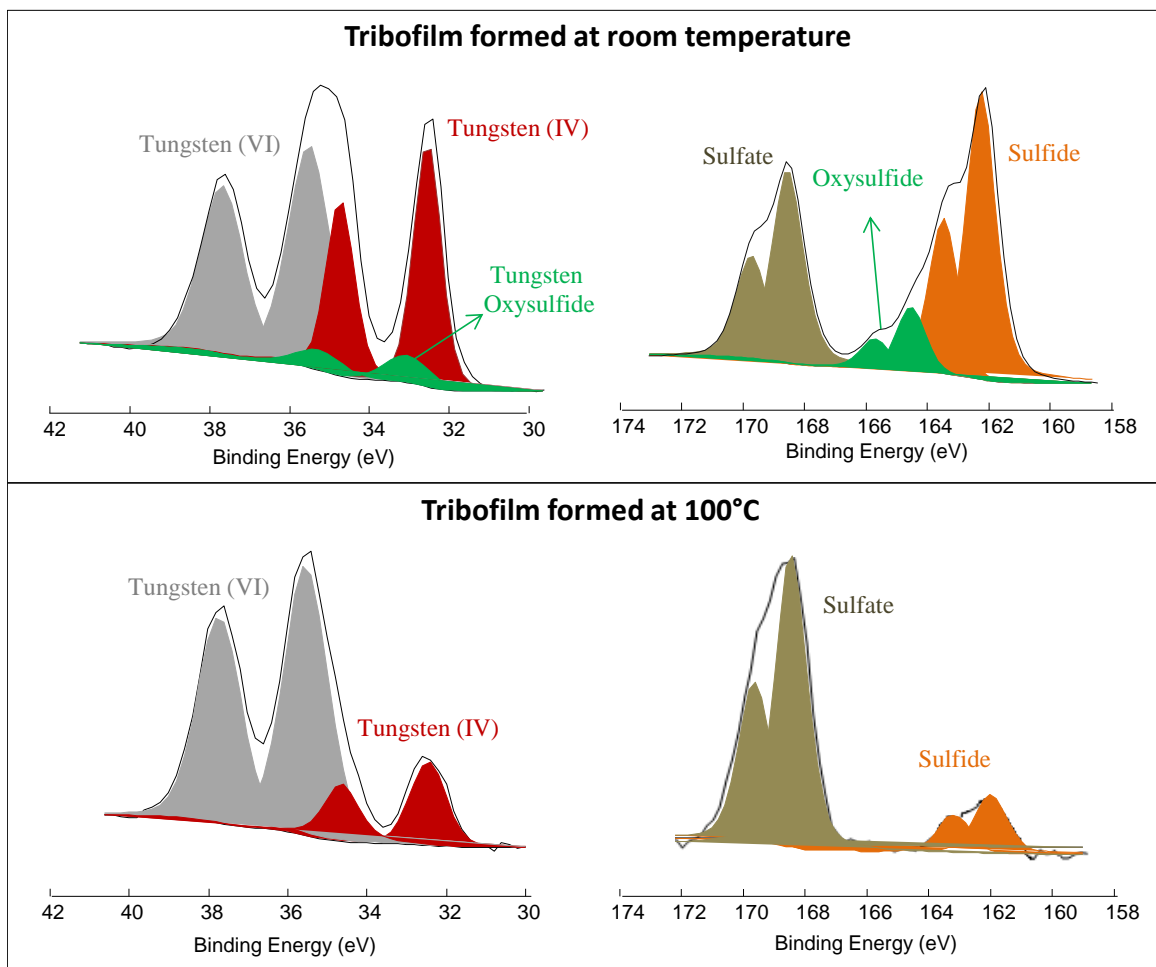
Figure 50. Tungsten and sulfur XPS spectra of the tribofilm by the nanoparticles at room temperature and at 100°C

The tungsten $W4f_{7/2}$ contribution at 32.6 eV (red peaks) and sulfur $S2p_{3/2}$ at 162.5 eV (yellow peaks) confirms the presence of tungsten disulfide. However, the important tungsten and sulfur contributions at 35.8 eV and 168.6 eV (grey and brown peaks) that correspond to these elements bonded to oxygen atoms prove that these elements are more oxidized in the tribofilm than in the nanoparticles powder. On the other hand, the green peaks at 33.1 eV and 163.5 eV correspond to tungsten oxysulfide which might come from partial oxidation of the tungsten disulfide. It can be seen that this contribution was not found at 100°C which indicates that oxidation was completed at high temperatures. This agrees with the

large quantities of tungsten in a tungsten oxide form found in the tribofilm formed at 100°C which was estimated to be around 85% while it was 47% at room temperature.

It can be concluded that tungsten oxide and sulfur bonded to oxygen atoms are present in larger quantities in the tribofilm than in the nanoparticles powder at both working temperatures. This suggests that an oxidation reaction has taken place. This oxidation seems to be more important at 100°C. In order to check the nanoparticles chemical stability at the working temperature, thermogravimetric analysis (TGA) of the sample bought from Nanomaterials Ltd. was carried out. The curve obtained using a heating rate of 25°C/min from 25 to 100°C can be seen in Figure 51.
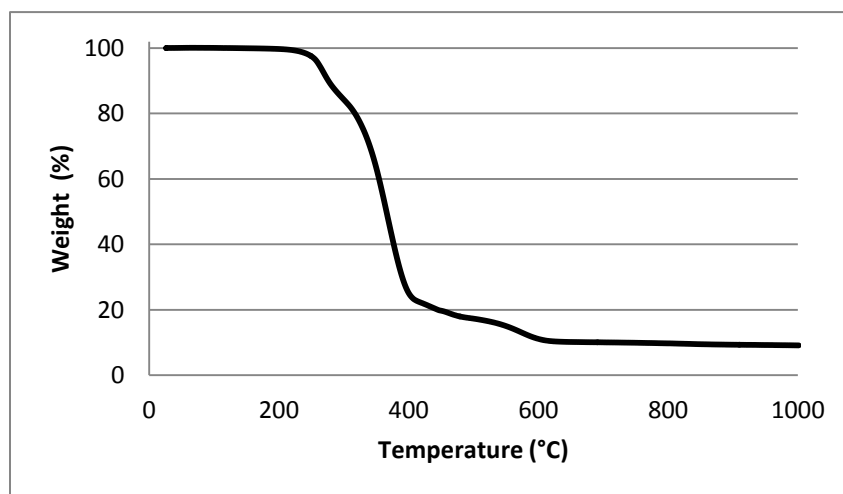
Figure 51. TGA curve of the sample bought from nanomaterials company.

It can be observed that the first weight loss occurs above 200°C so the sample is not expected to undergo any changes at the working temperature (100°C). Oxidation must then have happened by the dual effect of shear and high temperature.

Little information can be found on the oxidation degree of the tungsten or molybdenum in the tribofilms formed by metal dichalcogenides nanoparticles in the literature. At room temperature, only Kogovsek et al. (*92*) speak about WS_2 nanoparticles oxidation. Their EDX analysis carried out after lubricating steel surfaces with MoS_2 and WS_2 nanoparticles in base oil, revealed large amount of oxygen on the worn surfaces of the sample lubricated by the WS_2 nanoparticles. As a consequence, the authors claim that WS_2 oxidizes more easily than MoS_2. Nevertheless, no EDX quantification of the spectra is shown and no XPS analyses were carried out to verify whether oxygen was bonded to tungsten/ sulfur or not. On the contrary, information is more complete concerning molybdenum oxidation degree when using MoS_2 nanotubes in base oil for the lubrication of steel surfaces at room temperature. The XPS analyses carried out on the worn surfaces lubricated by MoS_2 nanotubes done by Kalin et al. (*119*) revealed that in the tribofilm the amount of molybdenum and sulfur in oxide forms were 22 and 14% respectively, which are higher than the 2 and 0 wt% reported for the raw material. These results suggest that nanoparticles do

undergo oxidation. However, it is difficult to know either this oxidation occurred during the friction test or after when the tribofilm was exposed to the air.

On the other hand, when working under 100°C, Ratoi et al. (*103*) have shown that a tribofilm with a thickness of around 100 to 200nm was formed with WS$_2$ nanoparticles. After carrying out XPS depth profile analyses, the authors suggested that this tribofilm has a layered structure as illustrated in Figure 52. The upper part is composed of WS$_2$ sheets, tungsten oxide and iron oxides and sulfides whereas the deeper layers consist of tungsten oxide and elemental tungsten and iron. Additionally, elemental tungsten and iron were found on the steel substrate. However, it is known that sputtering process significantly affects the ion-bombarded material since it might result in atomic mixing and strong oxidation state reduction. As a consequence, attention must be payed concerning the information given from the deconvolution of XPS depth profile spectra because reduction may have occurred. Thus, no conclusions can be done about the oxidation state and chemical environment of the elements found in the tribofilm after sputtering. This may explain the presence of elementary tungsten and iron in the tribofilm reported by the authors. Nevertheless, the information about the film thickness and the extreme surface composition is still reliable. However, no quantification of the amount of tungsten and sulfur in an oxide form in neither the tribofilm nor the raw nanoparticles is presented in their work.
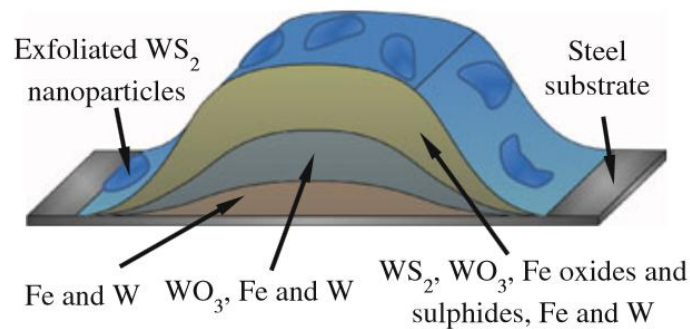
Figure 52. Composition of the tribofilm generated by WS$_2$ NP in PAO oil at 100°C proposed by Ratoi et al. (*103*)

On the contrary, XPS analyses done by Sgroi et al. (*122*) after lubricating a valve train system with a MoS$_2$-fully formulated lubricant, revealed that molybdenum and sulfur were highly oxidized (77 and 55 % respectively) in the tribofilm. After etching, a decrease of the peaks that correspond to the oxide species was accompanied by the increase of peak that corresponds to the Mo-S bond. For this reason the authors claim that oxidation occurred after the engine test due to the air exposure. As said before, sputtering process can affect the oxidation state of the elements. As a consequence, it is possible to think that the lower binding energies that were attributed to Mo-S could correspond to a reduction of the S-O and Mo-O peaks. Thus, oxidation could have happened during the engine test as it happened during the friction test done at 100°C using WS$_2$ nanoparticles. Once again, it is difficult to know whether this oxidation occurred during the friction test or after it when the tribofilm was exposed to atmospheric air.

It can be concluded that only the quantitative information about the molybdenum in an oxide form in the tribofilms formed at room temperature (22%) and at 100°C (77%) can be found in the literature.

These results can be compared to those obtained in this work with the industrially produced tungsten disufide nanoparticles where more tungsten oxide was found in the tribofilm formed at 100°C (85%) than at room temperature (47%). It is possible to think that the large quantities of tungsten oxide found in the tribofilm formed at 100°C might have a role in the reproducibility problems and the friction coefficient fluctuations observed during the friction tests. This will be discussed further in this work.

In order to determine the thickness of the tribofilm formed both at room temperature and 100°C, a transversal FIB cut of the tribofilms was carried out. A protective platinum layer was deposited on the tribofilm. First, a thin Pt layer was deposited by the electron beam followed by a thicker Pt layer deposited by the ion beam. The TEM images of the transversal FIB cuts showing the thickness of the tribofilms formed at room temperature and at 100°C can be seen in Figure 53a and b, respectively. The yellow dotted lines delimit the tribofilm. The light gray protective layer corresponds to the Pt deposited by the electron beam while the darker layer corresponds to the ion beam deposit. The EDX spectra recorded from the tribofilm formed at room temperature and at 100°C can be observed in Figure 53c and d, respectively.
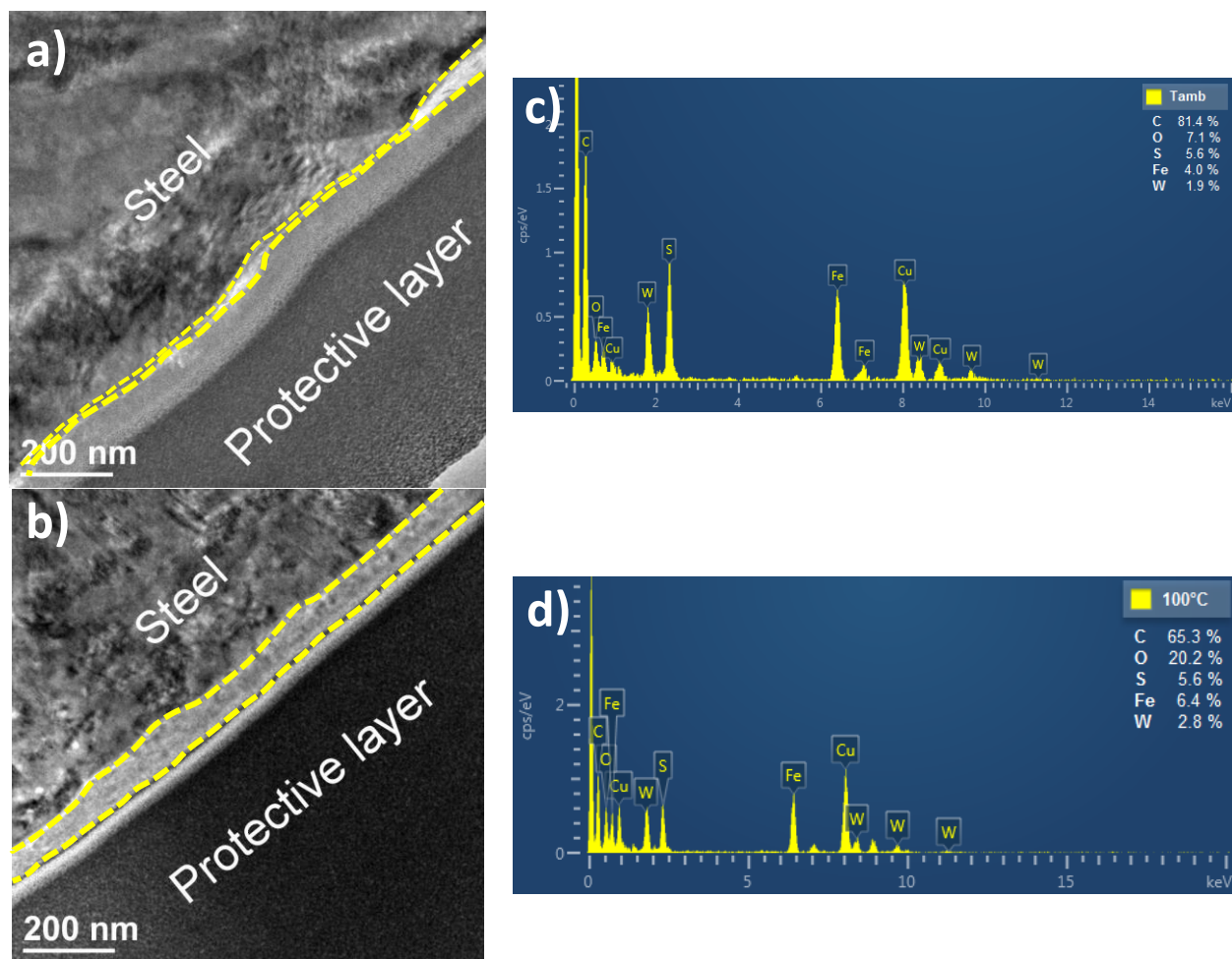
Figure 53.TEM images and EDX spectra of the tribofilms formed with the WS$_2$ nanoparticles in PAO at room temperature (a and c) and 100°C (b and d). The yellow doted lines delimit the tribofilm.

It can be observed that at room temperature, a thin and patchy tribofilm was formed on the steel surface. On the other hand, a more uniform tribofilm with a thickness of around 80nm was formed at 100°C. These results can be compared to those reported by Ratoi et al. (*103*) after lubricating smooth steel surfaces with tungsten disulfide nanoparticles in a MTM experiment at 40°C and 100°C. The authors found a patchy and thin tribofilm on the steel surface of around 30 nm thickness at 40°C and a more uniform tribofilm with an average thickness of 100 nm at 100°C. The thickness of the tribofilms was measured using 3D SLIM light interference imaging and Alicona 3D optical imaging in their work.

From the EDX spectra, it can be seen that oxygen concentration is higher for the tribofilm formed at 100°C than for the one formed at room temperature which agrees with the XPS results shown above.

6.2.1.1 *Tribological behavior of tungsten oxide nanoparticles*

The previous results suggest that the presence of tungsten oxide may be responsible for high friction coefficient and fluctuations when lubricating smooth surfaces with WS_2 nanoparticles at 100°C. In order to prove this, investigation on the tribological behavior of tungsten oxide nanoparticles under the same test conditions was done. Tungsten oxide nanoparticles were purchased from Sigma Aldrich as a powder with particle size of less than 100 nm. The sample tested consisted of 1 wt% of WO_3 in PAO base oil. The results were compared to those obtained using 1 wt% WS_2 nanoparticles in the base oil. The friction curves obtained for both samples can be observed in Figure 54.
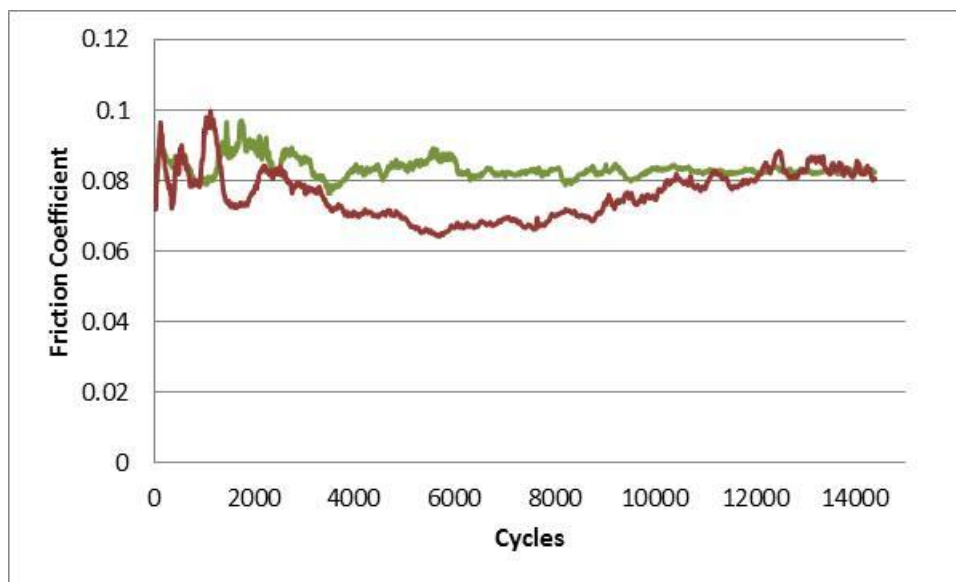
Figure 54. Friction coefficient as a function of cycles for the WS_2 nanoparticles (red) and the WO_3 (green) nanoparticles in PAO base oil at 100°C

Tungsten oxide nanoparticles give a steady stable friction coefficient of 0.08. This friction coefficient value corresponds to the highest value obtained for the fluctuations when using the WS_2 nanoparticles.

On the other hand, the scar diameters obtained for both samples are very similar as observed in Figure 55.
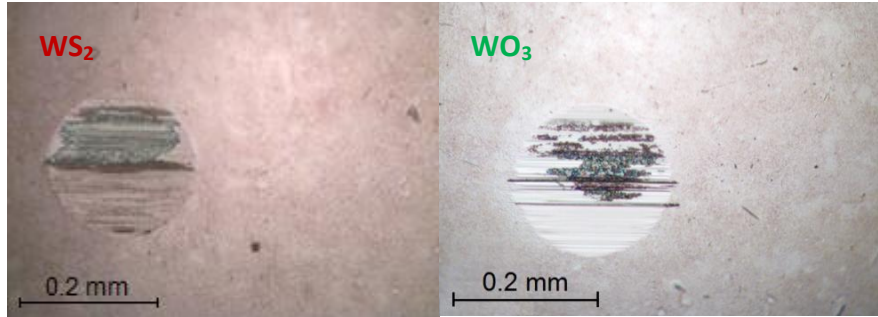
Figure 55. Wear scars after the test for the WS$_2$ nanoparticles (red, left) and the WO$_3$ nanoparticles (green, right) at 100°C

The fact that the nanoparticles may undergo an oxidation process can then explain the friction coefficient fluctuations observed, where 0.06 correspond to the lubrication provided by the WS$_2$ nanoparticles and 0.08 by the WO$_3$ ones. Therefore, in order to obtain low and stable friction coefficient oxidation should be avoided. This suggestion will be explored in the further in this work.

6.2.2   Nanoparticles behavior on rough surfaces

The industrial use of nanoparticles requires investigation on their lubricating properties under real life conditions. The research done on the lubricating properties of nanoparticles at the laboratory scale has mainly been done on smooth surfaces. Only, some research on the influence of surface roughness on the tribological properties of NT-MoS$_2$ at ambient temperature can be found in the literature, as discussed in section 3.4.1.6. However, industrial applications normally run at high temperatures and industrial surfaces are rougher than those tested by Kogovsek et al. (*91*) (arithmetical mean surface roughness Ra=6nm and Ra=40 nm). For this reason, it is important to study the effect of nanoparticles when lubricating rough surfaces where they could be blocked or trapped on the grooves (higher roughness than nanoparticles size). The TEM images showed that nanoparticles size varied between 50 to 130 nm. As a consequence, in this part of the work, disks with a roughness of 300 nm were used.

The friction tests were carried out using the industrial WS$_2$ nanoparticles on rough disks (Ra=300nm, Rz=1.21 µm), at room temperature and 100°C using the pin-on-flat tribometer described in section 6.2. The friction curves obtained are plotted in Figure 56.
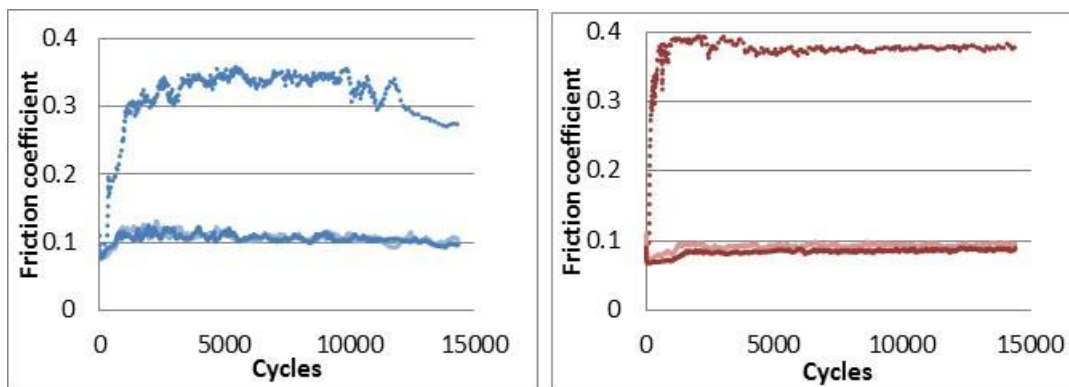
Figure 56. Friction coefficient as a function of the cycles for PAO (dotted lines) with and without (full lines) WS₂ nanoparticles on rough surfaces at room temperature (blue, left) and 100°C (red, right).

The results show that, as expected due to the asperities of the rough surfaces, the friction coefficient obtained are higher than for the smooth samples at both temperatures when using PAO as lubricant. Clear reduction of COF can be observed when the nanoparticles are used. Actually, a friction coefficient of around 0.1 was obtained for both temperatures with the use of nanoparticles whereas friction coefficient as high as 0.35 where obtained for the PAO alone.

The wear scars of the pins at the end of the test can be seen in Figure 57. Large wear can be observed for the base oil at both working temperature compared to the samples that contained the nanoparticles. Thus, it is evident that nanoparticles dramatically reduced wear on the rough surfaces too.
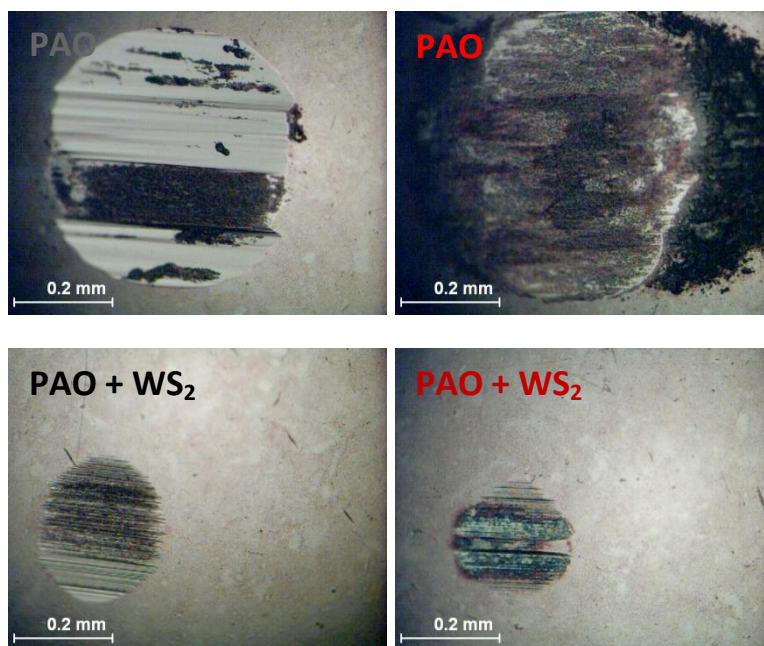
Figure 57. Wear scars of the pins when lubricating rough surfaces with PAO and PAO + WS₂ nanoparticles at ambient temperature (blue, left) and 100°C (red, right)

These results show that the use of nanoparticles reduced significantly not only the friction coefficient (50% at room temperature and 78% at 100°C), but also the wear (70%) at both temperatures. The value of COF obtained at both temperatures is close to 0.1 which is higher than for the smooth surfaces. According to the previous section, this may indicate that nanoparticles have undergone oxidation. Actually, the tribofilm may have been more easily oxidized on the rough surfaces than on the smooth ones because of the harder contact conditions. In order to verify the tungsten concentration in an oxide form in the tribofilms, XPS analyses were carried out on the worn surfaces. The spot size was 50 µm with a power of 12.5W. The analyses were made twice for each sample and showed good reproducibility. The tungsten spectra recorded for the tribofilm formed at room temperature and at 100°C are shown in Figure 58.
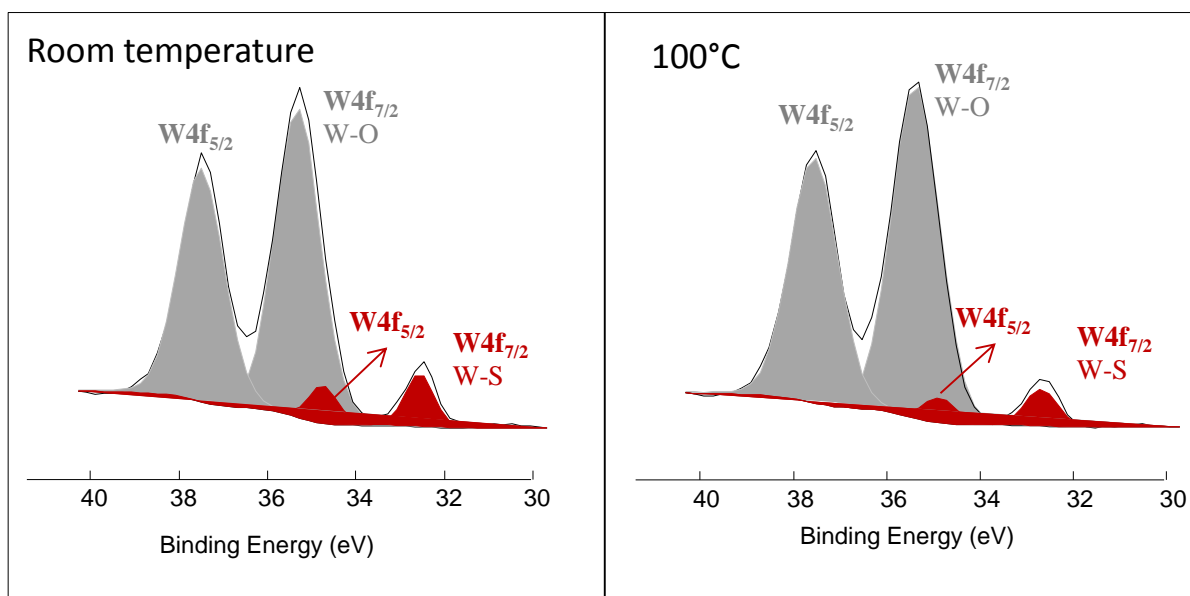
Figure 58. Tungsten XPS spectra of the tribofilm formed at room temperature and at 100°C

It can be seen that tungsten is mainly found bonded to oxygen atoms in both tribofilms. Actually, approximately 90% of the total tungsten was found in a tungsten oxide form. This might explain the higher friction coefficients obtained on the rough surfaces compared to the smooth ones. Nevertheless, contact between the asperities of the rough surfaces cannot be neglected and may also explain the higher friction coefficients obtained compared to the smooth surfaces. Actually this might explain why a slightly higher friction coefficient was obtained at room temperature than at 100°C on the rough surfaces. As seen before, a thinner tribofilm is formed at room temperature than at 100°C. It is then possible that contact between the asperities might have happened more often at room temperature than at 100°C, where a thicker tribofilm can be formed.

Even if friction tests were conducted at room temperature and at 100°C in this work, the following section presents only the analyses of the worn surfaces for the tests done at 100°C.

A contour GT-K1 Bruker interferometer was used to study the topography of the wear tracks on the rough flats. The images obtained can be seen in Figure 59. The complete wear track obtained when lubricating the surfaces with PAO and with the nanoparticles containing sample can be observed in Figure 59a and c, respectively. A closer look of the wear tracks can be observed in Figure 59b and d. It is important to note Figure 59aand c are at the same scale whereas Figure 59b and d are not. Actually, in order to be able to observe better the wear track obtained with the use of the nanoparticles the scale was changed on purpose. From these images it can be seen that a larger and deeper wear track is obtained with the use of PAO alone than when the nanoparticles are used. The roughness inside the wear track was measured for both samples. The results showed that the roughness for PAO increased from 300 nm (initial roughness of the flat) to 560 nm whereas it decreased to 45 nm for the samples containing the nanoparticles. This clearly shows that abrasive wear occurred for the first samples and suggest the presence of a tribofilm for the second one.
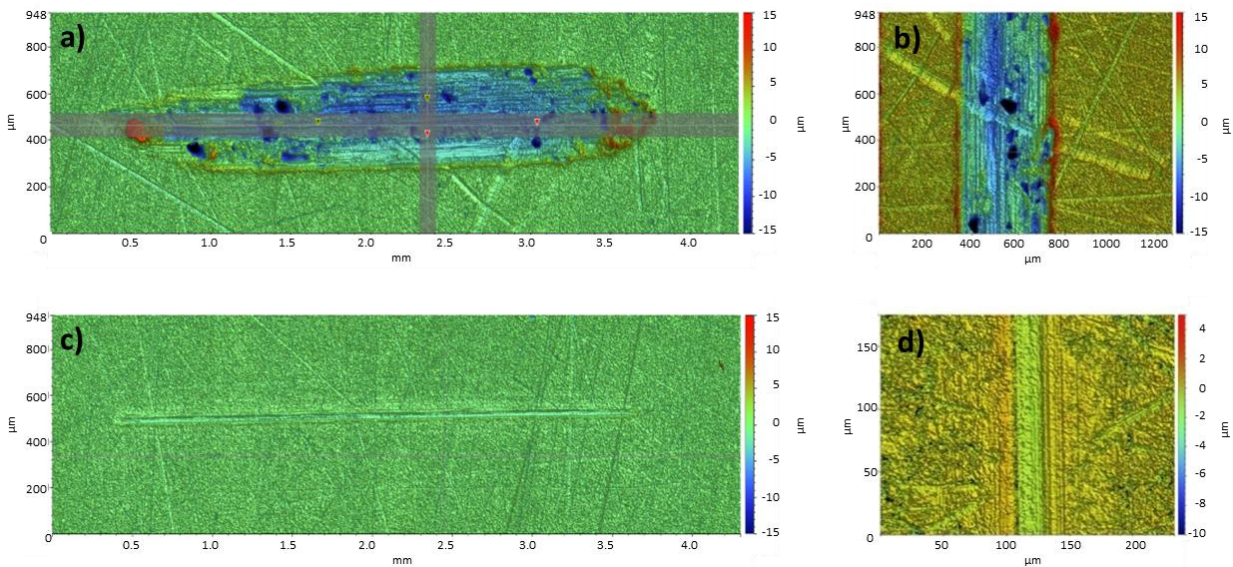
Figure 59. Wear scars of experiments carried out at 100°C on the rough flats, where a) and b) correspond to the images of the complete wear track and a closer view of the rough flat lubricated with PAO while c) and d) correspond to those of the flat lubricated with the nanoparticles in PAO

In order to prove the presence of such tribofilm observations and a chemical mapping of the wear track were done using a XL30 Low vacuum and Environmental Scanning Electron Microscopy (ESEM-FEG) equipped with EDX (spot size 10nm). The presence of tungsten sulfur and oxygen on the wear track testifying the presence of a tribofilm on the rubbed surface can clearly be seen in Figure 60. It can be seen that tungsten and sulfur signals are much more important in the zones where large groves are observed, than in the rest of the wear track.
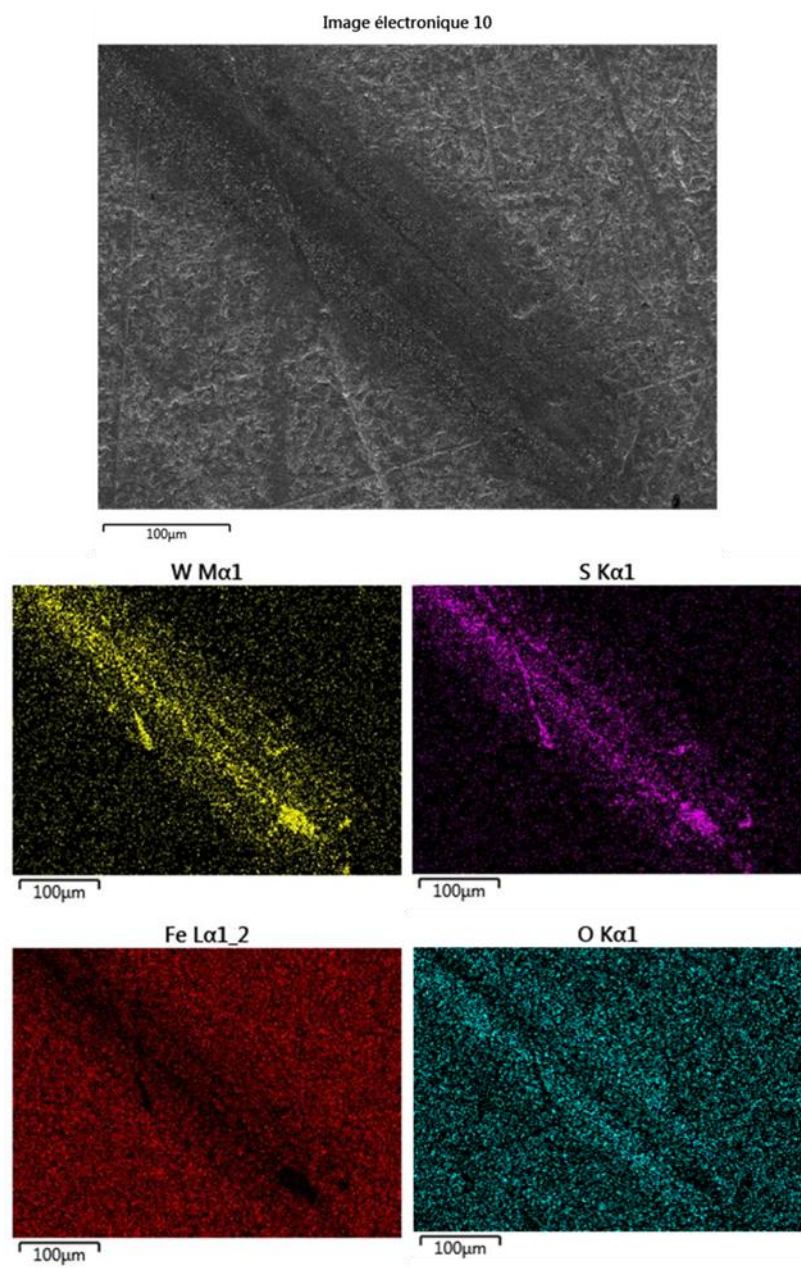
Figure 60. Chemical mapping of the wear track obtained when using the industrial WS$_2$ nanoparticles on a rough flat at 100°C

A closer look at these zones can be observed in Figure 61. The roughness of these zones measured by the Bruker profilometer was 20 nm which is lower than for the rest of the wear track.
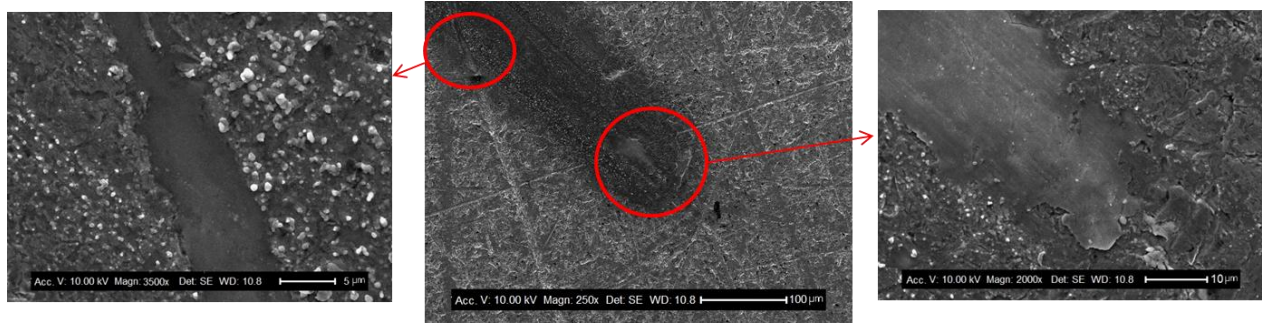
Figure 61. Closer looking of the zones with important tungsten and sulfur signals

The images shown in Figure 60 and Figure 61 suggest that nanoparticles have been trapped in the grooves of the flat surface. Kogovsek et al. (91) have demonstrated that MoS2 nanotubes accumulate at steel surface grooves in the wear scar at room temperature. However, no evidence that the groove was completely filled by the nanoparticles was provided. As a consequence, a transversal FIB cut was carried out on a fresh sample in one of these zones to prove this. The chemical mapping as well as the area chosen for the cut can be observed in Figure 62.
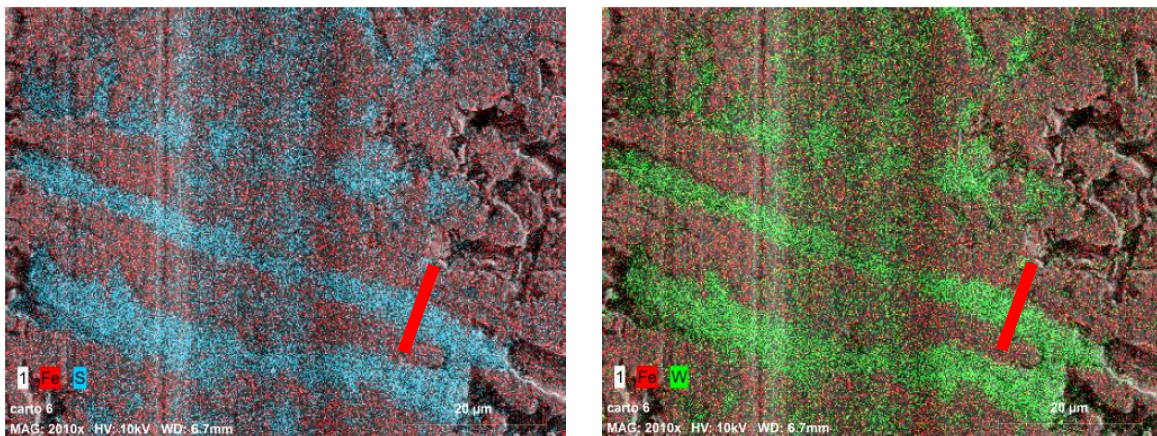
Figure 62. Iron, tungsten and sulfur chemical mapping of the wear track for the cross FIB cut. The red line indicates the zone where the transversal cut was done

SEM and TEM imaging revealed that the groove was around 4 μm width and 1 μm deep as seen in Figure 63 and Figure 64 respectively.

89
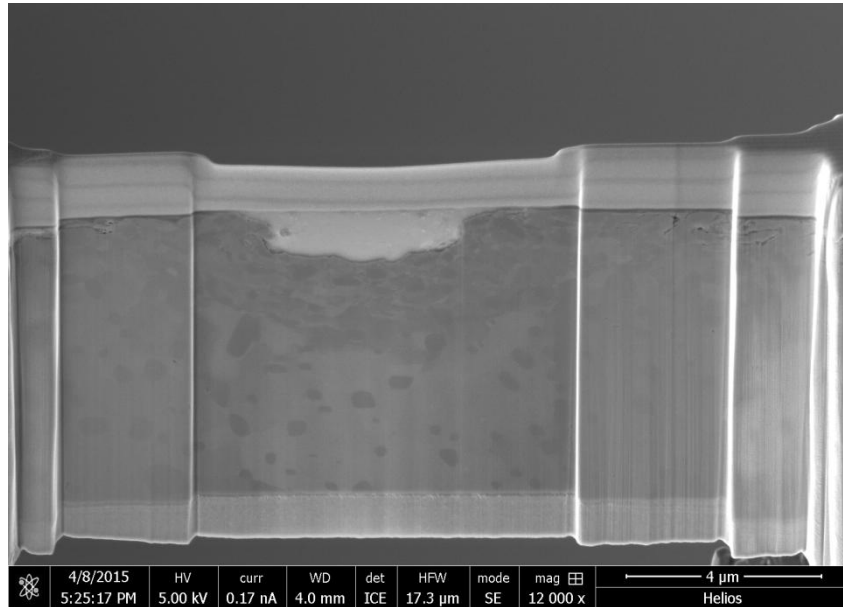
Figure 63. SEM image of the FIB transversal cut showing the groove
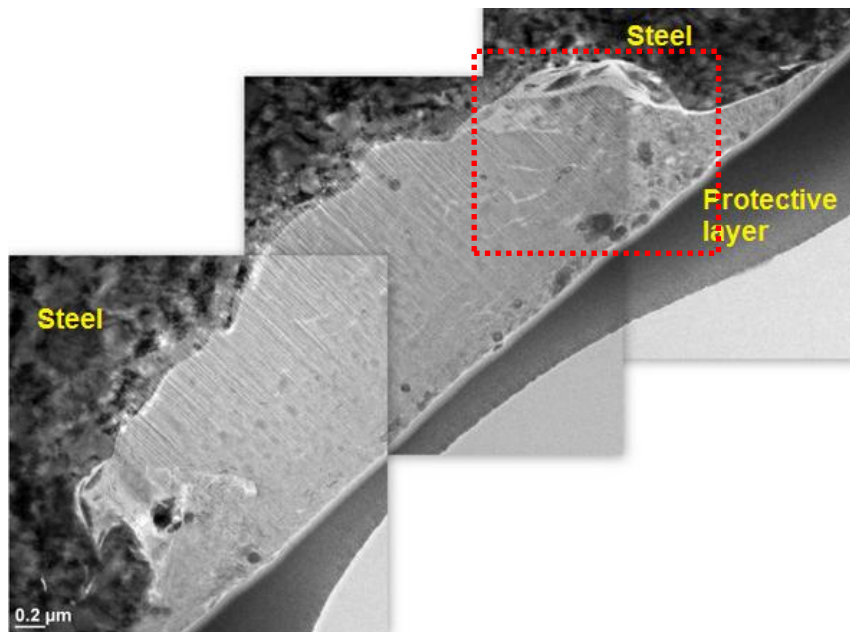
Figure 64.TEM image of the groove. The red rectangle shows the area where EDX mapping was done

Some damage of the sample during the FIB milling seems to have taken place where some lines are observed (Figure 64.). These lines are mainly present near the steel on the deepest part of the groove suggesting that curtaining effect has occurred. This phenomenon is mainly caused by cutting though very different materials, just like in this case. EXD mapping of the zone delimited by the red rectangle in Figure 64 was carried out. The results revealed the presence of tungsten and sulfur everywhere inside the groove as can be seen in Figure 65.
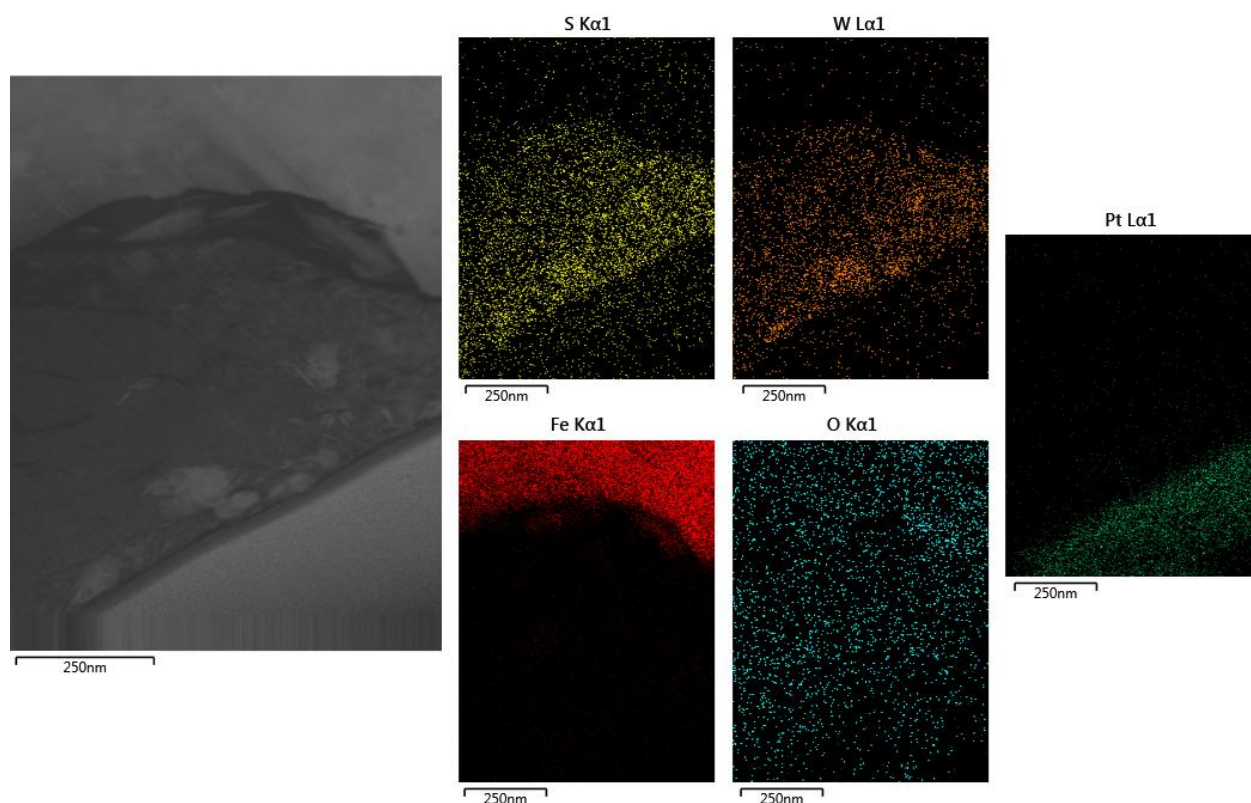
Figure 65. Chemical mapping of the red rectangle area shown in Figure 64, proving the presence of tungten and sulfur inside the groove

Even if some damage occurred during the preparation of the cross-cut, the presence of some nanoparticles and some sheets of WS_2 could be observed by TEM as it can be seen in Figure 66. They were mainly found in the right and upper part of the groove shown in Figure 64.
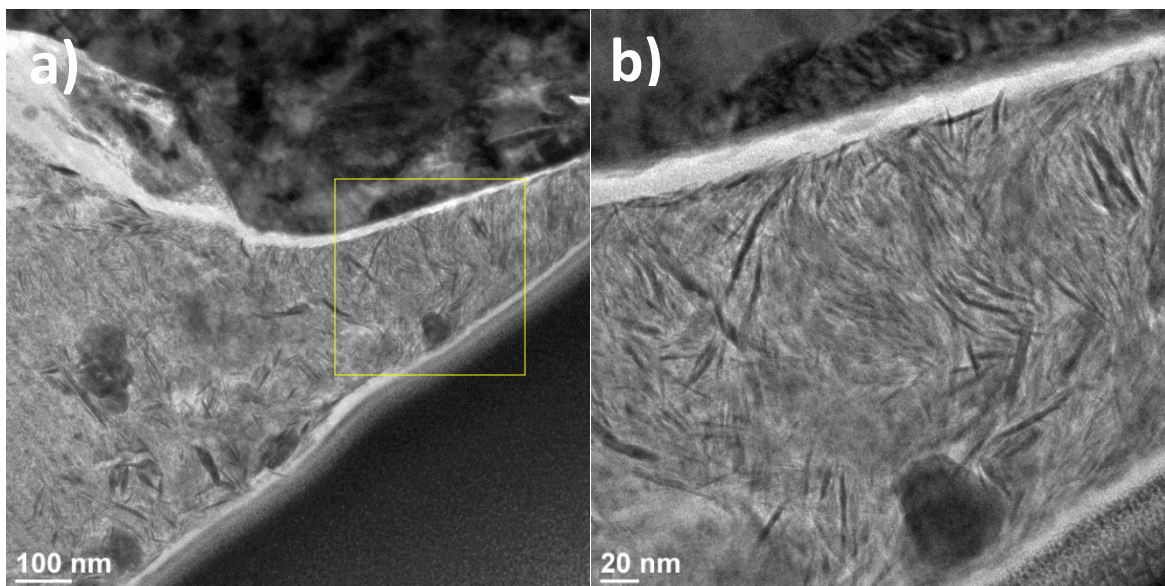
Figure 66. Presence of some nanoparticles and sheets of WS$_2$ inside the groove

It is possible that the nanoparticles trapped in the steel grooves may be liberated to provide proper lubrication in the case of deficient feeding of nanoparticles to the contact. To prove this, an additional experiment where PAO alone was used to lubricate a preformed tribofilm on the rough surface was carried out. The experiment consisted of two steps of one hour each. The disk and the ball were both cleaned with a heptane wet wipe between the two steps. The same experiment was also carried out on the smooth surfaces for comparison. The friction coefficient as a function of the number of cycles obtained on both surfaces can be observed in Figure 67. The vertical yellow line represents the change of the lubricant from PAO + 1% WS$_2$ to PAO alone.
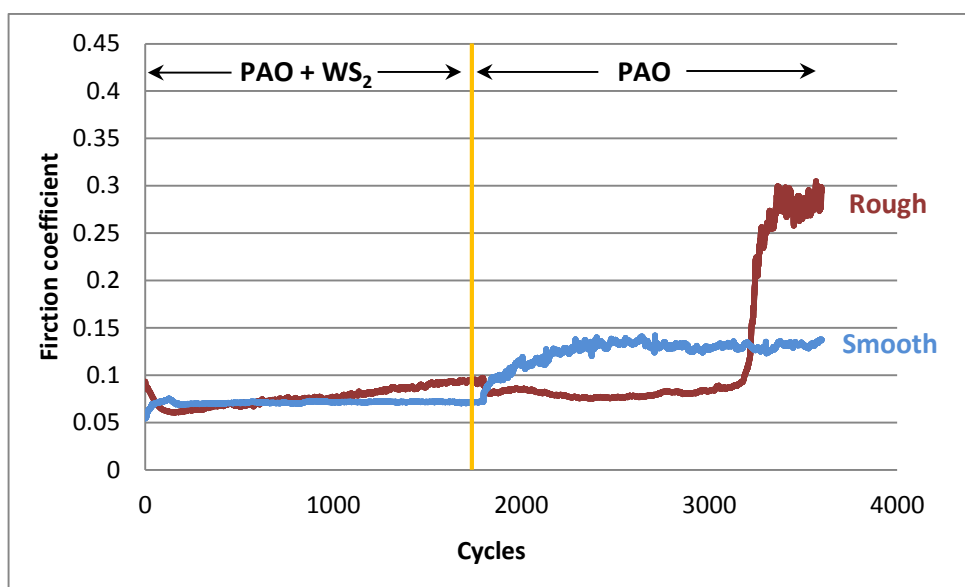
Figure 67. Friction curves obtained for the two step experiments on the rough (red) and the smooth (blue) surfaces. The yellow line represents lubricant change from PAO + WS$_2$ to PAO alone

It can be seen that in the case of the rough flat, the friction coefficient stays low for almost 45 minutes after the lubricant replacement before going up until 0.3 whereas an immediate increase is observed in the case of the smooth flat, reaching a value close to what we usually have in these conditions with pure PAO base oil (0.1). This high value of friction coefficient which is actually very close to the one obtained by the PAO on the rough surfaces suggests that the tribofilm formed by the nanoparticles has been rubbed off. This proves that the tribofilm formed on the rough surfaces can provide good lubrication to the contact during deficient nanoparticles fed during short periods. In order to compare this behavior with the molecular additives used nowadays an additional experiments was carried out under the same test conditions using 1 wt% MoDTC in PAO on the rough surfaces. The friction curve obtained can be observed in Figure 68.
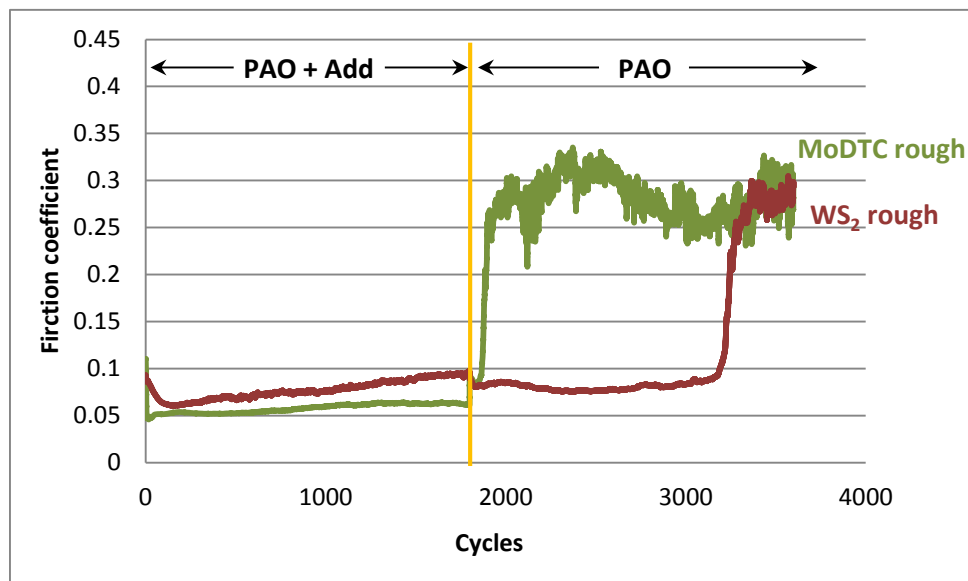
Figure 68. Friction curves obtained for the two step experiments on the rough surfaces with either MoDTC or WS₂ in PAO. The yellow line represents lubricant change to PAO alone

It can be seen that in the case of MoDTC the friction coefficient increases immediately after the lubricant change to a value of 0.3 showing that the MoDTC preformed tribofilm has been removed faster than the one formed by the nanoparticles.

7. Tribological behavior of industrial WS₂ nanoparticles in the presence of additives commonly used in the automotive industry

To be able to formulate an efficient nanoparticle-doped lubricant, minimum wear and maximum friction reduction needs to be guaranteed. The previous section showed that a friction coefficient of 0.06 can be achieved when lubricating steel surfaces with industrially produced WS₂ nanoparticles in PAO base oil. Nevertheless, lubricants are a complex mixture of different additives (as exposed in section 3.3) that can have either a synergistic or an antagonistic effect with the nanoparticles. As a consequence, the tribological behavior of the nanoparticles in the presence of the additives commonly used in the industry must be investigated. As exposed in section 3.4.1.4.1.2, only the effect of dispersant additives on the tribological behavior of nanoparticles has been studied in detail. The research has demonstrated that succinimide based dispersants, inhibit nanoparticles to create a tribofilm on steel surfaces (*104*) when used at the treat-rates used in the automotive industry. Thus, other dispersion alternatives must be considered in the formulation of nanoparticles-doped lubricants.

In order to provide clues for the formulation of efficient nanoparticles containing lubricants and with the aim of avoiding tungsten oxide formation due to oxidation under high temperatures, the effect of additives with anti-oxidant properties was first studied in this work. As described in section 3.3.2, aromatic amines sulfur and phosphorous compounds are commonly used as anti-oxidant additives. Therefore, a diphenylamine and a secondary zinc dithiophosphate were used to investigate the effect of anti-oxidants on the tribological performance of industrially produced WS₂ nanoparticles. Then, the nanoparticles performance in the presence of a mixture of ZDDP and calcium phenate detergent was studied at the end of this section.

7.1 WS₂ nanoparticles tribological behavior in the presence of a diphenylamine anti-oxidant

In the automotive industry, lubricants undergo oxidation due to heat, severe pressure, the presence of metal and air. Oxidation results in the decomposition of base oils and additives, which affects lubricants efficiency and shortens its life. The oxidation process of lubricants is known to happen on a three step process. In the first step, called initiation; a free radical is formed. In the second step, known as propagation, the free radical reacts with oxygen to give peroxide radicals. These radicals produce more radicals after reaction with other components of the lubricant. In the third step, called termination, two radicals combine and form a stable compound. Figure 69 shows a schematic representation of this three-step process.

Initiation	$RH \rightarrow R\cdot + H\cdot$
Propagation	$R\cdot + O_2 \rightarrow ROO\cdot$
	$ROO\cdot + RH \rightarrow ROOH + R\cdot$
Termination	$R\cdot + R' \rightarrow R - R'$
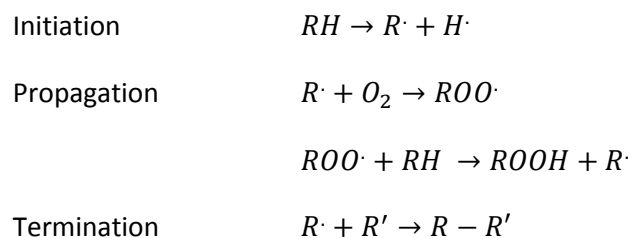
Figure 69. Lubricants oxidation schema

Diphenylamine antioxidants are widely used anti-oxidant additives in the automotive industry. They act as hydrogen donors to stop radical propagation process. Figure 70 illustrates a generic structure of diphenylamine.
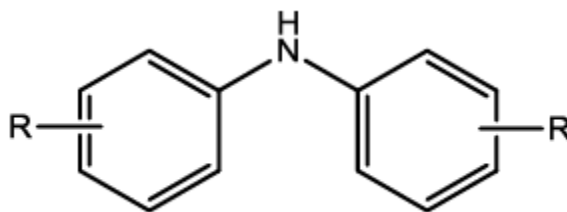
Figure 70. Generic structure of diphenylamines

Tribological testing of nanoparticles in the presence of an alkyl diphenylamine antioxidant was carried out using the pin-on-flat tribometer shown in Figure 46 at 100°C under the test conditions summarized in Table 4. The tungsten disulfide nanoparticles were dispersed in a concentration of 1 wt% in PAO base oil with 2 wt% antioxidant. The results were compared to the reference sample that consisted of 2 wt% antioxidant in the PAO base oil. The friction curves obtained are plotted in Figure 71, where the purple dotted line represents the reference sample and the two orange curves represent the results obtained for the sample that contained the nanoparticles. Once again, reproducibility problems and friction coefficient fluctuations from 0.06 and 0.08 were observed with the use of the nanoparticles. On the other hand, a friction coefficient of around 0.1 was obtained for the reference sample. This is the same COF value that was obtained for the PAO when tested alone (Figure 47). Actually, no information can be found on the tribological behavior of diphenylamine anti-oxidants because they are not expected to react with the steel surfaces.
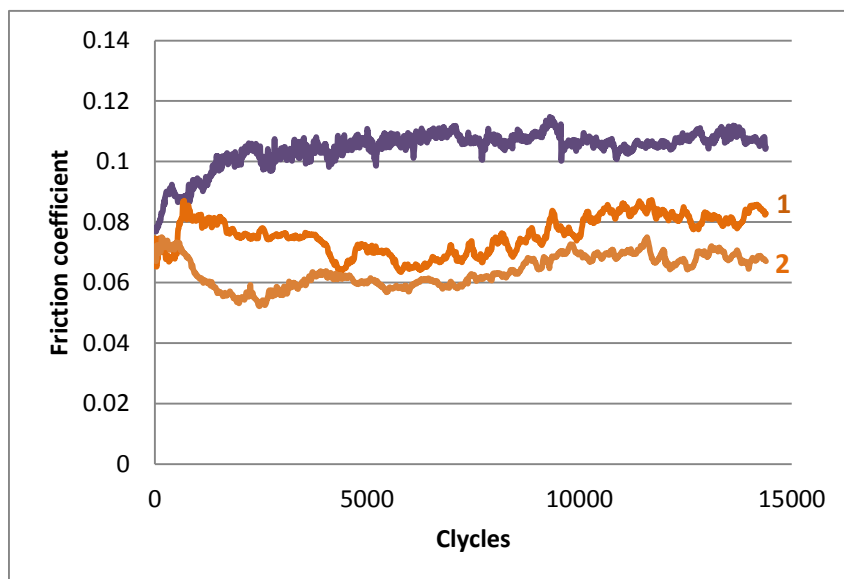
Figure 71. Friction curves obtained for the diphenylamine antioxidant in PAO (purple) and for the WS$_2$ nanoparticles in the presence of the antioxidant at 100°C (orange 1 and 2)

These results suggest that diphenylamine antioxidant don't interfere in nanoparticles tribofilm formation. To prove this, chemical characterization of the tribofilm formed by the nanoparticles after the friction tests was done using XPS. Both worn surfaces were analyzed (curve 1 and 2 in Figure 71). The analyses were done twice and showed good reproducibility. The spot size used for the analysis was 50 μm with a power of 12.5 W. The same elements were observed in the survey scans done for both tribofilms. The survey scan spectrum obtained is illustrated in Figure 72a. It can be seen that only sulfur, tungsten, iron, oxygen and carbon were detected while no nitrogen peak was identified (N1s peak position is at around 400 eV). This clearly shows that the antioxidant didn't take part in tribofilm formation. This proves that no interaction between the nanoparticles and the antioxidant occurred which agrees with the friction curves obtained. The only difference observed between both friction curves obtained was seen in the tungsten oxide content. Around 80% of the total tungsten corresponded to tungsten oxide; in the case of the tribofilm that gave the friction curve number 1 whereas 52% for number 2 (Figure 72b and c, respectively).
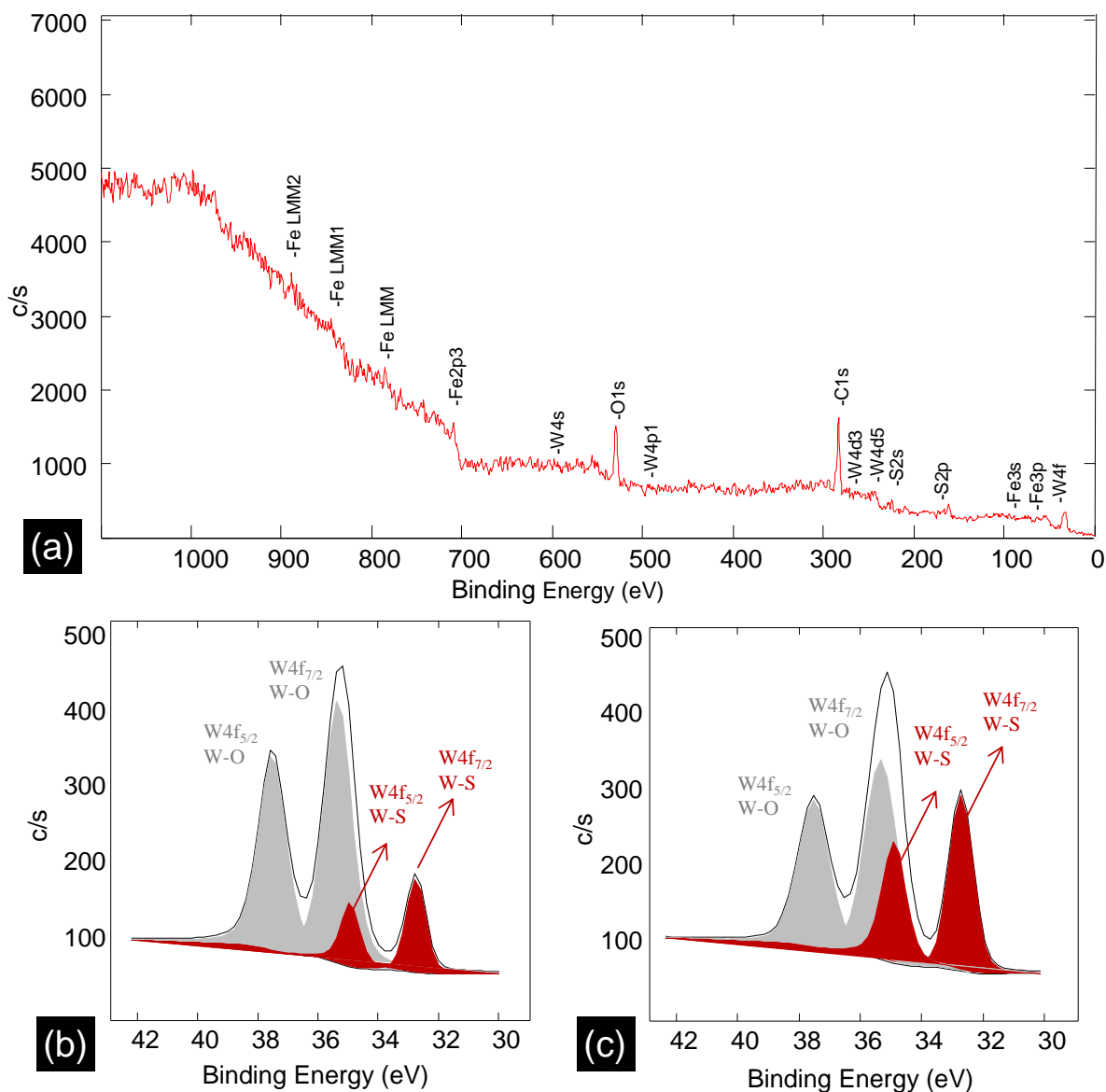
Figure 72. XPS spectra of the tribofilm formed by the nanoparticles in the presence of a diphenylamine antioxidant; a) survey scan; b) W4f spectrum of the tribofilm that gave the friction curve marked as 1 in Figure 71 and c) W4f spectrum of the tribofilm that gave the friction curve marked as 2 in Figure 71

These results show that this anti-oxidant additive, of which key role is to inhibit base oil oxidation process, does not have any detrimental effect on the tribological performance of nanoparticles so it can be used in the formulation of nanoparticles-doped lubricants.

7.2   Interaction between ZDDP and WS$_2$ nanoparticles

Zinc-dialkyl dithiophosphate additive is one of the most commonly used additives in the automobile industry. It is mainly known as an anti-wear additive but it also has anti-oxidant and extreme pressure properties. ZDDP anti-wear properties seem to be linked to the ability of phosphate glasses to digest oxides. Synergistic effect between MoDTC and ZDDP additive due to MoS$_2$ formation has been reported by several authors (*58, 59, 123*)

The effect of ZDDP on the tribological behavior of WS$_2$ nanoparticles must now be investigated.

7.2.1   WS$_2$ nanoparticles in the presence of ZDDP additive on smooth surfaces

A commercial secondary ZDDP additive was used for the experiments. The tribological tests were carried out on the smooth surfaces at 100°C. The usual additive treat rate for engine applications is 1 wt%. As a consequence, the sample consisted of 1 wt% WS$_2$ blended with 1 wt% ZDDP in PAO. The results were compared to those previously obtained by the nanoparticles in the base oil. The reference for the ZDDP (1 wt%) in PAO (without nanoparticles) was also plotted for comparison. The friction curves obtained for the different samples are plotted in Figure 73. The average friction coefficient measured for the samples can be observed in Figure 74.
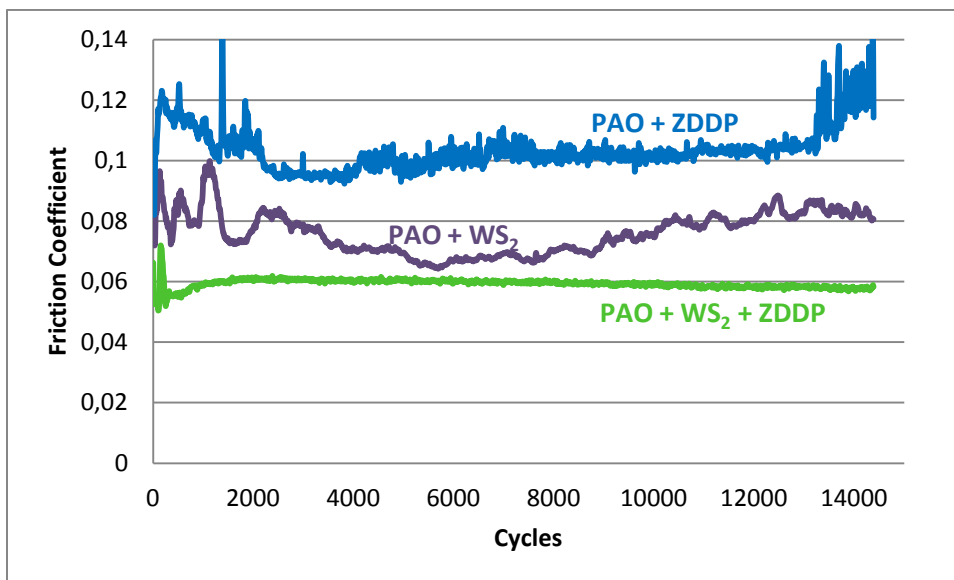
Figure 73. Coefficient of friction as a function of cycles for the different samples
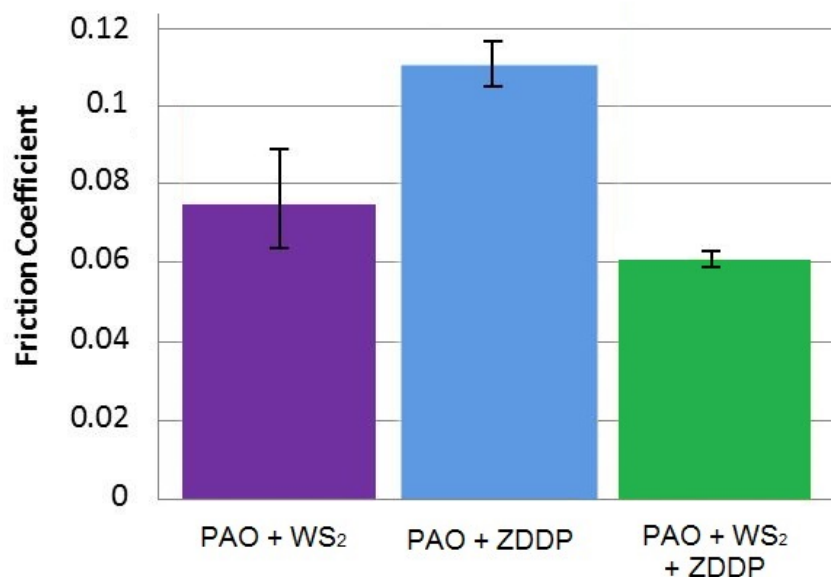
Figure 74. Average friction coefficient for the different samples

It can be seen that the ZDDP reference sample (PAO + ZDDP) gives a friction coefficient that rises up to 0.12 during the first 100 cycles and then decreases progressively until stabilization at approximately 0.1 after 1h. The addition of nanoparticles to this sample (PAO + WS$_2$ + ZDDP) gives a low and stable COF during all test length. Moreover good reproducibility was observed. This was not the case for the nanoparticles in the base oil (PAO + WS$_2$) where not only important friction coefficient fluctuations but also reproducibility problems were seen.

Concerning wear, the nanoparticles blended with the ZDDP also gave better results compared to the two other samples as observed from the images of the wear scars in Figure 75 and the calculated wear coefficients in Figure 76.
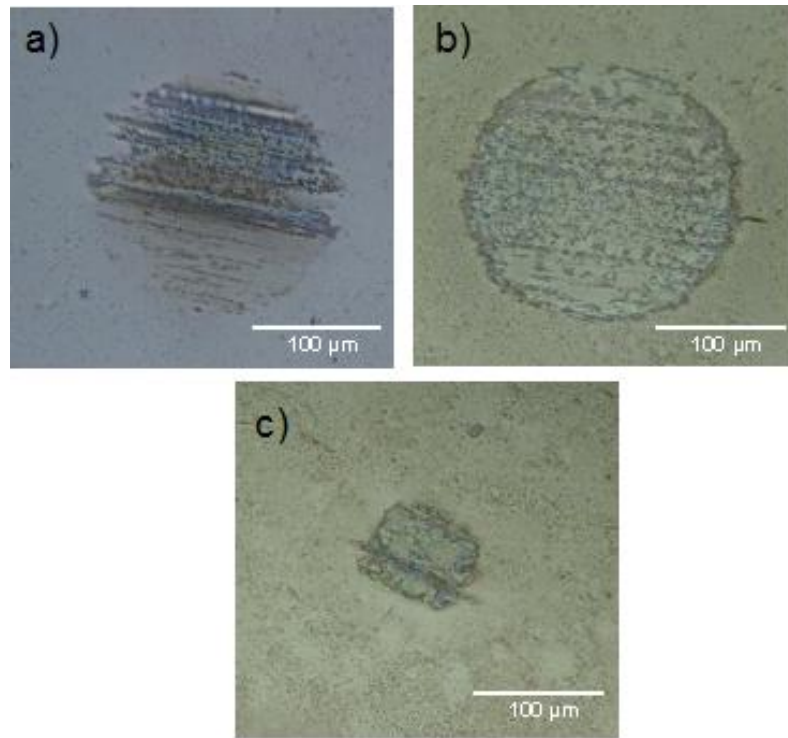
Figure 75. Wear scars of a) PAO + WS$_2$, b) PAO + ZDDP and c) PAO + WS$_2$ + ZDDP
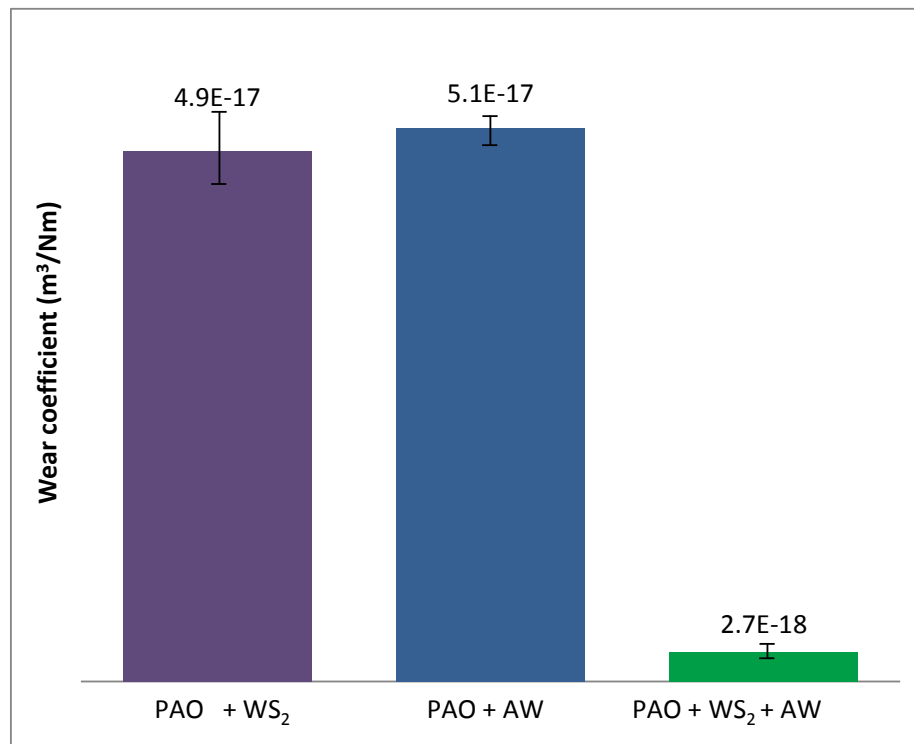
Figure 76. Wear coefficient for the different samples

These results demonstrate that ZDDP not only allows stabilization of the friction coefficient to the lowest value, but also that the friction reducing properties of the particles are enhanced by the ZDDP properties. This means, that ZDDP additive can be used in the formulation of industrial nanoparticle-doped lubricants.

In order to understand the better results exhibited by the nanoparticles in the presence of ZDDP a chemical characterization of the tribofilm formed on the steel flat was carried out using XPS technique. The XPS analyses were made twice for each sample and showed good reproducibility. The spot size was 18 µm with a power of 4.6W. The results are summarized in Figure 77. The general spectrum (Figure 77a) shows the presence of sulfur, phosphorus, zinc, tungsten, oxygen and carbon, confirming the contribution of the two additives (ZDDP and WS_2) in the tribofilm formation. Iron is also detected in a low concentration (<1%). Figure 77b and c show respectively the W4f and S2p XPS spectra. Two $W4f_{5/2}$ peaks are observed in Figure 77b, one corresponding to W-S at 32.5 eV and another one which corresponds to W-O bond at 35.9 eV. Sulfur is also present in two chemical states: as sulfide (WS_2 or FeS_2) at 162.03 eV and as sulfate (SOx) at 168.8 eV (Figure 77c). Thus, tungsten and sulfur are found in the same chemical environments in the nanoparticles and the tribofilm.

Figure 77. XPS spectra of the tribofilm formed by the nanoparticles in the presence of ZDDP additive on the smooth steel flat; a) survey scan; b) W4f energy region and c) S2p energy region

These results were compared to those obtained with the nanoparticles in base oil (without ZDDP). Additionally, the tribofilm formed by the ZDDP reference sample (PAO + ZDDP) was also characterized so the P2p and Zn2p peaks can be compared to those obtained with the nanoparticles/ ZDDP system. The binding energies of the main fitted peaks and corresponding chemical species for the three samples studied are shown in Table 5.

Table 5. XPS binding energies and corresponding chemical species in the tribofilms formed on the steel surface for the nanoparticles in PAO, the ZDDP in PAO and the nanoparticles with the ZDDP in PAO

Sample	P 2p peaks	Zn 2p peaks	S 2p peaks	W 4f peaks
PAO + WS$_2$	- -	- -	162.4 eV Sulfide (11%)	32.7 eV WS$_2$ (15%)
			168.7 eV Sulfate (89%)	35.8 eV WO$_x$ (85%)
PAO + ZDDP	133.7 eV Phosphate (100%)	1021,9 eV ZnS/ZnO/Zn phosphate (100%)	162.0 eV Sulfide (98%)	- -
			168.7 eV Sulfate (2%)	
PAO + WS$_2$ + ZDDP	133.8 eV Phosphate (100%)	1022,2 eV ZnS/ZnO/Zn phosphate (100%)	162.2 eV Sulfide (95%)	32.5 eV WS$_2$ (85%)
			168.6 eV Sulfate (5%)	35.9 eV WO$_x$ (15%)

It can be observed that the concentration of tungsten in an oxide form on the tribofilm formed by the nanoparticles in the presence of ZDDP is 15 wt% which is very low compared to the sample without ZDDP (85%) but slightly higher than for the nanoparticles powder (5.5 wt%). This result seems to line with the fact that in-situ tungsten oxide generation during the friction test might be responsible for the reproducibility problems and the friction coefficient fluctuations observed for the nanoparticles in base oil at 100°C.

In order to study the changes in elementary composition through the tribofilm obtained with the nanoparticles in the presence of ZDDP, XPS with depth profiling sputtering was carried out. Figure 78a shows the depth profile of all the elements in the tribofilm. It can be seen that carbon was found on the surface, probably due to the degradation of the oil during the test. On the contrary, iron signal is very weak during the first minutes and then increases drastically for further stabilization and final increment when approaching the steel surface. When steel surface is reached by the ion beam, phosphorus and zinc signals decrease as expected. Figure 78b shows clearer tungsten and sulfur profiles. It can be seen that the low iron signal seen during the first etching minutes matches with a high concentration of tungsten and sulfur elements. The concentration of these two elements, sulfur and tungsten, decreases fast after the first etching 5 min. This suggests that they are present mainly at the top surface of the tribofilm.

From these XPS results, it can be concluded that the tribofilm is composed of a mixture of zinc/iron phosphate and WS$_2$ compound, with a higher concentration of W and S in the upper part of the tribofilm. However, XPS technique does not allow commenting on the morphology of this WS$_2$ present on the top surface of the tribofilm.
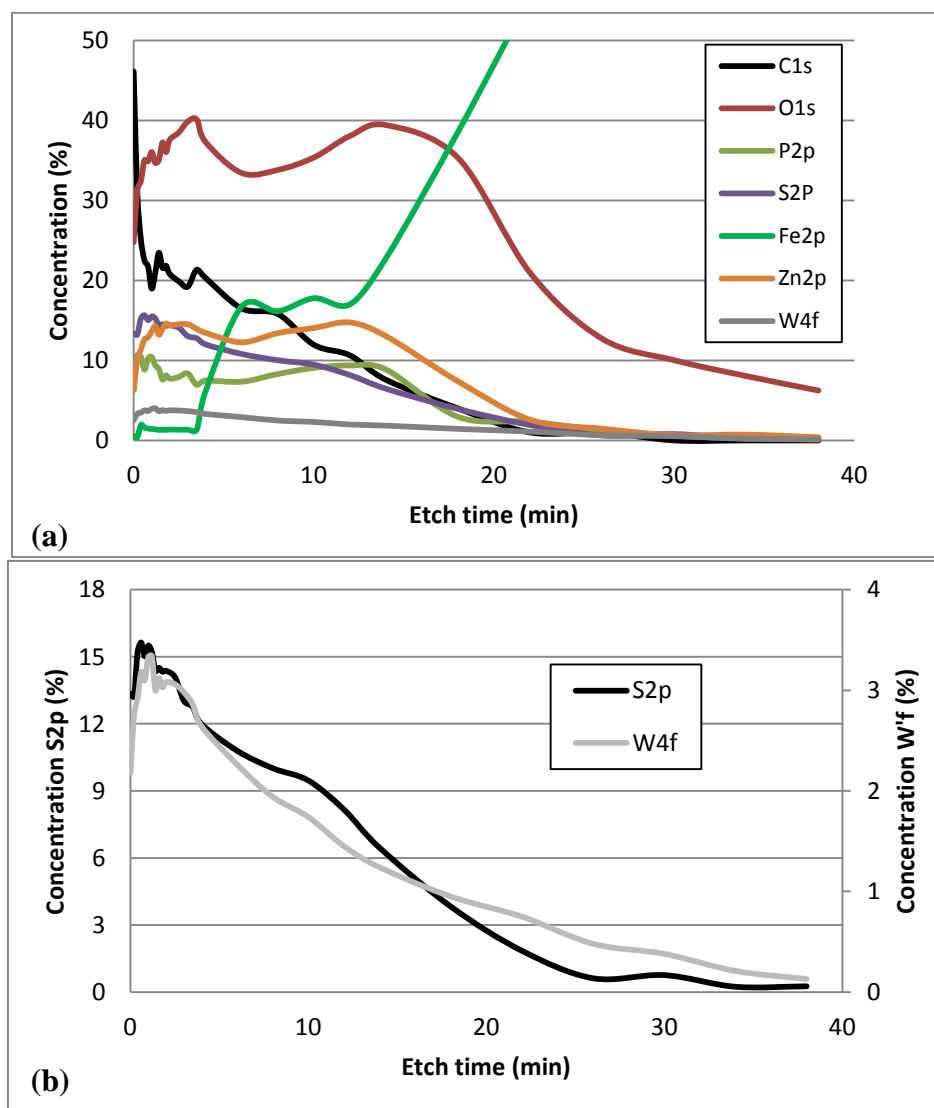
Figure 78: XPS depth profile on the tribofilm formed by the nanoparticles in the presence of ZDDP; a) Evolution of the concentration of all the elements, b) zoomed on tungsten and sulfur elements

As a consequence, to clarify the composition of this tribofilm and its thickness, a transversal cut was made by FIB technique in the wear track. The TEM images of the FIB cut, Figure 79 and Figure 80, revealed that thickness of the tribofilm varies between 50 and 60 nm. The tribofilm is mainly composed of zinc phosphate generated by the ZDDP anti-wear additive (lower part of the tribofilm, Figure 79b) with 2H-WS$_2$ sheets found mainly in the upper part of the tribofilm (Figure 80a and b) confirming the XPS results. Few non-exfoliated WS$_2$ nanoparticles were also observed in the tribofilm (Figure 79a). The EDX spectrum recorded from this particle (Figure 79c) confirms that it is mainly composed of tungsten and sulfur. The interplanar distance corresponding to the d002 was measured from Figure 80b and was

found to be approximately 0.64 nm. The same d002 value was found by Parigrahi and Pathak [25]. The value of the corresponding d002 spacing for the bulk $2H\text{-}WS_2$ is 0.618 nm (from JCPDS file).
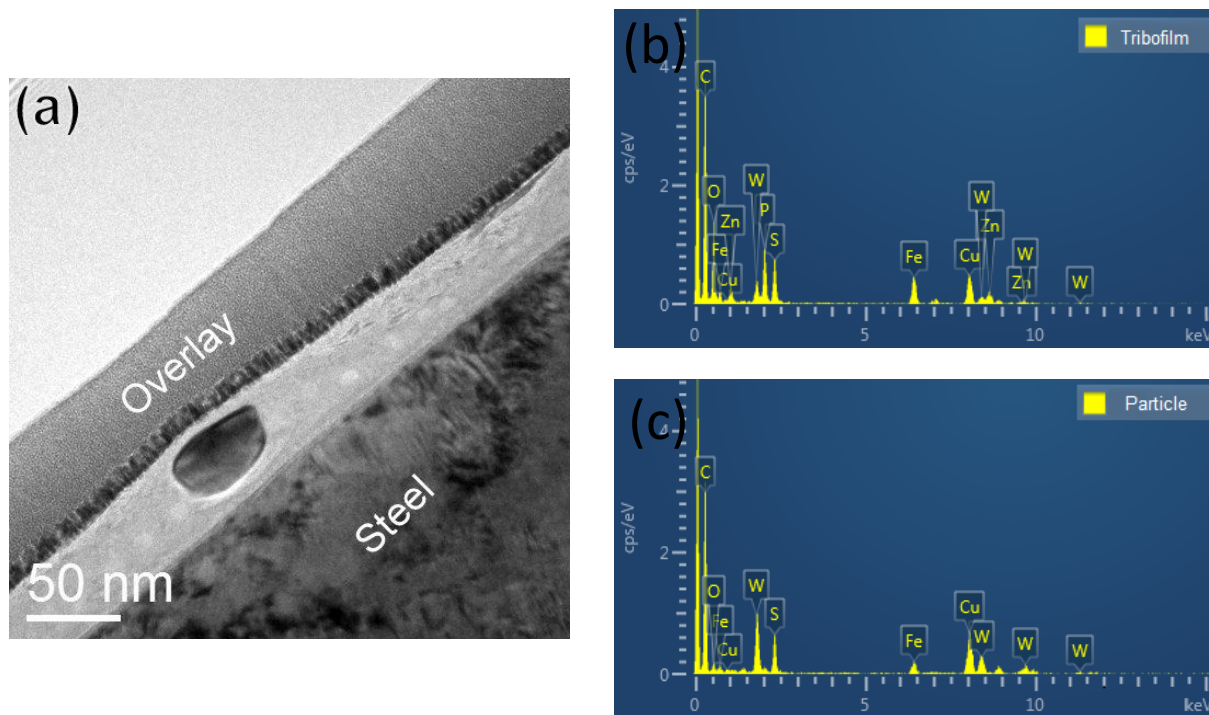
Figure 79. a) TEM image of the tribofilm showing the presence of WS$_2$ sheets, and the presence of a WS$_2$ nanoparticle embedded in the tribofilm formed by the nanoparticles in the presence of ZDDP. b) EDX spectra recorded from the tribofilm and c) EDX spectrum recorded from the nanoparticle
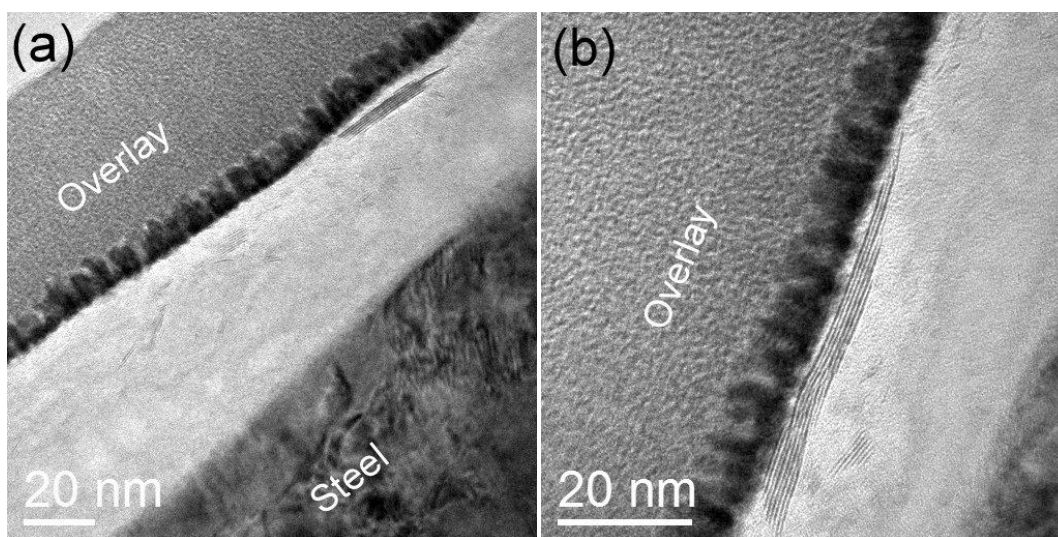
Figure 80. TEM images of the tribofilm showing the presence of WS$_2$ sheets in the tribofilm formed by the nanoparticles in the presence of ZDDP additive

The results obtained up to this point suggest that there is synergistic effect between the nanoparticles and ZDDP additive. However, in order to prove synergy between the two additives an additional test was carried out with 0.5 wt% of nanoparticles and 0.5 wt% of ZDDP in PAO so the total additive concentration was equal to 1 wt%. The friction curve obtained for this sample can be observed in Figure 81. It can be seen that the results are similar to those obtained with the sample containing higher concentration of both additives (wear behavior was also the same).
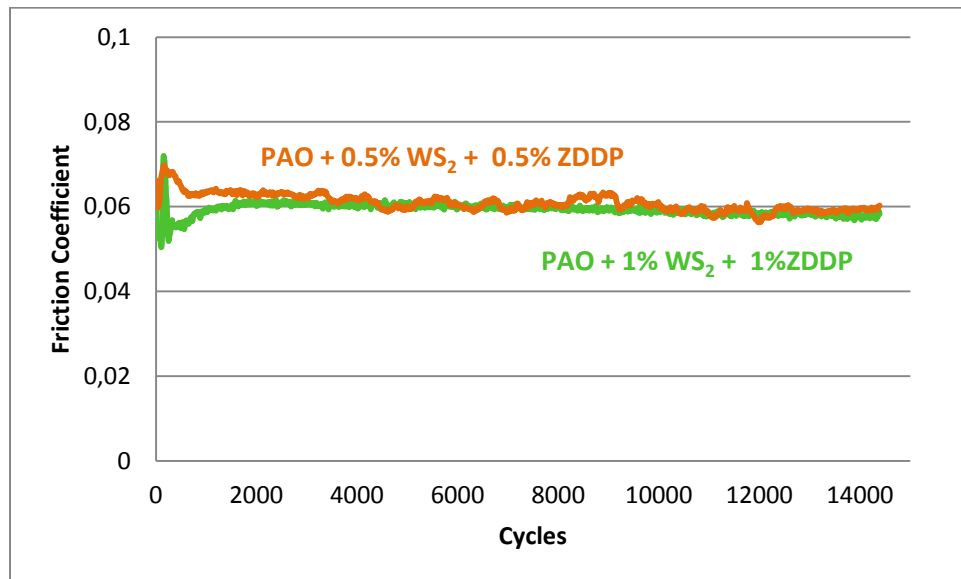
Figure 81. Friction coefficient for the ZDDP and nanoparticles containing samples

These results clearly show the synergetic effects between the WS_2 nanoparticles and the ZDDP anti-wear additive at high temperature (100 °C). The combination of these additives looks primordial in order to obtain tribological properties that neither the particles alone nor the ZDDP can provide in such severe test conditions (very high contact pressure and temperature of 100 °C). ZDDP would serve the action of the nanoparticles as friction modifier, while the nanoparticles would serve the anti-wear properties of the ZDDP. These results can directly be compared to those obtained in the literature between MoDTC and ZDDP additives where a synergetic effect has also been observed (*43, 92, 124*) . As described by Morina et al. (*56*), ZDDP is known for its anti-wear properties but high friction coefficients are obtained at high temperatures. As explained in section 3.3.2.1.2, MoDTC is known for its ability to reduce the friction coefficient by *in-situ* generation of MoS_2. As a consequence, the authors studied the effect of adding MoDTC to ZDDP. The results showed that the blend proved to be effective in friction reduction (*56*). Moreover, their results showed that the induction time for MoS_2 generation is reduced by half when the MoDTC is mixed with ZDDP than when it is alone in the base oil.

Few studies can be found on the interaction between ZDDP additives and nanoparticles. Tomala et al. (*125*) have recently studied the tribological properties of three different MoS_2 nanoparticles in a preformed ZDDP tribofilm on steel surfaces at 40°C. The authors studied the tribological behavior of IF-

MoS$_2$, rhenium-doped MoS$_2$ and MoS$_2$ nanotubes. The Re-MoS$_2$ nanoparticles outperformed the others in terms of friction reduction when direct lubrication of the steel samples was carried out. With the prerubbing of the surfaces with ZDDP, low and stable friction coefficients were obtained for the three different nanoparticles. TEM images of a cross-cut of the tribofilm formed on the ZDDP tribofilm-containing steel surface showed the presence of exfoliated nanosheets on the top of the ZDDP tribofilm. The authors conclude that nanoparticles get easily embedded onto the preformed ZDDP tribofilm allowing high reproducibility of the results and a stable and low friction coefficient. These results are in agreement with those obtained in the present work with WS$_2$ nanoparticles. On the contrary, Jenei et al (*126*) state that ZDDP additive inhibits WS$_2$ nanoparticles to reduce friction at room temperature. The authors came to this conclusion when comparing the results obtained by the mixtures of ZDDP additive in PAO with those obtained with the nanoparticles. However, it can be seen from their EDS chemical analyses made on the worn surface that no tribofilm was formed on the steel surface. In our work, experiments were done at 100°C so ZDDP chemical tribofilm was created. Thus, it looks like ZDDP tribofilm must be formed to obtain synergy between these two additives. This synergism is explained by the anti-oxidant properties of the ZDDP additive that allows the formation of a tribofilm with a low tungsten oxide concentration.

7.2.2   WS$_2$ nanoparticles in the presence of ZDDP additive on rough surfaces

In the previous section, synergy between ZDDP and the nanoparticles was proven on smooth steel surfaces. As industrial surfaces are not smooth but rough, it is important to verify that the same effect occurs on rough surfaces. The friction and wear results obtained at 100°C for the sample containing both the nanoparticles and the ZDDP additive were compared to those obtained by the individual additives as shown in Figure 82.
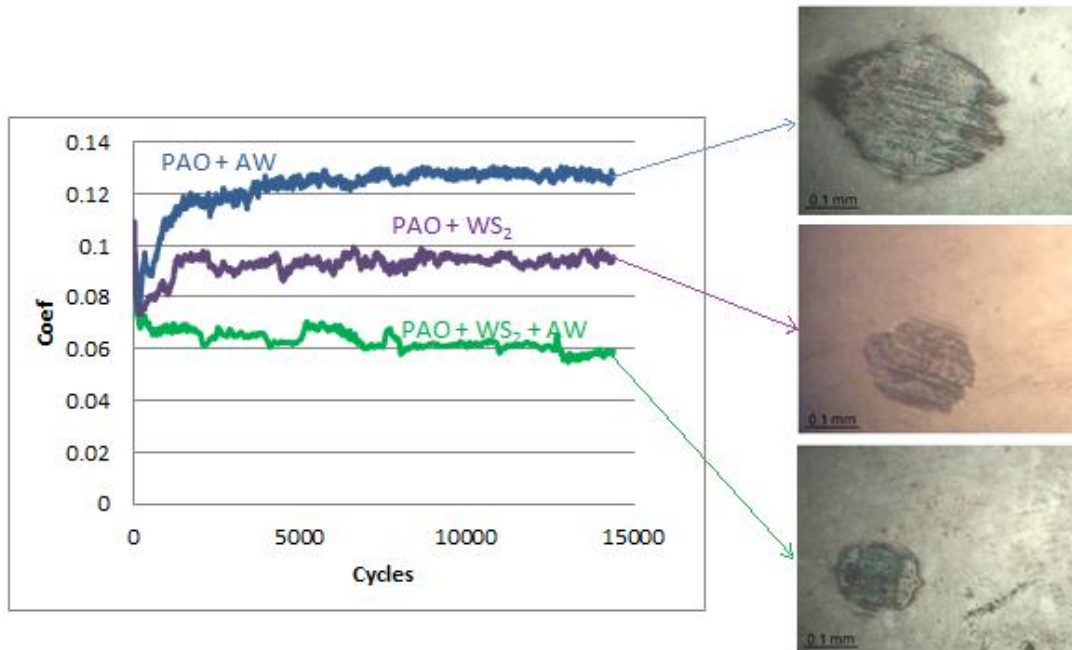
Figure 82. Friction coefficient and wear scars obtained for the rough surfaces lubricated by the different samples

It is important to remember that PAO on the rough surfaces gave a friction coefficient of approximately 0.4 (Figure 56). Thus, the addition of anti-wear additive reduced significantly not only friction coefficient, but also wear.

From Figure 82, it can be seen, once again, that the best friction and wear reduction are obtained for the sample that contained both the ZDDP additive and the nanoparticles. These results can be directly compared to those obtained for the smooth surfaces (Figure 73) where actually the same value of COF was obtained (0.06). In order to understand the good results obtained here, XPS chemical characterization of the tribofilm formed on the rough surface was done. The XPS survey scan (Figure 83a) revealed the presence of all the elements coming from both additives present in the lubricant used in the friction test. The tungsten spectrum (Figure 83b) showed that tungsten was present in a tungsten disulfide and in a tungsten oxide form whereas the sulfur spectrum (Figure 83c) revealed the presence of only sulfide species. The tungsten atomic concentration in an oxide form was calculated to be around 17%. These results are actually very similar to those obtained for the tribofilm formed by the same lubricant on the smooth surfaces (Figure 77), where also all the elements from the additives present in the lubricants were detected in the tribofilm and tungsten oxide concentration was calculated to be around 15%. It is then possible to conclude that the same value of friction coefficient was obtained because the same kind of tribofilm was formed on the steel surface and that the tribofilm was thick enough to avoid contact between the asperities.
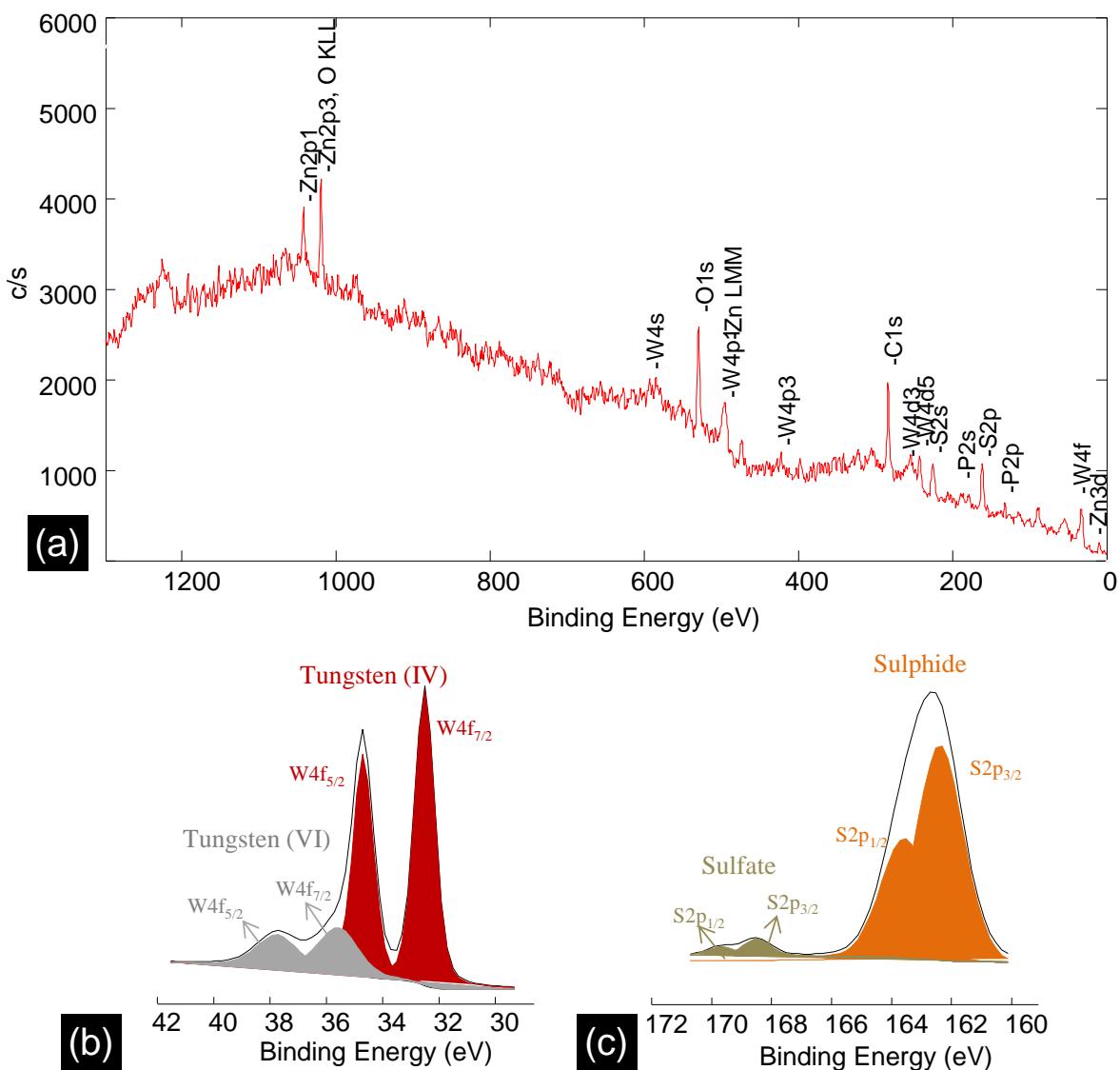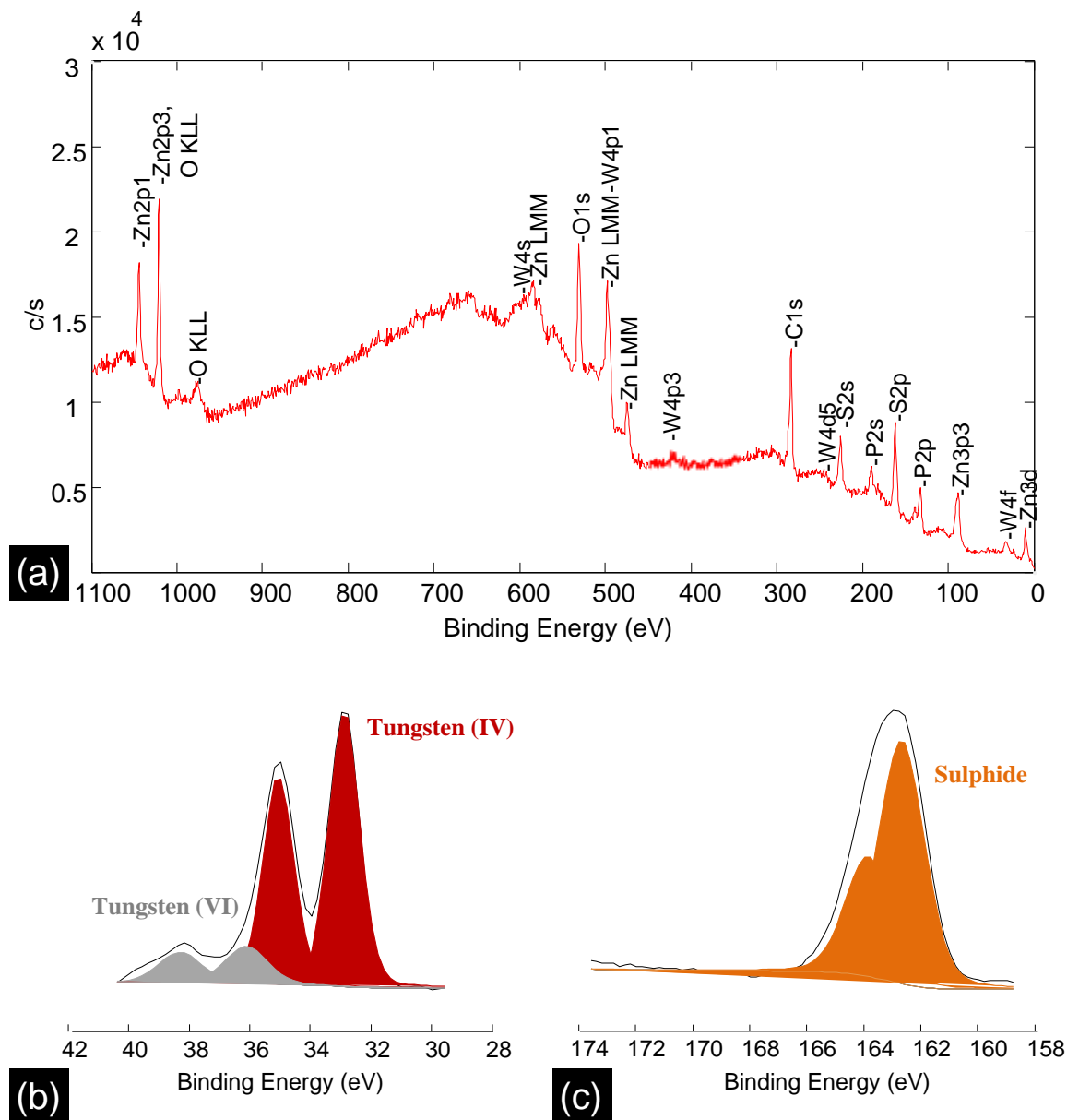
Figure 83. XPS spectra of the tribofilm formed by the nanoparticles in the presence of ZDDP additive on the rough steel flat; a) survey scan; b) W4f energy region and c) S2p energy region

7.3 WS$_2$ nanoparticles tribological behavior in the presence of ZDDP antiwear additive and calcium phenate detergent

Detergents are necessary constituents in engine oil formulation. They are used to ensure surface cleanness of the different engine components. The main function of these additives is to neutralize corrosive combustion acids and prevent the formation of harmful deposits. As exposed in section 3.3.2, they have a micellar structure with an alkaline core surrounded by surfactant chains and can have neutral pH or be overbased in order to neutralize acid compounds which could be generated. Sulfonates, phenates, salicylates and phosphonates are commonly used in the lubricants industry.

Synergism between ZDDP additive and WS$_2$ nanoparticles was proven in the previous chapter so it can be used in the formulation of nano-doped lubricants. However, as explained in section 3.3.2.1.1.3, ZDDP additive is known to interact with detergent additives. From the tribological point of view, the researchers do not agree in whether synergism or antagonism between these two additives exists. In this way, antagonism has been reported by Wan et al. (*55, 127, 128*) and Rounds et al. (*129*) whereas synergism has been reported by Yu et al. (*130*), Greenall et al. (*131*),and Ramakumar et al. (*132*). Though, the authors do agree in the fact that the metal from the detergent additive incorporates to the phosphate network to form calcium phosphate (*51, 53, 55, 127, 128, 130, 131, 133-139*). As detergents are necessary components in oil formulation, the investigation on the tribological properties of WS$_2$ nanoparticles in the presence of both ZDDP and detergent additives needs now to be done.

The tribological properties of the industrially produced nanoparticles of tungsten disulfide were studied in the presence of both an anti-wear and a detergent additive. An overbased calcium alkyl phenate sulfide detergent, better known as sulfurized calcium phenate was used for this study. A schematic representation of the chemical structure of this detergent is presented in Figure 84.
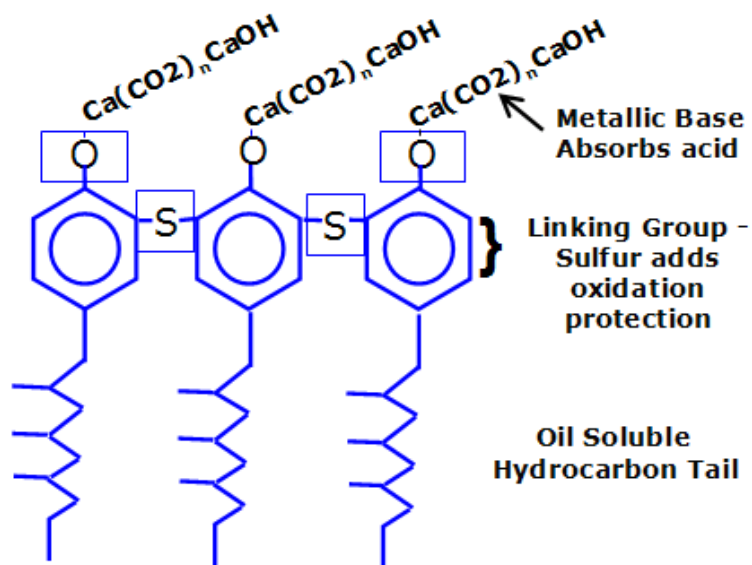
Figure 84.Schema of the chemical structure of a calcium phenate detergent

The detergent was blended at a concentration of 3 wt% in the base oil, while the ZDDP and nanoparticles were blended at a concentration of 1 wt%. Two samples were prepared for the experiments. The first one consisted on the ZDDP and the detergent in the base oil (without nanoparticles) and served as reference for the second sample, which consisted of both additives and the nanoparticles in the same base oil. The tests were carried out using the home made tribometer described in section 6.2 under the test conditions summarized in Table 4, at 100°C.

As described in section 3.3.2.1.1.3 of the *State of the art* part, longer tribofilm formation times are obtained for the mixture of anti-wear with detergent additives compared to the individual components (ZDDP in base oil or detergent in base oil) in the literature. In order to be able to compare the induction time needed to form a tribofilm with these two additives with and without nanoparticles, the electrical contact resistance (ECR) was measured along the friction tests.

The friction curves obtained for both samples are plotted in Figure 85a, whereas the ECR results can be seen in Figure 85b. The wear scars, where the presence of a tribofilm for both samples can be observed, are shown in Figure 86.
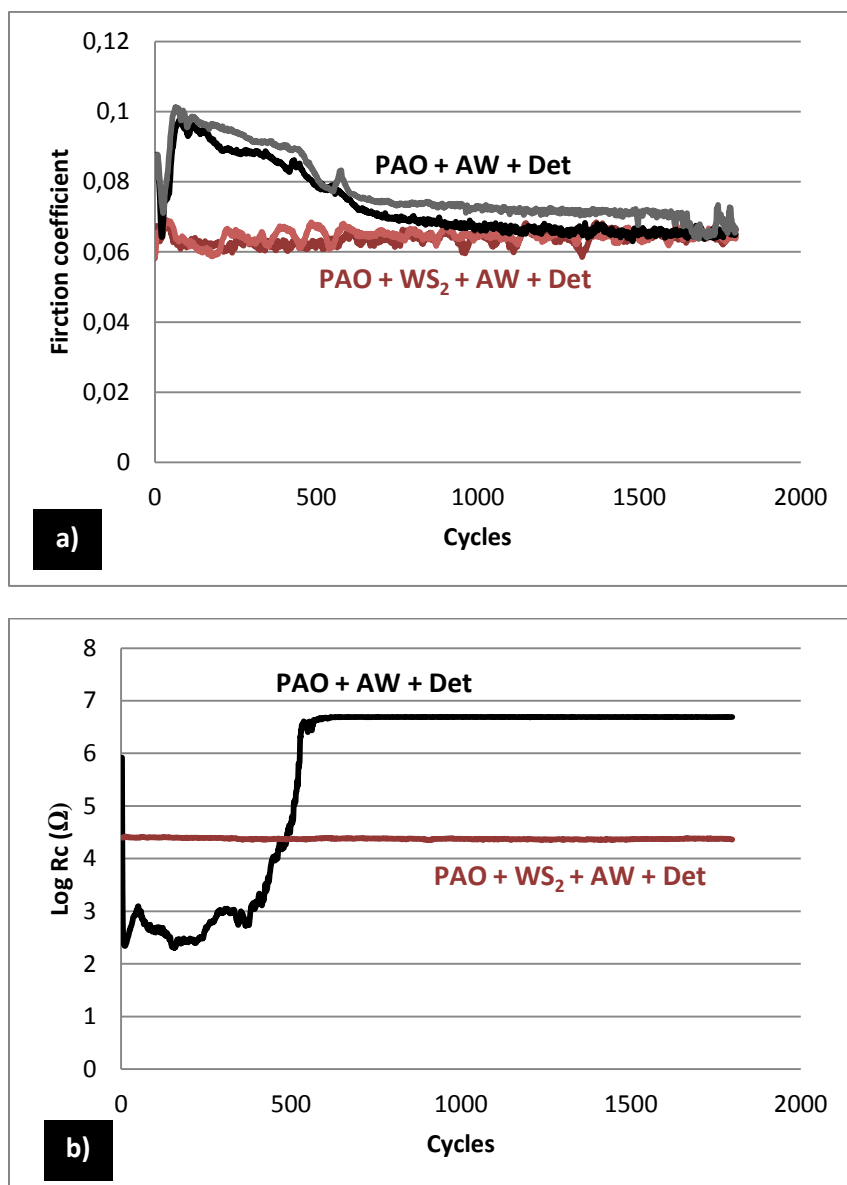
Figure 85. Results obtained for the samples containing both anti-wear (AW) and detergent additive with (red) and without (blue), a) friction curves; b) ERC curves
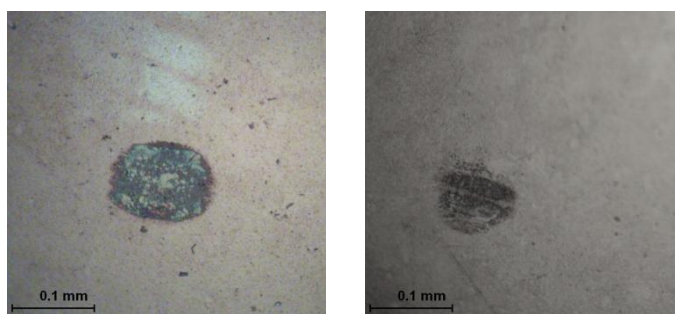
Figure 86. Wear scars for the sample containing ZDDP and detergent without (left) and with (right) the nanoparticles

From Figure 85, it can be seen that friction coefficient for the reference sample rises up to 0.1 during the first 100 cycles, after that to decrease continuously until reaching a steady state low value of 0.06 after 700 cycles. Comparison of the ECR measurements for this sample reveals that the high friction coefficient observed during the first 700 cycles corresponds to low electric resistance values which suggest that contact between the steel surfaces occurs. The rise of ECR value and further stabilization is a clear evidence of tribofilm formation that avoids contact between the friction pairs. Thus, the high friction coefficients obtained at the beginning of the test may be explained by the long tribofilm formation time needed for ZDDP and detergent blends. The significant decrease in friction coefficient observed for this sample can be due to an important contact pressure drop due to extensive wear during the first cycles. However, the wear scar diameter measured at the end of the tests is 100 nm for this sample and 92 nm for the one that contained the nanoparticles. These values are very close to the calculated Hertz diameter (92 nm), evidencing that no wear occurred for any of the samples. The results presented previously in this work, obtained for the ZDDP in base oil under the same test conditions, showed a higher friction coefficient and larger wear scar than for the ZDDP and the detergent blend. This suggest that the better results obtained herein are mainly due to the presence of the detergent in the mixture. Several authors have reported that overbased detergents possess extreme pressure, anti-scuffing, good friction and anti-wear properties (*139, 140*); although the origins of these properties are not fully understood but is thought to be due to the adsorption and packing of calcium carbonate particles on the surface (*141*). In order to prove whether the detergent exhibited such good properties under the test conditions used in this work an additional experiment was carried out using 3 wt% of detergent in base oil. The friction curve and the wear scar obtained can be observed in Figure 87. It can be seen that a stable friction coefficient of 0.07 is obtained by the detergent and that the wear scar diameter is very close to the Herz diameter. These results prove that the calcium phenate detergent additive do have anti-wear and friction reduction properties under the test conditions used in this work.
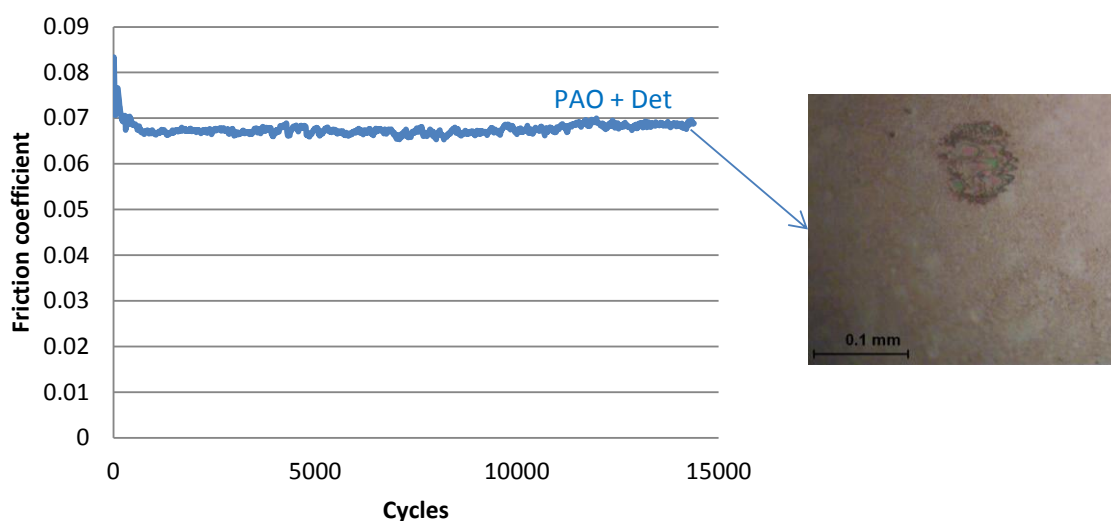
Figure 87.Friction curve for the detergent in PAO as a function of cycles and wear scar of the pin at the end of the test

On the other hand, the nanoparticle-containing sample gave not only a stable friction coefficient of 0.06 from the first cycles of the friction test but also a stable ECR measure since the very first cycles, suggesting that a tribofilm had been formed very quickly at the beginning of the test. To verify this hypothesis, XPS analyses were carried out on the worn surfaces after stopping the friction tests at 100 cycles. The spot size used was 50 μm with a power of 12.5 W. The survey scan obtained for both samples can be seen in Figure 88.
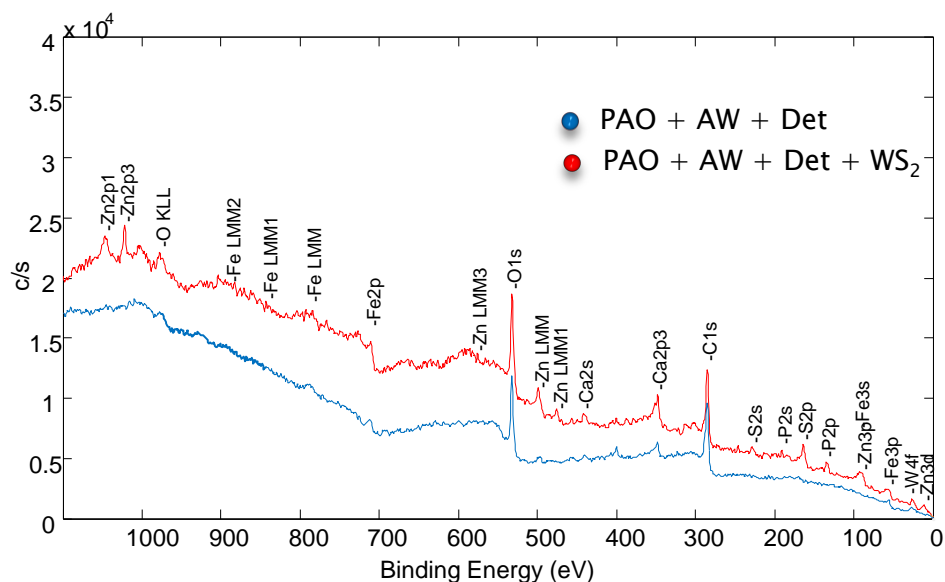
Figure 88. XPS survey scan of the tribofilm formed for both samples after 100 cycles

It can be seen that only oxygen, carbon, iron and some residual calcium are detected for the reference sample; both calcium and carbon disappear after 0.5 minutes sputtering time proving that no tribofilm had been formed. This is in agreement with the images of the worn surfaces after stopping the test during this period. Figure 89 shows the images of the worn surfaces (pin and flat) at the end of the test and after 100 cycles for the reference sample. It can be clearly observed that no tribofilm has been formed on the steel surface after 100 cycles whereas the presence of a tribofilm can be observed at the end of the test which agrees with the electric resistance measurements. As stated before, the presence of adsorbed calcium carbonate particles on the steel surface might be responsible of the good anti-wear properties observed for detergent additives (*140, 141*). Thus, it is possible to think that the residual calcium detected in the survey scan may have protected the steel surface against wear during the first cycles.
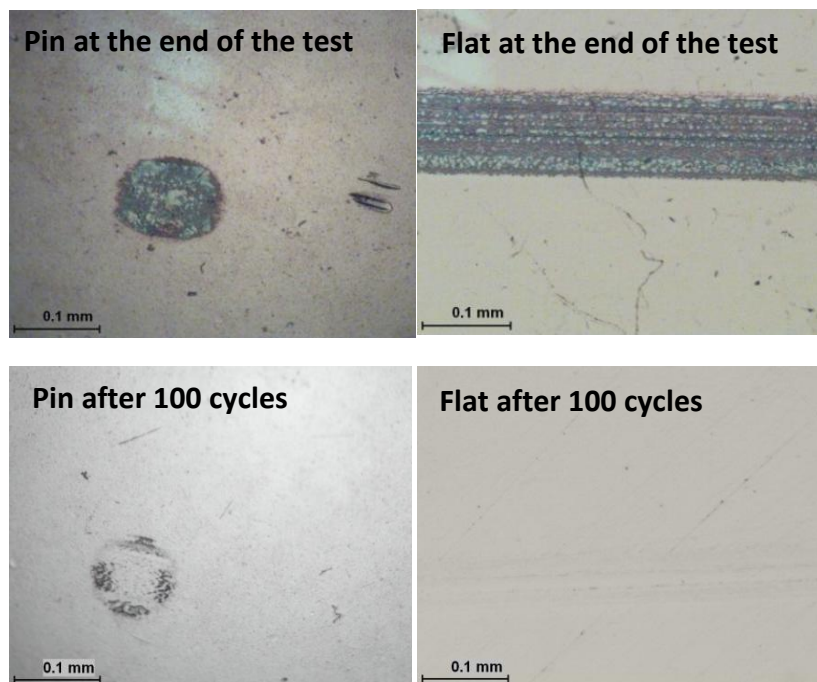
Figure 89. Images of the worn surfaces (pin and flat) lubricated by the reference sample at the end of the test and after 100 cycles

Concerning the nanoparticles-containing sample after 100 cycles, not only oxygen, carbon, iron, tungsten and sulfur are found on the worn surface, but also zinc, phosphorus, and calcium which come from the detergent and the anti-wear additives. Thus, it looks like nanoparticles presence helps fixation of the elements coming from the detergent and the anti-wear additive although this point is not understood. In order to prove that a chemical tribofilm was formed on the steel surface for this sample, XPS depth profiling of the tribofilm was done. Actually, this technique can be used to get an estimation of the thickness of the tribofilm. The etching rate was calculated from sputtering of the iron oxide layer on steel flat which is known to be 4 to 5 nm thick. The etching rate was found to be approximately 6 to 7 nm/min. Figure 90 shows the XPS depth profile of the tribofilm formed by this sample after 100 cycles.
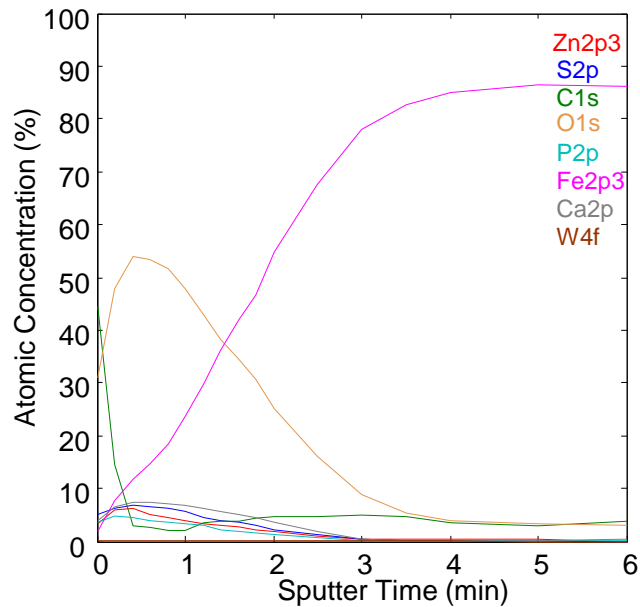
Figure 90.XPS depth profile on the tribofilm formed by the sample containing the nanoparticles and both anti-wear and detergent additives

It can be observed that at the same time that iron signal increases, the signals of all the characteristic elements from the additives used decreases at apparently the same rate at the same time that proving a tribofilm of some nm, composed of all the elements was formed on the steel surface. Iron signal is weak during the first minutes and then increases drastically until stabilization, proving that the steel surface was been reached after 3 minutes sputtering. As a consequence, the tribofilm thickness is estimated to be around 15 to 21 nm. However, it is important to note that the sputtering speed is dependent of the material and this thickness value was calculated using the etching rate of the iron oxide layer present on a steel surface. On the other hand, carbon signal decreases rapidly during the first minute suggesting that mainly C-C adventitious carbon which may come whether from the degradation of the oil during the test or the exposure of the sample to the atmosphere is found on the top of the tribofilm. Verification of the different contributions of the C1s peak can be seen in Figure 91.
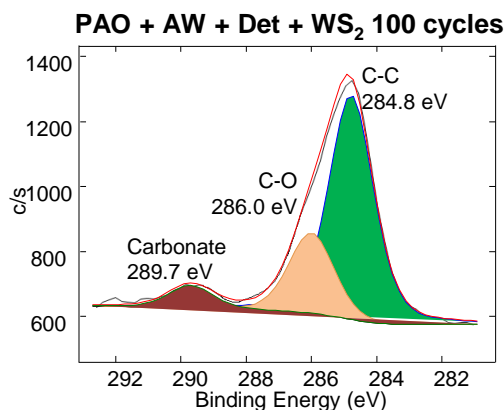
Figure 91. XPS spectra of the C1s peak showing the different contributions present in the tribofilm

The two main contributions at 284.8 eV and 286.0 eV correspond to adventitious carbon, whereas the third contribution at 289.7 eV corresponds to carbonate ion which may come from calcium carbonate.

In order to identify the different species present in the tribofilm (phosphates, sulfates, and sulfides), treatment of the XPS spectra of the main peaks detected in the survey scan was done. The binding energies of the main fitted peaks and corresponding chemical species are summarized in Table 6. (Adventitious carbon contributions are not taken into account making carbonate contribution to be 100%).

Table 6. XPS binding energies and corresponding chemical species in the tribofilms formed on the steel surface by the nanoparticles in the presence of ZDDP and calcium phenate detergent after 100 cycles

Element	Peak	% at
C 1s	289.7 eV Carbonate (100%)	7%
Ca 2p	347.6 eV Ca^{2+} (100%)	20%
P 2p	133.4 eV Phosphate (100%)	23%
Zn 2p	1022,3 eV ZnS/ZnO/Zn phosphate (100%)	16%
S 2p	162.1 eV Sulfide / phosphate (100%)	32%
W 4f	32.5 eV WS_2 (58%) 35.5 eV WO_x (42%)	2%

It can be seen that calcium atomic concentration is 20% while only 7% of carbonate was detected. This means that some of the initial calcium carbonate has undergone a chemical reaction. As mentioned before, it has been reported in the literature that calcium from the detergent additive incorporates to the ZDDP phosphate glass to form calcium phosphate. The phosphate contribution at 133.4 eV can be seen. The partial replacement of zinc by calcium to form a mixed zinc/calcium phosphate has been reported by (*128, 134, 135*). This reaction can be explained by the hard and soft acid and bases principle

because Ca^{2+} is harder lewis acid than Zn^{2+}. The zinc peak at 1022.3 eV which corresponds to Zn^{2+} cation can be an evidence of zinc phosphate, although it can also correspond to zinc sulfide or oxide which corresponding contributions in the S2p (162.1 eV) and O1s (530.6 eV, not shown in here) were also detected. However, once again those contributions can be related to other species like sulfur in the phosphate ion or in tungsten disulfide, and calcium or iron oxide, in the case of the sulfur and the oxygen peak respectively. Other analyses techniques like X-ray absorption near edge structure XANES) should be used to distinguish between the different phosphate, sulfide and oxide species present in the tribofilm. Concerning tungsten, it can be seen that it is mainly found in a tungsten disulfide form which explains the good friction behavior observed in the friction tests.

It has been shown that the same friction coefficient was obtained for both the nanoparticles containing sample and for the reference in steady stable conditions. Even if the presence of a tribofilm that gives a friction coefficient of 0.06 has been proven after 100 cycles, the possibility that the same kind of tribofilm can be obtained for both samples after a certain time cannot be excluded at this point. Thus, XPS chemical analysis was carried out at the end of the test to verify whether nanoparticles made part of the formed tribofilm at the end of the test or not. Figure 92 shows the survey scan and the depth profiles of the tribofilm for both samples at the end of the experiments.

It can be clearly seen that a tribofilm was present on the steel surface for both samples at the end of the test. The presence of calcium from the detergent and of zinc, sulfur and phosphorus from the anti-wear was observed in both tribofilms. However, tungsten was also detected in the case of the sample that contained the nanoparticles. The survey scan obtained for this sample is pretty similar to the one obtained after 100 cycles, where the same elements were also found. Thus, it looks like the fact that the same value of friction coefficient is reached with both samples under steady stable conditions seems to be just a coincidence.
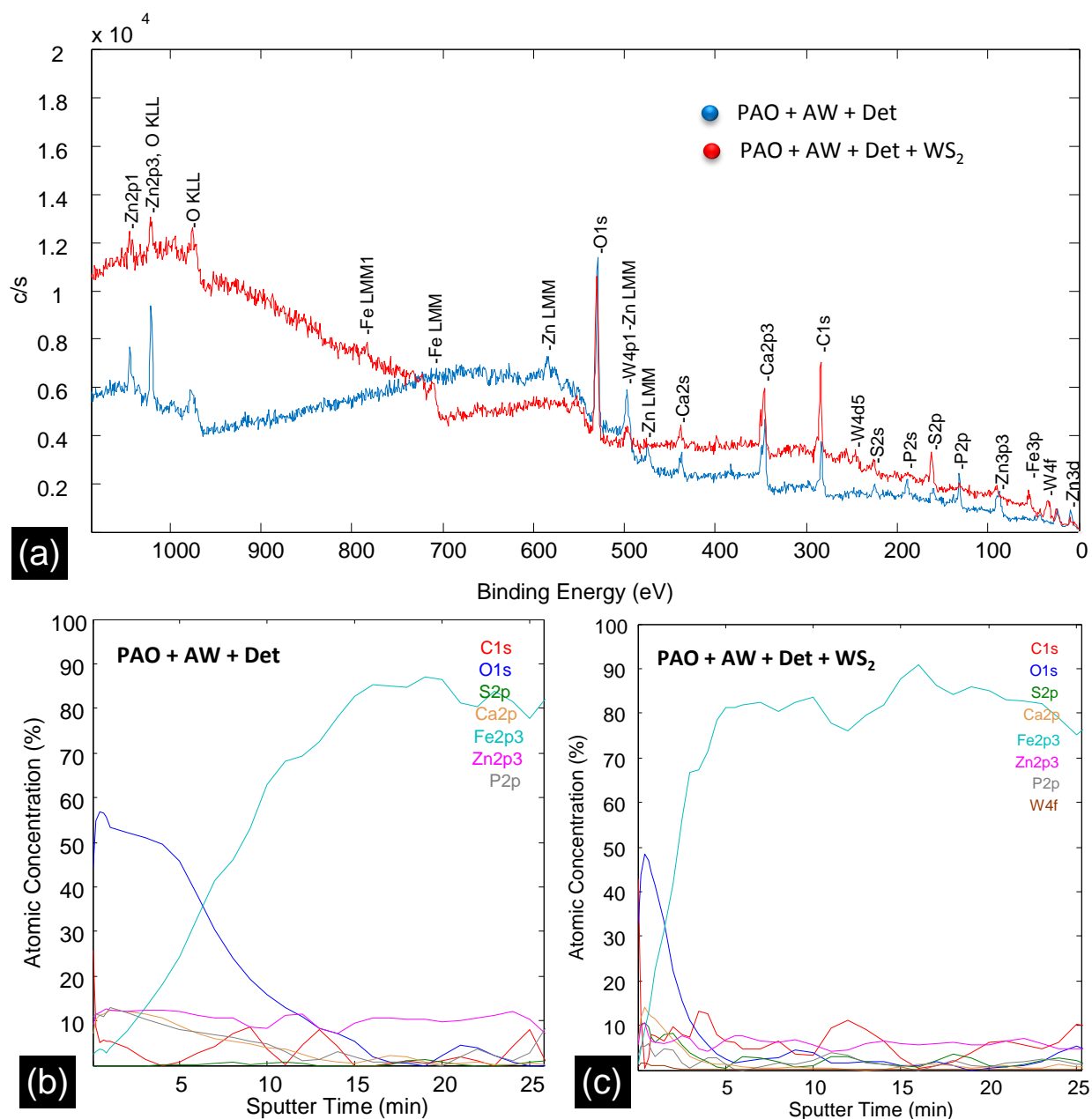
Figure 92. XPS spectra of the tribofilm formed by both samples at the end of the test a) survey scan b) elementary depth profile of the tribofilm formed by the reference sample and c) elementary depth profile of the tribofilm formed by the sample that contained the nanoparticles

From the depth profiles, it can be seen that more than 10 minutes etching are needed to reach the steel surface for the reference sample whereas less than 5 minutes are needed for the other sample. This shows that a thicker tribofilm was formed by the first sample than by the one that contained the nanoparticles which agrees with the wear scars observed in Figure 86. The fluctuations observed in the

depth profiles are due to the lower resolution used for the recording of these spectra compared to the one shown in Figure 90. Actually, the resolution of the spectra was reduced in purpose so the whole profile of the thick tribofilm could be recorded in reasonable time of analysis.

The results presented above show that the tribofilm formed by the nanoparticles, in the presence of the detergent and the anti-wear additive at the end of the test, is formed by the same elements than the tribofilm present on the surface after 100 cycles (Figure 92a and Figure 88, respectively). Additionally, less than 5 minutes of sputtering were needed to reach the steel surface in the XPS depth profiles for both tribofilms suggesting that both tribofilms may have a similar thickness (Figure 92c and Figure 90, respectively). All these result may indicate that the tribofilm present at the end of the test was formed since the very beginning of the test. To prove this, treatment of the XPS spectra of the different elements found in the tribofilm for this sample was done. The binding energies of the main fitted peaks and corresponding chemical species are summarized in Table 7 (Adventitious carbon contributions are not taken into account).

Table 7. XPS binding energies and corresponding chemical species in the tribofilms formed on the steel surface by nanoparticles in the presence of the ZDDP and the detergent in PAO at the end of the test

Element	Peak	% at
C 1s	289.7 eV Carbonate (100%)	0%
Ca 2p	347.6 eV Ca^{2+} (100%)	37%
P 2p	133.4 eV Phosphate (100%)	7%
Zn 2p	1022,1 eV ZnS/ZnO/Zn phosphate (100%)	7%
S 2p	162.1 eV Sulfide / phosphate (83%) 168.6 sulfate (17%)	40%
W 4f	32.5 eV WS_2 (74%) 35.5 eV WO_x (26%)	10%

The results were compared to those obtained with the samples containing nanoparticles after 100 cycles (Table 6). Two main differences were found between the tribofilms. First, the carbonate contribution detected at 100 cycles was no longer detected at the end of the test. Additionally, the presence of sulfate contribution that was not detected at 100 cycles, was identified at the end at the test. To understand whether these two differences between the tribofilms were due to the different reactions that seem to take place during the first 500 cycles between the anti-wear and the detergent additive, the treatment of the XPS spectra of the reference sample was done. Neither carbonate, not sulfate were detected for this sample at the end of the test. However the calcium, phosphorus, zinc and sulfur (in a sulfide form) were all detected. Thus, it looks like carbonate is no longer in the tribofilm at the end of the test and that the calcium detected corresponds to calcium phosphate. Concerning the sulfate peak, it has been previously observed in all our XPS results so it should come from our nanoparticles. Due to the complexity of the system which contains a lot of elements it is difficult to understand and analyze the

different reactions that occur in the contact. To get a better understanding, first an investigation on the different reactions that can happen between these additives in the oil (without friction) should be done. Additionally, the use of other surface analysis techniques like XANES would help distinguishing between the different species formed.

It can be seen that tungsten is present in an oxide form in a concentration of 26% which is lower than the tungsten oxide concentration detected in the tribofilm after 100 cycles. In the previous section it was seen that the WS_2 sheets were predominantly found on the top layer of tribofilm when lubricating steel surfaces with ZDDP additive. XPS technique allows the identification of the elemental composition of the top surface (10 nm usually). In order to check whether the nanoparticles were only found on the top of the surface or not, a FIB cross cut of the tribofilm was carried out. Figure 93 shows the TEM images of the tribofilm formed by the nanoparticles in the presence of calcium phenate and ZDDP additive and the different positions where EDX was carried out. The EDX results are summarized in Table 8.
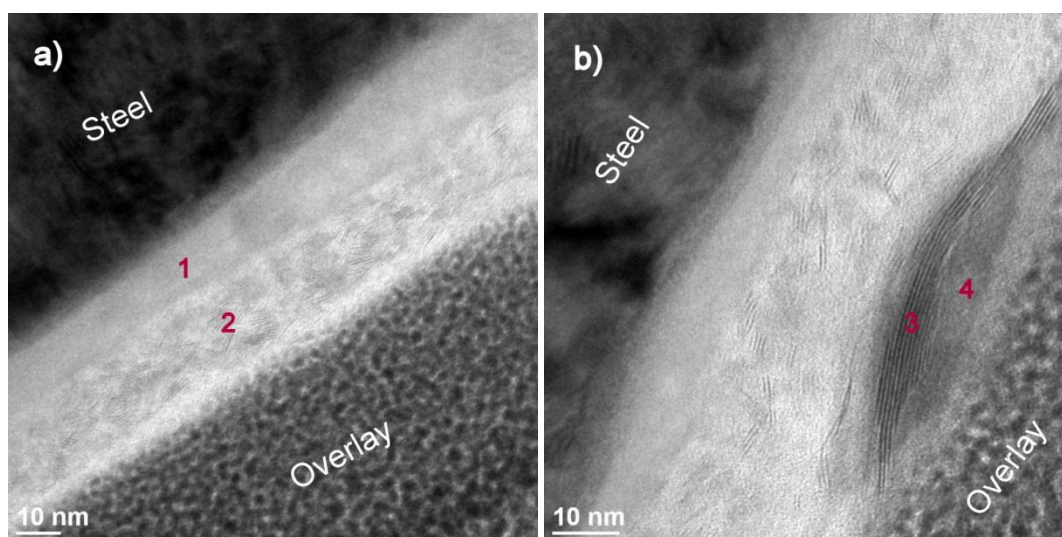
Figure 93. TEM images of the FIB cross cut of the tribofilm formed by the nanoparticles in the presence of calcium phenate and ZDDP

Table 8. EDX results of the different points of the tribofilm observed in Figure 93

Position	C	O	P	S	Ca	Zn	W
1	51.8	30.6	7.7	2.1	5.3	1.2	1.3
2	61.5	23.0	0.8	7.8	0.6	0.0	6.3
3	53.8	0.0	0.0	28.6	0.0	0.0	17.6
4	49.2	27.8	1.8	6.9	1.1	0.4	12.8

From the images, it can be concluded that the tribofilm thickness varies from 20 to 35 nm. The tribofilm has a layered structure. The presence of tungsten disulfide sheets can be clearly observed in the second layer (lighter zone on the top of the darker first layer). The presence of some smashed nanoparticles on the top of the tribofilm was confirmed by EDX analysis (position number 3). It can be seen that the first layer, located on the steel surface (position 1), contains all the elements coming from the different additives that were present in the lubricant whereas no zinc was detected in the second layer (position 2). This may be an evidence of zinc replacement by the calcium atoms in the phosphate glass (calcium and phosphorous were detected in small quantities). Nevertheless, zinc was again detected in the top of the tribofilm in small quantities (position number 4). Even if no sheets were seen on the first layer (on the top of the steel), the EDX analysis revealed the presence of tungsten in it. The analysis techniques available nowadays don't allow concluding on the chemical state of the elements in this first layer. Additionally, the second layer is richer in tungsten and sulfur elements than the first one which agrees with the TEM images where sheets of tungsten disulfide can be clearly seen.

It is possible that the first layer located on the steel surface might be formed during the first cycles and that the second layer was formed on it after a certain time. Actually, not only the impoverishment in phosphorous and zinc content but also the larger tungsten quantity detected by EDX in the second layer compared to the first layer one are in line with the XPS results of the tribofilm at 100 cycles (Table 6) and those of the tribofilm at the end of the test (Table 7). However, in order to prove this point, a transversal FIB cut of the tribofilm obtained after 100 cycles should be done.

8. Conclusions

The tribological performance of industrially produced WS_2 nanoparticles was studied in this part of this work. The results showed that these nanoparticles (as those produced at the laboratory scale) have interesting friction reduction and anti-wear properties when tested in PAO base oil in the boundary lubrication regime, at room and 100°C on both smooth and rough surfaces. However, some reproducibility problems were observed at 100°C on the smooth surfaces where chemical analysis revealed important quantities of tungsten in an oxide form. It is then believed that the oxidation of the nanoparticles may alter their tribological performance due to the in-situ production of tungsten oxide.

On the other hand, the morphological and chemical analyses made on the rough surfaces lubricated by the WS_2 nanoparticles at 100°C revealed the presence of a tribofilm on the wear track that reduced importantly the roughness of the worn surface. Additionally, it was observed that nanoparticles trapped on the grooves of the steel can provide proper lubrication in case of nanoparticles starvation in the contact.

With the aim of using nanoparticles in commercial lubricant oils, their good performance must be guaranteed in real temperature conditions and in the presence of the additives commonly used in the industry. Thus, we analyzed the tribological response of WS_2 nanoparticles in the presence of a diphenylamine anti-oxidant, a ZDDP anti-wear and a blend of ZDDP with calcium phenate detergent additive at 100 °C in boundary lubrication regime. The results showed that the diphenylamine antioxidant does not have any effect on the tribological behavior of the tungsten disulfide nanoparticles so it can be used in the formulation of nanoparticles containing lubricants.

Conversely, a better tribological performance was obtained when the nanoparticles were used in presence of ZDDP additive. Actually not only a stable and low friction coefficient was obtained but also high reproducibility of the results was observed. The analyses showed the presence of a 50–60-nm-thick tribofilm protecting the steel surface. The presence of sheets of WS_2 observed on the top of the tribofilm might explain both good friction and wear results. Under the WS_2-rich layer a typical ZDDP tribofilm composed by zinc and iron polyphosphates was found. In this work, synergetic effects between the WS_2 nanoparticles and ZDDP anti-wear additive were observed under severe test conditions. Actually, ZDDP seems to protect WS_2 sheets from oxidation, thus leading to improved friction modifier properties, while the presence of WS_2 nanoparticles seems to increase the anti-wear properties of the ZDDP.

On the other hand, when the nanoparticles were tested in the presence of ZDDP anti-wear and calcium phenate detergent a low and stable friction coefficient was obtained since the very beginning of the test whereas a certain time was needed to get a friction coefficient reduction for the reference sample (ZDDP and calcium phenate in PAO without nanoparticles). The results showed that a tribofilm composed of all the elements from the different additives that were present in the lubricant was present on the steel surface since the very first cycles. However, it is important to note that the same value of friction

coefficient and anti-wear behavior was obtained for the ZDDP-calcium phenate blend with and without the nanoparticles under steady stable conditions. Nevertheless, the most important point to be remembered is that no antagonism was seen between these additives.

As stated before engines and gearboxes are very complex machines with many different processes and phenomena. The investigation on the tribological behavior of these industrially produced nanoparticles needs to be continued so the formulation of a nanoparticles-doped lubricant can be done. At the same time, a research focused on the efficient dispersion of the nanoparticles combined with the tribological behavior of the dispersion is also needed. Additionally, an optimization on the scaled-up synthesis of tungsten and molybdenum disulfide nanoparticles should continue to take place so more homogeneous samples than the one tested in this work can be proposed for the formulation of new lubricants.

Résumé. Partie 1.
Propriétés lubrifiantes des nanoparticules de disulfure de tungstène produites à l'échelle industrielle

L'évolution des méthodes de synthèse rendent possible la production et la commercialisation des nanoparticules de disulfure de tungstène à l'échelle industrielle. Cependant, la recherche a démontré que les propriétés lubrifiantes des nanoparticules dépendent de leurs caractéristiques intrinsèques. Pour cette raison et dans le but d'utiliser ces nanoparticules dans les lubrifiants automobiles, leur comportement tribologique doit être étudié.

Dans cette partie de la thèse, nous avons donc étudié les propriétés tribologiques de ces nanoparticules dans une huile de base (PAO) en présence de surfaces en acier. Des premiers essais tribologiques ont été réalisés en utilisant une MTM (Mini Traction Machine) et un tribomètre pion/plan. Les résultats obtenus par MTM ont permis de définir les conditions opératoires à considérer pour les essais sur le tribomètre pion/plan. Un effet réducteur de frottement a été observé dans les courbes de Stribeck pour des vitesses faibles correspondant au régime de lubrification limite. Les résultats obtenus avec le tribomètre pion/plan font apparaitre les propriétés réductrice de frottement et anti-usure des nanoparticules en présence de surfaces lisses (R_a < 20nm) mais aussi de surfaces rugueuses (R_a = 300 nm) à température ambiante et à 100°C dans le régime de lubrification limite. Cependant, des problèmes de répétabilité ont été observés lors des essais à 100°C sur les surfaces lisses. Les analyses chimiques (menées par XPS) du tribofilm formé sur les surfaces en acier ont mis en évidence une concentration importante de tungstène sous une forme oxyde pour les essais menés à 100°C. Les problèmes de répétabilité ont donc été attribués à la production *in-situ* d'oxyde de tungstène lors des tests de frottement. Dans le but de vérifier cette hypothèse, des nanoparticules d'oxyde de tungstène ont été testées dans les mêmes conditions opératoires. Les résultats ont montré que le coefficient de frottement obtenu avec ces nanoparticules correspond au coefficient le plus haut mesuré avec les nanoparticules de disulfure de tungstène. De la même manière, les résultats en usure sont très similaires. Il a donc été conclu que les problèmes de répétabilité rencontrés lors des essais de frottement étaient bien liés à la formation d'oxyde de tungstène, à l'origine de propriétés tribologiques moindres.

Concernant les surfaces rugueuses, les caractérisations (MEB couplé avec EDX, XPS et HRTEM) ont permis de démontrer pour la première fois que les nanoparticules restent piégées dans les rugosités propres des surfaces. Ces nanoparticules peuvent lubrifier le contact en cas de sous-alimentation. Des essais comparatifs avec le MoDTC, additif très utilisé dans l'industrie comme modificateur de frottement, ont mis en évidence que les tribofilms formés par les nanoparticules sur les surfaces rugueuses sont plus durables que ceux obtenus avec le MoDTC. Cela constitue un atout important pour ces matériaux comparés aux chimies dites «solubles» utilisées aujourd'hui.

Etant donné que les lubrifiants sont un mélange complexe de plusieurs additifs, nous nous sommes ensuite intéressés à l'interaction des nanoparticules avec ces additifs. Dans le but d'essayer d'obtenir des tribofilms avec une faible quantité d'oxyde de tungtène, nous avons d'abord étudié l'effet d'une diphénylamine, additif antioxydant, sur les propriétés tribologiques des nanoparticules. Les résultats

montrent que cet additif n'a aucun effet sur la performance des nanoparticules. Ceci peut être expliqué par leur mode d'action antioxydant qui agit comme donneur d'hydrogène pour arrêter la propagation des radicaux des chaînes carbonés de l'huile de base.

Nous avons ensuite étudié l'interaction de l'additif anti-usure ZDDP avec les nanoparticules sachant que cet additif présente aussi des propriétés antioxydantes et anticorrosion. Les résultats montrent qu'il existe une synergie entre ces deux additifs à 100°C dans le régime de lubrification limite indépendamment de la rugosité de la surface testée. Non seulement un coefficient de frottement bas et stable a été obtenu avec les nanoparticules en présence de ZDDP, mais un renforcement des propriétés anti usure du ZDDP a également été observé avec les nanoparticules. La caractérisation chimique du tribofilm a mis en évidence que le tungstène se trouve majoritairement sous forme disulfure de tungstène. Le ZDDP est quant à lui présent dans le mélange. Les résultats des analyses XPS ainsi que les images MET d'une lame FIB du tribofilm couplées aux analyses EDX ont démontré la présence de feuillets et nanoparticules de WS_2 dans un tribofilm chimique de ZDDP. Une couche riche en feuillets de WS_2 a été observée en extrême surface, expliquant ainsi les bons résultats en frottement. Il est important de noter que la même valeur du coefficient de frottement a été obtenue avec le ZDDP et les nanoparticules indépendamment de la rugosité des surfaces testées.

Enfin, les propriétés tribologiques de ces nanoparticules en présence de l'additif détergent phénate de calcium mélangé au ZDDP, a été étudié à 100°C dans le régime de lubrification limite. Les résultats montrent qu'un coefficient de frottement bas et stable peut être obtenu avec le mélange des trois additifs tandis qu'un certain temps est nécessaire pour attendre une telle valeur avec le mélange binaire détergent-ZDDP. La présence d'un tribolfilm composé par tous les éléments des différents additifs dès les premiers cycles a été mise en évidence par les analyses chimiques (XPS).

Les résultats obtenus lors de cette première partie montrent qu'il n'existe pas d'antagonisme entre les additifs testés (diphénylamine, ZDDP et phénate de calcium) et les nanoparticules. Pour cette raison, ces additifs peuvent être utilisés lors de la formulation des lubrifiants contenant des nanoparticules.

Part 2. Lubrication of gears by tungsten disulfide nanoparticles

The aim of this second part is to present the results of the investigation on the performance of WS$_2$ nanoparticles (used both in dispersion in base oil and fully formulated oil) when used in gearbox lubrication. Preliminary laboratory scale test and scaled-up tests using gearboxes from vehicles were carried out. A characterization of the rubbed surfaces for the scaled up tests was done using X-Ray Photoelectron Spectroscopy (XPS), Scanning Electron Microscopy and High Resolution Transmission Electron Microscopy (HRTEM).

9. Introduction

Despite all the research work done until now on the tribological properties of nanoparticles, only a few studies reported the effect of the nanoparticles in real life conditions (*122*). Thus, the nanoparticles effect in gears and bearings must therefore be studied before considering their use in gearboxes and engines.

Rolling contact fatigue is known to be one of the most common forms of failure fatigue in gears (*11, 12*). Thus, the reduction of wear in gearboxes requires the use of powerful lubricants able to minimize the disastrous consequences of this wear mode.

Pitting of gears is related to many causes: intrinsic metallurgy, teeth profiles, surface roughness, lubrication conditions, etc. The validation of a new lubricant is generally done at the laboratory scale on a FZG test rig and at the industrial scale on a complete gearbox. Therefore, both tests were carried out to evaluate the potential benefit of nanoparticles on gears in this work.

Due to the high cost of the transmission tests on complete gearboxes, the FZG tests were carried out as preliminary experiments to evaluate the potential effect of using nanoparticles on the lubrication of gears. As a consequence, only the lubricants that gave the best results on the laboratory scaled experiments were selected for the scaled-up ones.

10. FZG tests

The preliminary tests at the laboratory scale were conducted on a back-to-back spur gear test rig with power recirculation, better known as FZG (Forschungstelle für Zahnräder und Getriebebau, English translation: research test rig for gears and transmissions) test rig. In this machine, the drive gearbox connects the test pinion and wheel though two shafts. The test pinion shaft is separated into two parts by the load clutch. One part of the clutch can be locked using the locking pin, while in the other part of the clutch, different static torques can be applied using the load lever and dead weights. A Schema of the FZG tests rig can be observed in Figure 94.

The gears used for the experiments were made of 20MnCr5 steel. The roughness of the surface was measured on three different teeth for each gear. The average roughness for all the samples was Ra=0.35±0.1μm.
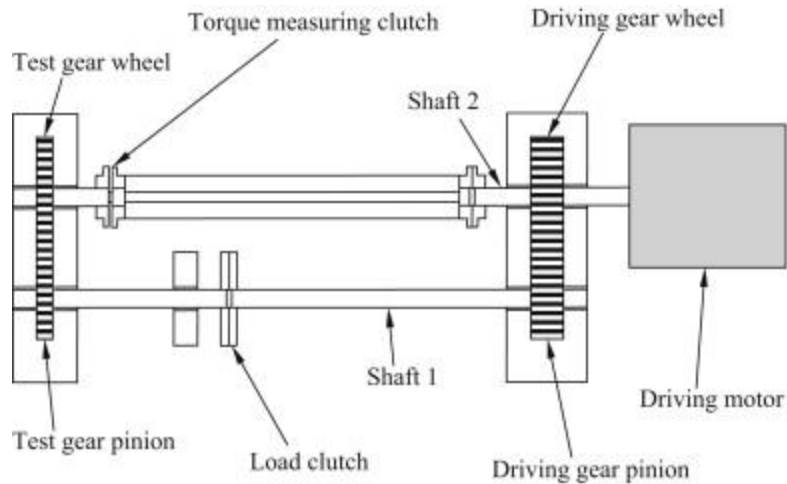
Figure 94. Schema of the FZG tests rig

The tests were carried out at constant temperature (110°C) and rotational speed (2900 rpm). Five torque load stages of 20 hours were defined as summarized in Figure 95. The tests were conducted until the area of a pit surpassed 5 mm^2. Therefore, visual inspection of the teeth was done at different moments during the tests. The first visual inspection was done at the end of the first stage, each 10 hours at stage s2 and, every 5 hours since the third load stage because pits are expected to appear faster under high loads. The experiments were extended under the conditions of the stage s5 until the pitted area met the criteria to stop the test.
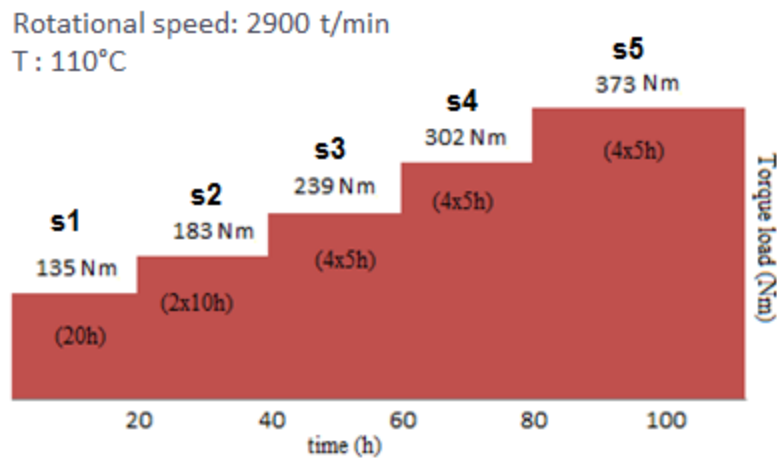
Figure 95. FZG testing program (rotational speed and temperature were constant across the load stages)

In order to study the effect of nanoparticles on the lubrication of gears, two systems were studied. The first one consisted on the nanoparticles in base oil whereas the second one consisted of the nanoparticles in base oil with a commercial package of additives. The results obtained with these

130

samples were compared to their respective reference sample: base oil for the first case and base oil with the package of additives for the second case. All the information about the samples is summarized in Table 9.

Table 9. Composition of the different samples used for the tests and their kinematic viscosity at 40°C and at 100°C

Sample	Composition	KV at 40°C (mm^2/s)	KV at 100°C (mm^2/s)
A	Base oil	125.6	18.3
B	Base oil + WS$_2$ nanoparticles	129.7	19.3
C	Base Oil + package of additives	127.3	18.5
D	Base oil + package of additives + WS$_2$ nanoparticles	133.1	19.5

The base oil used for the experiments was a mixture of 80 wt% PAO and 20 wt% polyol-ester. The package of additives used contained an anti-wear, a dispersant, an anti-corrosion, an anti-foam, a defoamant and a viscosity modifier.

The results obtained for the different samples are summarized in Table 10. Sample A (base oil) was stopped after 65 h under the s4 test conditions whereas sample B (nanoparticles in base oil) was stopped after 85h under the s5 test conditions. On the other hand, lubricants containing the package of additives, gave as expected, better results compared to sample A and B. Sample C (base oil with the package of additives) was stopped at 105h and sample D (nanoparticles in base oil with the package of additives) at 110 hours both under the s5 conditions. We can see that sample B and D stood out because of their better performances compared to their respective references sample A and C. The sample containing the nanoparticles (Sample D) performed best of all. These results clearly demonstrate the beneficial effect of the particles on the fatigue life of gears. As a consequence, sample B and D were chosen to be used for the scaled-up tests using real gearboxes that are commonly used in vehicles.

Table 10. FZG results for the different samples tested

Sample	Duration of the test (h)	Stage load (Nm)
A	65	302
B	85	373
C	105	373
D	110	373

11. Transmission tests

Once the preliminary lab-scale tests were completed, real scale experiments with gearboxes commonly used in vehicles were conducted using the nanoparticles containing samples (B, D).

For the transmission tests, five-speed gearboxes made of steel with a coating of manganese phosphate were used. The gearboxes were tested using an electrically operated test rig. The test was run up to either mechanical failure or up to 426 hours, whether comes first. The rig uses a re-circulating power loop principle at constant temperature (110°C) with a torque load of 148 Nm and a rotation speed of 3000 rpm. Third gear ratio was engaged for the duration of the test. Gears were made of 27CrMo4 steel and had all approximately the same roughness. The roughness of the steel was measured on three different teeth for each gear. The average roughness for the samples was Ra=0.75±0.1μm. Characterization of the gears before the fatigue tests was done by XPS and SEM. The XPS spectra, see Figure 96, confirms the presence of manganese phosphate with a pic at 133.5 eV and its doublet in the P2p energy region that corresponds to the phosphate anion (*142*) and the Mn(II) pic at 641.9 eV with its doublet and its satellite feature in the Mn2p region (*143*). The manganese phosphate crystals can be observed in the SEM image on Figure 97.
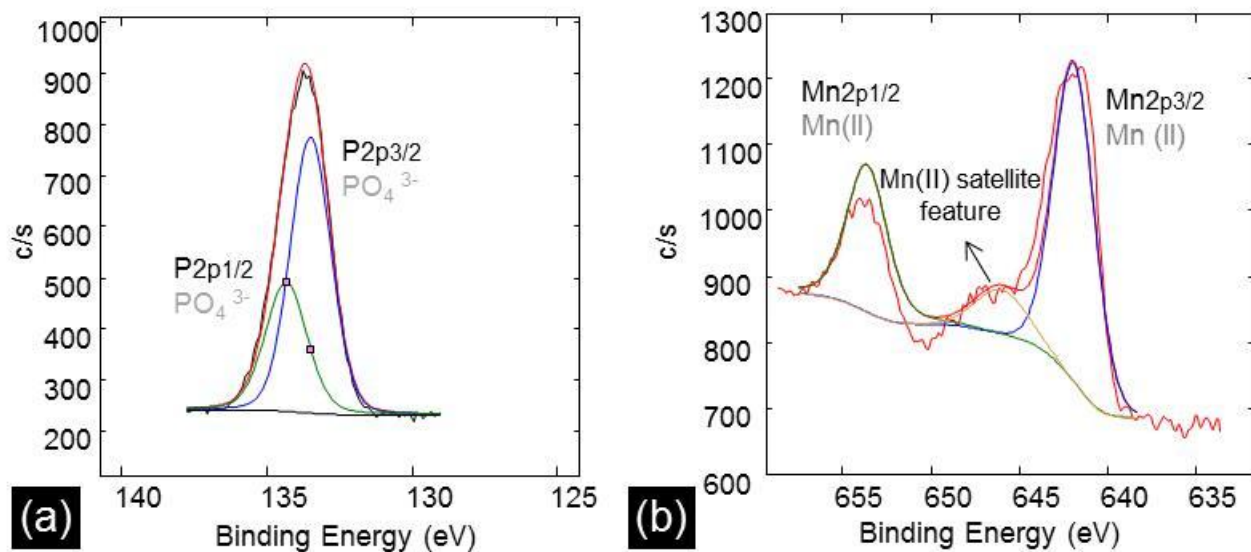
Figure 96. XPS spectra of the manganese phosphate coating zoomed on a) P2p energy region, and b) Mo2p3 energy region
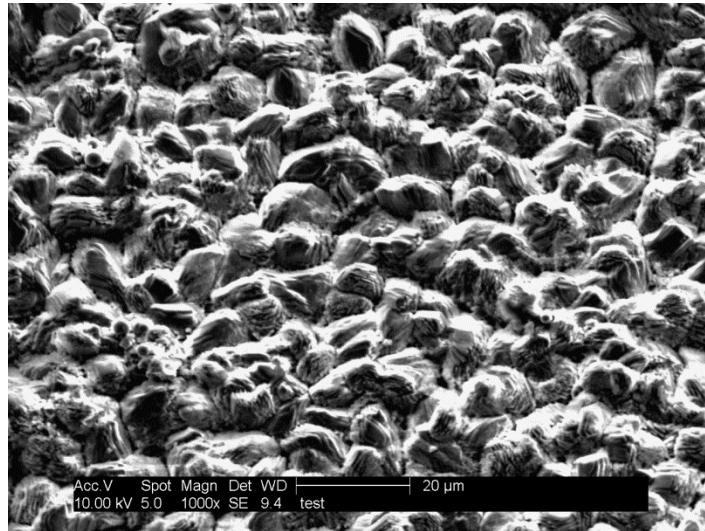
Figure 97. SEM image of the manganese phosphate coating present on the steel surface of the gears before the transmission test

The duration of the tests for each sample as well as the information on the damage observed at the end of each test on the surface of the teeth are reported in Table 11. Figure 98 shows the images of the gears after the tests.

Table 11. Information about the duration of each test and the damages observed on the surface after the transmission tests

Sample	Duration of the test	Number of pinion teeth damaged	Damage on surface
B	Stopped at full duration (426h)	3	No damage (small pits)
D	Stopped at extended time (600h)	0	No damage

The transmission tests carried out with Sample B was stopped at 426h and very few pits were seen on the teeth of the gear. Every 142 hours, visual inspection of the gears was done, quantifying the number of pits and measuring the pitted areas, the information about the evolution of the pits measured after each visual inspection for sample B is summarized in Table 12. Two pits of less than 3 mm^2 were seen on the surface of the gear's teeth at 142 hours and a third pit of less than 1 mm^2 was observed at 284 hours. No evolution of any of these pits was observed during the test. Additionally, at the end of the test no new pits were seen. The fact that the area of the pits didn't changed during time suggests that somehow they were sealed by the lubricant.

Figure 98. Surface of the gears after the experiments for a) Sample B and b) Sample D

Table 12. Evolution of the pit area measured for sample B

Time (h)	Number of pinion teeth damaged	
	Pit area ≤ 1 mm^2	$1<$Pit area<3mm^2
142	0	2
284	1	2
426	1	2

On the other hand, the test lubricated by sample D (with nanoparticles and package of additives) did not lead to any visible pitting after 426h, so it was pursued until 600h with no visible surface damage of the teeth at the end of the test. These results demonstrate the beneficial effect of the particles in the reduction of spalling when used as additives in base oil. Moreover, the presence of the additives package in the lubricant does not alter the performances of the particles. No antagonist effect was observed and the anti-fatigue performances of the nanoparticles were actually enhanced in the presence of the other

additives. In order to understand how the particles interact with the surfaces, chemical analyses and observations were made on the worn surfaces of the gears lubricated with the nanoparticles (Samples B and D).

First of all we wanted to verify that the nanoparticles were able to form a tribofilm on the steel surface. So, XPS analyses were made on a tooth of the gearboxes lubricated with sample B and D at the end of the tests. As contact conditions are known to be the most critical bellow the pith diameter, analyses were made on the surface of the dedendum area of the tooth (see Figure 99). The spot size was 50 µm with a power of 12.5W. The gears were cleaned with heptane and the teeth were cut from the gears using a cutting metal machine equipped with a resinoid cut-off wheel from Presi enterprise. Cutting was carried out under dry conditions to avoid contamination from cutting fluids. The temperature was monitored by a thermocouple and was not allowed to exceed 120°C. The teeth were washed with heptane and sonicated for ten minutes before the XPS analyses.
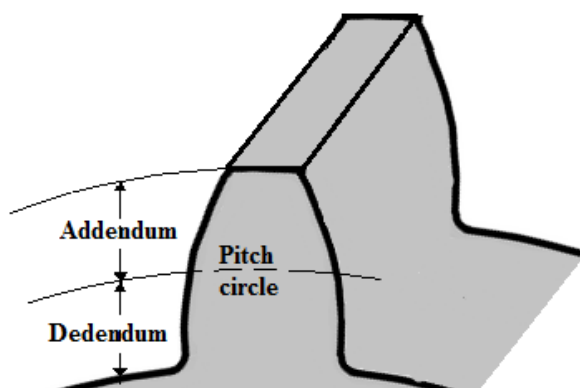
Figure 99. Gear tooth terminology

Figure 100 shows the XPS results for sample B. The survey scan (Figure 100a) shows the presence of sulfur, tungsten, iron and oxygen at the surface of the material. Neither manganese nor phosphorus is detected, letting think that either the coating was rubbed and replaces by a tribofilm or that a tribofilm thicker than 10 nm composed of the elements said before was created over the coating. Decomposition of the tungsten spectra (Figure 100b) shows the presence of two peaks $W4f_{5/2,}$ one at 32.4 eV which corresponds to W-S bond and another one at 35.9 eV that corresponds to W-O bond. The atomic concentration of tungsten in an oxide form is 58%. Treatment of the sulfur spectra (Figure 100c) shows one peak $S2p_{3/2}$ at 162.2 eV corresponding to sulfide (WS_2 or FeS_2) and another one at 168.6 eV which can be attributed to a contribution of sulfur oxide. Tungsten and sulfur elements come undoubtedly from the nanoparticles. However, the nanoparticles were probably oxidized during the test or during the cutting of the teeth. Nevertheless, previous works reported in the literature shows oxidation of nanoparticles when tested at 100°C in base oil (*103, 144*).
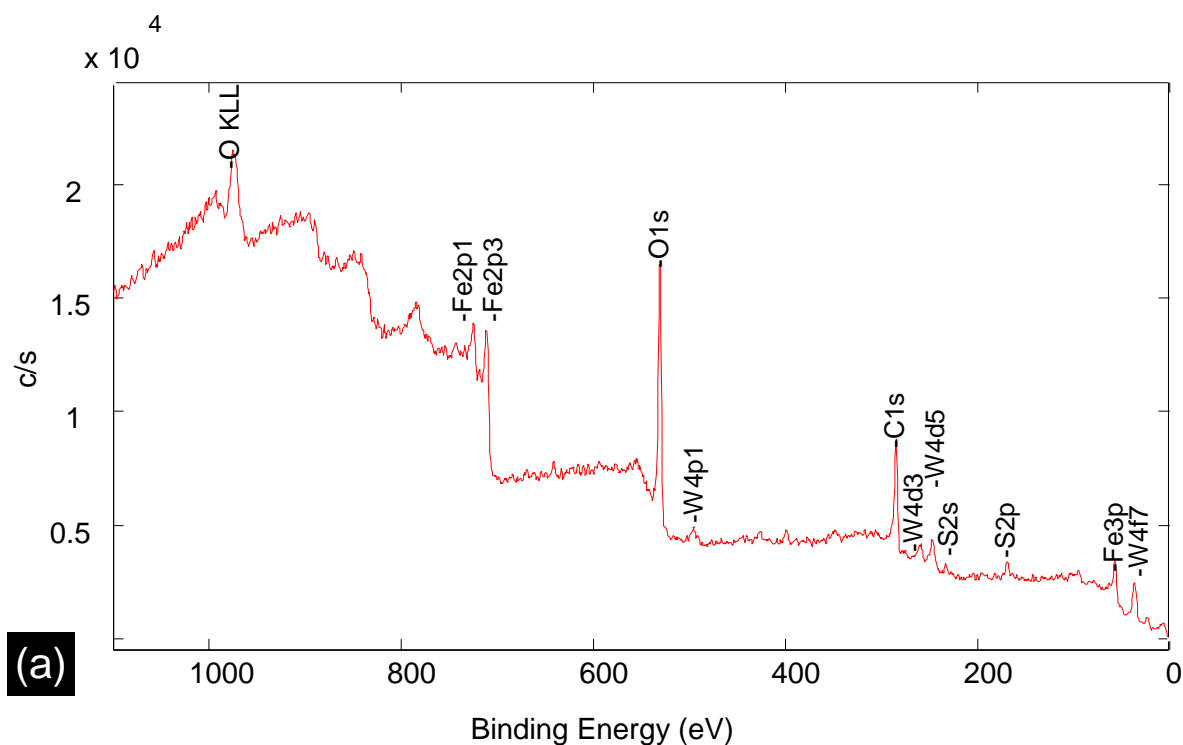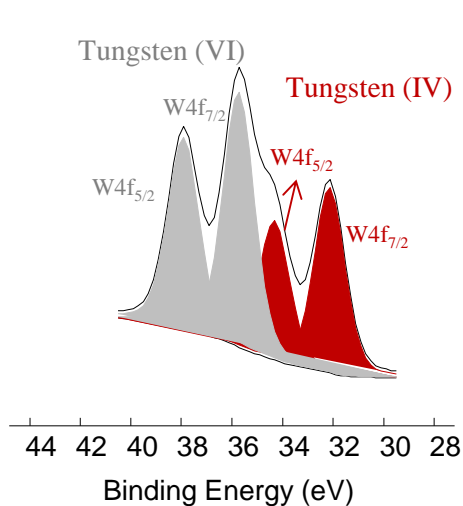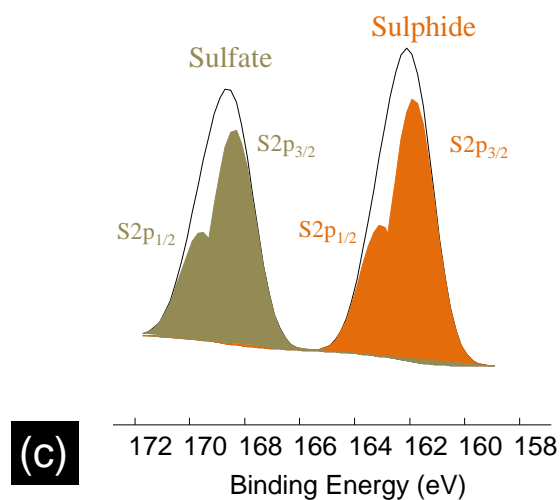
Figure 100. XPS spectra of the tribofilm formed on the gear surface for sample B, a) zoomed on the W4f energy region (b) and S2p energy region (c)

Analyses made for the gear lubricated with sample D (Figure 101) show the presence of not only tungsten and sulfur elements, that come from the nanoparticles, but also of calcium and phosphorous which come from the package of additives. The presence of other additives in the formulation does not seem to prevent the nanoparticles to interact with the surface of the teeth of the gear. Once again, no

phosphorus or manganese is detected. In order to verify if the coating was rubbed from the surface SEM images of the surface teeth and of a transversal cut were done.
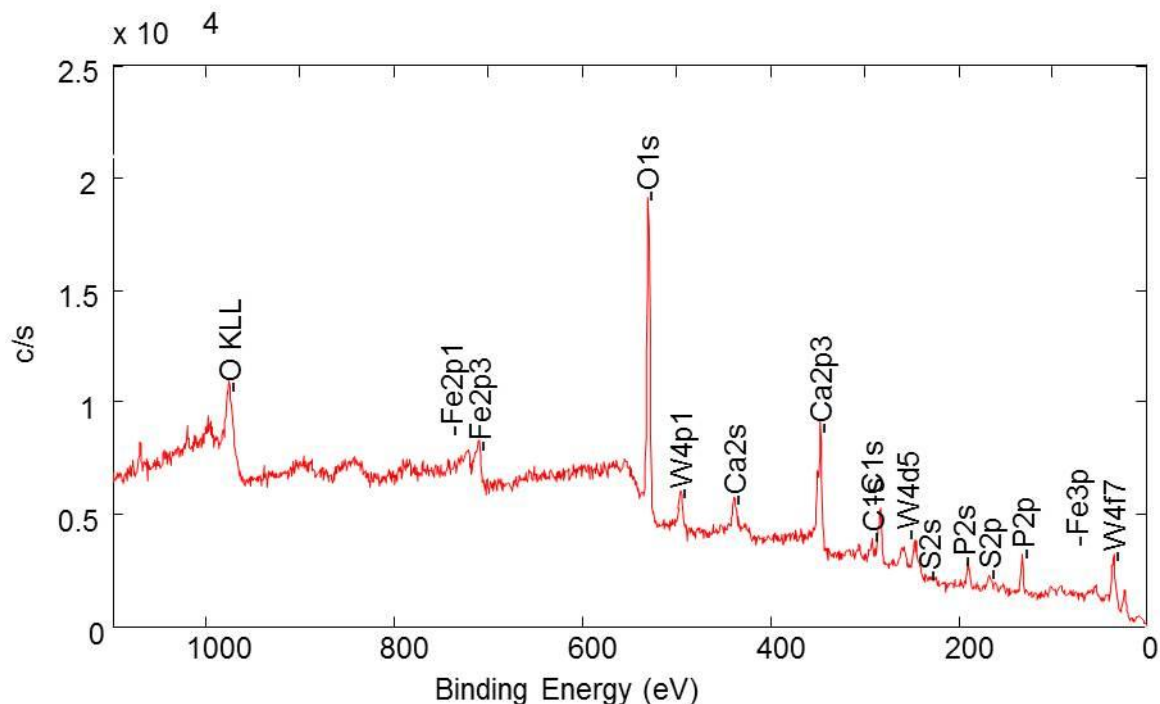
Figure 101. XPS spectra of the tribofilm formed on the gear surface for sample D

The SEM images of the surface of the teeth after the experiments for sample B and D can be observed in Figure 102a and c respectively. It is possible to see at the bottom of these images the phosphate coating crystals that was not rubbed because of the geometry of the gears. Figure 102b and d show SEM images of the same teeth (respectively Sample B and D) after cross-sectional cuts made from the teeth using a well diamond wire saw. Figure 102b and d were recorded approximately 400 µm above the remaining phosphate manganese layer. From these images, it can be observed that the phosphate layer was rubbed during the experiments.
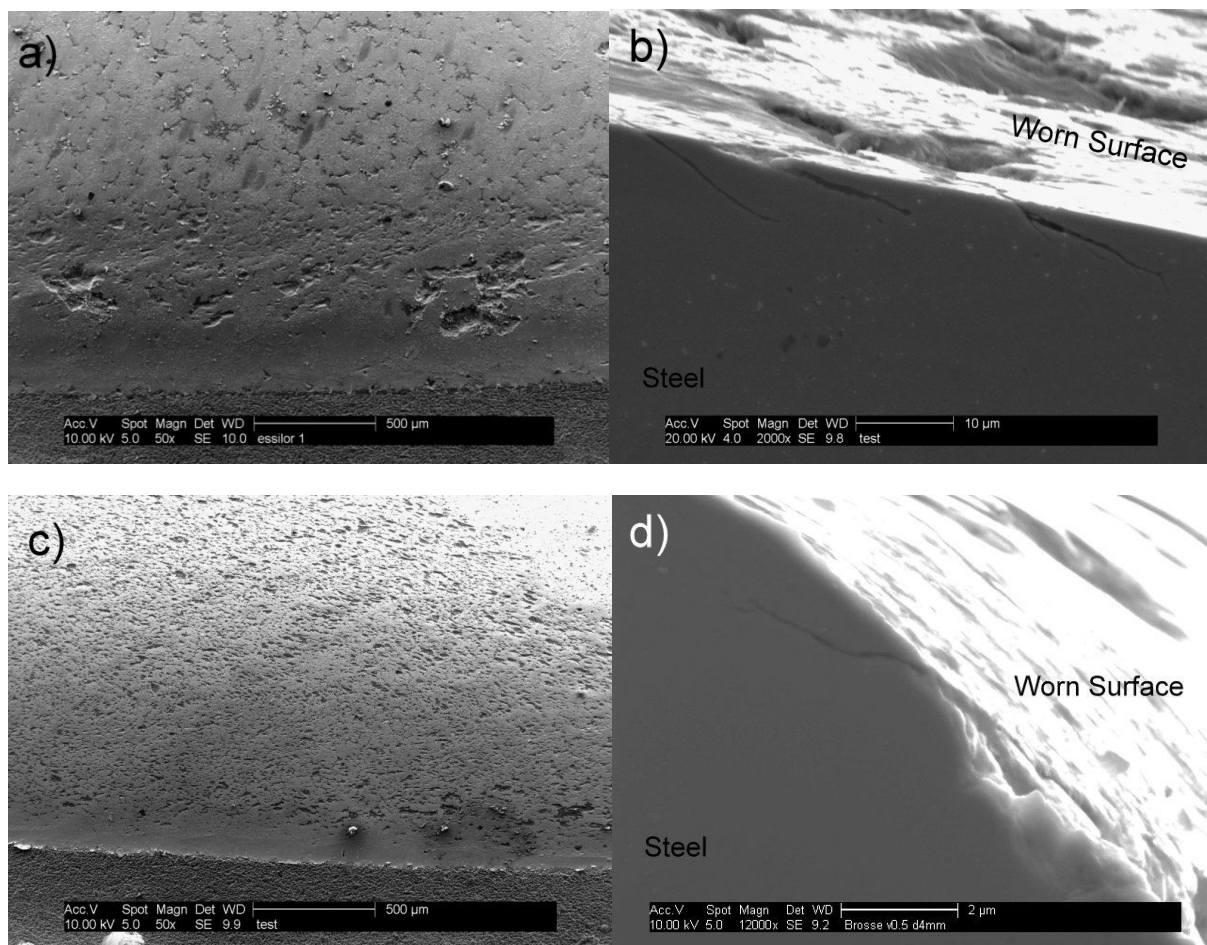
Figure 102. SEM images of the teeth after test for sample B and D showing the presence of cracks; (a) Surface of the tooth for sample B, (b) cracks for sample B, (c) surface of the tooth for sample D, (d) cracks for sample D

The cross-sectional cuts made for the teeth of the gears lubricated with sample B and D revealed the presence of cracking in the material. A net of cracks close to the surface with a depth in the range of 5 to 10 μm and an angle to the surface between 15 and 30 degrees was seen for sample D. These cracks are one form of fatigue named micropitting (*20-23, 145*). Even though small cracks were also seen for sample B (Figure 102b), pitting and spalling were also observed (Figure 102a). Additionally a net of deep non oriented cracks was also observed in a cross sectional cut made for Sample B in a spalled region as illustrated in Figure 103. According to the literature, micropitting can escalate into full scale pitting (*22*). Micropitting resistance is known to be strongly affected by lubricant properties, especially the base oil type, viscosity and the lubricant chemistry (*146, 147*), therefore it is not possible to do a direct comparison of the results obtained with sample B and D because of the different chemistry of the samples. However, we can say that more cracks were observed for sample D which can be explained by the presence of the package of additives which is normally detrimental for micropitting as explained in Chapter 1. Further investigations would be needed to bring a new insight in the synergetic effect between the nanoparticles and the additives package.
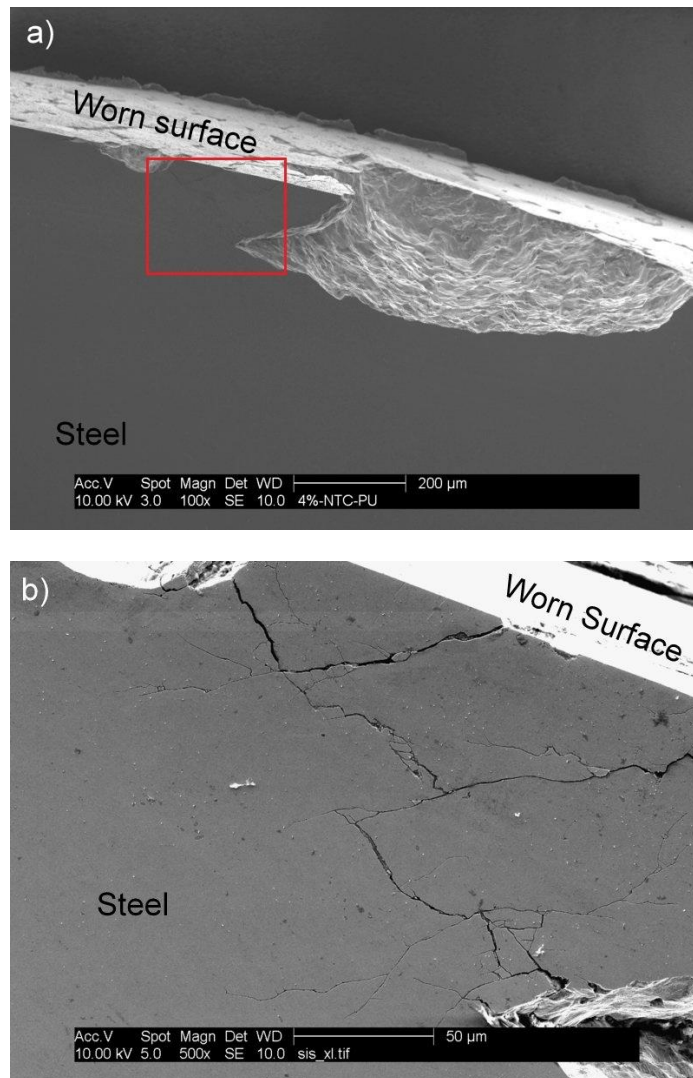
Figure 103. SEM image of the cross-sectional cut made from a tooth of the gear after the test for sample B on a spalled zone; a) localization of the cracks; b) zoom of the red rectangle showing the presence of deep cracks

We have seen that the nanoparticles formed a tribofilm on the steel surface and that there was cracking for both samples. However, this does not explain how nanoparticles can act against crack growth that was the phenomena seen for sample B. As a consequence, the following part of this work focuses on this sample too try to understand these results.

Figure 104 shows the hole left by a spall in the dedentum zone of the tooth. In the right upper part of the figure, the phosphate coating that was not rubbed during the test (due to the geometry of the contact) can be observed. EDX mapping was carried out. It reveals more intense signals for both tungsten and sulfur elements on the walls of the hole left by the spall. Because of the topography of the tooth surface

and the location of the detector, information of some zones (the deeper ones) could not be collected. This results in the observation of some black parts on the mapping.
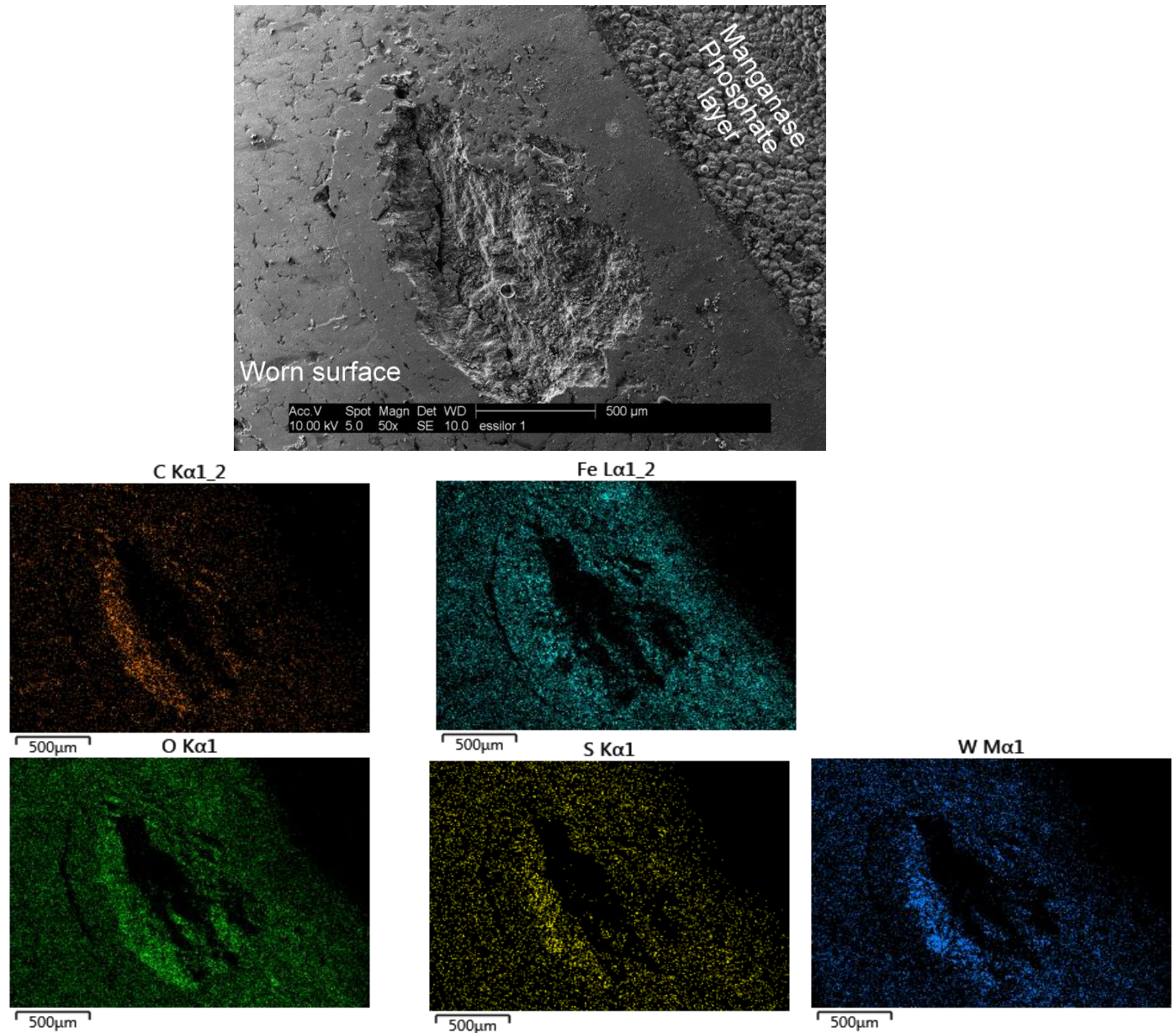
Figure 104. Chemical mapping characterization of a spall observed for sample B

Several chemical mapping where done on the tooth surface for sample B (another example can be observed in Figure 105). All of them revealed important signal for tungsten and sulfur in the places

where defects were seen on the surface of the gear. Figure 102b and d, showed that cracks look like lines or defects on the surface similar to those observed in the left of the hole left by a spall in Figure 105.
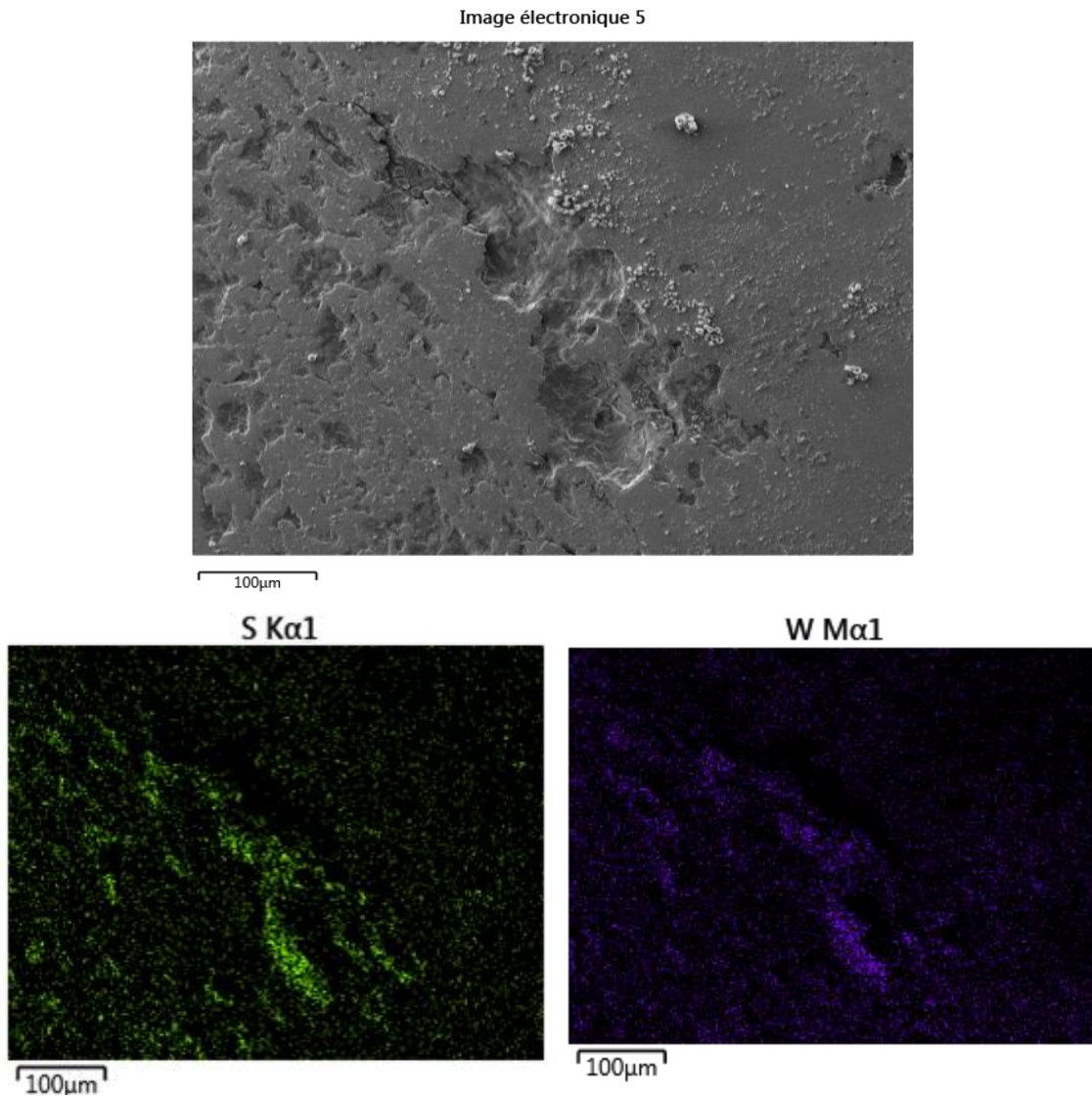
Figure 105. Chemical mapping characterization for sample B where different defect on the surface can be observed

As explained in Chapter 1, lubricants can promote crack propagation due to oil hydraulic pressure caused by oil penetrated into the cracks. The whole process is sketched in Figure 106.

1. Crack opening under lateral tensile stress
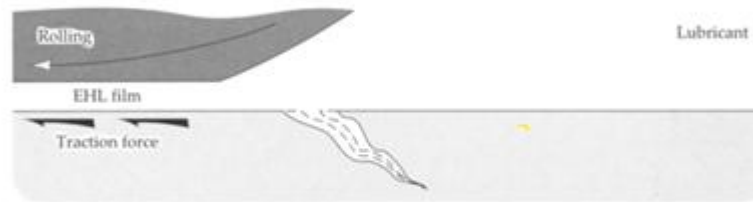
2. Lubricant forced into crack by extreme pressure
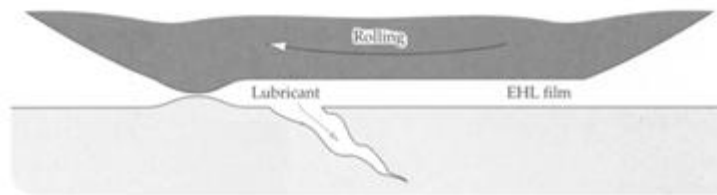
3. Crack extension by compressed lubricant
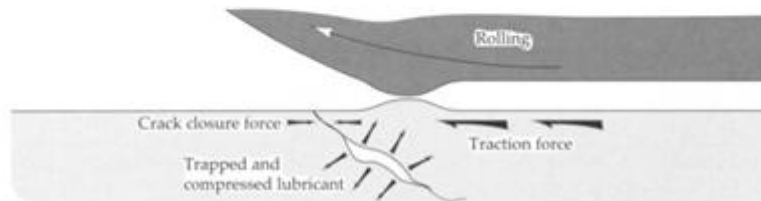
Figure 106. Crack propagation by oil hydraulic pressure (*19*)

Our results so far have shown that a tribofilm has been formed on the steel surface and that there is an important nanoparticles concentration in the places where some defects can be seen in the surface. It is possible that a mechanical blockage of the mouth of the cracks by the solid nanoparticles could have limited oil seepage reducing crack growth due to hydraulic pressure as proposed in Figure 107. However, quantification of oil seepage into the cracks is not possible today so this mechanism cannot be proven and will remain a hypothesis until a reliable measurement method becomes possible.
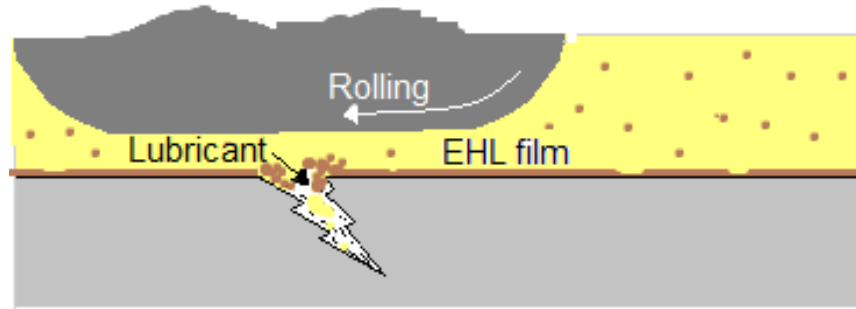
Figure 107. Proposed mechanism against crack growth

As described in Chapter 1, the fact that additives can go inside cracks and react with crack faces has already been demonstrated by Meheux et al. (*40*). We have seen that nanoparticles create a tribofilm on the steel surface and that an important concentration of them at the mouth of the cracks may limit oil seepage and reduce hydraulic pressure inside cracks. However, we do not know if the tungsten disulfide nanoparticles entered the cracks or not. In order to verify this point, two cross-sectional cuts were prepared by FIB and were observed by TEM after the test done with Sample B. The first one was done on the surface of the tooth to be able to observe the tribofilm formed during the transmission test whereas the second one was done in the bulk of the material, 100 μm bellow the worn surface to verify whether the nanoparticles (or exfoliated WS$_2$ sheets) can go deep inside the cracks or not. Localization of the fist cut can be seen in Figure 108.
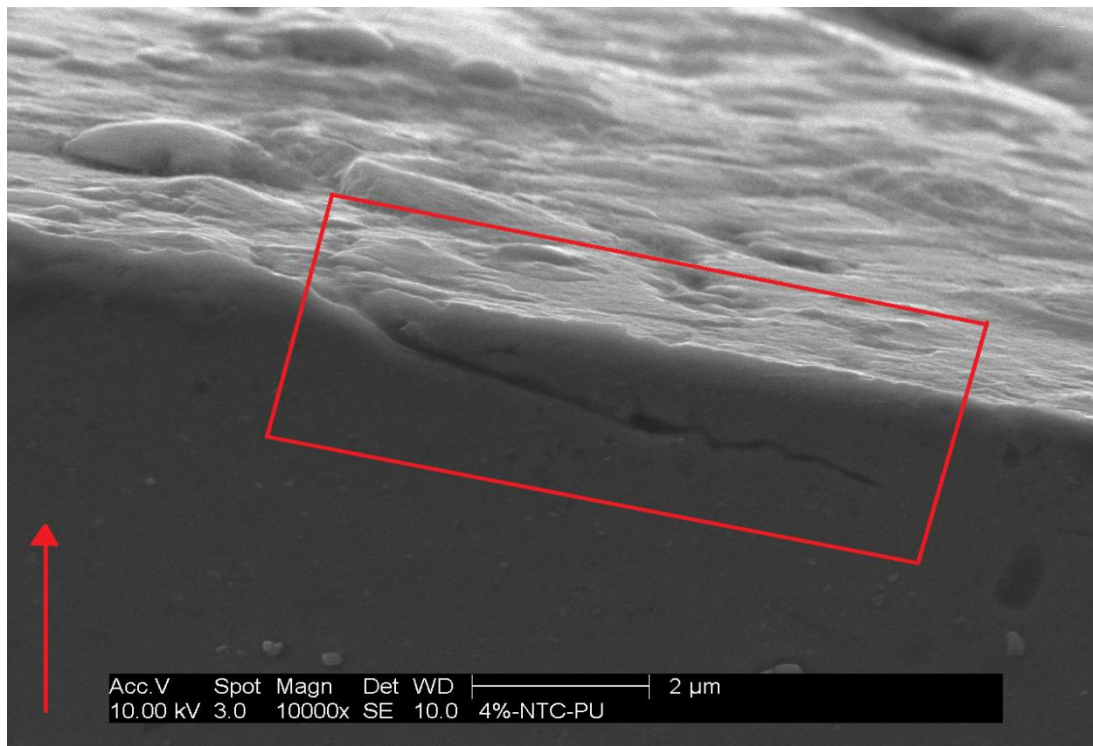
Figure 108. Localization of the cross-sectional cut made by FIB on the surface of the gear tooth (Sample B). The arrow represents the direction of the cut

TEM images and chemical analyses for this first cut can be seen in Figure 109 and Figure 110 respectively. A small crack close to the surface can be seen in its entirety in Figure 109a. A 100 nm thick tribofilm can also be observed between the protective film and the surface of the steel. From this figure, the walls of the crack seem also to be covered by a film which has the same aspect than the tribofilm formed on the steel surface. Figure 109b shows a zoomed part of the Figure 109a where a flake of steel looks surrounded by the tribofilm on its upper part and the layer formed on the walls of the cracks. The thickness of the film formed into the cracks is approximately the same than the tribofilm observed on the surface. EDX analysis shows that both the tribofilm (Figure 110a) and the layer formed into the crack (Figure 110b) are composed of the same elements: sulfur, tungsten, oxygen and iron. However, more iron is seen in the tribofilm than in the film formed on the walls of the track. Copper comes from the grid in where the FIB cut is fixed and carbon may come from contamination. The whitest zone in the middle of the crack is mainly composed of carbon which may also come from contamination during the cut. The presence of some sheets of tungsten disulfide is also regularly observed all along the crack as illustrated in Figure 109c that was taken inside the crack, 4 micrometers from its beginning.
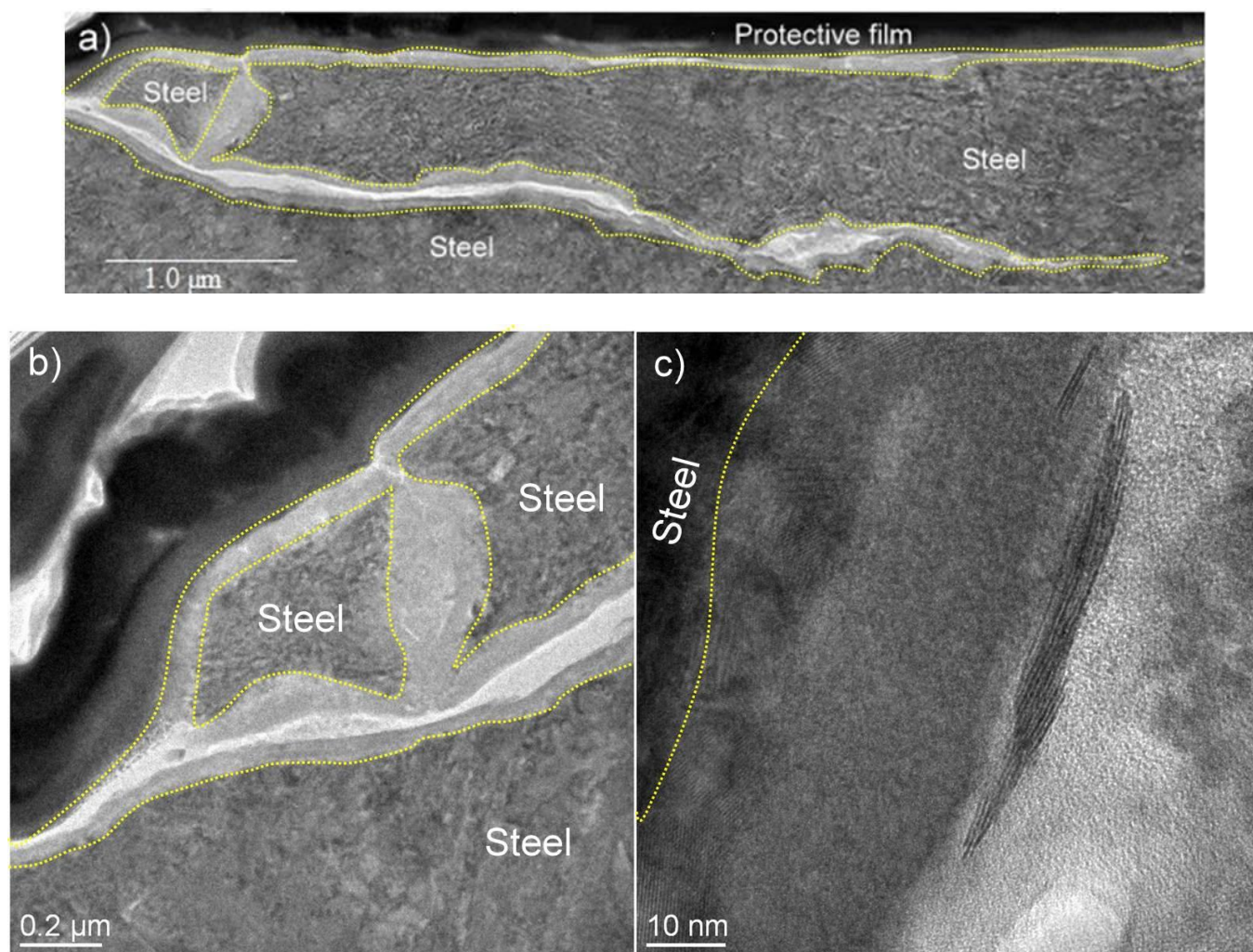
Figure 109. a) TEM image of the FIB preparation (Sample B), b) zoom-in at the beginning of the crack, and c) zoom-in on a zone containing sheets of WS_2
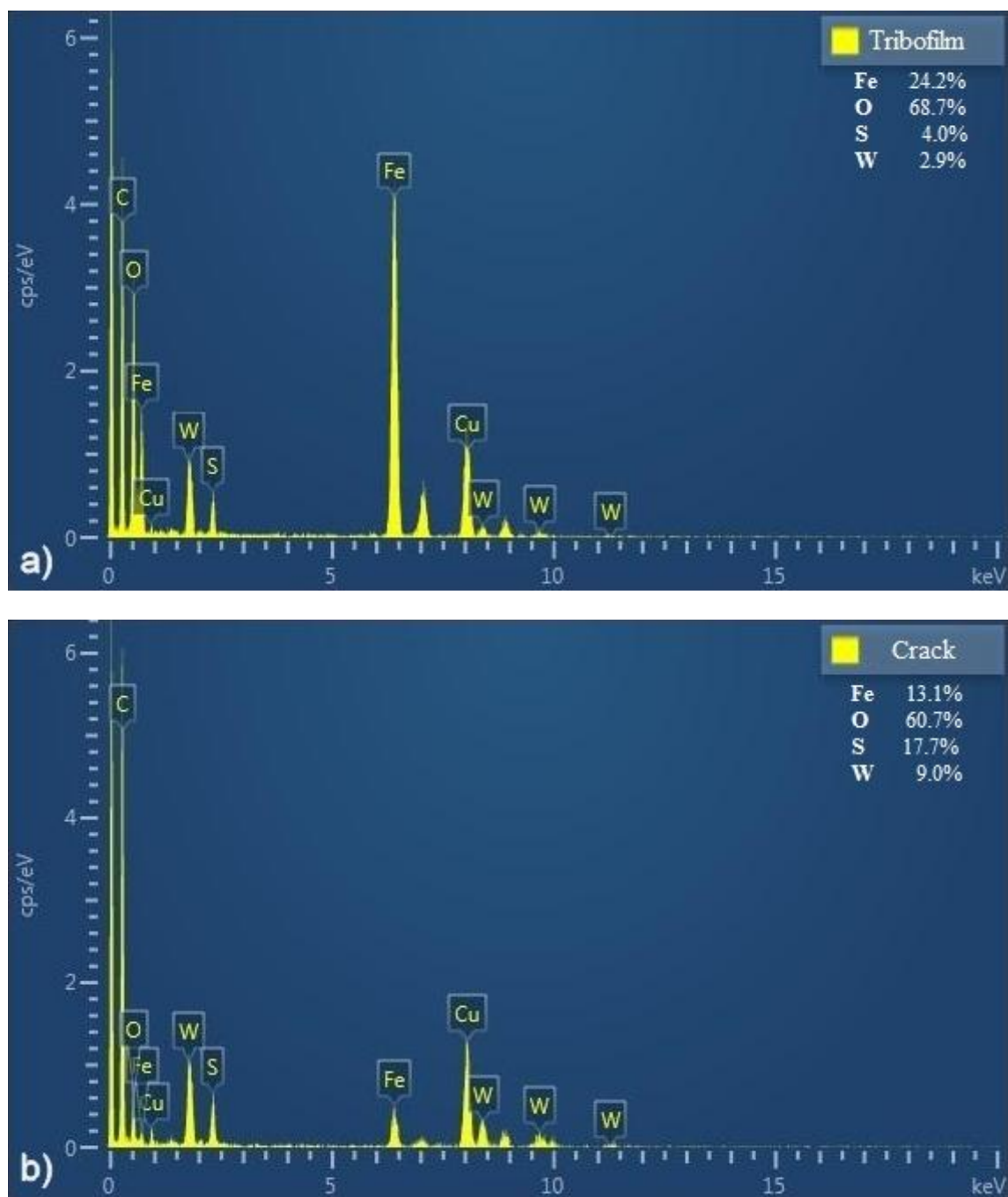
Figure 110. EDX spectra of a) the tribofilm and b) of the layer formed into the crack

The second cross-cut was done in the spalled region where a net of deep non-oriented cracks was observed (Figure 111).
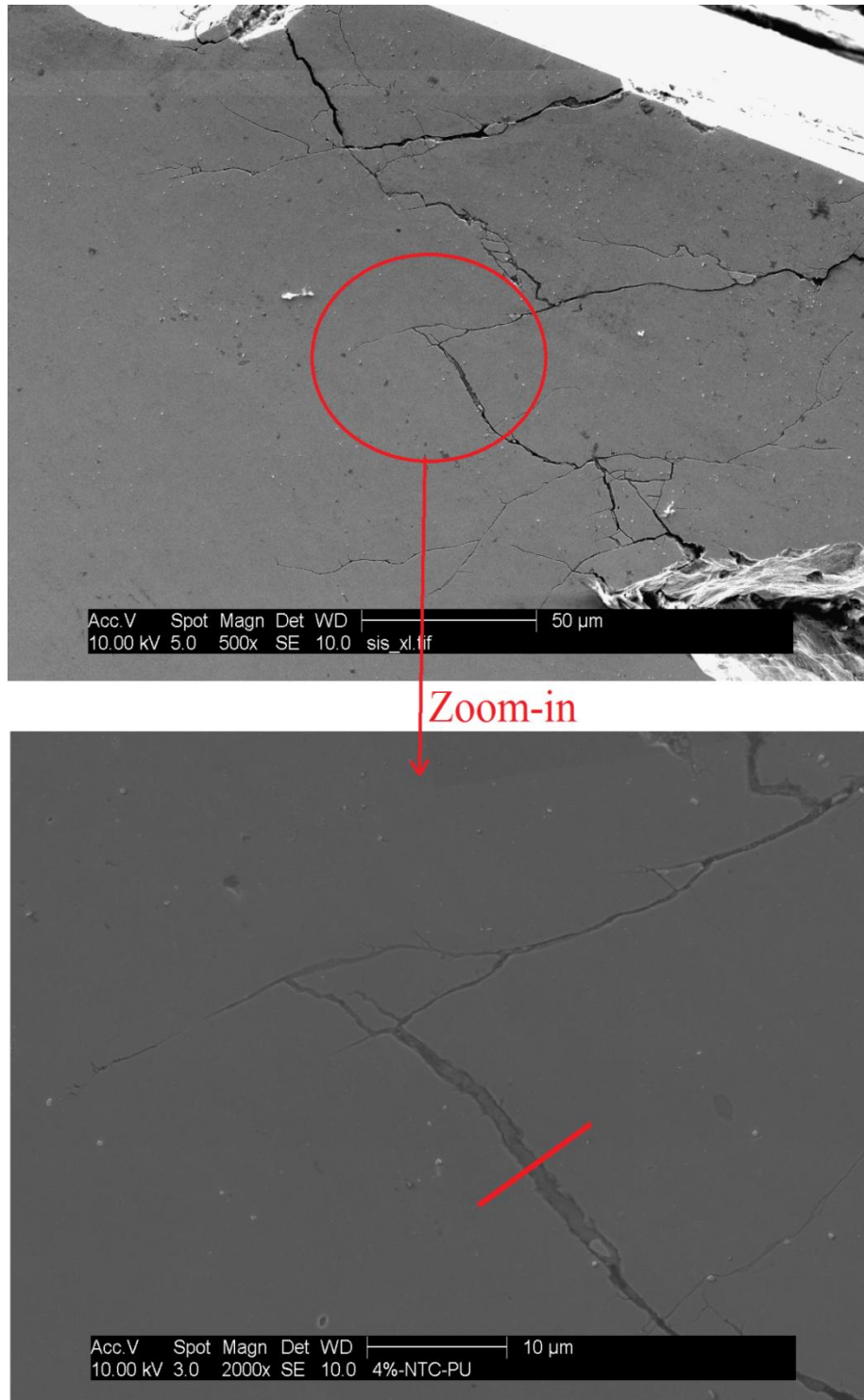
Figure 111. Localization of FIB cut number two (Sample B)

TEM images for this cut reveal also the presence of a gray layer all along the walls of the cracks (Figure 112). EDX demonstrated the presence of tungsten and sulfur also in this gray zone. The zoom (Figure 112 b, c and d) made on the gray layer reveals the presence of sheets of WS_2 surrounding all the gray zones in the thickest part. Additionally, some spherical particles can be observed on the left part of the image in Figure 112a. EDX analysis made on these particles is shown in Figure 113. They are composed of tungsten, iron, oxygen and sulfur. Ga comes from the FIB preparation, Cu and Co comes from the grid used as sample holder.

It is known that contact fatigue is generally accompanied by the release of spherical particles with sizes from 1 to 5 µm consisting of a mixture of metal and oxide (*19*). The origin of these particles is thought to be the detachment of material from the walls of the cracks which are in relative movement under the stress cycles causing them to close and slide against each other. Then, the movement of the cracks rolls the particle providing them the spherical shape. The spherical particles observed inside the cracks may have been formed by this way. Then, the metal and oxide particles formed by fatigue may have taken tungsten and sulfur from the layer that was formed on the walls of the cracks.
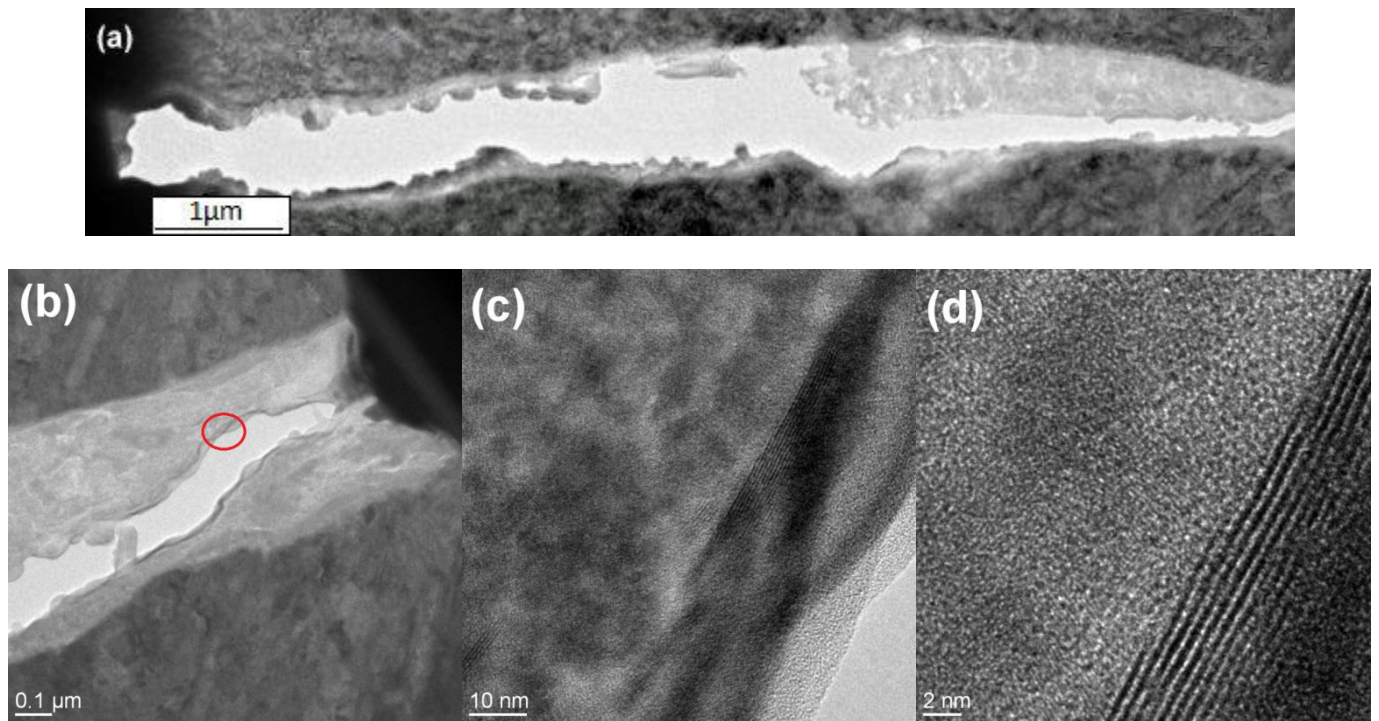
Figure 112. TEM image of the FIB cut made in the bulk of the steel (Sample B) showing: a) the presence of a gray layer on the walls of the crack, b) a zoom of the upper right side of figure a), c) a zoom of the red circle of the figure b), and d) a zoom of the figure c) revealing the presence of WS_2 sheets in the border of the gray zone
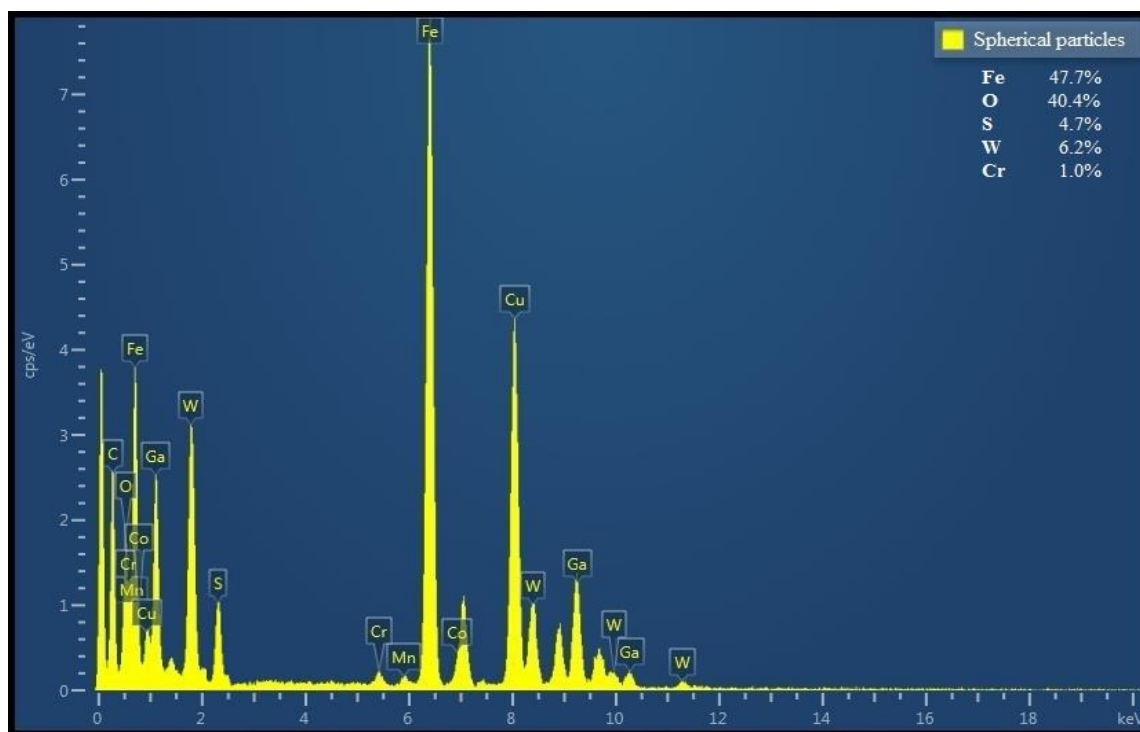
Figure 113. EDX analysis of the spherical particles observed in Figure 112a

The surfaces analyses made for sample B showed that sulfur and tungsten elements were not only found on the surface of the tooth (as XPS results showed) but also inside the cracks as proven by TEM and EDX. The film seen on the crack faces may have been formed by the action of shear when the crack is closed under the cycles of load. Moreover, fragments (sheets) of WS_2 nanoparticles were found far inside the cracks, up to 100 μm. Additionally, the flake of steel observed in Figure 109b seems to be attached to the tooth by the tungsten and sulfur layer. These results clearly show that nanoparticles are able to go deep inside the cracks. This film formed on the surface of the gear and on the walls of the cracks may protect steel against hydrogen embrittlement and avoid cracks propagation. Endo et al. (*29*) claim that the formation of a protective layer film on steel formed during fatigue tests can increase contact fatigue life. As a matter of fact, Niste et al. (*148*) have demonstrated that tribofilms formed on the surface of steel rolling element bearing, when lubricated by WS_2 nanoparticles dispersed in base oil at high temperatures, do act as a barrier to hydrogen permeation. To get to this conclusion, the authors performed tribological tests in a ball-on-disc setup rig at 120°C and a Hertz pressure of 4.8 GPa (boundary lubrication regime) and measured the hydrogen content in the steel samples using a TDS (Thermal Desorption Spectroscopy) apparatus. Their results showed that the WS_2-additized sample reduced significantly the amount of hydrogen permeated in the steel compared to the PAO alone. Our results showed that a tribofilm is not only present on the surface of the gears but also on the walls of the cracks. Additionally, this is the first time that the presence of a solid lubricant additive is demonstrated inside cracks.

12. Conclusion

The use of nanoparticles as lubricant additives in the automobile industry involves the study and comprehension of their effect into the mechanical parts of a car. In this work, we studied the effect of WS_2 nanoparticles in gearboxes when added to base oil and in the presence of a package of additives. Results have shown that nanoparticles increase the lifespan of gear drives when added to base oil. Furthermore, the presence of the package of additives in the base oil seems to increase the action of the nanoparticles.

The chemical analyses revealed that the nanoparticles are able to form a tribofilm on the steel surface even in the presence of a commercial package of additives. Different phenomena were observed on the gears lubricated by the samples. Micropitting, pitting and spalling were observed in the case of the nanoparticles in base oil, whereas only micropitting was seen in the case of the nanoparticles in base oil in the presence of the commercial package of additives.

The investigation done on the gear lubricated by the nanoparticles in base oil revealed an important concentration of tungsten and sulfur in the places where some defects were seen. This nanoparticles concentration is thought to be able to limit oil seepage inside the cracks which would release hydraulic pressure and reduce crack propagation. Nevertheless, this cannot be proven with the technology currently available. Additionally, the chemical analyses revealed not only the presence of a tungsten and sulfur containing tribofilm in the surface of the tooth, but also that a film formed by the same elements coming from the nanoparticles (as well as sheets of nanoparticles) were found all along the wall of the cracks even 100 micrometers below the surface. It has been demonstrated by another research group that this tribofilm may act as a barrier against hydrogen embrittlement increasing life span of the gear drive.

Further investigation should be done on the hydrogen permeability of tribofilms produced by tungsten disulfide nanoparticles in the presence of a commercial package of additives.

Résumé. Partie 2.
Lubrification de boîtes de vitesse par des nanoparticules de disulfure de tungstène

Dans cette deuxième partie de la thèse, le potentiel des nanoparticules pour une application boîte de vitesse a été exploré. Dans un premier temps, des essais à l'échelle laboratoire ont été menés par l'intermédiaire d'une FZG avec un protocole spécialement adapté dans le but de tester l'endurance des engrenages lubrifiés par des huiles contenant des nanoparticules. Pour ces essais, les nanoparticules ont été dispersées dans une huile de base composée à 80 wt% par de la PAO et 20 wt% par un polyol-ester. L'influence d'un paquet d'additif commercial sur la performance des nanoparticules a aussi été étudiée. Les premiers résultats ont montré que les échantillons contenant des nanoparticules donnent des durées de vies plus importantes que leurs références respectives.

Pour cette raison, nous avons décidé de tester les huiles dopées aux nanoparticules sur des boîtes de vitesse réelles que l'on trouve dans les véhicules. A nouveau, un protocole d'endurance a été utilisé pour les essais. L'évolution d'écailles sur les dents est suivie périodiquement lors de ces essais. De très bons résultats ont été obtenus avec les deux huiles testées. Dans le cas de l'engrenage lubrifié par les nanoparticules dans l'huile de base, trois petites écailles ont été observées au niveau des dents à la fin du test. Les données récoltées lors des inspections périodiques des engrenages permettent de mettre en évidence que deux des trois écailles étaient déjà apparues avant la première inspection visuelle et que leur aire n'a pas évoluée dans le temps. On retrouve le même résultat pour la troisième écaille, apparue avant la deuxième inspection visuelle. On constate donc une évolution très lente des écailles lors de cet essai. Dans le cas de la boîte de vitesse lubrifiée avec le paquet d'additifs et les nanoparticules, les résultats ont été tellement surprenants que nous avons poursuivi le test au-delà de la durée standard. Aucune écaille n'a été observée sur les dents des engrenages lors de cet essai.

Les analyses XPS menées sur la surface des engrenages ont montré que les nanoparticules forment un tribofilm même en présence d'un paquet d'additifs commercial. Des analyses de surfaces faites sur les dents des engrenages ont montré la présence de fissures pour les deux boîtes de vitesse. Cependant, des fissures plus grandes et interconnectées ont été observées dans le cas de l'engrenage lubrifié par les nanoparticules dans l'huile de base. De cette manière on parle de phénomènes de pitting et d'écaillage pour cet essai et de micro pitting pour le deuxième.

L'investigation faite sur les engrenages lubrifiés par les nanoparticules dans l'huile de base ont permis de voir qu'il existe une concentration importante de nanoparticules dans les endroits où il y a des défauts sur la surface des dents. Nous pensons donc que cette concentration importante de nanoparticules peut limiter la quantité d'huile qui rentre dans les fissures réduisant la pression hydraulique exercée par le liquide piégé dans les fissures et ensuite leur propagation. Cependant, il n'existe pas aujourd'hui la technologie nécessaire pour prouver cette hypothèse.

Enfin, des lames FIB observées par HR-TEM et analysées par EDX, ont mis en évidence la présence d'un film sur l'acier à l'intérieur des fissures. Ce film est composé par les mêmes éléments que le tribofilm formé sur les dents. Ce film composé par de l'oxygène, du fer, du tungstène et du soufre montre que les

nanoparticules rentrent dans les fissures et réagissent avec les surfaces métalliques pour créer un film. Il a été démontré récemment que ce type de film peut protéger l'acier contre une perte de sa ductilité causé par l'attaque par des atomes d'hydrogène.

General conclusions and perspectives

The potential of industrially produced fullerene like WS$_2$ nanoparticles for an automotive application was studied throughout this research work.

With the aim of understanding the motivations and industrial context that motivated this research a state of the art on tribology science in general, and on the lubricating properties of nanoparticles in particular was exposed in the first section of this work. Although metal diacolgenide nanoparticles have shown interesting friction reduction and anti-wear properties under specific laboratory test conditions, some key issues such as the nanoparticle lubricating properties in the presence of additives commonly used in industrial lubricants and under real life conditions was still missing. In consequence, this research work is divided in two main parts that intended to address these two issues.

In the first part of this work, the industrially produced IF tungsten disulfide nanoparticles were characterized and tribologically tested under different test conditions. Then, their behavior in the presence of additives that are commonly used in lubricants was studied. The results showed that despite the fact that the sample used in this work was heterogeneous in terms of shape and size, the nanoparticles produced at the industrial scale do have interesting friction and wear properties when tested in PAO base oil in the boundary lubrication regime (as those produced at the laboratory scale). Actually the friction reduction and anti-wear properties of these nanoparticles were observed at ambient and 100°C on both smooth and rough surfaces. However, some reproducibility problems that are believed to be due to the in situ generation of tungsten oxide were observed at 100°C on the smooth surfaces. The friction tests carried out with binary blends (nanoparticles with either diphenylamine or ZDDP additive in PAO) at 100°C in the boundary lubrication regime on the smooth surfaces, revealed that the presence of diphenyl anti-oxidant does not have any effect on the tribological properties of these nanoparticles whereas a synergistic effect was seen between the nanoparticles and ZDDP additive under these tests conditions. The chemical analyses showed low tungsten oxide concentration in the tribofilm with the use of ZDDP which might explain the good tribological results obtained for this binary blend. This synergistic effect was also observed on the rough surfaces where actually the obtained value of friction coefficient was the same than for the smooth surfaces. On the other hand, the friction tests carried out for the ternary blend (that consisted of ZDDP, calcium phenate and nanoparticles) in base oil gave the same friction coefficient and wear results than the blend without the nanoparticles in steady conditions. Such good results obtained for the ZDDD and the detergent additive in PAO base oil are not fully understood and some research should be done to address this point. Nevertheless, the use of nanoparticles allowed to get a low and stable friction coefficient from the very first cycles which was not the case for the other sample that needed some time to reach the steady stable condition. From this first part, it can be concluded that the industrially produced tungsten disulfide nanoparticles do exhibit interesting friction reduction and anti-wear properties in PAO base oil and that no antagonism was observed with any of the tested additives so they can be used in the formulation of nanoparticles-doped lubricants. Although this is a step forward in the formulation of more efficient lubricants, the comparison between the beneficial effects of using this additive instead of MoDTC still need to be studied. This

investigation should be done first under specific laboratory test conditions and then, under the conditions found in the real life applications. The effect of aging of both additives on their lubricating properties should also be investigated. It is important to note that this research work was carried out using industrially produced tungsten disulfide nanoparticles that were synthetized with the synthesis techniques available three or four years ago. As said before, research has demonstrated that nanoparticle size and shape have a direct impact on their tribological properties. For this reason, it is important to keep in mind that the evolution and optimization of the synthesis techniques may allow in the future the production of more uniform nanoparticles with a given size and shape in large scales.

In the second part of this work, the effect of using industrially produced fullerene like WS_2 nanoparticles in gearboxes when added to base oil and in the presence of a commercial package of additives was investigated. The results showed that nanoparticles can be used to increase the lifespan of gear drives. The nanoparticles formed a protective tribofilm on the gear surface even in the presence of the package of additives. The investigation done on the gear lubricated with nanoparticles in base oil revealed an important concentration of tungsten and sulfur in the places where some defects were seen. This nanoparticle accumulation is thought to be able to limit oil seepage inside the cracks which would have a direct impact in reducing crack propagation. However, this cannot be proven with the technology currently available. The chemical analyses revealed not only the presence of a tungsten and sulfur containing film on the contact surface of the tooth, but also all along the wall of the cracks even 100 micrometers below the surface. It has been demonstrated by another research group that this tribofilm may act as a barrier against hydrogen embrittlement increasing life span of the gear drive. Further investigation should be done on the hydrogen permeability of tribofilms produced by tungsten disulfide nanoparticles in the presence of a commercial package of additives. The results obtained in this part of this work opens the door to the use of nanoparticles in applications affected by rolling contact fatigue such as wind turbines where gearbox failure remains the leading cause of downtime (*149*).

The research done in this work serves as a ground for the formulation of nanoparticle-doped lubricants. However, some key issues still need to be addresses before these lubricants could be commercialized. From the formulation point of view, one of the biggest challenges is to ensure an optimal dispersion of the nanoparticles without affecting their tribological properties. On the other hand, from the legislative point of view, the assessment of nanoparticles toxicity towards humans and the environment needs to be done. This would help to fill the regulatory gaps and to fix guidelines for safe nanoparticles handling, use and disposal.

Conclusions générales et perspectives

Les nanoparticules de dichalcogénures métalliques rencontrent un intérêt croissant en raison de leurs propriétés réductrices de frottement et anti-usure. Les recherches antérieures ont démontré que les fullerènes inorganiques de type WS_2 ou MoS_2 ont des propriétés tribologiques intéressantes qui en font des concurrents potentiels aux additifs utilisés aujourd'hui. Cependant, ces nanoparticules ont été produites à l'échelle du laboratoire et ont été testées dans des conditions de sollicitation très spécifiques (surfaces lisses, température ambiante). Dans le but d'utiliser ces nanoparticules dans des applications industrielles, elles doivent d'abord pouvoir être synthétisées à l'échelle industrielle et être testées dans des conditions de contact plus représentatives des applications réelles (surfaces rugueuses, hautes températures, présence d'autres additifs dans l'huile).

L'objectif de ce travail de thèse a été d'étudier le comportement tribologique des fullerènes inorganiques de WS_2 produits industriellement et de sonder leurs performances dans une application transmission.

Dans la première partie de la thèse, nous avons tout d'abord caractérisé ces nanoparticules avant de les tester sous différentes conditions de sollicitation et en présence d'additifs couramment utilisés dans l'industrie automobile. Nous avons donc travaillé avec un échantillon comprenant des nanoparticules de différentes formes et tailles. Les résultats tribologiques montrent que ces nanoparticules sont capables de réduire le coefficient de frottement ainsi que l'usure, dans des conditions de lubrification limite, lorsqu'elles sont dispersées dans une huile de base indépendamment de la rugosité de la surface testée. Cependant, des problèmes de répétabilité ont été observés lors des essais à 100°C sur les surfaces lisses. Ces problèmes ont été attribués à la formation d'oxyde de tungstène pendant le test de frottement. Les résultats tribologiques de mélanges binaires (nanoparticules avec diphénylamine ou ZDDP dans l'huile de base) ont montré que le diphénylamine n'a pas d'effet sur les propriétés tribologiques des nanoparticules, tandis qu'une synergie entre le ZDDP et les nanoparticules existe à 100°C dans le régime de lubrification limite. Les analyses chimiques ont mis en évidence que l'utilisation du ZDDP permet d'obtenir des tribofilms avec une faible quantité d'oxyde de tungstène ce qui expliquerait les bons résultats obtenus. Cette synergie permet d'obtenir la même valeur du coefficient de frottement sur les surfaces lisses et rugueuses. Dans le cas des tests réalisés avec le mélange ternaire : ZDDP, phénate de calcium, nanoparticules dans l'huile de base, un coefficient bas et stable a été obtenu dès les premiers cycles. Cependant, la même valeur du coefficient de frottement a également été obtenue avec le ZDDP et le phénate de calcium, en l'absence de nanoparticules, mais après un temps plus long. Plus d'études devraient être menées pour comprendre ces résultats.

Etant donné que nous n'avons pas observé d'effet antagoniste de ces additifs avec les nanoparticules, nous pouvons donc conclure de cette première partie que les additifs diphénylamine, ZDDP et phénate de calcium peuvent être utilisés dans la formulation des lubrifiants contenant des nanoparticules. Nous avons aussi démontré pour la première fois que les nanoparticules peuvent être piégées dans les rugosités propres des plans rugueux et que les tribofilms formés par les nanoparticules sont plus durables que ceux formés par le MoDCT. Ce point constitue un atout majeur pour l'utilisation des

nanoparticules vis-à-vis des additifs dits « solubles » utilisés aujourd'hui. Toutefois, une étude comparative entre ces deux additifs doit être faite sous différentes conditions de sollicitation et en tenant compte du vieillissement des huiles pour pouvoir en sortir des conclusions.

Dans la deuxième partie de cette thèse, nous avons étudié les performances des nanoparticules dans une application industrielle. L'application transmission a été visée. Des essais réalisés à l'échelle laboratoire ainsi que sur des boîtes de vitesse réelles ont montré que les nanoparticules de disulfure de tungstène produites industriellement peuvent être utilisées pour augmenter la durée de vie des engrenages. Les analyses de surface ont mis en évidence que les nanoparticules forment un tribofilm sur les dents des engrenages même en présence d'un paquet d'additifs commercial. Les bons résultats obtenus avec l'utilisation des nanoparticules ont été attribués à une possible diminution de la quantité d'huile qui rentre dans les fissures ainsi que par la formation d'un tribofilm composé de tungstène, d'oxygène, de soufre et de fer sur les parois de la fissure, lequel protégerait l'acier de l'attaque par l'hydrogène. Nous avons démontré pour la première fois que les nanoparticules rentrent dans les fissures et réagissent avec les parois métalliques. Pour compléter cette partie, il serait intéressant de mesurer le coefficient de diffusion de l'hydrogène à travers des films formés par les nanoparticules soit par expérimentalement soit à l'aide de la simulation numérique.

Les résultats obtenus lors de cette thèse ouvrent la voie à l'utilisation des nanoparticules dans d'autres types d'applications tels que les turbines d'éoliennes où la défaillance des engrenages par la fatigue est une des premières causes de temps d'arrêt. Cependant, des progrès doivent être faits concernant la dispersion des nanoparticules dans l'huile. En effet, la stabilité des nanoparticules dans le lubrifiant constitue encore un verrou. Cette instabilité apparait très souvent sur le long terme, mais aussi en fonction des contraintes telles que la centrifugation dans le cas de vitesses périphériques ou de rotations élevées. La sédimentation des mélanges non seulement dans des systèmes statiques, mais également avec des contraintes gravitationnelles (centrifugation) devrait donc être étudiée. A cela devrait s'ajouter l'étude de l'influence de la nature des surfaces frottantes telles que les surfaces DLC et les alliages d'aluminium.

Enfin, d'un point de vu réglementaire, l'élaboration des normes en matière d'utilisation des nanoparticules ainsi que les règles sur l'élimination des déchets les contenant reste à fixer au niveau national, européen et international. Enfin, une étude de marché sur l'impact de la couleur des lubrifiants auprès des consommateurs devrait être menée dans le but d'évaluer l'acceptation des huiles de couleur noire.

Bibliography

1.   I. E. Agency, "Key World Energy Statistics," (2014).
2.   K. Holmberg, P. Andersson, A. Erdemir, Global energy consumption due to friction in passenger cars. *Tribology International* **47**, 221-234 (2012).
3.   ExxonMobil, "The outlook for energy: 2040," (2015).
4.   J. Dulac, Paris, 2013.
5.   B. Bhushan, *Modern Tribology Handbook*. C. Press, Ed., (2000), vol. 1, pp. 1760.
6.   K. Hokkirigawa, K. Kato, An experimental and theoretical investigation of ploughing, cutting and wedge formation during abrasive wear. *Tribology International* **21**, 51-57 (1988).
7.   S. C. Tung, M. L. McMillan, Automotive tribology overview of current advances and challenges for the future. *Tribology International* **37**, 517-536 (2004).
8.   C. M. Taylor, Automobile engine tribology—design considerations for efficiency and durability. *Wear* **221**, 1-8 (1998).
9.   S. Culley, T. McDonnell, The impact of passenger car motor oil phosphorus levels on engine durability, oil degradation, and exhaust emissions in a field trial. *SEA technical paper* **952344**, (1995).
10.   S. Culley, T. McDonnell, D. Ball, C. Kirby, The impact of passenger car motor oil phosphorus levels on automotive emission control systems. *SAE technical paper* **961898**, (1996).
11.   A. F. Bower, The Influence of crack face friction and trapped fluid on surface initiated rolling contact fatigue cracks. *Journal of Tribology* **110**, 704-711 (1988).
12.   W. J. Bartz, V. Krüger, Influence of lubricants on the pitting fatigue of gears. *Wear* **35**, 315-329 (1975).
13.   G. Fajdiga, M. Sraml, Fatigue crack initiation and propagation under cyclic contact loading. *Engineering Fracture Mechanics* **76**, 1320-1335 (2009).
14.   *CRC Handbook of lubrication. Theory and practice of tribology*. (Robert W. Bruce, 1983), vol. II.
15.   E. Bamberger, T. Harris, W Kackmarsky, C. Moyer, R. Parker, J. Sherlock, E. Zaretsky, Life adjustment factors for ball and roller bearings: An engineering design guide. *American Society of Mechanical Engineers*, (1971).
16.   R. E. Cantley, The Effect of water in lubricating oil on bearing fatigue life. *ASLE Transactions* **20**, 244-248 (1977).
17.   I. M. Felsen, R. W. McQuaid, J. A. Marzani, Effect of seawater on the fatigue life and failure distribution of flood-lubricated angular contact ball bearings. *ASLE Transactions* **15**, 8-17 (1972).
18.   P. Schatzberg, Inhibition of water-accelerated rolling-contact fatigue. *Journal of Tribology* **93**, 231-233 (1971).
19.   G. Stachowiak, A. Batchelor, *Engineering Tribology*. (ed. Fourth, 2013), pp. 884.
20.   N. F. R. Cardoso, R. C. Martins, J. H. O. Seabra, A. Igartua, J. C. Rodriguez, R. Luther, Micropitting performance of nitrided steel gears lubricated with mineral and ester oils. *Tribology International* **42**, 77-87 (2009).
21.   A. Cardis, M. Webster, Gear oil micropitting evaluation. *Gear Technology* **September - October**, (2000).
22.   L. Canale, R. Mesquita, G. Totten, *Failure Analysis of Heat Treated Steel Components*. (ASM international, 2008).
23.   I. Kudish, M. Covitch, *Modeling and analytical methods in tribology*. (Chapman & Hall/CRC, Boca Raton, FL, 2010), pp. 905.
24.   S. Way, Pitting due to rolling contact. *ASME transactions, Journal Appl. Mechanics*, A49-A58 (1935).

25. M. Kaneta, Y. Murakami, Effects of oil hydraulic pressure on surface crack growth in rolling/sliding contact. *Tribology International* **20**, 210-217 (1987).
26. N. P. Suh, H. C. Sin, The genesis of friction. *Wear* **69**, 91-114 (1981).
27. H. Uyama, H. Yamada, H. Hidaka, N. Mitamura, The effects of hydrogen on microstructural change and surface originated flaking in rolling contact fatigue. *Tribology Online* **6**, 123-132 (2011).
28. K. Hiraoka, T. Fujimatsu, N. Tsunekage, A. Yamamoto, Generation process observation of micro-structural change in rolling contact fatigue by hydrogen-charged specimens. *Japanese Journal of Tribology* **52**, 673-683 (2007).
29. T. Endo, D. Dong, Y. Imai, Y. Yamamoto, in *Tribology and Interface Engineering Series,* M. P. G. D. a. A. A. L. D. Dowson, Ed. (Elsevier, 2005), vol. Volume 48, pp. 343-350.
30. Y. Wang, J. E. Fernandez, D. G. Cuervo, Rolling-contact fatigue lives of steel AISI 52100 balls with eight mineral and synthetic lubricants. *Wear* **196**, 110-119 (1996).
31. H. K. Trivedi, N. H. Forster, C. S. Saba, Rolling contact fatigue testing of a 3 cSt polyolester lubricant with and without TCP and DODPA/PANA at 177 °C. *Tribology Letters* **16**, 231-237 (2004).
32. H. Trivedi, N. Forster, L. Rosado, Rolling contact fatigue evaluation of advanced bearing steels with and without the oil anti-wear additive tricresyl phosphate. *Tribology Letters* **41**, 597-605 (2011).
33. A. A. Torrance, J. E. Morgan, G. T. Y. Wan, An additive's influence on the pitting and wear of ball bearing steel. *Wear* **192**, 66-73 (1996).
34. G. T. Y. Wan, E. V. Amerongen, H. Lankamp, Effect of extreme-pressure additives on rolling bearing fatigue life. *Journal of Physics D: Applied Physics* **25**, A147 (1992).
35. E. Lainé, A. V. Olver, T. A. Beveridge, Effect of lubricants on micropitting and wear. *Tribology International* **41**, 1049-1055 (2008).
36. V. Brizner, H. R. Pasaribu, G. E. Morales-Espejel, Micropitting performance of oil additives in lubricated rolling contacts. *Tribology Transactions* **56**, 739-748 (2013).
37. F. G. Rounds, Some effects of additives on rolling contact fatigue. *A S L E Transactions* **10**, 243-255 (1967).
38. W. Tuszynski, An effect of lubricating additives on tribochemical phenomena in a rolling steel four-ball contact. *Tribology Letters* **24**, 207-215 (2006).
39. W. Tuszyński, W. Piekoszewski, Effect of the type and concentration of lubricating additives on the antiwear and extreme pressure properties and rolling fatigue life of a four-ball tribosystem. *Lubrication Science* **18**, 309-328 (2006).
40. M. Meheux, C. Minfray, F. Ville, T. Le Mogne, A. A. Lubricht, J. M. Martin, H. P. Lieurade, G. Thoquenne, Effect of lubricant additives in rolling contact fatigue. *J. Engineering Tribology* **224**, 947-955 (2010).
41. L. Arizmendi, A. Rincon, J. M. Bernardo, The effect of a solid additive on rolling fatigue life. *Tribology International* **18**, 17-20 (1985).
42. E. F. Rico, I. Minondo, D. G. Cuervo, Rolling contact fatigue life of AISI 52100 steel balls with mineral and synthetic polyester lubricants with PTFE nanoparticle powder as an additive. *Wear* **266**, 671-677 (2009).
43. H. Spikes, The history and mechanisms of ZDDP. *Tribology Letters* **17**, 469-489 (2004).
44. M. A. Nicholls, T. Do, P. R. Norton, M. Kasrai, G. M. Bancroft, Review of the lubrication of metallic surfaces by zinc dialkyl-dithiophosphates. *Tribology International* **38**, 15-39 (2005).
45. J. Martin, Antiwear mechanisms of zinc dithiophosphate: a chemical hardness approach. *Tribology Letters* **6**, 1-8 (1999).

46. T. Onodera, Y. Morita, A. Suzuki, R. Sahnoun, M. Koyama, H. Tsuboi, N. Hatakeyama, A. Endou, H. Takaba, M. Kubo, C. Del Carpio, C. Minfray, J. M. Martin, A. Miyamoto, A theoretical investigation on the abrasive wear prevention mechanism of ZDDP and ZP tribofilms. *Applied Surface Science* **254**, 7976-7979 (2008).

47. G. W. Kennerly, W. L. Patterson, Kinetic studies of petroleum antioxidants. *Industrial & Engineering Chemistry* **48**, 1917-1924 (1956).

48. T. Colclough, J. I. Cunneen, 923. Oxidation of organic sulphides. Part XV. The antioxidant action of phenothiazine, zinc isopropylxanthate, zinc di-isopropyldithiophosphate, and zinc dibutyldithiocarbamate, in squalene. *Journal of the Chemical Society (Resumed)*, 4790-4793 (1964).

49. W. W. Hanneman, R. S. Porter, The thermal decomposition of dialkyl phosphates and O,O-dialkyl dithiophosphates1. *The Journal of Organic Chemistry* **29**, 2996-2998 (1964).

50. R. Jones, R. Coy, The chemistry of the thermal degradation of zinc dialkyldithiophosphates additives. *ASLE transactions* **24**, 91-97 (1979).

51. P. A. Willermet, D. P. Dailey, R. O. Carter Iii, P. J. Schmitz, W. Zhu, Mechanism of formation of antiwear films from zinc dialkyldithiophosphates. *Tribology International* **28**, 177-187 (1995).

52. D. R. Armstrong, E. S. Ferrari, K. J. Roberts, D. Adams, An examination of the reactivity of zinc di-alkyl-di-thiophosphate in relation to its use as an anti-wear and anti-corrosion additive in lubricating oils. *Wear* **217**, 276-287 (1998).

53. P. Kapsa, J. M. Martin, C. Blanc, J. M. Georges, Antiwear mechanism of ZDDP in the presence of calcium sulfonate detergent. *Journal of Lubrication Technology* **103**, 486-494 (1981).

54. E. S. Yamaguchi, P. R. Ryason, S. W. Yeh, T. P. Hansen, Boundary film formation by ZnDTPs and detergents using ECR. *Tribology Transactions* **41**, 262-272 (1998).

55. Y. Wan, M. Kasrai, G. M. Bancroft, J. Zhang, Characterization of tribofilms derived from zinc dialkyldithiophosphate and salicylate detergents by X-ray absorbance near edge structure spectroscopy. *Tribology International* **43**, 283-288 (2010).

56. A. Morina, A. Neville, M. Priest, J. H. Green, ZDDP and MoDTC interactions and their effect on tribological performance – tribofilm characteristics and its evolution. *Tribology Letters* **24**, 243-256 (2006).

57. A. Morina, A. Neville, M. Priest, J. H. Green, ZDDP and MoDTC interactions in boundary lubrication—The effect of temperature and ZDDP/MoDTC ratio. *Tribology International* **39**, 1545-1557 (2006).

58. C. Grossiord, J. M. Martin, K. Varlot, B. Vacher, T. Le Mogne, Y. Yamada, Tribochemical interactions between ZnDTP, MoDTC and calcium borate. *Tribology Letters* **8**, 203-212 (2000).

59. M. Muraki, Y. Yanagi, K. Sakaguchi, Synergistic effect on frictional characteristics under rolling-sliding conditions due to a combination of molybdenum dialkyldithiocarbamate and zinc dialkyldithiophosphate. *Tribology International* **30**, 69-75 (1997).

60. P. C. H. Mitchell, Oil-soluble MO-S compounds as lubricant additives. *Wear* **100**, 281-300 (1984).

61. Y. Yamamoto, S. Gondo, T. Kamakura, N. Tanaka, Frictional characteristics of molybdenum dithiophosphates. *Wear* **112**, 79-87 (1986).

62. C. Grossiord, K. Varlot, J. M. Martin, T. Le Mogne, C. Esnouf, K. Inoue, MoS_2 single sheet lubrication by molybdenum dithiocarbamate. *Tribology International* **31**, 737-743 (1998).

63. J.-M. Martin, C. Grossiord, T. Le Mogne, J. Igarashi, Transfer films and friction under boundary lubrication. *Wear* **245**, 107-115 (2000).

64. M. I. De Barros Bouchet, J. M. Martin, T. Le Mogne, P. Bilas, B. Vacher, Y. Yamada, Mechanisms of MoS_2 formation by MoDTC in presence of ZnDTP: effect of oxidative degradation. *Wear* **258**, 1643-1650 (2005).

65. F. Dassenoy, L. Joly-Pottuz, J. M. Martin, D. Vrbanic, A. Mrzel, D. Mihailovic, W. Vogel, G. Montagnac, Tribological performances of $Mo_6S_3I_6$ nanowires. *Journal of the European Ceramic Society* **27**, 915-919 (2007).

66. T. Onodera, Y. Morita, A. Suzuki, M. Koyama, H. Tsuboi, N. Hatakeyama, A. Endou, H. Takaba, M. Kubo, F. Dassenoy, C. Minfray, L. Joly-Pottuz, J. M. Martin, A. Miyamoto, A Computational Chemistry Study on Friction of h-MoS_2. Part I. Mechanism of Single Sheet Lubrication. *The Journal of Physical Chemistry B* **113**, 16526-16536 (2009).

67. J. Graham, H. Spikes, S. Korcek, The Friction Reducing Properties of Molybdenum Dialkyldithiocarbamate Additives: Part I — Factors Influencing Friction Reduction. *Tribology Transactions* **44**, 626-636 (2001).

68. L. Rapoport, Y. Feldman, M. Homyonfer, H. Cohen, J. Sloan, J. L. Hutchison, R. Tenne, Inorganic fullerene-like material as additives to lubricants: structure–function relationship. *Wear* **225–229, Part 2**, 975-982 (1999).

69. E.-o.-l. Ettefaghi, H. Ahmadi, A. Rashidi, A. Nouralishahi, S. S. Mohtasebi, Preparation and thermal properties of oil-based nanofluid from multi-walled carbon nanotubes and engine oil as nano-lubricant. *International Communications in Heat and Mass Transfer* **46**, 142-147 (2013).

70. H. D. Huang, J. P. Tu, L. P. Gan, C. Z. Li, An investigation on tribological properties of graphite nanosheets as oil additive. *Wear* **261**, 140-144 (2006).

71. L. Joly-Pottuz, N. Matsumoto, H. Kinoshita, B. Vacher, M. Belin, G. Montagnac, J. M. Martin, N. Ohmae, Diamond-derived carbon onions as lubricant additives. *Tribology International* **41**, 69-78 (2008).

72. J. L. Viesca, A. Hernández Battez, R. González, R. Chou, J. J. Cabello, Antiwear properties of carbon-coated copper nanoparticles used as an additive to a polyalphaolefin. *Tribology International* **44**, 829-833 (2011).

73. A. Hernandez Battez, J. E. Fernandez Rico, A. Navas Arias, J. L. Viesca Rodriguez, R. Chou Rodriguez, J. M. Diaz Fernandez, The tribological behaviour of ZnO nanoparticles as an additive to PAO6. *Wear* **261**, 256-263 (2006).

74. S. Ingole, A. Charanpahari, A. Kakade, S. S. Umare, D. V. Bhatt, J. Menghani, Tribological behavior of nano TiO_2 as an additive in base oil. *Wear* **301**, 776-785 (2013).

75. P. Ye, X. Jiang, S. Li, S. Li, Preparation of $NiMoO_2S_2$ nanoparticle and investigation of its tribological behavior as additive in lubricating oils. *Wear* **253**, 572-575 (2002).

76. V. Narayanunni, B. A. Kheireddin, M. Akbulut, Influence of surface topography on frictional properties of Cu surfaces under different lubrication conditions: Comparison of dry, base oil, and ZnS nanowire-based lubrication system. *Tribology International* **44**, 1720-1725 (2011).

77. L. Joly-Pottuz, F. Dassenoy, M. Belin, B. Vacher, J. M. Martin, N. Fleisher, Ultralow-friction and wear properties of IF-WS_2 under boundary lubrication. *Tribology Letters* **18**, 477-485 (2005).

78. Q. H. Wang, K. Kalantar-Zadeh, A. Kis, J. N. Coleman, M. S. Strano, Electronics and optoelectronics of two-dimensional transition metal dichalcogenides. *Nat Nano* **7**, 699-712 (2012).

79. M. Ghorbani-Asl, N. Zibouche, M. Wahiduzzaman, A. Oliveira, A. Kuc, T. Heine, Electromechanics in MoS_2 and WS_2: nanotubes vs. monolayers. *Sci. Rep.* **3**, (2013).

80. F. J. Claus, Solid Lubricants and Self-Lubricating Solids. *Academic Press*, (1972).

81. A. Margolin, F. L. Deepak, R. Popovitz-Biro, M. Bar-Sadan, Y. Feldman, R. Tenne, Fullerene-like WS_2 nanoparticles and nanotubes by the vapor-phase synthesis of WCl_n and H_2S. *Nanotechnology* **19**, 095601 (2008).

82. R. Tenne, L. Margulis, M. Genut, G. Hodes, Polyhedral and cylindrical structures of tungsten disulphide. *Nature* **360**, 444-446 (1992).

83. L. Margulis, G. Salitra, R. Tenne, M. Talianker, Nested fullerene-like structures. *Nature* **365**, 113-114 (1993).

84. I. Lahouij, B. Vacher, J.-M. Martin, F. Dassenoy, IF-MoS$_2$ based lubricants: Influence of size, shape and crystal structure. *Wear* **296**, 558-567 (2012).

85. I. Lahouij, E. W. Bucholz, B. Vacher, S. B. Sinnott, J. M. Martin, F. Dassenoy, Lubrication mechanisms of hollow-core inorganic fullerene-like nanoparticles: coupling experimental and computational works. *Nanotechnology* **23**, 375701 (2012).

86. I. Lahouij, F. Dassenoy, B. Vacher, J.-M. Martin, Real Time TEM Imaging of Compression and Shear of Single Fullerene-Like MoS$_2$ Nanoparticle. *Tribology Letters* **45**, 131-141 (2012).

87. I. Lahouij, B. Vacher, F. Dassenoy, Direct observation by in situ transmission electron microscopy of the behaviour of IF-MoS$_2$ nanoparticles during sliding tests: influence of the crystal structure. *Lubrication Science*, **26**, 164-173 (2013).

88. J. Tannous, F. Dassenoy, A. Bruhács, W. Tremel, Synthesis and tribological performance of novel Mo$_x$W$_{1-x}$S$_2$ (0 ≤ x ≤ 1) inorganic fullerenes. *Tribology Letters* **37**, 83-92 (2010).

89. R. Greenberg, G. Halperin, I. Etsion, R. Tenne, The effect of WS$_2$ nanoparticles on friction reduction in various lubrication regimes. *Tribology Letters* **17**, 179-186 (2004).

90. L. Joly-Pottuz, F. Dassenoy, in *Nanolubricants*. (John Wiley & Sons, Ltd, 2008), pp. 15-92.

91. J. Kogovšek, M. Remškar, A. Mrzel, M. Kalin, Influence of surface roughness and running-in on the lubrication of steel surfaces with oil containing MoS$_2$ nanotubes in all lubrication regimes. *Tribology International* **61**, 40-47 (2013).

92. J. Kogovšek, M. Kalin, Various MoS$_2$-, WS$_2$- and C-Based Micro- and nanoparticles in boundary lubrication. *Tribology Letters* **53**, 585-597 (2014).

93. J. Kogovšek, M. Remškar, M. Kalin, Lubrication of DLC-coated surfaces with MoS$_2$ nanotubes in all lubrication regimes: Surface roughness and running-in effects. *Wear* **303**, 361-370 (2013).

94. L. Rapoport, O. Nepomnyashchy, I. Lapsker, A. Verdyan, A. Moshkovich, Y. Feldman, R. Tenne, Behavior of fullerene-like WS$_2$ nanoparticles under severe contact conditions. *Wear* **259**, 703-707 (2005).

95. K. Hu, X. Hu, Y. Xu, F. Huang, J. Liu, The effect of morphology on the tribological properties of MoS$_2$ in liquid paraffin. *Tribology Letters* **40**, 155-165 (2010).

96. H. D. Huang, J. P. Tu, T. Z. Zou, L. L. Zhang, D. N. He, Friction and wear properties of IF–MoS$_2$ as additive in paraffin oil. *Tribology Letters* **20**, 247-250 (2005).

97. C. P. Koshy, P. K. Rajendrakumar, M. V. Thottackkad, Evaluation of the tribological and thermo-physical properties of coconut oil added with MoS$_2$ nanoparticles at elevated temperatures. *Wear* **330–331**, 288-308 (2015).

98. Y. Zhang, C. Li, D. Jia, D. Zhang, X. Zhang, Experimental evaluation of MoS$_2$ nanoparticles in jet MQL grinding with different types of vegetable oil as base oil. *Journal of Cleaner Production* **87**, 930-940 (2015).

99. M. Gulzar, H. H. Masjuki, M. Varman, M. A. Kalam, R. A. Mufti, N. W. M. Zulkifli, R. Yunus, R. Zahid, Improving the AW/EP ability of chemically modified palm oil by adding CuO and MoS$_2$ nanoparticles. *Tribology International* **88**, 271-279 (2015).

100. R. R. Sahoo, S. K. Biswas, Effect of layered MoS$_2$ nanoparticles on the frictional behavior and microstructure of lubricating greases. *Tribology Letters* **53**, 157-171 (2014).

101. L. Cizaire, B. Vacher, T. Le Mogne, J. M. Martin, L. Rapoport, A. Margolin, R. Tenne, Mechanisms of ultra-low friction by hollow inorganic fullerene-like MoS$_2$ nanoparticles. *Surface and Coatings Technology* **160**, 282-287 (2002).

102. R. Rosentsveig, A. Gorodnev, N. Feuerstein, H. Friedman, A. Zak, N. Fleischer, J. Tannous, F. Dassenoy, R. Tenne, Fullerene-like MoS$_2$ nanoparticles and their tribological behavior. *Tribology Letters* **36**, 175-182 (2009).

103. M. Ratoi, V. Niste, J. Walker, J. Zekonyte, Mechanism of action of WS_2 lubricant nanoadditives in high-pressure contacts. *Tribology Letters* **52**, 81-91 (2013).

104. P. Rabaso, F. Dassenoy, F. Ville, M. Diaby, B. Vacher, T. Le Mogne, J. M. Martin, J. Cavoret, An Investigation on the Reduced Ability of IF-MoS_2 Nanoparticles to reduce friction and wear in the presence of dispersants. *Tribology Letters*, **55**, 503-516 (2014).

105. A. Moshkovith, V. Perfiliev, A. Verdyan, I. Lapsker, R. Popovitz-Biro, R. Tenne, L. Rapoport, Sedimentation of IF-WS_2 aggregates and a reproducibility of the tribological data. *Tribology International* **40**, 117-124 (2007).

106. L. Rapoport, A. Moshkovich, V. Perfilyev, A. Laikhtman, I. Lapsker, L. Yadgarov, R. Rosentsveig, R. Tenne, High lubricity of Re-doped fullerene-like MoS_2 nanoparticles. *Tribology Letters* **45**, 257-264 (2012).

107. L. Yadgarov, V. Petrone, R. Rosentsveig, Y. Feldman, R. Tenne, A. Senatore, Tribological studies of rhenium doped fullerene-like MoS_2 nanoparticles in boundary, mixed and elasto-hydrodynamic lubrication conditions. *Wear* **297**, 1103-1110 (2013).

108. R. R. Sahoo, S. K. Biswas, Deformation and friction of MoS_2 particles in liquid suspensions used to lubricate sliding contact. *Thin Solid Films* **518**, 5995-6005 (2010).

109. S. Aralihalli, S. Biswas, Grafting of dispersants on MoS_2 nanoparticles in base oil lubrication of steel. *Tribology Letters* **49**, 61-76 (2013).

110. Y. Cho, J. Park, B. Ku, J. Lee, W. Park, J, Lee, S. Kim, Synergistic effect of a coating and nano-oil lubricant on the tribological properties of friction surfaces. *International Journal of Precision Engineering and Manufacturing* **13**, 97-102 (2012).

111. J. Jelenc, M. Remskar, Friction on a single MoS_2 nanotube. *Nanoscale Research Letters* **7**, 208 (2012).

112. M. Stefanov, A. N. Enyashin, T. Heine, G. Seifert, Nanolubrication: How do MoS_2-based nanostructures lubricate? *The Journal of Physical Chemistry C* **112**, 17764-17767 (2008).

113. L. Rapoport, Y. Bilik, Y. Homyonfer, S. R. Cohen, R. Tenne, Hollow nanoparticles of WS_2 as potential solid-state lubricants. *Nature* **387**, 791-793 (1997).

114. P.-Z. Si, C.-J. Choi, J.-W. Lee, D.-Y. Geng, Z.-D. Zhang, Synthesis, structure and tribological performance of tungsten disulphide nanocomposites. *Materials Science and Engineering: A* **443**, 167-171 (2007).

115. L. Rapoport, V. Leshchinsky, Y. Volovik, M. Lvovsky, O. Nepomnyashchy, Y. Feldman, R. Popovitz-Biro, R. Tenne, Modification of contact surfaces by fullerene-like solid lubricant nanoparticles. *Surface and Coatings Technology* **163–164**, 405-412 (2003).

116. P. Njiwa, A. Hadj-Aïssa, P. Afanasiev, C. Geantet, F. Bosselet, B. Vacher, M. Belin, T. Le Mogne, F. Dassenoy, Tribological properties of new MoS_2 nanoparticles prepared by seed-assisted solution technique. *Tribology Letters*, 1-9 (2014).

117. J. Tannous, F. Dassenoy, A. Bruhács, W. Tremel, Synthesis and tribological performance of novel $Mo_xW_{1-x}S_2$ ($0 \leq x \leq 1$) inorganic fullerenes. *Tribology Letters* **37**, 83-92 (2010).

118. M. Kalin, J. Kogovšek, M. Remškar, Nanoparticles as novel lubricating additives in a green, physically based lubrication technology for DLC coatings. *Wear* **303**, 480-485 (2013).

119. M. Kalin, J. Kogovšek, J. Kovač, M. Remškar, The formation of tribofilms of MoS_2 nanotubes on steel and DLC-coated surfaces. *Tribology Letters*, 1-11 (2014).

120. S. J. Castillo Marcano, S. Bensaid, F. A. Deorsola, N. Russo, D. Fino, Nanolubricants for diesel engines: Related emissions and compatibility with the after-treatment catalysts. *Tribology International* **72**, 198-207 (2014).

121. I. Jenei, F. Svahn, S. Csillag, Correlation studies of WS_2 fullerene-like nanoparticles enhanced tribofilms: a scanning electron microscopy analysis. *Tribology Letters* **51**, 461-468 (2013).

122. M. Sgroi, F. Gili, D. Mangherini, I. Lahouij, F. Dassenoy, I. Garcia, I. Odriozola, G. Kraft, Friction reduction benefits in valve-train system using IF-MoS$_2$ added engine oil. *Tribology Transactions* **58**, 207-214 (2014).

123. S. Bec, A. Tonck, J. M. Georges, G. W. Roper, Synergistic effects of MoDTC and ZDTP on frictional behaviour of tribofilms at the nanometer scale. *Tribology Letters* **17**, 797-809 (2004).

124. M. Nicholls, G. Bancroft, P. Norton, M. Kasrai, G. De Stasio, B. Frazer, L. Wiese, Chemomechanical properties of antiwear films using X-ray absorption microscopy and nanoindentation techniques. *Tribology Letters* **17**, 245-259 (2004).

125. A. Tomala, B. Vengudusamy, M. Rodriguez Ripoll, A. Naveira Suarez, M. Remskar, R. Rosentsveig, Interaction between selected MoS$_2$ nanoparticles and ZDDP tribofilms. *Tribology Letters* **59**, 1-18 (2015).

126. I. Jenei, F. Svahn, S. Csillag, Correlation studies of WS$_2$ fullerene-like nanoparticles enhanced tribofilms: A scanning electron microscopy analysis. *Tribology Letters* **51**, 461-468 (2013).

127. Y. Wan, M. L. Suominen Fuller, M. Kasrai, G. M. Bancroft, K. Fyfe, J. R. Torkelson, Y. F. Hu, K. H. Tan, Effects of detergent on the chemistry of tribofilms from ZDDP: studied by x-ray absorption spectroscopy and XPS, *Tribology Series* **40**, 155-166 (2002).

128. Y. Wan, M. Kasrai, G. M. Bancroft, X-ray absorption study of tribofilms from ZDDP and overbased salicylate detergents. *Chinese Chemical Letters* **20**, 119-122 (2009).

129. F. G. Rounds, Additive interactions and their effect on the performance of a zinc dialkyl dithiophosphate. *ASLE Transactions* **21**, 91-101 (1978).

130. L. G. Yu, E. S. Yamaguchi, M. Kasrai, G. M. Bancroft, The chemical characterization of tribofilms using XANES — Interaction of nanosize calcium-containing detergents with zinc dialkyldithiophosphate. *Canadian Journal of Chemistry* **85**, 675-684 (2007).

131. A. Greenall, A. Neville, A. Morina, M. Sutton, Investigation of the interactions between a novel, organic anti-wear additive, ZDDP and overbased calcium sulphonate. *Tribology International* **46**, 52-61 (2012).

132. S. S. V. Ramakumar, A. M. Rao, S. P. Srivastava, Studies on additive-additive interactions: Formulation of crankcase oils towards rationalization. *Wear* **156**, 101-120 (1992).

133. G. Pereira, A. Lachenwitzer, M. Kasrai, G. M. Bancroft, P. R. Norton, M. Abrecht, P.U. Gilbert, T. Regier, R. I. Blyth, J. Thompson, Chemical and mechanical analysis of tribofilms from fully formulated oils Part 1 – Films on 52100 steel. *Tribology - Materials, Surfaces & Interfaces* **1**, 48-61 (2007).

134. P. A. Willermet, R. O. Carter, P. J. Schmitz, M. Everson, D. J. Scholl, W. H. Weber, Formation, structure, and properties of lubricant-derived antiwear films. *Lubrication Science* **9**, 325-348 (1997).

135. M. Kasrai, M. S. Fuller, G. M. Bancroft, P. R. Ryason, X-Ray absorption study of the effect of calcium sulfonate on antiwear film formation generated from neutral and basic ZDDPs: Part 1—phosphorus species. *Tribology Transactions* **46**, 534-542 (2003).

136. M. Burkinshaw, A. Neville, A. Morina, M. Sutton, Calcium sulphonate and its interactions with ZDDP on both aluminium–silicon and model silicon surfaces. *Tribology International* **46**, 41-51 (2012).

137. M. Najman, M. Kasrai, G. Michael Bancroft, R. Davidson, Combination of ashless antiwear additives with metallic detergents: interactions with neutral and overbased calcium sulfonates. *Tribology International* **39**, 342-355 (2006).

138. J. McGeehan, E. Yamaguchi, J. Adams, paper presented at the SAE technical papers. Procidings of the international fuels and lubricants meeting and exposition, Tulsa, Oklahoma; October, 1985.

139. M. T. Costello, R. A. Urrego, Study of surface films of the ZDDP and the MoDTC with crystalline and amorphous overbased calcium sulfonates by XPS. *Tribology Transactions* **50**, 217-226 (2007).

140.	F. Chinas-Castillo, H. A. Spikes, Film formation by colloidal overbased detergents in lubricated contacts. *Tribology Transactions* **43**, 357-366 (2000).

141.	S. Giasson, T. Palermo, T. Buffeteau, B. Desbat, J. M. Turlet, Study of boundary film formation with overbased calcium sulfonate by PM-IRRAS spectroscopy. *Thin Solid Films* **252**, 111-119 (1994).

142.	X.-B. Chen, X. Zhou, T. B. Abbott, M. A. Easton, N. Birbilis, Double-layered manganese phosphate conversion coating on magnesium alloy AZ91D: Insights into coating formation, growth and corrosion resistance. *Surface and Coatings Technology* **217**, 147-155 (2013).

143.	V. Di Castro, G. Polzonetti, XPS study of MnO oxidation. *Journal of Electron Spectroscopy and Related Phenomena* **48**, 117-123 (1989).

144.	P. Aldana, B. Vacher, T. Le Mogne, M. Belin, B. Thiebaut, F. Dassenoy., Action mechanism of WS_2 nanoparticles with ZDDP additive in boundary lubrication regime. *Tribology Letters*, 1-10 (2014).

145.	K. Lipp, G. Hoffman, Design for rolling contact fatigue. *The international journal of Power Metallurgy* **39**, (2003).

146.	R. Errichello, Selecting oils with high-pressure-viscosity coefficient. *Machinery Lubrication* **4**, 48-52 (2004).

147.	R. Errichello, Morphology of micropitting. *Gear Technology* **Nov/dic**, 74-81 (2012).

148.	V. B. Niste, H. Tanaka, M. Ratoi, J. Sugimura, WS_2 nanoadditized lubricant for applications affected by hydrogen embrittlement. *RSC Advances* **5**, 40678-40687 (2015).

149.	S. Sheng, "Report on wind turbine subsystem reliability. A survey of various databases," (United States National Renewable Energy Laboratory, 2013).

AUTORISATION DE SOUTENANCE

Vu les dispositions de l'arrêté du 7 août 2006,

Vu la demande du Directeur de Thèse

Monsieur F. DASSENOY

et les rapports de

Monsieur M. KALIN
Professeur - Laboratory for Tribology and Interface Nanotechnology - University of Lubljana
Faculty of Mechanical Engineering - Bogisiceva 8 - 1000 Lubljana - Slovénie

Et de

Monsieur S. CSILLAG
Professeur - Stockholms Universitet Instrumenteringsfysik - 106 91 Stockholm - Suède

Madame USSA ALDANA Paula

est autorisée à soutenir une thèse pour l'obtention du grade de **DOCTEUR**

Ecole doctorale MATERIAUX

Fait à Ecully, le 8 janvier 2016

P/Le directeur de l'E.C.L.
La directrice des Etudes

M-A. GALLAND

Abstract

The growing environmental concerns, along with the continuous increase of energy demand, have encouraged research to improve energy efficiency in every technological field. In the transport industry, responsible of more than half of the world's oil consumption, manufacturers have bet on hybrid fuel technologies, more aerodynamic car profiles, innovative tires and even downsizing of engines and gearboxes to reduce the weight of the vehicles to face the problem. However, according to VTT Technical Research Centre of Finland, in passenger cars one third of fuel consumption is due to friction loss. This means that several millions of liters of fuel are used every year to overcome friction around the world. As a consequence, reduction on the friction losses would have a direct impact in oil consumption. For this reason, research in the tribology field has specially focused in the development of low friction materials and more efficient lubricants. This work investigates the potential of metal dichalcogenide nanoparticles as lubricant additives for automobile applications with the aim of formulating more efficient lubricants. These nanoparticles which were synthetized for the first time in the 90's have shown interesting tribological properties when added to base oil under specific laboratory test conditions. However, their future use in real-life mechanical systems needs a better comprehension of their behavior on rough surfaces and in the presence of additives commonly used in industrial lubricants.Industrially produced tungsten disulfide nanoparticles were used in this work. First of all, the industrial context of this work and the basis of tribology science in general and of tribology in the automotive industry in particular are exposed in the state of the art part. In this section, a literature review of the lubricating properties of laboratory scale produced metal dichalcogenides nanoparticles of tungsten and molybdenum disulfide is exposed. The effect of different conditions (temperature, concentration in oil, contact pressure, among others) is also presented in this first section. The research work done for this thesis is divided in two main parts. In the first one, the nanoparticles were first morphologically and chemically characterized and their tribological potential in base oil was investigated on smooth and rough surfaces under different test conditions. Then, their tribological behavior in the presence of additives that are commonly used in industrial applications, in the boundary lubrication regime and at 100°C was studied.In the second part, the use of nanoparticles for a gearbox application was explored. The potential of the nanoparticles in base oil and in the presence of a commercial package of additives for this application was studied, first at the laboratory scale, and then in scaled-up tests with gearboxes used in cars. The results suggest that nanoparticles can be used to increase life span of the mechanical parts of gears.

Key words: Nanoparticles, lubrication, gears, additives, rough surfaces.

Résumé

Les normes environnementales toujours plus sévères associées à une constante augmentation de la demande énergétique rendent nécessaires les actions à entreprendre en vue d'améliorer l'efficacité énergétique. Dans le domaine du transport, responsable à lui seul de plus de la moitié de la consommation des ressources pétrolières, les actions visant à optimiser la consommation énergétique se traduisent par la mise en place de nouvelles technologies hybrides, par un travail sur l'aérodynamisme des véhicules, la conception de pneumatiques plus performants ou bien encore la réduction de la taille des moteurs et des boites de vitesse afin de réduire le poids des véhicules. Cependant, selon le VTT (Centre de recherche technique finlandais), dans les voitures particulières, les pertes par frottement représentent un tiers de la consommation totale de carburant. Plusieurs millions de litres de carburant sont ainsi utilisés dans le monde chaque année pour vaincre les forces de frottement. Pour cette raison la recherche en tribologie dans le domaine de l'automobile s'est plus particulièrement focalisée ces dernières années sur le développement de matériaux à faible coefficient de frottement ainsi que lubrifiants plus performants. Ce travail de thèse a pour objectif d'étudier le potentiel des nanoparticules de dichalcogénures métalliques en tant qu'additifs de lubrification pour applications automobiles dans le but de développer de nouveaux lubrifiants hautement performants. Ces nanoparticules, synthétisées pour la première fois dans les années 90, ont déjà montré des propriétés tribologiques intéressantes lors de tests effectués en laboratoire, en régime de lubrification limite. Toutefois, leur utilisation dans des systèmes mécaniques réels nécessite une meilleure compréhension de leurs performances dans des conditions plus proches de la réalité, à savoir en présence de surfaces rugueuses ainsi qu'en présence d'additifs couramment utilisés dans les lubrifiants industriels. Au cours de ce travail, nous nous sommes focalisés sur des nanoparticules de bisulfures de tungstène produites industriellement. Le contexte industriel de ce travail de thèse ainsi que les bases de la tribologie seront exposés dans un premier chapitre consacré à l'état de l'art. Dans ce même chapitre, une revue bibliographique des propriétés lubrifiantes des nanoparticules de bisulfures métalliques (MoS2, WS2) observées lors d'essais tribologiques effectués en laboratoire sera également présentée. L'influence de certains paramètres tels que les conditions d'essais, l'effet de la température, de la concentration, de la cristallinité sera également présentée dans ce premier chapitre.Les résultats de mon travail de thèse seront présentés à travers deux grandes parties. Dans une première, les caractéristiques morphologiques et chimiques des nanoparticules étudiées seront présentées. Leurs propriétés tribologiques dans l'huile de base en présence de surfaces en acier de différentes rugosités seront discutées. Enfin, leurs performances en présence d'additifs couramment utilisés dans les applications industrielles ont également été étudiées. Tous ces essais ont été réalisés en régime de lubrification limite et à 100°C. Dans une seconde partie, le potentiel des nanoparticules pour une application boîte de vitesses a été exploré. Des essais tribologiques ont été réalisés à la fois dans une huile de base ainsi qu'en présence d'un cocktail d'additifs, tout d'abord à l'échelle du laboratoire puis lors de tests réels effectués avec des boites de vitesses utilisées dans l'automobile. Les résultats montrent que les nanoparticules peuvent être utilisées pour augmenter la durée de vie des engrenages.

Mots cléfs : Nanoparticules, lubrification, engrainages, additifs, surfaces rugueuses.